

**THE PATHOGENESIS OF UTERINE  
ADENOMYOSIS**

Thesis submitted for the degree of

**Doctor of Philosophy**

At the University of Leicester

By

**Mohamed Khairy Mehaseb**

MBBCh, MSc, MD, MRCOG

Reproductive Sciences Section

Department of Cancer Studies and Molecular Medicine

University of Leicester

**2010**

# THE PATHOGENESIS OF UTERINE ADENOMYOSIS

**Mohamed Khairy MEHASSEB**

## ABSTRACT

The exact aetiology and pathogenesis of uterine adenomyosis are not clear. Increased endometrial invasiveness has been proposed in the literature, but without conclusive evidence. This thesis was undertaken to examine the pathogenesis of adenomyosis and the differences between affected and unaffected uteri, testing two possibilities with adenomyosis: (i) that the myometrium is permissive to invasion by a normal basal endometrium, or (ii) that the basal endometrium has a higher invasive potential and penetrates a normal myometrium.

To examine the early phases of development of adenomyosis, a mouse model was used, where adenomyosis was induced by dosing female pups with tamoxifen. The same experiment was used on C57/BL6J strain to examine strain differences in response to tamoxifen and predisposition to adenomyosis. Adenomyosis in the human uterus was characterised, examining the immunohistochemical, light and electron microscopy structure, and RNA microarrays of affected and unaffected uteri. The invasive properties of the stroma and its interaction with the underlying myometrium were further studied in a co-culture model.

Adenomyosis was successfully induced in the CD1 mice, with abnormal development and disruption of the inner circular myometrium. However, the C57/BL6J did not develop adenomyosis in spite of the presence of inner myometrial abnormalities comparable to the CD1 mice. Affected human uteri showed distinct myometrial features such as reduced myometrial cellular density and enlarged nuclei with hypertrophy and hyperplasia seen on light microscopy. Electron microscopy revealed ultrastructural features (e.g. reduced caveolae and increased myelin bodies, intermediate filaments and dense bands) in adenomyotic uteri. A large number of dysregulated genes were detected between affected and unaffected uteri, with *Wnt5a* being a key downregulated gene. Steroid receptor expression was equally altered in cases of adenomyosis (e.g. reduced progesterone receptors and increased estrogen receptor beta). Increased vimentin immunostaining was equally observed in the inner myometrium of diseased uteri. An increased adenomyotic stromal invasiveness and increased myometrial permissiveness was observed in the co-culture model.

The thesis demonstrates that the endometrial – myometrial interface behaves differently in uteri with adenomyosis, concluding that adenomyosis is a uterine disease characterized by both increased endometrial invasiveness and myometrial defects that play a facilitative role for this invasion. Both the myometrium and endometrial stroma of diseased uteri show a unique phenotype, gene expression and protein expression profiles.

## ACKNOWLEDGEMENTS

This research was carried out in the Reproductive Sciences Section of the Department of Cancer Studies and Molecular Medicine at the University of Leicester, between 2005 and 2008. The research was supported by a clinical fellowship awarded to me by the University Hospitals of Leicester NHS Trust to which I am really grateful.

First, I would like to acknowledge the contribution of all the women who took part in the studies for this thesis. Without their generosity and understanding I would not have been able to carry out my work.

I am indebted to my supervisors, Mr Marwan Habiba, Professor Stephen Bell and Dr James Howard Pringle. Without their constant support, patience, ideas and input this thesis would not have been possible. They were always there for me, encouraged me in hard times and helped me maintain progress towards my goals.

I would like to thank the staff in the Reproductive Sciences Section for their help, especially Mrs Susan Spurling and Mrs Muna Abbas for their technical assistance; Mrs Stephanie Moutrey and Mrs Zoe Skidmore for their excellent administrative and secretarial support. A special recognition would go for Dr Anthony Taylor for his invaluable help, support and scientific advice through the thesis, Dr Rina Panchal and Dr Sarah Philip for their help and camaraderie.

During this research, I had recourse to specialised areas of expertise. I would like to acknowledge Dr Ian White and the Division of Biomedical Services for their help in the mouse experimental model. I would also like to thank the staff in the Electron Microscopy facilities in the University of Leicester, and Dr Bryan Eyden from the University of Manchester for their help and advice. Special thanks go to all the staff in the Department of Genetics for their help and support in the microarray analysis, and for the Department of Infection, Immunity and Inflammation for their help in the proteomics analysis.

## DEDICATION

*To my Mother and Father, for all they have done to me*

*To my wife Racha, for her patience and support*

*To Hussein, who gives a meaning to my life*

*To Yasmine, who taught me to never give up*

*And to Yahia ...*

# LIST OF CONTENTS

<b>Chapter 1: Introduction.....</b>	<b>1</b>
1.1 DEFINITIONS.....	2
1.2 ASSOCIATED PATHOLOGY .....	6
1.3 PREVALENCE .....	8
1.4 CLINICAL CORRELATES OF ADENOMYOSIS.....	10
1.4.1 Menstrual disorders.....	12
1.4.2 Endometriosis .....	13
1.4.3 Infertility .....	14
1.5 IMAGING AND DIAGNOSIS OF ADENOMYOSIS .....	15
1.5.1 Hysterosalpingography .....	15
1.5.2 Pelvic Ultrasonography.....	16
1.5.3 Magnetic resonance imaging (MRI).....	18
1.6 THE ENDOMETRIAL-MYOMETRIAL INTERFACE (EMI) .....	21
1.6.1 Normal myometrial zonal differentiation .....	24
1.7 PATHOGENESIS OF UTERINE ADENOMYOSIS .....	26
1.7.1 Endometrial-myometrial interface invasion and physical disruption .....	26
1.7.2 Disordered proliferation/regeneration.....	27
1.7.3 Role of endometrial stromal and stem cells in adenomyosis.....	28
1.7.4 Altered hormonal milieu .....	31
1.7.5 Immunological and biochemical abnormalities.....	34
1.7.6 Genetic basis of uterine adenomyosis.....	36
 <b>Chapter 2: The effects of tamoxifen and estradiol on myometrial differentiation and organisation during early uterine development in the CD-1 mouse.....</b>	 <b>41</b>

2.1	INTRODUCTION .....	42
2.2	METHODS .....	44
2.2.1	Samples and materials .....	44
2.2.2	Immunohistochemistry .....	44
2.3	RESULTS .....	45
2.3.1	Morphology and uterine development.....	46
2.3.1.1	Normal uterine development of CD-1 mice .....	46
2.3.1.2	Uterine development following tamoxifen administration .....	48
2.3.1.3	Uterine development following estradiol administration 49	
2.3.2	Immunohistochemical markers.....	52
2.3.2.1	$\alpha$ -Smooth muscle actin ( $\alpha$ -SMA) expression.....	52
2.3.2.2	Desmin expression.....	52
2.3.2.3	Vimentin expression .....	53
2.3.2.4	Laminin and fibronectin expression .....	53
2.3.2.5	ER-alpha expression .....	54
2.4	DISCUSSION.....	60

**Chapter 3: The effects of tamoxifen on myometrial differentiation and organisation during early uterine development in the C57/BL6J mouse .... 65**

3.1	INTRODUCTION .....	66
3.2	MATERIALS AND METHODS.....	66
3.3	RESULTS .....	67
3.3.1	Morphology and uterine development.....	67
3.3.1.1	Normal uterine development of C57/BL6J mice.....	67
3.3.1.2	Uterine development following tamoxifen administration .....	68

3.3.2	Immunohistochemical markers.....	72
3.3.2.1	$\alpha$ -Smooth Muscle Actin ( $\alpha$ -SMA) expression .....	72
3.3.2.2	Desmin expression.....	72
3.3.2.3	Vimentin expression .....	73
3.3.2.4	Laminin and fibronectin expression .....	73
3.3.2.5	ER-alpha expression .....	73
3.4	DISCUSSION.....	81

**Chapter 4: Phenotypic characterization of the inner and outer myometrium in normal and adenomyotic uteri .....86**

4.1	INTRODUCTION .....	87
4.2	MATERIALS AND METHODS.....	89
4.2.1	Samples.....	89
4.2.2	Immunohistochemistry .....	91
4.2.3	Image analysis & validation .....	91
4.2.4	Measurements .....	92
4.2.5	Statistical analysis.....	93
4.3	RESULTS .....	93
4.4	DISCUSSION.....	106

**Chapter 5: Ultrastructural study of the inner and outer myometrium in uteri with and without adenomyosis..... 109**

5.1	INTRODUCTION .....	110
5.2	PATIENTS AND METHODS.....	111
5.3	RESULTS .....	113
5.3.1	Myometrium ultrastructure in the absence of adenomyosis .....	113
5.3.2	Myometrial ultrastructure in the presence of uterine adenomyosis .....	116
5.4	DISCUSSION.....	119

**Chapter 6: Estrogen and Progesterone receptors distribution in uteri with and without adenomyosis through the menstrual cycle ..... 124**

6.1	INTRODUCTION .....	125
6.2	MATERIALS AND METHODS.....	127
6.2.1	Patients and samples .....	127
6.2.2	Immunohistochemistry .....	128
6.2.3	Images capture and analysis .....	129
6.2.4	Statistical analysis.....	130
6.3	RESULTS .....	130
6.3.1	Estrogen receptor alpha (ER- $\alpha$ ) distribution.....	130
6.3.2	Estrogen receptor beta (ER- $\beta$ ) distribution.....	133
6.3.3	Progesterone receptors (PR-A and PR-B) distribution.....	135
6.4	DISCUSSION .....	138

**Chapter 7: Microarray analysis comparison of the inner and outer myometrium in uteri with and without adenomyosis ..... 143**

7.1	INTRODUCTION .....	144
7.2	METHODS .....	145
7.2.1	Patients and samples .....	145
7.2.2	Sample size calculation:.....	146
7.2.3	RNA preparation, array hybridization and scanning .....	146
7.2.3.1	Total RNA extraction.....	146
7.2.3.2	RNA Quantification and Quality Assessment .....	147
7.2.3.3	Microarray .....	147
7.2.3.4	cRNA Direct Hybridisation Assay .....	148
7.2.3.5	Data Analysis.....	148
7.2.4	Validation of the microarray data by Real-Time polymerase chain reaction (RT-PCR).....	149

7.3	RESULTS .....	150
7.3.1	Comparison of inner myometrium in uteri with and without adenomyosis, in the proliferative phase.....	150
7.3.2	Comparison of inner myometrium in uteri with and without adenomyosis, in the secretory phase.....	151
7.3.3	Comparison of outer myometrium in uteri with and without adenomyosis, in the proliferative phase.....	151
7.3.4	Comparison of outer myometrium in uteri with and without adenomyosis, in the secretory phase.....	152
7.3.5	Overall comparison of the myometrium in uteri with and without adenomyosis.....	152
7.3.6	Validation of microarray data by Quantitative Real-Time PCR (QT-PCR) and correlation with steroid receptors immunohistochemistry data (chapter 6) .....	155
7.4	DISCUSSION.....	158

**Chapter 8: Study of stromal – myometrial interaction in a three-dimensional co-culture model and proteomic analysis ..... 163**

8.1	INTRODUCTION .....	164
8.2	MATERIALS AND METHODS.....	165
8.2.1	Samples .....	165
8.2.2	Construction of the in-vitro cell-culture model .....	166
8.2.3	Histology and immunohistochemistry .....	169
8.2.4	Proteomic analysis .....	170
8.2.4.1	Samples and arrays preparation .....	170
8.2.4.2	Surface Enhanced Laser Desorption/Ionization – Time of Flight – Mass Spectrometry (SELDI-TOF-MS) Analyses... ..	171
8.3	RESULTS .....	172
8.3.1	Co-culture invasion assay .....	172

8.3.2 Protein expression analysis:.....	175
8.4 DISCUSSION.....	179
<b>Chapter 9: Discussion .....</b>	<b>182</b>
9.1 GENERAL DISCUSSION .....	183
9.2 SUGGESTED MODEL FOR THE PATHOGENESIS OF UTERINE ADENOMYOSIS .....	195
9.3 FUTURE RESEARCH.....	195
<b>APPENDIX 1: Additional figures and plates for Chapter 6: Estrogen and Progesterone receptors distribution in uteri with and without adenomyosis through the menstrual cycle.....</b>	<b>196</b>
<b>APPENDIX 2: Additional tables for Chapter 7: Microarray analysis comparison of the inner and outer myometrium in uteri with and without adenomyosis.....</b>	<b>230</b>
<b>APPENDIX 3: Publications arising from the thesis.....</b>	<b>257</b>
<b>APPENDIX 4: Oral Presentations arising from the thesis.....</b>	<b>258</b>
<b>APPENDIX 5: Poster Presentations arising from the thesis.....</b>	<b>260</b>
<b>APPENDIX 6: Copy of Ethics Committee approval letters.....</b>	<b>262</b>
<b>BIBLIOGRAPHY .....</b>	<b>266</b>

# LIST OF TABLES

## **Chapter 1**

Table 1.1 .....	5
Table 1.2 .....	8
Table 1.3 .....	9
Table 1.4 .....	12
Table 1.5 .....	18
Table 1.6 .....	20

## **Chapter 2**

Table 2.1 .....	50
Table 2.2 .....	55

## **Chapter 3**

Table 3.1 .....	70
Table 3.2 .....	75

## **Chapter 4**

Table 4.1 .....	94
Table 4.2 .....	95

## **Chapter 5**

Table 5.1 .....	111
Table 5.2 .....	118

## **Chapter 6**

Table 6.1 .....	132
Table 6.2 .....	134
Table 6.3 .....	136
Table 6.4 .....	137

## **Chapter 7 (see appendix 2 for Tables 1 – 12)**

Table 7.13 .....	155
Table 7.14 .....	156
Table 7.15 .....	157

## **Chapter 8**

Table 8.1 .....	172
Table 8.2 .....	178

## **Appendix 2**

Table 7.1 .....	231
-----------------	-----

Table 7.2 .....	234
Table 7.3 .....	237
Table 7.4 .....	238
Table 7.5 .....	241
Table 7.6 .....	243
Table 7.7 .....	245
Table 7.8 .....	248
Table 7.9 .....	251
Table 7.10 .....	252
Table 7.11 .....	255
Table 7.12 .....	256

# LIST OF FIGURES

## Chapter 1

Figure 1.1 .....	3
Figure 1.2 .....	4
Figure 1.3 .....	7
Figure 1.4 .....	16
Figure 1.5 .....	17
Figure 1.6 .....	19
Figure 1.7 .....	22

## Chapter 2

Figure 2.1 .....	56
Figure 2.2 .....	57
Figure 2.3 .....	58
Figure 2.4 .....	59

## Chapter 3

Figure 3.1 .....	76
Figure 3.2 .....	77
Figure 3.3 .....	78
Figure 3.4 .....	79
Figure 3.5 .....	80

## Chapter 4

Figure 4.1 .....	90
Figure 4.2 .....	96
Figure 4.3 .....	102
Figure 4.4 .....	103
Figure 4.5 .....	104
Figure 4.6 .....	105
Figure 4.7 .....	105
Figure 4.8 .....	106

## Chapter 5

Figure 5.1 .....	115
Figure 5.2 .....	117
Figure 5.3 .....	118

## Chapter 7

Figure 7.1 .....	153
Figure 7.2 .....	154
Figure 7.3 .....	157
<b>Chapter 8</b>	
Figure 8.1 .....	168
Figure 8.2 .....	173
Figure 8.3 .....	176
Figure 8.4 .....	177
<b>Appendix 1</b>	
Figure 6.1 .....	197
Figure 6.2 .....	198
Figure 6.3 .....	199
Figure 6.4 .....	200
Figure 6.5 .....	201
Figure 6.6 .....	202
Figure 6.7 .....	203
Figure 6.8 .....	204
Figure 6.9 .....	205
Figure 6.10.....	206
Figure 6.11.....	207
Figure 6.12.....	208
Figure 6.13.....	209
Figure 6.14.....	210
Figure 6.15.....	211
Figure 6.16.....	212
Figure 6.17.....	213
Figure 6.18.....	214
Figure 6.19.....	215
Figure 6.20.....	216
Figure 6.21.....	217
Figure 6.22.....	218
Figure 6.23.....	219
Figure 6.24.....	220
Figure 6.25.....	221
Figure 6.26.....	222

Figure 6.27.....	223
Figure 6.28.....	224
Figure 6.29.....	225
Figure 6.30.....	226
Figure 6.31.....	227
Figure 6.32.....	228
Figure 6.33.....	229

## LIST OF ABBREVIATIONS

AR	Androgen receptor
bFGF	Basic fibroblast growth factor
BSA	Bovine serum albumin
CTSb	Cathepsin B
DAB	3,3'-diaminobenzidine
DES	Diethylstilbestrol
DMSO	Dimethyl sulfoxide
DNA	Deoxyribonucleic acid
ECM	Extracellular matrix
EM	Electron microscopy
EMI	Endometrial myometrial interface
EMT	Epithelial-mesenchymal transition
EP	Early proliferative
ER	Estrogen receptor
ES	Early secretory
FGF-R	Fibroblast growth factor receptor
GALT	Galactose 1-phosphatase uridyl transferase
GPCRs	G-Protein coupled receptors
GSTM1	Glutathione S-transferase M1
H&E	Hematoxylin and eosin
HCG	Human chorionic gonadotropin
HRT	Hormone replacement therapy
HSG	Hysterosalpingography
IEL	Intra epithelial leucocytes

IGF	Insulin growth factor
IUCD	Intrauterine contraceptive device
IVF	In-vitro fertilization
JZ	Junctional zone
LH	Luteinizing hormone
LP	Late proliferative
LS	Late secretory
MeSH	Medical subjects headings
MET	Mesenchymal-epithelial transition
MMP	Matrix metalloproteinase
MP	Mid-proliferative
MRI	Magnetic resonance imaging
MS	Mid-secretory
NGF	Nerve growth factor
PI	Proliferation index
PND	Post natal days
PR	Progesterone receptor
RNA	Ribonucleic acid
SELDI-TOF-MS	Surface Enhanced Laser Desorption/Ionization – Time of Flight – Mass Spectrometry
SERM	Selective estrogen receptor modulator
SMA	Smooth muscle actin
SPA	Sinapinic acid
TFA	Trifluoroacetic acid
TGF $\beta$ i	Transforming growth factor beta induced
TVS	Transvaginal sonography

## **Chapter 1**

### **Introduction**

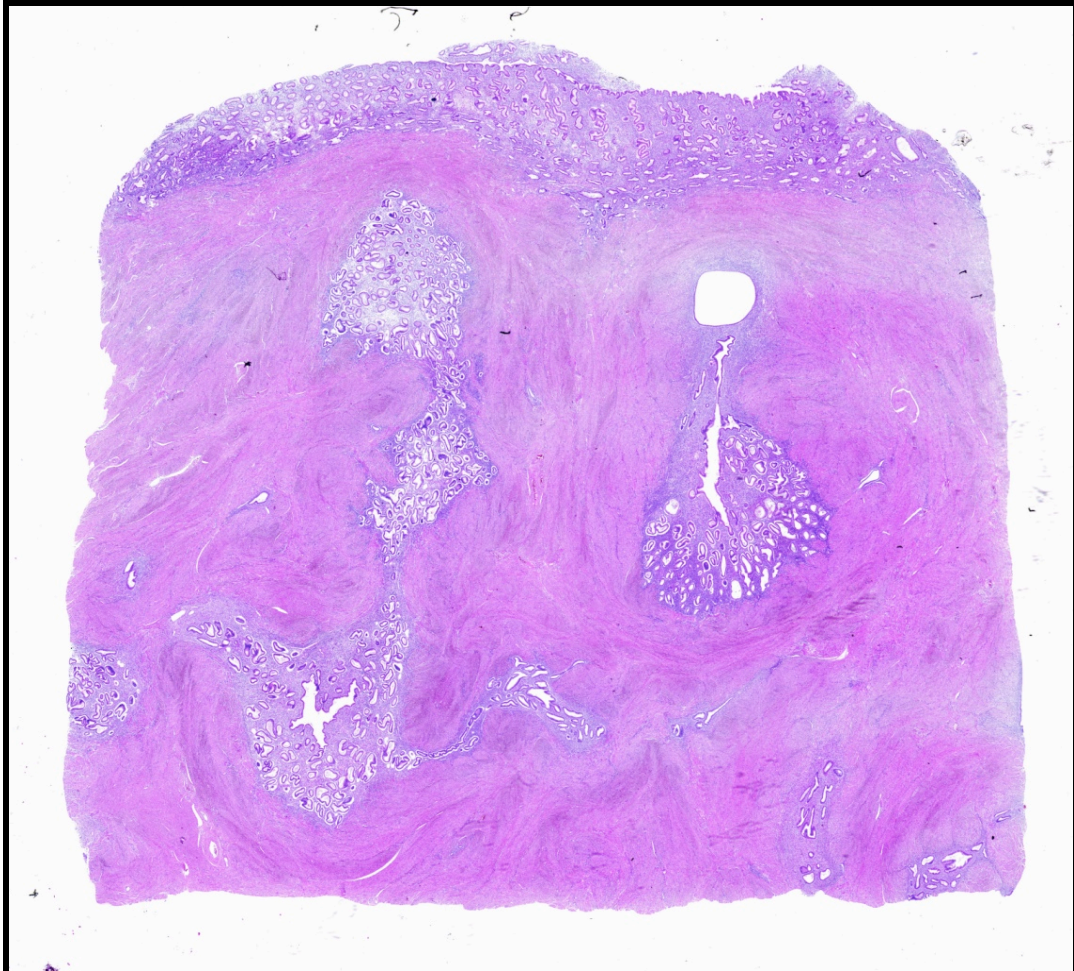
# Chapter 1

## Introduction

### 1.1 DEFINITIONS

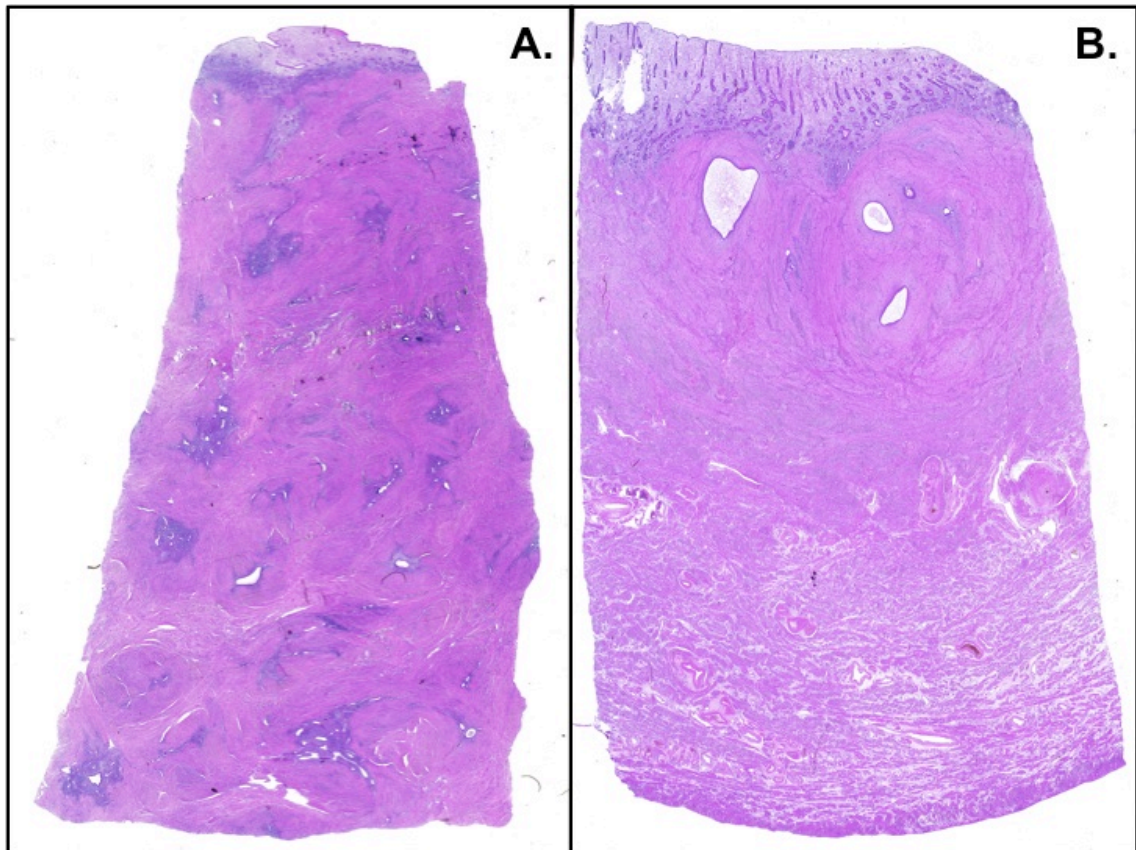
Uterine adenomyosis is defined by the presence of endometrium within the myometrium. Microscopically, ectopic, non-neoplastic, endometrial glands and stroma are surrounded by hypertrophic and hyperplastic myometrium (Figure 1.1). Early description of the condition was made by *Rokitansky* in 1860 (Rokitansky, 1860) and by *von Recklinghausen* in 1896 (von Recklinghausen, 1896). The first systematic description of what is known today as adenomyosis was the work of *Thomas Stephen Cullen* who, at the turn of the 19<sup>th</sup> century, fully researched the ‘mucosal invasion’ already observed by a number of investigators in several parts of the lower abdominal cavity. Cullen clearly identified the epithelial tissue invasion as being made of ‘uterine mucosa’ and defined the mechanism through which the mucosa invades the underlying tissue (Cullen, 1908). The term “*adenomyosis uteri*” was then introduced by *Frankl* in 1925 (Frankl, 1925). The term itself is also often used to describe deep endometriosis nodules, which can create some confusion, and it is notable that the condition does not have its separate entry under the *Medical Subjects Headings (MeSH)*. The exact aetiology of adenomyosis uteri remains unknown. There is little research specifically directed to the condition, and much of the published reviews include extrapolations from endometriosis research.

**Figure 1.1: Histological section of uterine adenomyosis showing endometrial glands and stroma deep in the myometrium and separate from the overlying endometrium (magnification x5).**



Adenomyosis can be ‘focal’ or ‘diffuse’ and the degree of invasion is variable and may involve the whole uterine wall up to the serosa or only the deep myometrial layer (Figure 1.2). There has been no consistent definition on how deep the endometrial penetration into the myometrium must be in order to diagnose adenomyosis, which makes the collation of historical studies difficult.

**Figure 1.2: Histological sections of uterine adenomyosis showing A: Diffuse deep adenomyosis, and B: localised superficial adenomyosis with distended glands, mimicking fibroids (magnification x5).**



There is no consensus on the depth of endometrial penetration needed to diagnose adenomyosis - ranging from one high power field to more than 25% of the myometrial thickness -, which makes comparisons between different studies difficult. A cut-off point of >2.5mm for glandular extension below the endometrial-myometrial interface (EMI) is advocated (Uduwela et al., 2000). A characteristic feature of the EMI is the lack of a submucosa. As a result, the endometrial glands and stroma lie in direct contact with the myometrium. The EMI is also irregular over its entire surface. The term ‘adenomyosis sub-basalis’ has been defined as minimally invasive adenomyosis extending <2 mm beneath the basal endometrium although this term/definition is not in widespread use (Bird et al., 1972) (Table 1.1).

**Table 1.1: Different definitions of adenomyosis** (Parazzini et al., 1997, Sasmour et al., 2002, Bird et al., 1972, Molitor, 1971, Raju et al., 1988, Owolabi and Strickler, 1977, Daisley, 1987, Rao and Persaud, 1982, Vavilis et al., 1997, Shaikh and Khan, 1990, Bergholt et al., 2001, Levgur et al., 2000, Nikkanen and Punnonen, 1980, Whitted et al., 2000, Curtis et al., 2002, Panganamamula et al., 2004, Blum, 1981, Kilkku et al., 1984)

<b>Reference</b>	<b>Depth from endometrial-myometrial junction</b>
Novak and Woodruff (1967) <i>Gynecologic and Obstetric Pathology</i>	> high-power field (0.5-0.75mm)
Kurman (1994) <i>Pathology of the Female Genital tract</i> ; Parazzini et al (1997)	> 0.5 of low-power field (1mm)
Gompel and Silverberg (1985) <i>Pathology in Gynecology and Obstetrics</i> ; Sasmour et al (2002)	> medium-power field (2mm)
Ackerman (1989) <i>Surgical Pathology</i> ; Bird et al. (1972); Molitor (1971); Raju et al (1988), Owolabi and Strickler (1977); Daisley (1987); Rao and Persaud (1982); Vavillis et al (1997)	> low-power field (2mm)
Hendrickson and Kempson (1990) <i>Surgical Pathology of the Uterine Corpus</i> ; Shaikh and Khan (1990)	Penetration of more than 25% of the total thickness of the uterine wall
Bergholt et al. (2001)	>3mm
Levgur et al (2000)	> 2.5mm
Nikkanen and Punnonen (1980); Whitted (2000); Curtis et al (2002); Thomas et al (1987); Panganamamalu et al (2004); Blum (1981); Kilkku et al (1984)	Unspecified depth

In diffuse adenomyosis, the uterus becomes enlarged and globular. Glandular foci may contain brown haemosiderin deposits (Azziz, 1989). ‘Focal’ lesions can resemble leiomyomata; hence the older term adenomyoma although the process is not neoplastic (Hendrickson and Kempson, 1980). Adenomyosis has poorly defined margins and

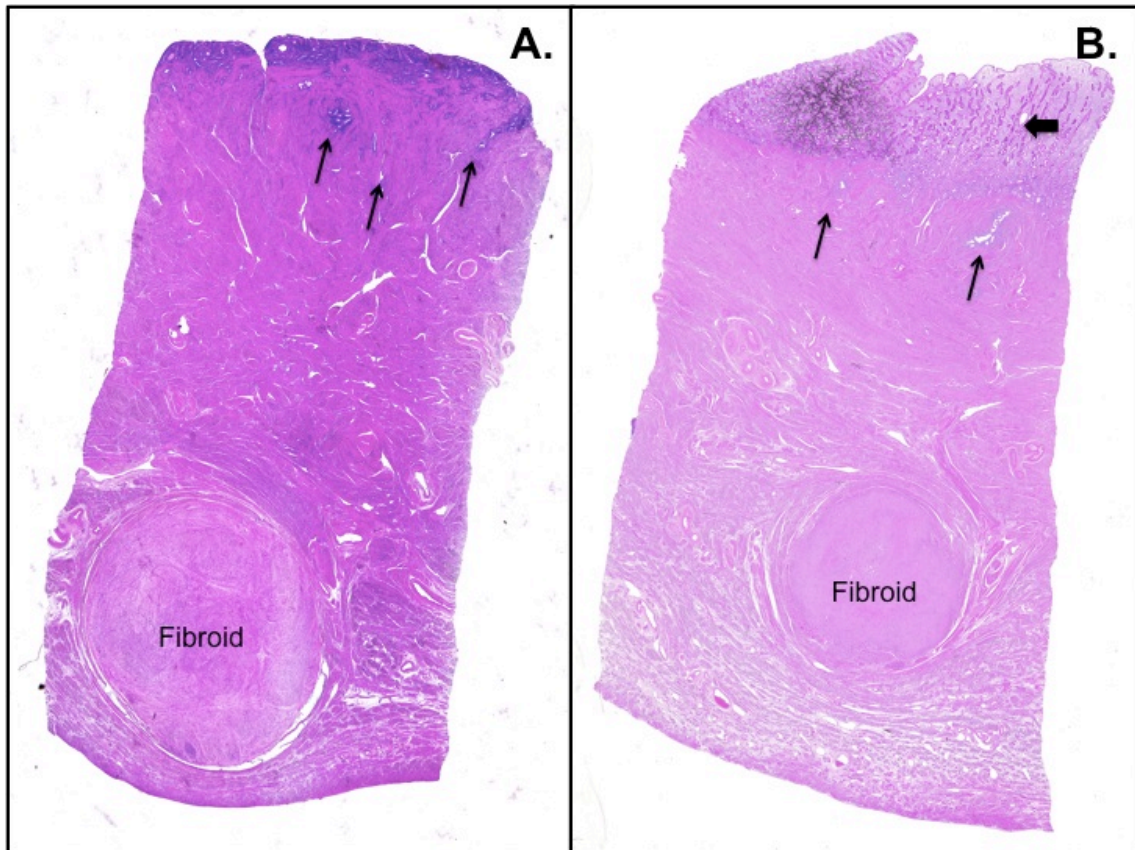
cannot be enucleated. Endometrial glands and stroma in adenomyosis resemble the basalis endometrium, and show limited changes with the menstrual cycle, but secretory changes, including stromal decidualization, may be seen during pregnancy and in women receiving exogenous progestogens, the changes being mediated by estrogen and progesterone receptors (Ferenczy, 1998).

The precise reason for myometrial hyperplasia/hypertrophy around deep focal adenomyotic lesions is not known, but may be an attempt at controlling endometrial invagination or may represent smooth muscle bundles pushed aside by the ingrowing endometrium. Myometrial hypertrophy is often absent in postmenopausal women. Morphologically, the endometrial glands and stroma in adenomyotic foci resemble the basalis endometrium and seldom respond to hormonal stimuli.

## **1.2 ASSOCIATED PATHOLOGY**

Up to 80% of uteri containing adenomyosis also contain other lesions, the most frequent being leiomyomata (Figure 1.3). Endometrial polyps, hyperplasia, with and without atypia, and adenocarcinoma are more frequent in uteri also containing adenomyosis (Table 1.2) (Bergholt et al., 2001). Pelvic endometriosis is observed in 6-24% of women with adenomyosis. Women with endometrial carcinoma were reported to have a higher (60%) incidence of adenomyosis compared to woman without cancer (39%), but adenomyosis has no adverse effect on cancer survival (Hall et al., 1984).

**Figure 1.3: Histological sections of uterine adenomyosis in association with A: Subserosal fibroid, and B: Subserosal fibroid and endometrial hyperplasia and thickening (thick arrow). Adenomyosis foci are highlighted with the thin arrows (magnification x5).**



Adenocarcinoma may rarely involve foci of adenomyosis. Whether adenocarcinoma located in both the overlying endometrium and foci of adenomyosis represent separate entities or the extension of the former into adenomyotic foci is not known. When carcinoma is limited to adenomyotic foci, it should be considered intramucosal since it does not make the prognosis worse than the carcinoma for which the patient has had surgery (Hall et al., 1984).

**Table 1.2: Incidence of concomitant pathology in hysterectomy specimens containing adenomyosis (Bergholt et al., 2001)**

<b>Disease</b>	<b>%</b>
Leiomyomas	20.5 – 70
Pelvic endometriosis	6.3 – 24
Salpingitis isthmica nodosa	1.4-19.8
Endometrial polyps	2.3 – 14.7
Endometrial hyperplasia	7.3 – 13.6
Endometrial hyperplasia with atypia	3.5
Adenocarcinoma	2.2 – 5.3

### **1.3 PREVALENCE**

Histological examination of hysterectomy specimens remains the mainstay for diagnosis, but this introduces selection bias when estimating the prevalence of the disease. The percentage of hysterectomy specimens containing adenomyosis varies from 5% up to 70% (Azziz, 1989). This wide variation may be partly explained by the histological criteria used and/or by the number of tissue blocks examined. The exact prevalence of adenomyosis in the population is unknown. The specificity of preoperative diagnosis based on clinical picture is poor, ranging from 2.6 – 26% (Reinhold et al., 1998). The sensitivity and specificity of MRI and ultrasound are highlighted in table 1.3.

**Table 1.3: Accuracy of TVS and MRI in the diagnosis of adenomyosis** (Fedele et al., 1992a, Ascher et al., 1994, Brosens et al., 1995b, Reinhold et al., 1995, Kocak et al., 1998, Bromley et al., 2000, Bazot et al., 2001, Dueholm et al., 2002, Mark et al., 1987, Reinhold et al., 1996)

<b>Accuracy of TVS in diagnosis of adenomyosis</b>		
<b>Investigators</b>	<b>Sensitivity (%)</b>	<b>Specificity (%)</b>
Fedele et al., 1992	87	99
Ascher et al., 1994	53	75
Brosens et al., 1995	86	50
Reinhold et al., 1995	86	86
Kocak et al., 1998	89	88
Bromley et al., 2000	84	84
Bazot et al., 2001	65	98
Dueholm et al., 2002	68	65
<b>Accuracy of MRI in the diagnosis of adenomyosis</b>		
<b>Investigators</b>	<b>Sensitivity (%)</b>	<b>Specificity (%)</b>
Mark et al., 1987	61	100
Ascher et al., 1989	88	66
Reinhold et al., 1996	89	89
Bazot et al., 2001	78	93
Dueholm et al., 2002	70	86

The incidence of adenomyosis in asymptomatic women is less known. Using MRI criteria, *Hauth et al.* identified adenomyosis in 12 out of 100 healthy women (Hauth et al., 2007). In another study, the diagnosis of adenomyosis was suggested by MRI in 19 of 204 (9.1%) women following term deliveries and in 16 of 104 (15.4%) women following preterm delivery; the overall incidence was 11.3% (Juang et al., 2007). *Lewinski* (1931) reported an incidence of 54% in 54 autopsies (Lewinski, 1931). In one series, 7 cases were reported in which mothers and daughters were affected (Emge, 1962).

## 1.4 CLINICAL CORRELATES OF ADENOMYOSIS

Despite lack of agreement on the histological criteria, adenomyosis is frequently reported following hysterectomy. However, as the incidence of the disease in the general population remains unclear, and because of its common association with other pathologies such as fibroids, the clinical significance of adenomyosis remains uncertain.

Numerous surgical series and epidemiologic studies described the clinical correlates and associations of uterine adenomyosis (Parazzini et al., 1997, Sammour et al., 2002, Bird et al., 1972, Molitor, 1971, Raju et al., 1988, Owolabi and Strickler, 1977, Daisley, 1987, Rao and Persaud, 1982, Vavilis et al., 1997, Shaikh and Khan, 1990, Bergholt et al., 2001, Levгур et al., 2000, Nikkanen and Punnonen, 1980, Whitted et al., 2000, Curtis et al., 2002, Panganamamula et al., 2004, Blum, 1981, Kilkku et al., 1984).

However, few studies have been correctly designed and powered to detect moderate increases in relative risks.

The majority of cases are reported in women aged 40 to 50 years (Bird et al., 1972), and there is a positive association with parity (Lee et al., 1984, Parazzini et al., 1997, Vercellini et al., 1995, Vavilis et al., 1997). Adenomyosis occurs relatively frequently in pregnancy. It is reported in 27 of 151 (17%) of caesarean hysterectomy specimens (Azziz, 1989), and was diagnosed using MRI in 11.3% postpartum women (Juang et al., 2007). There is no relation to the age at first childbirth, and prior caesarean section does not seem to be a predisposing factor (Parazzini et al., 1997, Nikkanen and Punnonen, 1980). Four large studies (Bergholt et al., 2001, Panganamamula et al., 2004, Curtis et al., 2002, Levгур et al., 2000) failed to demonstrate an increased incidence with caesarean delivery. The average incidence of caesarean section delivery in adenomyosis patients was 6-6.4% (Levgur et al., 2000, Harris et al., 1985). Older women tend to be

more symptomatic, whilst symptoms in younger women are relatively mild or absent (Benson and Sneed, 1958). The relative importance of parity and age remains unanswered, as parous women also tend to be older. No association is seen with age at menarche, menopausal status, age at hysterectomy or its indication (Parazzini et al., 1997, Vercellini et al., 1995, Vavilis et al., 1997). Spontaneous miscarriage has been observed more frequently in women with adenomyosis. Whether miscarriage is the cause or the result of adenomyosis remains to be explained (Parazzini et al., 1997, Vercellini et al., 1995, Vavilis et al., 1997, Levgur et al., 2000).

Sharp curettage during abortion or following early pregnancy loss increases the risk, possibly by disrupting the EMI and facilitating embedding of the endometrium within the myometrium (Levgur et al., 2000, Curtis et al., 2002). This practice has largely been superseded by suction curettage. Interestingly, sharp curettage in the non-pregnant status does not increase the risk (Panganamamula et al., 2004, Bergholt et al., 2001, Curtis et al., 2002, Levgur et al., 2000). This differential effect might be related to the disruption of the EMI by the invading trophoblasts. Focal disruption of the EMI in early pregnancy can be observed using MRI, which reverts to normal 2-24 weeks after delivery (Barton et al., 1993).

Women who smoke tend to be at reduced risk of adenomyosis (Parazzini et al., 1997). The use of oral contraception (Parazzini et al., 1997), IUCD or tubal sterilization (Thomas and Clark, 1989) does not appear to be associated with increased risk of adenomyosis. Adenomyosis has been reported in 60% of postmenopausal women on long term tamoxifen therapy, and it is possible that tamoxifen reactivates pre-existing adenomyosis (Cohen et al., 1997). *Kunz et al.* (2005) found a high incidence of

adenomyosis in their cohort of infertile patients with endometriosis (28%) (Kunz et al., 2005). A summary of clinical correlates is presented in table 1.4.

**Table 1.4: Summary of risk factors and symptoms of adenomyosis** (Vercellini et al., 1995, Paganamamula et al., 2004, Curtis et al., 2002, Levgur et al., 2000, Harris et al., 1985, Parazzini et al., 1997, Devlieger et al., 2003, Chrysostomou et al., 1991, Vavilis et al., 1997, Nikkanen and Punnonen, 1980, Kunz et al., 2005)

Increased risk	Decreased risk	No risk
Parity	Smoking	Age at menarche
Spontaneous miscarriage		Menopausal status
Endometriosis		Age at first childbirth
Menorrhagia		Oral contraceptives, IUCD, Tubal sterilization
Infertility		Indication of and Age at surgery
Abortion and curettage in pregnancy		Endometrial carcinoma
Endometrial Hyperplasia		Caesarean section
Preterm birth		Dilatation and curettage

### 1.4.1 Menstrual disorders

About 35% of women with adenomyosis are asymptomatic. Symptomatic women mostly present with menorrhagia (40-50%), dysmenorrhoea (10-30%) and metrorrhagia (10-12%), and occasionally, dyspareunia or dyschezia (Vavilis et al., 1997, Parazzini et al., 1997). Typically, the symptoms start one week prior to the menstrual flow (Azziz, 1989). The precise cause of abnormal bleeding is not known (McCausland, 1992).

Menorrhagia was associated even with superficial adenomyosis (~1mm of endometrial penetration) (McCausland, 1992). Menorrhagia could be due to dysfunctional

contractility of the myometrium (Brosens et al., 1995b). Mefenamic acid administration can reduce blood loss suggesting that prostaglandins may be involved (Azziz, 1989). Other factors that might be involved are anovulation or endometrial hyperplasia. The extent and spread of adenomyosis may correlate with pelvic pain and dysmenorrhea and to a lesser degree, with menorrhagia and dyspareunia (Sammour et al., 2002). These symptoms do not correlate with the depth of foci (Sammour et al., 2002).

#### **1.4.2 Endometriosis**

Pelvic endometriosis coexists with adenomyosis in 2 - 24% of cases, suggesting that the two conditions may be linked (Parazzini et al., 1997, Vavilis et al., 1997, Bird et al., 1972, Molitor, 1971, Owolabi and Strickler, 1977, Daisley, 1987, Rao and Persaud, 1982, Shaikh and Khan, 1990, Nikkanen and Punnonen, 1980, Curtis et al., 2002). *Kunz et al.*, hypothesize that pelvic endometriosis and uterine adenomyosis are variants of the same disease, involving dislocation of the basal endometrium both in the underlying myometrium and peritoneal cavity (Kunz et al., 2000). They postulate that chronic uterine dysfunctional peristalsis and hyperperistalsis are important causal factors. Women with endometriosis displayed a marked uterine hyperperistalsis that differed significantly from the peristalsis of the controls during the early and mid-follicular and mid-luteal phases. During the late follicular phase of the cycle, uterine peristalsis in women with endometriosis became dysperistaltic, arrhythmic and convulsive in character, while in controls peristalsis continued to show long and regular cervico-fundal contractions. Using MRI in a cohort of infertile women, 126 out of 160 (79%) women with and 19 out of 67 (28%) women without endometriosis had adenomyosis (Kunz et al., 2005).

### 1.4.3 Infertility

Because of its association with multiparity, scant attention has been paid in the past to a possible relation between adenomyosis and infertility. Research has also linked adenomyosis to life-long infertility in baboons (Barrier et al., 2004). Advances in imaging and delayed pregnancies may have contributed to the condition being encountered more frequently in fertility clinics (Devlieger et al., 2003). Reported studies included a cohort of infertile women with poorly defined demographics and a high incidence of endometriosis. The authors suggested that adenomyosis impaired uterine sperm transport (Kunz et al., 2005), an effect that could not be confirmed in the absence of endometriosis.

It has been proposed that the abnormal structure of the EMI and myometrium in adenomyosis, especially at the fundus, could interfere with normal fertilization and implantation, possibly by interfering with normal directional uterine peristalsis (Leyendecker et al., 1996). According to *Kunz et al.*, invasion of basal endometrial glands and stroma leads to disruption of the normal architecture of the underlying myometrium. This would result in dysfunctional myometrial hyperperistalsis, increased intrauterine pressure, and impairment of the uterine mechanism of rapid and sustained directed sperm transport during the late follicular phase (Kunz et al., 2000). In fact, directed sperm transport into the tube ipsilateral to the dominant follicle provided by uterine peristalsis is claimed to be one of the fundamental uterine functions in the early reproductive process (Wildt et al., 1998).

Another putative mechanism is the over-expression of nitric oxide. Nitric oxide affects human sperm function, fertilization, implantation and embryo development. Over-expression of endothelial nitric oxide synthase in adenomyosis, may be triggered by

immune response acting on macrophages or endometrial cells (Ota et al., 1998).

However, evidence from recipients of sibling oocytes in IVF suggests that adenomyosis as diagnosed by ultrasound has no impact on implantation rate (Camargo et al., 2001).

The latter observation does not contradict the view that adenomyosis can affect normal fertility, as IVF bypasses the uterine directed sperm transport and sperm function.

## **1.5 IMAGING AND DIAGNOSIS OF ADENOMYOSIS**

Management of adenomyosis is hindered by the lack of a reliable non-invasive diagnostic test. No serum markers are currently available. The role of invasive hysteroscopic or laparoscopic biopsy remains limited, with small series reported. The small size of the obtained biopsies may be insufficient to rule out the disease, especially that the diagnosis has been shown to be influenced by the number of uterine sections examined.

### **1.5.1 Hysterosalpingography**

Hysterosalpingography (HSG) is an early imaging modality used for the diagnosis of adenomyosis, but has a low sensitivity and specificity. Features suggestive of adenomyosis on HSG done as part of infertility workup are multiple small ( $1\pm 4$  mm) spicules extending from the endometrium into the myometrium with saccular endings (Figure 1.4). A local accumulation of contrast material in the myometrium may provide a honeycomb appearance (Wolf and Spataro, 1988).

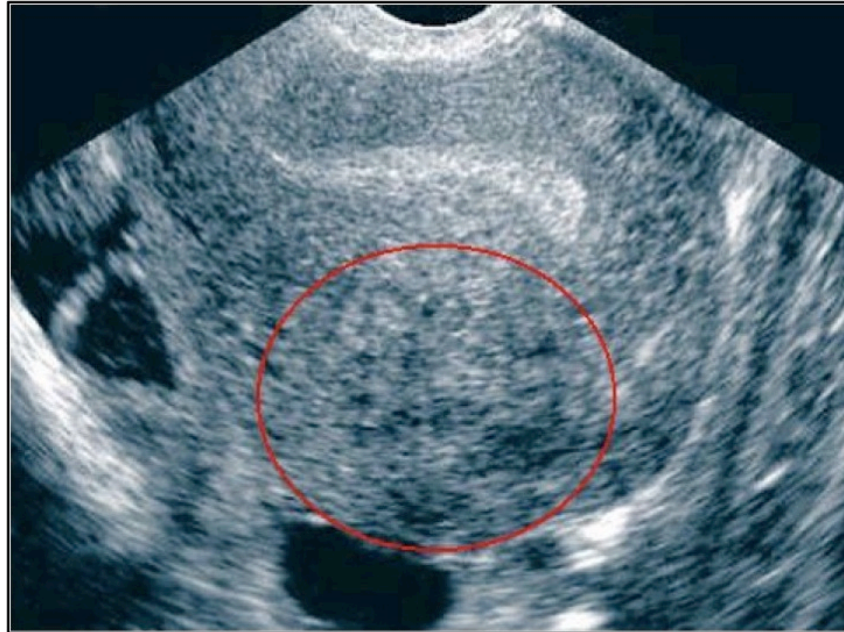
**Figure 1.4: Hysterosalpingogram showing dye spicules extending into the myometrium, suggestive of adenomyosis (Wolf and Spataro, 1988).**



### **1.5.2 Pelvic Ultrasonography**

Transvaginal ultrasound is superior to transabdominal ultrasound in demonstrating the subtle features suggestive of adenomyosis. The normal myometrium has three distinct sonographic layers. The middle layer is the most echogenic and is separated from the thin outer layer by the arcuate venous and arterial plexus. The inner layer is hypo-echoic relative to the middle and outer layers (subendometrial or myometrial halo). The presence of adenomyosis can alter or distort the sonographic appearance of these zones (Brosens et al., 1995b, Ascher et al., 1994, Fedele et al., 1992b, Hirai et al., 1995, Atri et al., 2000, Fedele et al., 1997, Reinhold et al., 1995) (Figure 1.5 and Table 1.5).

**Figure 1.5: Transvaginal ultrasound scan showing an area of altered and distorted sonographic appearance of the myometrium suggestive of adenomyosis in the posterior wall of the uterus** (Brosens et al., 1995b, Ascher et al., 1994, Fedele et al., 1992b, Hirai et al., 1995, Atri et al., 2000, Fedele et al., 1997, Reinhold et al., 1995)



Studies published on the accuracy of transvaginal sonography (TVS) reported variable accuracy indices with sensitivity and specificity of TVS varying between 53-87% and 50-99% respectively (see Table 1.3). The reported studies were conducted on selected women prior to surgery and caution is needed when TVS is used for other groups with low prevalence of adenomyosis. Three-dimensional ultrasonography offers advantages in determining organ volume and uterine pathology, including endometrial tumours. There are some reports on the use of 3D-TVS and 3D power Doppler in adenomyosis including vessel distribution and branching and differences in perfusion patterns in affected areas (Lee et al., 1999, Ahmed et al., 2007).

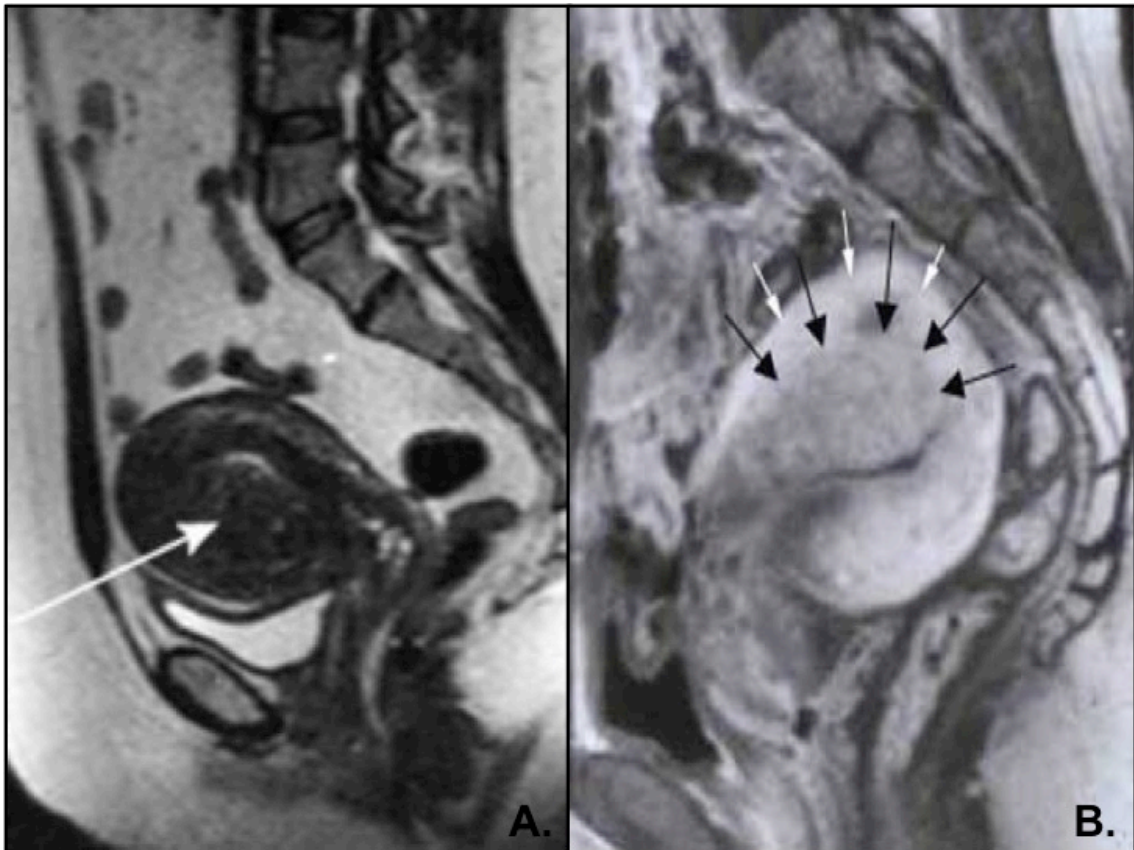
**Table 1.5: TVS criteria used to diagnose adenomyosis (Adenomyosis is most often diagnosed in the presence of three or more sonographic criteria)** (Brosens et al., 1995b, Ascher et al., 1994, Fedele et al., 1992b, Hirai et al., 1995, Atri et al., 2000, Fedele et al., 1997, Reinhold et al., 1995)

<b>TVS criteria for adenomyosis (used separately or in combination)</b>
Uterine enlargement in the absence of leiomyomas
Asymmetric enlargement of the anterior or posterior myometrial wall
Lack of contour abnormality or mass effects
Heterogeneous, poorly circumscribed areas within the myometrium
Hyperechoic islands or nodules, finger-like projections or linear striations, indistinct endometrial stripe
Anechoic lacunae or cysts of varying size

### **1.5.3 Magnetic resonance imaging (MRI)**

In women of reproductive age, three different zones can be identified within the uterus using MRI. The normal endometrium and endometrial secretions appear as a high signal-intensity type stripe on T2-weighted sagittal image. Immediately subjacent to this is a band of low signal intensity that represents the innermost layer of the myometrium: the Junctional Zone (JZ) (Brown et al., 1991). The outer layer of the myometrium is of intermediate signal intensity. There is considerable variation in the normal JZ thickness ranging from 2 to 8 mm (Lee et al., 1985, Hauth et al., 2007). The appearance of diffuse or focal widening of the JZ on MRI is suggestive of adenomyosis. Areas of low signal intensity corresponding to smooth muscle hyperplasia can also be seen, together with high signal intensity foci or linear striations representing the ectopic endometrial tissue (Figure 1.6 and Table 1.6).

**Figure 1.6: Sagittal section MRI showing A: Areas of high signal intensity foci and linear striations dye spicules extending into the myometrium on a T2-weighted images (white arrow) suggestive of adenomyosis, B: Similar findings on a T1-weighted image where areas of adenomyosis are outlined by black arrows.**



There is growing evidence for the role of MRI in the diagnosis of adenomyosis.

However, the high cost and limited availability hinder its routine use in the clinical setting. Several studies have compared the accuracy of TVS and MRI in the diagnosis of adenomyosis (table 1.3). Although the sensitivities and specificities of both techniques were comparable, MRI proved to be superior to TVS in women where associated leiomyomas or additional pathology was suspected (Bazot et al., 2001).

**Table 1.6: MRI features used to diagnose adenomyosis** (Brosens et al., 1995b, Ascher et al., 1994, Fedele et al., 1992b, Hirai et al., 1995, Atri et al., 2000, Fedele et al., 1997, Reinhold et al., 1995, Brown et al., 1991)

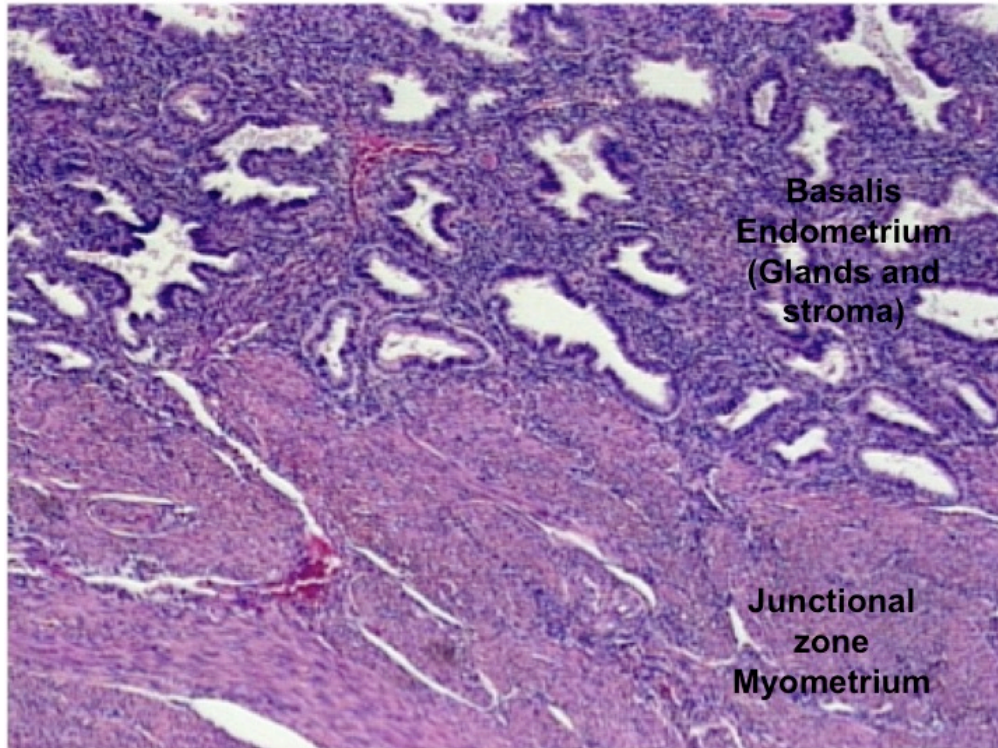
<b>MRI criteria suggestive of adenomyosis</b>
Focal or diffuse thickening of the junctional zone
Low signal intensity uterine mass with ill-defined border
Junctional zone thickness >5mm or >12mm
Poor definition of junctional zone border
Localized high signal foci within an area of low signal intensity
Linear striations of increased signal radiating out from the endometrium into the myometrium
Bright foci in endometrium isointense with myometrium (T1 weighted)
Ratio of Junctional zone/myometrium (ratio <sub>max</sub> ) > 40%

## 1.6 THE ENDOMETRIAL-MYOMETRIAL INTERFACE (EMI)

Both EMI components (basalis endometrium and subendometrial myometrium) are believed to have a common embryological origin from the paramesonephric ducts, whereas the outer myometrium is thought to be of non-paramesonephric mesenchymal origin (Noe et al., 1999, Uduwela et al., 2000). Examining autopsy material obtained from human abortuses and stillborn fetuses at different gestational ages (12-40 weeks), *Konishi et al.* observed that the outer part of the mesenchyme of the uterus gives rise to the myometrium and that the inner part corresponds to the endometrial stroma (Konishi et al., 1984). The Mullerian origin of the outer myometrium is also supported by *Robboy et al.*, who described the normal development of the human female reproductive tract and the alterations resulting from experimental exposure to diethylstilbestrol (Robboy et al., 1982).

This endometrial-subendometrial unit has also been described in the literature as the “*archimetra*” (the endometrium of older phylogenetic origin) (Leyendecker et al., 1998), with reference to *Werth and Grusdew* (1898), who used the term *archimyometrium* to describe the ontogenetically old character of the subendometrial myometrium (Werth and Grusdew, 1898). A distinctive feature of the EMI is the lack of an intervening connective tissue layer, or a protective submucosa (Figure 1.7). As a result, the endometrial glands and stroma lie in direct contact with the myometrium, allowing extensive free interaction (Emge, 1962, Marcus, 1961, Uduwela et al., 2000). The EMI is also irregular over its entire surface (Emge, 1962).

**Figure 1.7: Histological section showing the Endometrial-Myometrial Interface (EMI) and its components: the basalis endometrial glands and stroma, and the junctional zone myometrium, with no intervening submucosa or connective tissue layer. The EMI is irregular.**



Little is known regarding the molecular basis for the coordinated development of the endometrium and myometrium (Uduwela et al., 2000). Some studies identified that epithelial-mesenchymal interactions are crucial in the correct development of the mammalian female reproductive tract. Three members of the Wnt family of growth factors (Wnt4, Wnt5a, Wnt7a) were identified to play an important role in this context, in mice (Mericksay et al., 2004). Further interaction with  $\beta$ -Catenin and Cadherin pathways could play a role in the specification and proper arrangements of new cell types during tissue differentiation (Nelson and Nusse, 2004). Such factors have not been studied in humans.

The endometrium undergoes cyclic synchronized waves of proliferation and differentiation in response to the rise and fall of ovarian estrogen and progesterone. During the follicular phase of the cycle, the glandular, stromal, and vascular endothelial cells show a prominent proliferative response in the superficial, but not the basal, endometrial layer (Russell and Fraser, 1998) (Tabibzadeh et al., 1993). After ovulation, the functionalis layer undergoes extensive tissue remodeling in response to ovarian progesterone levels, a process that initially involves secretory transformation of the glandular epithelium, followed by edema and decidualization of the stromal compartment. These classical sex steroid hormone responses are absent in the basal endometrial layer, which is characterized by low proliferative activity, absence of glandular secretory transformation, and lack of a pre-decidualization reaction in the late luteal phase of the cycle. Cytokines and growth factors released by endometrial immune cells, including T cells, uterine natural killer (NK) cells, polymorphonuclear neutrophils, macrophages, and monocytes cells, are thought to play a pivotal role in establishing such microenvironments in the human endometrium (Tabibzadeh et al., 1993, Stewart et al., 1992, Tabibzadeh, 1991, King, 2000). Ovarian hormones also tightly control the spatial and temporal distribution of these cells. For instance, during the reproductive years lymphoid aggregates, consisting mainly of T cells and a few B cells, are characteristically found in the endometrial-myometrial junction (Stewart et al., 1992, Yeaman et al., 1998). These aggregates are small during the early proliferative phase and significantly increase in size during the second half of the cycle (Yeaman et al., 1998, Yeaman et al., 1997). It has been suggested that IFN-gamma in the human endometrium is secreted by lymphoid aggregates in the basal endometrial layer. Production of IFN-gamma is thought to contribute to the low apoptotic and proliferative activities in this layer and could account for the higher local expression of IFN-gamma-

dependent genes, such as class II major histocompatibility complex antigens and heat shock protein-70 (Tabibzadeh et al., 1993, Stewart et al., 1992) (Tabibzadeh, 1991, Arends, 1999, Koshiyama et al., 1995, Stephanou et al., 1999).

### **1.6.1 Normal myometrial zonal differentiation**

Although the myometrium seems at first sight to be homogenous under light microscopy, MRI has defined a structurally different “junctional zone” that forms the outer boundary of the EMI (Brosens et al., 1998).

Previous studies have suggested architectural and cellular differences between myocytes in the subendometrial and outer myometrium. Using image analysis of Fielgen nuclear-stained myometrial sections, *Scoutt et al.* demonstrated that the normal subendometrial myometrium is characterized by a threefold increase in nuclear area and decreased extracellular matrix per unit volume. They suggested that the increased nuclear area reflected both a higher smooth muscle density and an increased nucleocytoplasmic ratio of the myocytes. Extracellular space between individual fibers and fiber bundles was minimal in the junctional zone, but no difference was found in either the concentration or the composition of the most common components of the extracellular space (collagen, laminin, and fibronectin) compared to the outer myometrium. It was equally suggested that the junctional zone myometrium has lower water content than that of the endometrium or outer myometrium (Scoutt et al., 1991, Brosens et al., 1998, McCarthy et al., 1989a).

Using immunocytochemistry of the whole uterine wall, *Noe et al.* showed that the subendometrial myometrium exhibited a cyclic pattern of estrogen and progesterone receptors expression that paralleled that of the functionalis endometrium, whereas the

outer portion of uterine wall, which represented the bulk of the uterine musculature, did not exhibit such a pattern (Noe et al., 1999). This observation could back the view that the subendometrial myometrium is functionally distinct from the rest of the myometrium.

Using ultrasound scan and radioisotope scintigraphy, the subendometrial myometrium was suggested to have distinct contractile properties that varied with the phases of the normal menstrual cycle and recurred in a similar fashion each cycle. The contractions were antegrade (from fundus to cervix) during menstruation, and retrograde (from cervix to fundus) in the rest of the cycle. These contractions were suggested to play a role in sperm transport and proper implantation of the blastocyst (De Vries et al., 1990, Lyons et al., 1991). This contractile pattern could also help to control menstrual blood flow, thus its disturbance might explain some cases of menorrhagia (Brosens et al., 1995a).

## **1.7 PATHOGENESIS OF UTERINE ADENOMYOSIS**

### **1.7.1 Endometrial-myometrial interface invasion and physical disruption**

Conventionally, it is believed that adenomyosis results from the abnormal in-growth and invagination of the basal endometrium into the sub-endometrial myometrium at the endometrial-myometrial interface. This is supported by the observation of histological continuity between the basal endometrium and underlying adenomyosis in some tissue sections (Leyendecker et al., 2002).

During periods of regeneration, healing and re-epithelialization, the endometrium could invade a predisposed myometrium or a traumatized EMI (Ferenczy, 1998). Mechanical damage to and/or physical disruption of the EMI by dysfunctional uterine hyperperistalsis and/or dysfunctional contractility of the sub-endometrial myometrium (Kunz et al., 2000, Leyendecker et al., 2002) or by sharp curettage during pregnancy (Curtis et al., 2002) may allow for the dislocation of basal endometrium into the myometrial wall and the development of adenomyosis. The latter is supported by the association of adenomyosis with a history of intra-uterine procedures such as pregnancy termination (Levgur et al., 2000), as well as by animal experiments where transplantation of the anterior pituitary in the uterine lumen of adult SHN and SLN mice strains induced adenomyosis (Mori and Nagasawa, 1983). The EMI is also disturbed by the intra-myometrial penetration of trophoblast during early pregnancy and this may underlie the higher incidence in parous patients.

However, the early stages and sequence of events of the development of adenomyosis is unclear. It is not known which component of the EMI (i.e. basal endometrium or subendometrial myometrium) plays the key role in the development of adenomyosis.

Whether the endometrium in adenomyosis has a higher invasive potential and penetrates a normal subendometrial myometrium, or alternatively, the subendometrial myometrium in cases of adenomyosis is more permissive to invasion by a normal basal endometrium is not known. The interaction between the endometrial stroma and the underlying myometrium will be examined in this thesis.

### **1.7.2 Disordered proliferation/regeneration**

Spontaneously occurring adenomyosis has been reported in several animal species including non-human primates, dogs, cats, and laboratory rodents and rabbits (McCann and Myers, 1970, Suire et al., 1978). In CD-1 mice, spontaneous adenomyosis starts to appear in from about 6 months of age onwards, and over 80% are affected by 12 months of age, disease severity increases thereafter (Greaves and White, 2006).

The understanding of the early developmental stages of uterine lesions such as adenomyosis remains limited largely because these lesions are diagnosed after maturity. Animal models such as rodents allow us to examine the ontogeny of uterine mesenchymal differentiation under different circumstances. A study used short treatment of neonatal mice with Tamoxifen and found that these animals developed adenomyosis by 3 months of age. There was a notable disordered arrangement of the smooth muscle of the myometrium (Parrott et al., 2001). Smooth muscle changes were more extensive than the zones of abnormal glands, suggesting that the penetration of endometrial glands might follow the changes to myometrium rather than precede them. It has been proposed that paracrine signalling affects differentiation of uterine myocytes in the mesenchyme and, over a period of time, this may permit downgrowth of the endometrium.

The Tamoxifen treated neonatal CD-1 mice model with tamoxifen induces changes in the uterus similar to human adenomyosis and makes it possible to examine the histogenesis of uterine adenomyosis because of the short latency between the time of treatment and the development of the disease. Disruption of the mesenchymal layers surrounding the endometrium in the neonatal period can trigger disordered development of uterine stroma, smooth muscle, blood vessels and possibly innervation. This might form the basis of abnormal and aberrant endometrial tissue growth leading to adenomyosis.

This thesis will study the sequence of early uterine development changes and aberrations that lead to the final development of uterine adenomyosis observed by earlier studies, hypothesising that adenomyosis might be caused primarily by defects in the formation of the myometrium, allowing the penetration of the overlying endometrium. This work will examine the effect of Tamoxifen on the differentiation of the different muscle layers and the development of adenomyosis, as manifested by histological changes and patterns of expression of cytoskeletal proteins (actin, desmin, vimentin) and matrix differentiation (fibronectin, laminin). To examine the possible strain (genetic) predisposition in response to these hormonally active agents, the study will examine the effects of Tamoxifen on the C57/BL6J mouse strain that is not known to develop spontaneous adenomyosis.

### **1.7.3 Role of endometrial stromal and stem cells in adenomyosis**

The development and differentiation of myometrial smooth muscle is affected and directed by the uterine epithelial and stromal cells. Using uteri from BALB-c mice 1 to 60 days postpartum, uterine mesenchyme produced larger amounts of smooth muscle

when co-cultured with epithelium. This suggests that the endometrium plays a promotional role in the differentiation and spatial organisation of the myometrium (Cunha et al., 1989b) (Kurita et al., 2001).

*Mai et al.* (1997) used immunohistochemistry to study 10 cases of adenomyosis. They characterized isolated nodules of endometrial stromal cells without endometrial glands, along blood or lymphatic vessels – what they called type 1 nodules. The authors described these endometrial stromal nodules to arise from multipotent pericytes. They also suggested that due to the proliferative nature of the endometrial glands, the newly enlarged area of stroma serves as “new soil”, facilitating further downward growth of the endometrial glands. Hormonal, genetic, immunological and growth factors possibly play a role in this sequence of events (Mai et al., 1997).

There is evidence that metaplasia occurs in the endometrium. Decidual stromal cells express  $\alpha$ -smooth muscle actin and show ultrastructural similarities with myofibroblasts (Oliver et al., 1999). Cells having some features of smooth muscles were found among the usual endometrial stromal cells. In the follicular phase of the menstrual cycle, such cells resembled myofibroblasts, but in the luteal phase and during early pregnancy, they had more distinct cytoplasmic filaments with dense bodies and dense plaques and other well-developed characteristics of smooth muscle. This suggests that smooth muscle differentiation possibly occurs from multi-potential mesenchymal cells in the endometrial stroma (Fujii et al., 1989).

To determine whether myometrial smooth muscle is newly produced at the EMI of the adult uterus, *Fujii et al.* examined the ultrastructure of the mesenchymal components of the EMI during the menstrual cycle and early pregnancy (Fujii et al., 1989). Their finding of cells morphologically resembling myofibroblasts in the follicular phase and

differentiating into cells morphologically resembling smooth muscle cells in the luteal phase and early pregnancy, suggests that smooth muscle differentiation possibly occurs from mesenchymal cells in the endometrial stroma. It is unknown if the same phenomenon occurs around the endometrium of adenomyotic foci, contributing to the myometrial hypertrophy and hyperplasia surrounding the ectopic endometrium.

In neonatal rodent models, the use of Tamoxifen produces abnormal and aberrant endometrial tissue growth leading to adenomyosis. This is the result of the disruption of the mesenchymal layers surrounding the endometrium in the neonatal period, triggering a disordered development of the uterine stroma, smooth muscle, blood vessels and possibly innervation (Parrott et al., 2001).

Endometrial stromal fibroblasts produce tenascin, a fibronectin inhibitor that in turn facilitates epithelial migration. Tenascin mediates epithelial-mesenchymal interactions by inhibiting cell attachment to fibronectin, an action stimulated by hormonally regulated epidermal growth factors. Whether this interaction plays a role in the development of uterine adenomyosis or endometriosis is unclear (Chiquet-Ehrismann et al., 1989) (Ferenczy, 1998).

Previous studies have described some characteristics of this area in normal uteri, as described earlier, but little is known about the 'phenotype' of the EMI in uteri with adenomyosis. One of the objectives of this thesis will be to characterize the EMI in human uteri with and without adenomyosis, both on the histological and ultrastructural levels, testing the hypothesis that this layer is structurally and functionally different in uteri affected by adenomyosis. One key hypothesis to be tested is that adenomyosis may reflect a disordered pattern of mesenchymal differentiation and maturation (i.e. fibroblasts-smooth muscle pathway). This could point to a primary subendometrial

myometrial defect. This work will therefore examine the expression of a range of mesenchymal markers, which are expressed as the cell matures in this pathway i.e. fibroblast-myofibroblast-smooth muscle cells. These will include vimentin, desmin, and  $\alpha$ -smooth muscle actin (SMA).

#### **1.7.4 Altered hormonal milieu**

Although there is no clear evidence of an impaired systemic hormonal milieu, local hyperestrogenism may be involved in the development of uterine adenomyosis. Similar to uterine leiomyomata, estrogen was found to be synthesized and secreted by adenomyotic tissue (Yamamoto et al., 1993). Aromatase and estrone sulfatase activities were detected in adenomyosis foci using anion-exchange resin column chromatography, thin-layer chromatography, co-crystallization, and immunohistochemistry (Yamamoto et al., 1993). This might equally account for hypertrophy/hyperplasia in the surrounding myometrium. Interestingly, endometrial hyperplasia is often found in women with adenomyosis (Ferenczy, 1998). *Leyendecker* (1998) describes a model for the development of adenomyosis, where a key event appears to be an increase in the local production of estrogen secondary to a pathological expression of the P<sub>450</sub> aromatase enzyme. The starting event may be a hyperactivity of the endometrial inflammatory response or hyperactivity in the endometrial oxytocin receptor system or in the pathological expression of the P<sub>450</sub> aromatase system itself. This leads to uterine hyperperistalsis and endometrial hyperproliferation. Subsequently an infiltrative growth of the elements of the archimetra (endometrial-subendometrial unit) into the rest of the myometrium results in adenomyosis (Leyendecker et al., 1998). There is no proof or validation for this model.

Endometrial glands in adenomyotic tissue selectively expresses more *human chorionic gonadotrophin (HCG)/luteinizing hormone (LH) receptor mRNA* and immunoreactive protein than the non-invaginating eutopic glandular epithelium. This increased expression was also found in endometrial carcinoma and in invasive trophoblasts of choriocarcinoma (Lei et al., 1993). The increased receptor expression in the invaginating endometrial epithelium may be related to the potential to invaginate into the myometrium and to form adenomyotic foci.

The possible role of prolactin in the development of adenomyosis has been described in several animal studies. A high rate of uterine adenomyosis in mice was induced by intrauterine or ectopic anterior pituitary isograft (Jeffcoate and Potter, 1934, Sakamoto et al., 1992). Fluoxetine (a serotonin uptake inhibitor) was used by *Ficicioglu et al.* to induce hyperprolactinaemia in castrated and non-castrated rats. Adenomyosis uteri developed in the non-castrated group. The authors suggested that high prolactin concentrations cause myometrial degeneration in the presence of ovarian steroids, which may result in myometrial weakness and subsequent myometrial invasion by the endometrial basalis (Ficicioglu et al., 1995). To date, prolactin and its relation to adenomyosis has not been the subject of studies in humans. Other rodent models have described in-utero or neonatal dosing with tamoxifen or diethylstilbestrol (DES) to induce adenomyosis, all having in common the presence of marked myometrial disruption and pathology. These models raise the possibility of in-utero developmental events leading to adenomyosis.

Various forms of hormonal manipulation can enhance the development of adenomyosis in the mouse. These include hypothalamic auto-transplant induced hyperprolactinaemia

(Huseby and Thurlow, 1982, Mori and Nagasawa, 1983), prolonged estrogen (Guttner, 1980), or progesterone administration (Ostrander et al., 1985b).

One experimental model involved transplant of the anterior pituitary in the lumen of adult SHN and SLN mouse strains (Mori and Nagasawa, 1983, Mori et al., 1991).

Almost all animals developed adenomyosis in both uterine horns. Adenomyosis was also reported following neonatal administration of prolactin or dopamine antagonists (Mori et al., 1981). Prolonged exposure of BALB/c mice to progesterone, norethisterone or norethynodrel increased the incidence of adenomyosis (Lipschutz et al., 1967). Prolonged progesterone treatment following diethylstilbestrol also induced adenomyosis in ovariectomised mice, suggesting a link between progesterone and the development of adenomyosis (Ostrander et al., 1985a). On the other hand, estrogen unopposed by progestogen administered to ovariectomised rhesus monkeys induced adenomyosis (Baskin et al., 2002).

Adenomyosis has also been reported in postmenopausal breast cancer patients treated with the selective estrogen receptor modulator (SERM) Tamoxifen (Cohen et al., 1995). The associated risk of adenomyosis with conventional postmenopausal hormone replacement therapy (HRT) is not known. Adenomyosis was incidentally found in some HRT users having endometrial ablation for postmenopausal bleeding (Phillips, 1995). The use of oral contraceptives does not appear to be associated with a risk of adenomyosis (Parazzini et al., 1997).

Steroid receptors expression has been described in the normal uteri. It has been suggested that estrogen and progesterone receptors exhibit cyclic changes in the subendometrial myometrium but not in the overlying basalis endometrium. Studies on steroid receptors in adenomyotic tissue using immunohistochemistry showed that ER

was always present but in a reduced quantity when compared to the corresponding normal myometrium. In contrast, progesterone receptors (PR) were not always present. Androgen receptors (AR) have also been found in adenomyotic tissue (Tamaya et al., 1979). Using titration assay and Scatchard analyses in 319 human uteri, adenomyosis patients had higher PR and lower ER concentrations than normal uteri (van der Walt et al., 1986).

### **1.7.5 Immunological and biochemical abnormalities**

A number of immunological and biochemical abnormalities (cellular and humoral) have been described in adenomyosis by *Ota and co-workers* (Ota et al., 1998, Ota et al., 1996, Ota and Tanaka, 1997, Ota et al., 1992, Ota and Tanaka, 2001, Ota et al., 2001b, Ota et al., 2001a, Ota et al., 2000, Ota et al., 1999a, Ota et al., 1999b, Ota and Igarashi, 1993). They described changes in both cellular and humoral immunity (e.g. a strong expression of cell surface antigens or adhesion molecules, an increased number of macrophages or immune cells, and deposition of immunoglobulins and complements components). Using immunohistochemistry, increased expression of the major histocompatibility complex class II antigen (HLA-DR) in the gland cells of eutopic and adenomyotic endometrium has been described (Ota and Igarashi, 1993). Macrophages in the myometrium of adenomyotic uteri seemed to increase, possibly activating helper T-cells and B-cells to produce antibodies (Ota et al., 1998). Peripheral blood concentrations of autoantibodies were increased in adenomyosis (Ota et al., 1992). The deposition of complement components C3 or C4 in adenomyosis were increased in 74% and 89% of patients respectively. The expression of E-cadherin in the endometrial tissue of adenomyosis was equally found to be significantly higher (Ota et al., 1998).

Using immunohistochemistry, adenomyotic uteri showed excessive expression of superoxide dismutase throughout the menstrual cycle (Ota et al., 1999b). Similarly, glandular tissue in adenomyosis showed increased expression of glutathione peroxidase (Ota et al., 2000), cyclo-oxygenase-2 (Ota et al., 2001a) and xanthine oxidase (Ota et al., 2001b) when compared to eutopic endometrium.

Increased expression of basic fibroblast growth factor (bFGF) and its receptor (FGF-R) was found in the epithelium of adenomyosis compared with autologous endometrial epithelium in menopausal women. The authors suggested that bFGF might contribute to the pathogenesis of abnormal uterine bleeding associated with adenomyosis. However, they only included 6 uteri in their study and all their patients were postmenopausal (Propst et al., 2001). These findings could not be generalized or applied to the premenopausal patients without further research.

Intraepithelial leucocytes (IEL) are an immunological component of most mucosal surfaces although the function and significance of their presence is not really known. In the eutopic endometrium of patients with adenomyosis, IEL expression varied during the menstrual cycle, with *CD45+*, *CD43+* and *CD56+* cells increasing from the proliferative to the late secretory phase. IEL number was higher in the surface epithelium compared to the glands in the proliferative and early secretory phases. Throughout the menstrual cycle there were no significant differences in IEL between eutopic and ectopic endometrium in adenomyosis (Bulmer et al., 1998). Most of these observations were extrapolated from work on endometriosis, based on the assumption that these are similar diseases only different in the location of the ectopic endometrium.

### 1.7.6 Genetic basis of uterine adenomyosis

Experimental observations in animals suggest that hereditary factors may be involved in the pathogenesis of adenomyosis. The uteri of recombinant inbred SMXA mice develop spontaneously histological changes similar to adenomyosis (Kida, 1994). The uteri of F1 mice strain contain more prominent changes resembling human adenomyosis. It is not yet determined whether heredity plays an important role in the development of adenomyosis in humans.

Genetic polymorphism and linkage analysis implicate genes that encode for enzymes such as galactose 1-phosphatase uridyl transferase (GALT) located on 9p21 (Cramer et al., 1996) and glutathione S-transferase M1 (GSTM1) located on 1p13 (Baranova et al., 1997), have been implicated in the pathogenesis of endometriosis. In addition, microsatellite analysis of endometriosis has revealed loss of heterozygosity at candidate ovarian tumor suppressor gene loci (Jiang et al., 1996). It is unknown if the same factors may be involved in the pathogenesis of adenomyosis.

The clonal chromosome abnormality of *del [7] [q21.2q31.2]* has been observed in adenomyotic tissue culture (Pandis et al., 1995). This karyotypic abnormality is also frequently seen in leiomyomata, suggesting that adenomyosis could possibly be a neoplastic process. Microsatellite markers have been used to examine and determine the incidence of loss of heterozygosity in adenomyosis. Loci on *2p22.3-p16.1*, *3p24.2-p22* and *9p21* chromosomal regions exhibited imbalance (19.4%, 9.7% and 6.5%, respectively) (Goumenou et al., 2000). However, such chromosomal gain or loss was not observed using comparative genomic hybridization on frozen tissue samples (Wang et al., 2002).

Aberrant expression of ER- $\alpha$  might be partly involved in the onset or growth of adenomyosis and its poor response to anti-estrogen therapy. Using PCR/single strand conformation polymorphism analysis, *Oehler et al.* identified somatic estrogen receptor ER- $\alpha$  gene mutations in three out of 55 samples from adenomyosis uteri. Functional characterization revealed that two of the mutant ER- $\alpha$  proteins display severely impaired DNA-binding and transactivation properties secondary to an altered response to estrogens or changes in epidermal growth factor-mediated ligand-independent activation. A mutation-related silencing of estrogen responsiveness might render ectopic endometrial cells resistant to hypo-estrogenic conditions thereby accounting for poor response to estrogen-ablative therapy in adenomyosis (Oehler et al., 2004).

Whether hereditary or familial factors for adenomyosis exist is unknown. Only one personal series was identified for Emge who operated on 7 cases of adenomyosis in which mothers of the patients were operated upon for the same reason, raising the possibility of a hereditary background (Emge, 1962). The same paper refers to a description of adenomyosis in a fetus at term. Review of the literature did not identify any studies on adenomyosis in twins.

## HYPOTHESES

A review of the literature led to the identification of the following research hypothesis.

1. That the primary pathology in uterine adenomyosis is an abnormal development or behaviour of the endometrial-myometrial interface (EMI) (basal endometrium / subendometrial myometrium), postulating that this zone behaves differently in adenomyosis compared to normal uteri and as compared to the deeper myometrium.
2. Further to this hypothesis, this work will try to identify which component of the EMI (i.e. basal endometrium or subendometrial myometrium) plays the key role in the development of adenomyosis. The thesis will test two possibilities: (i) that the subendometrial myometrium is permissive to invasion by a normal basal endometrium, or (ii) that the basal endometrium has a higher invasive potential and penetrates a normal subendometrial myometrium.

In order to examine these hypotheses, the thesis will follow the following outline:

### **A: Experimental model of adenomyosis**

This section will examine the sequence of early uterine development changes and aberrations that lead to uterine adenomyosis. This work will examine the effect of Tamoxifen on the differentiation of the different muscle layers and the development of adenomyosis in the uteri of CD-1 mice. To examine the possible strain (genetic) predisposition in response to these hormonally active agents, this work will also examine the effects of Tamoxifen on the C57/BL6J mouse strain that is not known to develop spontaneous adenomyosis.

**B: Human uterine adenomyosis:**

**i. The role of the myometrium in the development of human uterine adenomyosis.**

This experimental work will attempt to identify the phenotypic and genotypic characteristics of the human myometrium in uteri affected by adenomyosis. The gross and ultrastructure of the myometrium will be examined. Then, the differences in genes expression between control and affected myometrium will be studied.

**ii. The role of the endometrial stroma in the development of human uterine adenomyosis.**

This experimental work will examine the characteristics of the endometrium in uteri with and without adenomyosis. The invasive properties of the endometrium and the interaction between the endometrium and myometrial layers will be further studied.

The emphasis of the human tissue work will be on “diffuse” rather than “focal” adenomyosis.

## **Section I**

### **Experimental Adenomyosis**

## **Chapter 2**

**The effects of tamoxifen and estradiol on myometrial differentiation  
and organisation during early uterine development in the CD-1 mouse**

## Chapter 2

### **The effects of tamoxifen and estradiol on myometrial differentiation and organisation during early uterine development in the CD-1 mouse**

#### **2.1 INTRODUCTION**

Elucidation of the mechanisms involved in the initiation and development of uterine adenomyosis in women is difficult. Development of an animal model will thus be useful for the study of the disease.

Adenomyosis was demonstrated in CD-1 mice following neonatal administration of tamoxifen (Green et al., 2005, Parrott et al., 2001). Oral administration of tamoxifen (200 µg/ml, at a dose of 5 µl/g body weight) to female pups between days 1 and 5 of age, induced adenomyosis in all uteri examined at 6 weeks post-natal. This was also associated with marked disorganisation of the myometrium and the mesenchyme. The ovaries of adult mice were noted to be normal and to contain corpora lutea, and as early uterine development was not assessed, the possibility remains that ovarian steroids may have a role in the pathogenesis of adenomyosis. It is also interesting to note that adenomyosis was not induced following the administration of an equivalent uterotrophic dose of estradiol, or following the administration of raloxifene which has no uterotrophic effect. Although adenomyosis was demonstrated, there was no study of the early developmental phases of the disease.

The mesenchyme surrounding the developing Mullerian duct gives rise to 90-95% of the uterine mass and forms both the myometrium and the endometrial stroma (Martin et

al., 1973), and has been shown to express estrogen receptor (ER). In contrast to the epithelium, which expresses ER at postnatal day 6-7, Mullerian duct mesenchyme in the CD-1 mouse, expresses ER from day 13 of gestation (Holderegger and Keefer, 1986, Eide, 1975, Stumpf et al., 1980).

ER- $\alpha$  mRNA was found in CD-1 mouse uterus as early as fetal day 14; in contrast, low level expression of ER- $\beta$  mRNA was only detected on the first postnatal day. However, whilst ER- $\alpha$  was detected using immunohistochemistry in stromal cells during late gestation and the postnatal period (Jefferson et al., 2000, Kurita et al., 2001), ER- $\beta$  immunolabelling was not detected before postnatal day 6 (Jefferson et al., 2000, Kurita et al., 2001, Parrott et al., 2001).

In this study, the CD-1 mouse model developed by Green et al. and Parrott et al. (Green et al., 2005, Parrott et al., 2001) is used to examine the histogenesis and the early developmental changes associated with uterine adenomyosis. The doses of tamoxifen and estradiol used in this work were derived from dose-response studies (Green et al., 2001) and have been previously described and utilised in similar experiments (Parrott et al., 2001, Green et al., 2003). First, the normal uterine development and morphogenesis are compared with those following tamoxifen and estradiol administration. Then the effect of tamoxifen and estradiol on the developing uterus, as manifested by changes in the patterns of expression of cytoskeletal proteins (actin, desmin, vimentin), extracellular matrix proteins (laminin, fibronectin), and ER- $\alpha$  is examined. This section examines the hypothesis that adenomyosis and the previously described myometrial changes are due to an abnormality in myometrial differentiation, or in the extracellular matrix proteins expression. It also examines the possible involvement of ER and its regulation by tamoxifen and estradiol, in relation to the development of adenomyosis.

## **2.2 METHODS**

### **2.2.1 Samples and materials**

The study was conducted under the authority of the United Kingdom Home Office, Animals (Scientific Procedures) Act 1986. Pregnant time-mated CD-1 mice were obtained (Charles River Ltd, Margate, Kent, UK) and their female pups were divided into three groups. The first group (n=27), were orally dosed on days 1- 5 after birth (day of birth being day 0) with 1mg/kg tamoxifen - suspended in peanut oil/lecithin/condensed milk mixture at a concentration of 200 µg/ml, at a dose of 5 µl/g body weight. The second group (n=24) received 0.1mg/kg estradiol benzoate - suspended in peanut oil/lecithin/condensed milk mixture at a concentration of 20 µg/ml, at a dose of 5 µl/g body weight. The control group (n=27) received vehicle only. Five mice from each group were culled on day 2 (before the 2<sup>nd</sup> dose), 5, 10, 15 and the remainder on day 42. Uteri were collected, weighed and fixed in 4% neutral buffered formalin for 24hrs at room temperature. Paraffin embedded cross sections (2µm to avoid overlap of cells) were cut and mounted on silane coated glass slides for histological and immunohistochemical examination.

### **2.2.2 Immunohistochemistry**

Sections were dewaxed in xylene, and rehydrated in graded alcohols and water. Epitope antigen retrieval using microwave and citrate buffer (pH = 6.0) was used for desmin, fibronectin, and ER- $\alpha$  staining. Endogenous peroxidase activity was blocked with 6% (v/v) hydrogen peroxide (H<sub>2</sub>O<sub>2</sub>) in water for 10 minutes. Specific mouse-on-mouse blocking reagent (Vector labs, Peterborough, UK) was applied for one hour where applicable. Sections were incubated overnight at 4°C with the primary antibodies

against desmin (mouse monoclonal clone DR33, 1:50 (v/v), Dako, Cambridge, UK), vimentin (mouse monoclonal, clone LN6, 1:50 (v/v), Chemicon, Millipore, Watford, UK), laminin (Rabbit polyclonal, 1:200 (v/v), Abcam, UK), fibronectin (Rabbit polyclonal, 1:500 (v/v), Abcam, UK), and ER- $\alpha$  (mouse monoclonal, clone ER-6F11, Novocastra, Newcastle upon Tyne, UK) and for one hour at room temperature for  $\alpha$ -SMA (clone SMM1, Vector labs, Peterborough, UK). Biotinylated rabbit anti-mouse or swine anti-rabbit secondary antibody (Dako, Cambridge, UK) was applied at a concentration of 1:400 (v/v) for 30 minutes at room temperature. Immunoreactivity was demonstrated with 3,3'-diaminobenzidine/ H<sub>2</sub>O<sub>2</sub> (DAB solution) (Vector labs, Peterborough, UK). Sections were lightly counterstained with haematoxylin, then dehydrated and cleared in graded alcohol and xylene, and finally covered with glass slips. The immunostaining was assessed for distribution and intensity using a visual score (- negative;  $\pm$  equivocal, + weak; ++ moderate, +++ strong).

Image capture and analysis was performed using Axioplan® 2 light microscopy (Carl Zeiss, Germany) and an image capture system. The system was based on a single chip colour video camera (Sony DXC-151P, Sony Inc., Japan) connected to a camera adapter (Sony CMA-151P, Sony Inc., Japan) that transmits the image to a Windows® based computer via a Meteor 2 MMC graphics display interface and the Axiovision image analysis software (version 4.0, Carl Zeiss, Germany).

## **2.3 RESULTS**

In the following subsections, the normal uterine development in the CD-1 mice is presented. Then, the morphological changes observed in the tamoxifen and estradiol treated groups are described. Finally, the data on immunohistochemical markers is

presented. The data is visually presented and summarised in figures 2.1 to 2.4 and tables 2.1 & 2.2.

### **2.3.1 Morphology and uterine development**

#### **2.3.1.1 Normal uterine development of CD-1 mice**

**Day 2:** The uterine cavity consisted of an oval-shaped lumen, elongated in the mesometrial-antimesometrial axis. The luminal epithelium consisted of a monolayer of low columnar cells, with large round nuclei and prominent nucleoli. The uterine wall thickness was formed of mesenchymal cells with large pale cytoplasm, large round nuclei and less prominent nucleoli. These cells were not differentiated into distinct layers or orientation. No discernible blood vessels could be seen. The perimetrium was composed of a single layer of cuboidal to low columnar epithelium.

**Day 5:** The monolayer luminal epithelium consisted of tall columnar cells with elongated nuclei arranged in palisade with some multilayered areas. There was no evidence of gland formation. In the uterine wall, the mesenchymal cells started to segregate into three layers: endometrial stroma, inner circular and prospective outer longitudinal muscle layers. The endometrial stroma occupied the inner half of the uterine wall thickness. The stromal cells retained their undifferentiated shape and loose arrangement with no particular spatial orientation. The prospective inner circular muscle layer was the most defined and densely staining layer, 5-6 cells thick. The cells were bundled, circularly orientated and tightly packed with elongated nuclei and minimal inter-cellular space. The prospective outer myometrium was formed of 1-2 layers of cells retaining their undifferentiated appearance. Vascular spaces started to appear, especially in the layer between the inner and outer myometrium.

**Day 10:** Uterine sections showed a more complex luminal epithelium invaginating the stroma to form simple tubular uterine glands. All layers of the uterine wall were more distinct. The stroma appeared more tightly packed and surrounded the endometrial glands. The inner circular muscle layer was thicker compared to the outer myometrium. The cells were organised into bundles with no surrounding connective tissue sheath. Longitudinally cut sections demonstrated elongated nuclei in this outer layer, confirming its longitudinal arrangement. Blood vessels were larger and observed in all layers of the uterine wall.

**Day 15:** The adult configuration of the uterus was apparent. The endometrium showed numerous simple tubular glands and a thick endometrial stroma. Stromal cells were randomly orientated except around the individual glands where they appeared more circular. A distinct loose vascular layer separated the inner and outer myometrial layers. The outer myometrial cells became grouped in bundles connected by loose connective tissue sheaths, and separated from the inner myometrium by a distinct loose vascular layer.

**Day 42:** The adult uterus was larger and more complex, but had the same configuration as the uterus on day 15. The endometrial glands were more complex and branching, but were confined to the endometrial layer. The inner myometrium was quite distinct. The intervening vascular layer harboured most of the large blood vessels. The outer longitudinal muscle layer was formed of prominent bundles with well-formed connective tissue sheaths.

### **2.3.1.2 Uterine development following tamoxifen administration**

**Day 2:** The uterine epithelium was hypertrophied, with large nuclei and prominent nucleoli. The mesenchymal cells in the uterine wall were uniform in shape and size, and did not show any specific spatial arrangement.

**Day 5:** The uterine lumen was markedly dilated with prominent secretions, and the uteri were significantly heavier than controls. The hypertrophied epithelium was formed of tall columnar cells with pale elongated nuclei. Blood filled spaces were seen throughout the uterine wall, which was thinner compared to controls. Some cells in the middle of the uterine wall appeared to adopt circular orientation, but these were loosely bundled and only formed a thin patchy ring encircling about 25-40% of the uterus. One section examined revealed deep glands involving >30% of the uterine thickness, representing early evidence of adenomyosis.

**Day 10:** The uterus was dilated and adenomyosis was observed in 3 out of 5 specimens. There was marked disorganisation of uterine development, with glands dispersed all through the uterine wall but not reaching the serosa. The original lumen was sometimes hard to identify. The stroma surrounding the glands was highly cellular with ovoid nuclei. The glandular epithelium was less hypertrophied. Otherwise, the myometrial layers were not distinct. Some cells had circular orientation but with no observable continuity and with some glands seen deeper to the circular layer. The outer muscle layer was less obvious, with some bundles observed on the periphery.

**Day 15:** Adenomyosis was observed in 80% of specimens. The same earlier disorganised development pattern was observed. The circular muscle layer disruption was more evident as cells acquired darker staining cytoplasm and more obvious circular orientation, and some glands extending deeper to the circular muscle layer. The outer

myometrium showed signs of differentiation into bundles surrounded by thin loose connective tissue. The intervening vascular layer was not obvious although some prominent blood vessels were seen scattered in the uterine wall.

**Day 42:** Adenomyosis was observed in all specimens to various degrees. The uteri were smaller than controls. Some glands reached the serosa forming subserosal cysts. The endometrial stroma was highly cellular. The circular myometrium showed marked loosening and increased intercellular space. The outer myometrium was well developed with obvious bundling. Overall, the muscle integrity was more preserved on the antimesometrial border of the uterus.

### **2.3.1.3 Uterine development following estradiol administration**

In general, the uterine development in estradiol treated CD-1 mice was similar to the control mice, but development and appearance of the different layers was observed at earlier chronological stages. By day 2, the cells in the middle third of the uterine wall already demonstrated a clear circular arrangement with dark cytoplasm staining. By day 5, the circular muscle layer was well developed, with tightly packed bundles of dark cells, and with minimal intercellular space. The uterine wall contained many blood filled spaces. Later on, the uterine layers were well developed and easily identified. The uterine size was generally larger compared to the control counterpart, but the different layers retained their proportions and relative sizes. Endometrial glands were abundant. There was no evidence of adenomyosis or myometrial disruption.

**Table 2.1: Histological features measured at different stage of development of neonatal CD-1 mice after administration of tamoxifen, estradiol or vehicle only. Measurements are in  $\mu\text{m}$ : median (range).**

	<b>Control</b>	<b>Tamoxifen *</b>	<b>Estradiol **</b>
<b><u>Day 2 (n=5)</u></b>			
Epithelial height	14 (10-16)	14 (13-15)	12 (10-15)
Uterine wall thickness	60 (40-75)	70 (60-75)	70 (60-75)
<b><u>Day 5 (n=5)</u></b>			
Epithelial height	18 (16-20)	25 (25-35)	20 (18-25)
Uterine wall thickness	110 (100-110)	70 (60-80)	90 (85-110)
Inner cellular layer (future stroma)	70 (60-80)	35 (35-40)	50 (45-60)
Inner circular muscle layer	30 (25-35)	20 (20-25)	30 (25-35)
Outer cellular layer (future outer myometrium)	12 (10-15)	12 (10-15)	20 (16-22)
<b><u>Day 10 (n=5)</u></b>			
Epithelium height	18 (16-20)	15 (12-20)	16 (15-18)
Uterine wall thickness	120 (110-130)	-	120 (110-130)
Inner cellular layer (future stroma)	90 (80-100)	-	90 (80-100)
Inner circular muscle layer	30 (25-35)	-	30 (25-35)
Outer cellular layer (future outer myometrium)	20 (15-25)	-	20 (15-25)

**Cont.**

**Table 2.1: Histological features measured at different stage of development of neonatal CD-1 mice (cont.)**

	<b>Control</b>	<b>Tamoxifen *</b>	<b>Estradiol **</b>
<b><u>Day 15 (n=5)</u></b>			
Epithelial height	18 (15-20)	18 (15-20)	18 (16-20)
Uterine wall thickness	170 (160-180)	-	150 (140-165)
Endometrial stroma	100 (90-110)	-	80 (75-90)
Inner circular myometrium	40 (35-40)	-	35 (30-40)
Intermediate vascular layer	10 (10-15)	-	10 (10-15)
Outer myometrium	25 (20-30)	25 (20-30)	30 (20-35)
<b><u>Day 42 (n=5)</u></b>			
Epithelial height	18 (15-20)	20 (15-20)	18 (16-20)
Uterine wall thickness	340 (320-360)	-	550 (450-600)
Endometrial stroma	120 (110-130)	-	160 (140-300)
Inner circular muscle layer	80 (75-90)	-	100 (80-120)
Intermediate vascular layer	50 (50-55)	-	50 (45-60)
Outer myometrium	90 (85-100)	50 (40-60)	110 (100-120)

\* The uteri in the tamoxifen group had wide irregular lumens and poorly defined layers characterised by penetrating stroma, markedly disrupted circular layer and no obvious vascular layer. The mean uterine diameter was 600  $\mu\text{m}$  (550-620). The whole uterine structure was so disorganized with glands and surrounding stroma dispersed throughout the uterine wall, with few scattered muscle fibers and blood vessels (no muscle or vascular layers as such) vessels everywhere. The wall thickness was measured from the luminal epithelium of the central lumen to the serosal edge. However, the central lumen was not identified in most specimens treated with tamoxifen. All the structures were intermingled and too indistinct to measure separately, hence the absence of some measurements (-).

\*\* Estradiol treated uteri had distinct well-developed layers from day 2.

## **2.3.2 Immunohistochemical markers**

### **2.3.2.1 $\alpha$ -Smooth muscle actin ( $\alpha$ -SMA) expression**

On day 2, control uteri were negative for  $\alpha$ -SMA. A narrow but distinct zone of variable intensity staining corresponding to the developing inner circular myometrium was seen in the middle of the uterine wall by day 5. On day 10,  $\alpha$ -SMA expression was strong and well defined in the inner circular ‘muscle’ layer; less intense expression was seen in the outer longitudinal muscle layer. Uteri from day 15 onwards exhibited well-defined, intense staining of both the inner and outer muscle layers.

In the tamoxifen group,  $\alpha$ -SMA expression was weaker, with fewer positive cells/area, reflecting disruption and loosening of the circular myometrium. Staining intensity was generally weaker in the inner circular compared to the outer longitudinal muscle layers.

In estradiol treated mice, positive immunostaining for  $\alpha$ -SMA was observed as early as day 2 in the middle section of the uterine wall. The staining was generally intense particularly in the compact thickened circular myometrium.

### **2.3.2.2 Desmin expression**

In control CD-1 mice, desmin expression followed a ‘wave’ of maturation from inside outwards. Firstly, on day 2, the whole uterine thickness was weakly immunopositive to desmin. The developing endometrial stroma then strongly expressed desmin, while the outer and middle parts of the uterine wall remained less intense. As the outer and longitudinal myometria developed, they acquired and expressed stronger immunostaining to desmin compared to the endometrial stroma that reverted to be

weakly positive. The blood vessels walls stained strongly positive, whilst endometrial epithelium was negative.

In tamoxifen treated mice, this “wave” of maturation was absent. The intensity of staining remained uniformly weak all through the developmental phases of the uterine wall structures. Generally, the intensity of staining was weaker than in controls.

However, in the adult uterus (day 42), the myometrial layers showed relatively stronger staining compared to the endometrial stroma. The endometrial epithelium remained negative.

Estradiol treated mice demonstrated an earlier (day 2) stronger desmin immunostaining. The undifferentiated uterine wall strongly expressed desmin and the early developing myometrial layers were more intense than the endometrial stroma. The endometrial epithelium stained negatively for desmin. All blood vessels walls stained strongly positive and were considered internal quality control for the immunostaining.

### **2.3.2.3 Vimentin expression**

Vimentin immunohistochemical expression was observed in the endometrial stroma and blood vessel wall starting on day 15 and day 42 (in all groups). No staining was seen in the myometrium. In some uteri, occasional staining was observed in the inner part of the uterine wall (developing stroma) by day 5, but this was not consistent. All blood vessels walls stained positive and were considered intrinsic quality control.

### **2.3.2.4 Laminin and fibronectin expression**

The undifferentiated mesenchyme showed a light diffuse expression for laminin and fibronectin on day 2. By day 5, laminin expression was more localised to the middle third of the developing uterus i.e. the prospective inner circular muscle layer, while fibronectin was differentially expressed in the prospective endometrial stroma (inner

third of the developing uterus). The same expression pattern was observed on day 10, and subsequently, as laminin was exclusively expressed in the extracellular matrix surrounding the smooth muscle layers (inner circular and outer longitudinal).

Fibronectin was exclusively expressed around the stromal cells and in the connective tissue sheaths separating the outer longitudinal muscle, and the intervening vascular layer. There was no difference in the localisation of laminin or fibronectin between the controls or treatment groups. However, laminin expression was reduced in the tamoxifen treated uteri, secondary to the disruption of the inner myometrium, and on day 5 possibly secondary to tissue oedema.

#### **2.3.2.5 ER-alpha expression**

In the control CD-1 mice, the whole thickness of the uterine wall expressed ER- $\alpha$  from day 2, while the epithelial lining remained negative till day 10, when both luminal and glandular epithelium exhibited strong positive staining. As the various layers developed in the mesenchyme, the ER- $\alpha$  expression was more intense in the stroma compared to the muscle layers. By day 42, there was more variability in staining intensity between specimens, due to different phases of the estrous cycle.

In tamoxifen treated mice, there was marked downregulation of the ER- $\alpha$ , with no or very weak staining in all layers in days 5 and 10. However, by day 15, the ER- $\alpha$  staining has recovered in the endometrial layers (epithelium and stroma), but was less obvious in the myometrium. On day 42, the glands and stroma were strongly positive (including in adenomyotic foci), but the muscle layers (inner and outer) remained less immunopositive. Overall, ER- $\alpha$  expression was attenuated compared to control uteri. In estradiol-administered mice, ER- $\alpha$  expression was comparable to control mice, although on day 5 and 10 ER- $\alpha$  was transiently over expressed in all layers.

**Table 2.2: Immunohistochemical expression of desmin and vimentin in the uterus CD-1 mice. The control group received vehicle only, study group received tamoxifen or estradiol from neonatal days 1 to 5. Uteri were examined on day 2, 5, 10, 15 and 42 of age.**

	Control		Tamoxifen		Estradiol	
	Desmin	Vimentin	Desmin	Vimentin	Desmin	Vimentin
<b><u>Day 2 (n=5)</u></b>						
Uterine wall	+	-	+	-	+++	-
<b><u>Day 5 (n=5)</u></b>						
Inner layer	+++	±	+	-	++	-
Middle layer	+	-	+	-	±	-
Outer layer	+	-	+	-	+	-
<b><u>Day 10 (n=5)</u></b>						
Stroma	+	-	±	-	+	-
Inner myometrium	++	-	±	-	++	-
Outer myometrium	+	-	±	-	++	-
<b><u>Day 15 (n=5)</u></b>						
Stroma	±	+	+	+	+	+
Inner myometrium	++	-	+	-	++	-
Outer myometrium	++	-	+	-	++	-
<b><u>Day 42 (n=7)</u></b>						
Stroma	±	+	+	+	+	+
Inner myometrium	+++	-	++	-	+++	-
Outer myometrium	+++	-	++	-	+++	-

**Figure 2.1: Control CD-1 mice: Uterine development and immunohistochemical staining pattern for alpha smooth muscle actin, desmin, vimentin, and ER-alpha. Magnification: Days 2, 5, 10, and 15 micrographs (x20), day 42(x10). (H&E: Hematoxylin and eosin, SMA: alpha smooth muscle actin).**

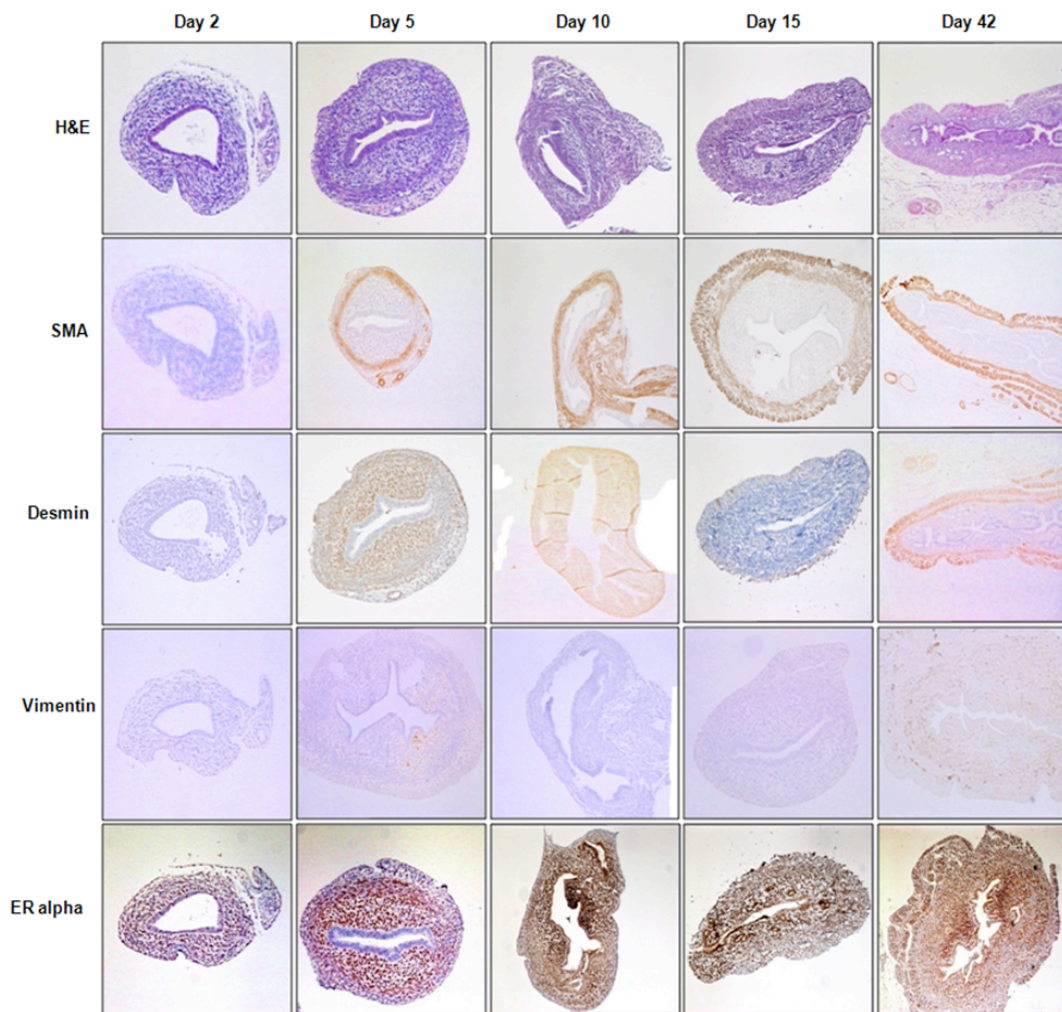


**Figure 2.2: Tamoxifen treated CD-1 mice: Uterine development and immunohistochemical staining pattern for alpha smooth muscle actin, desmin, vimentin, and ER-alpha. Magnification: Days 2, 5, 10, and 15 micrographs (x20), day 42(x10). Black arrows point to early invading glands (day 5), leading to adenomyosis (day 10). Note the marked disorganisation and disruption of the inner myometrium around the adenomyosis foci. Subserosal adenomyotic cysts are evident on day 42. Also note the reduced desmin expression in the myometrial layers. (H&E: Hematoxylin and eosin, SMA: alpha smooth muscle actin).**

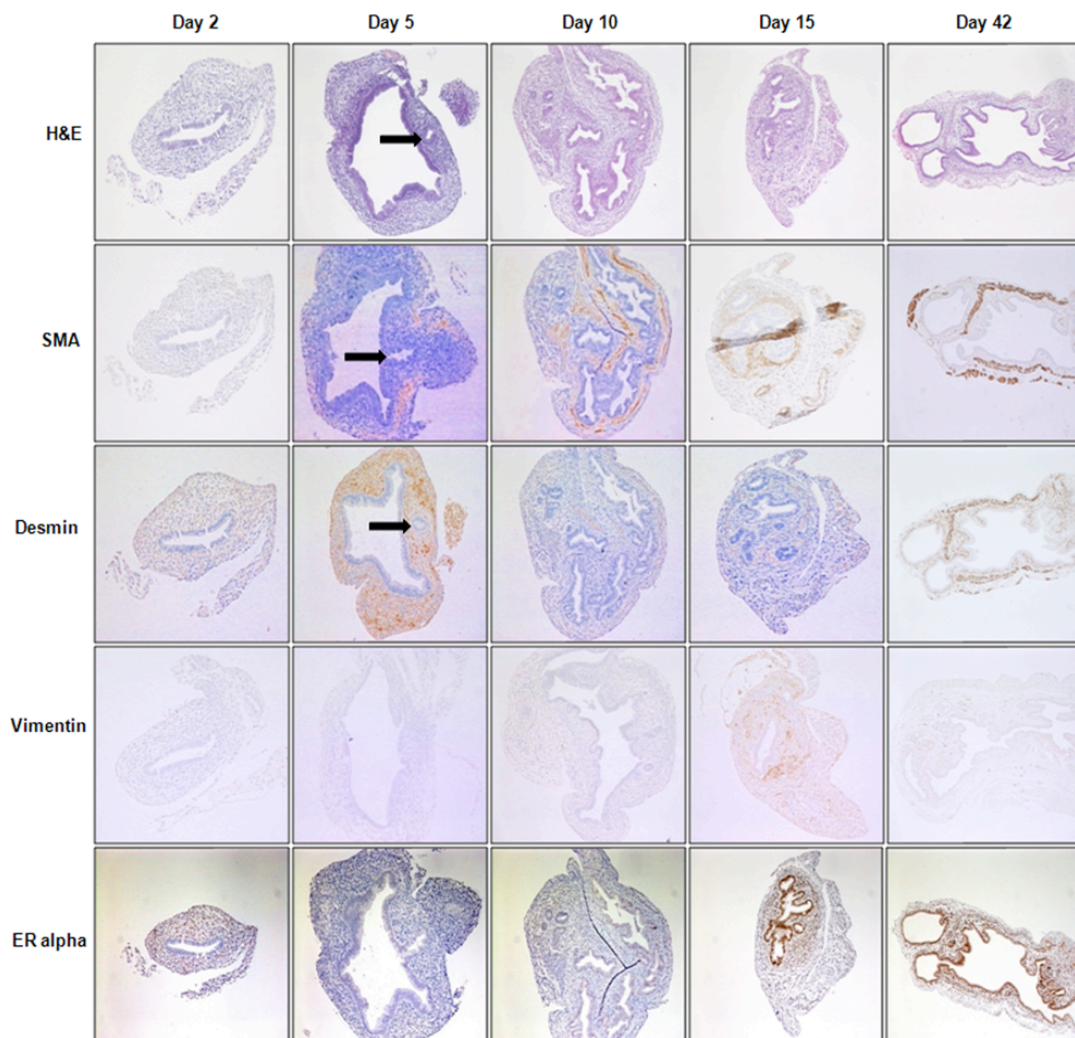


**Figure 2.3: Estradiol treated CD-1 mice: Uterine development and immunohistochemical staining pattern for alpha smooth muscle actin, desmin, vimentin, and ER-alpha. Magnification: Days 2, 5, 10, and 15 micrographs (x20), day 42(x10). (H&E: Hematoxylin and eosin, SMA: alpha smooth muscle actin).**

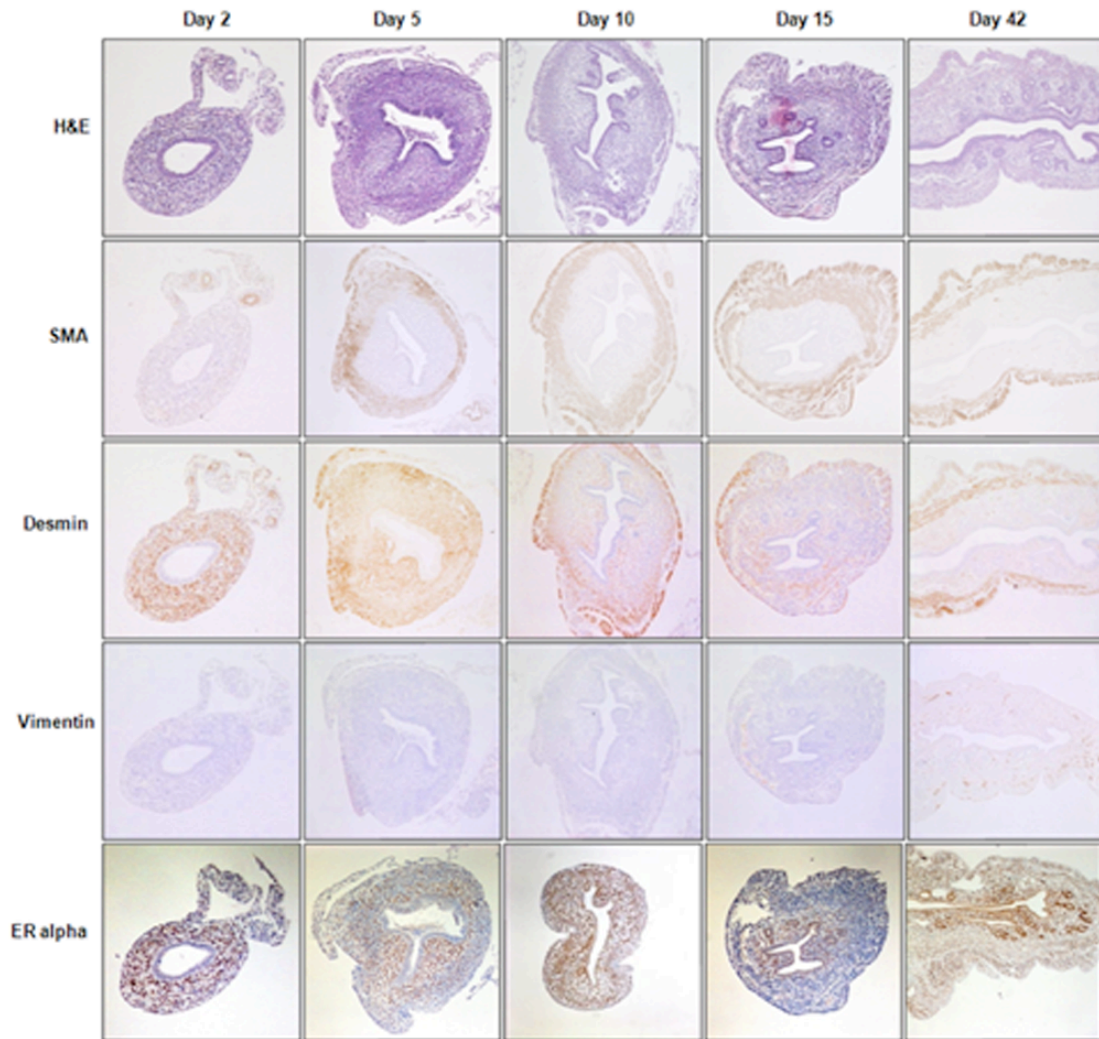
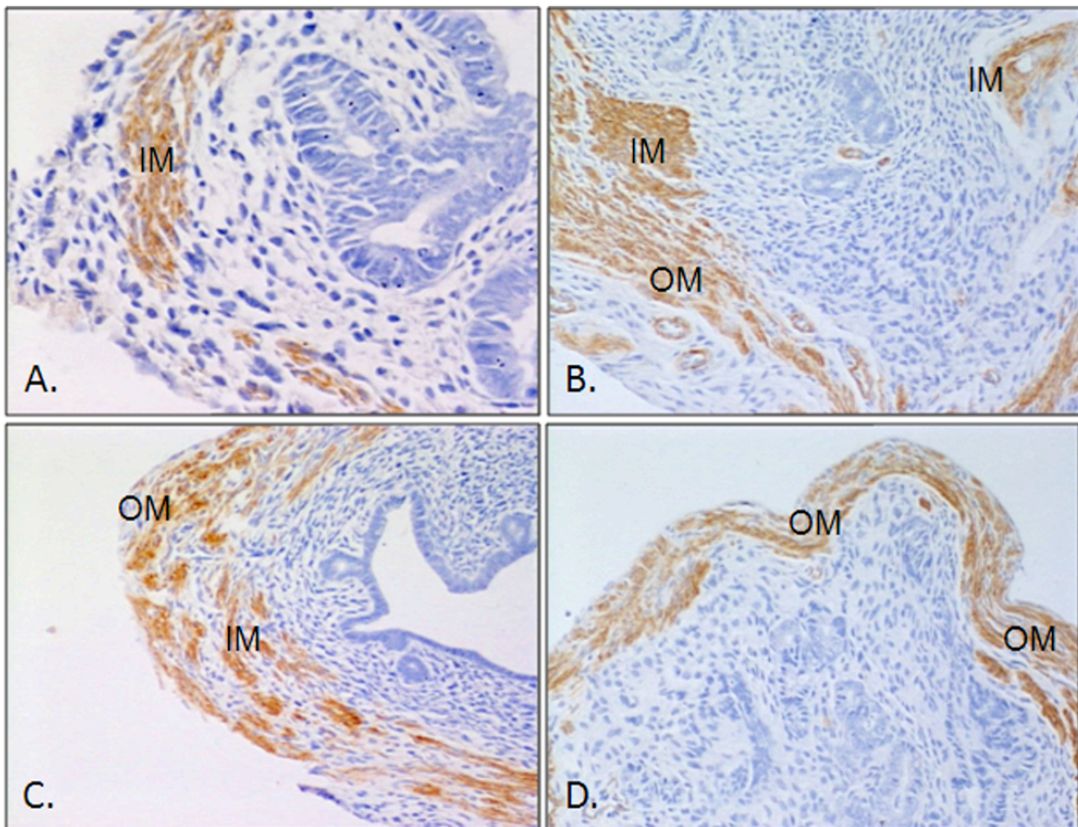


**Figure 2.4: Alpha smooth muscle actin immunostaining, demonstrating the myometrial abnormalities associated with the presence of uterine adenomyosis. A: Bundling and loosening of the inner myometrium. B: Disruption of the inner myometrium. C: Increased extracellular space. D: Normal outer myometrium immunostaining. (IM: inner myometrium, OM: outer myometrium)(x40)**



## 2.4 DISCUSSION

At birth, the uterus of CD-1 mice is made of simple low columnar epithelium supported by undifferentiated mesenchyme, and lacked endometrial glands. Uterine development involved differentiation and development of the endometrial glands from the luminal epithelium and the inner circular and outer longitudinal layers of muscle from the uterine mesenchyme. The described developmental stages in this study are in agreement with previous reports using CD-1 strain (Brody and Cunha, 1989, Cunha, 1976, Cunha et al., 1992).

Perinatal uterine development represents a critical phase for uterine morphogenesis and differentiation (Iguchi and Sato, 2000). This model demonstrated the early stages of development of uterine adenomyosis, in the absence of progestogenic effect.

Tamoxifen, but not estradiol neonatal exposure resulted in the development of adenomyosis in CD-1 mice as early as day 10, with disruption of the inner myometrial layer and in-growth of endometrial glands and stroma. The doses of tamoxifen and estradiol used in this work were derived from dose-response studies (Green et al., 2001) and have been previously described and utilised in similar experiments (Parrott et al., 2001, Green et al., 2003).

The exact genetic and environmental factors regulating cell line differentiation in the uterus are not fully known. Interaction of estrogen agonists with ER- $\alpha$  plays a key role in the initial uterine effect since immature ER- $\alpha$  knockout mice, when given tamoxifen, show no significant increase in uterine weight (Korach, 1994). The observed immunohistochemical changes are due to a direct action on the uterus, as the hypothalamic/pituitary axis is inactive as this early stage. Gene expression arrays demonstrated similar changes in 14 days old female mice uteri following estradiol,

genestein and diethylstilbestrol administration, which suggests that the actions of estrogens on the uterus are intrinsically similar (Moggs et al., 2004).

Epithelial-mesenchymal interactions are recognized to play an important role in the postnatal development and the spatial organisation of the uterus (Cunha, 1976, Cunha et al., 1992, Cunha et al., 1989a). Alpha Smooth Muscle Actin ( $\alpha$ -SMA) and the intermediate filaments (desmin and vimentin) were used as differential markers for myocytes, myofibroblasts and fibroblasts cellular differentiation, as they are tissue specific and their pattern of expression is developmentally regulated. Recent work has suggested that ER- $\beta$  could be involved in the differentiation process of stromal cells and fibroblasts into myofibroblasts in various breast tumours (Sapino et al., 2006a). It is possible that tamoxifen could alter the paracrine signalling in the uterus (via a receptor mediated mechanism), affecting the differentiation of uterine myocytes in the mesenchyme and, over a period of time, allowing invasion of the endometrium into the myometrium. However, this study suggests that the developing myometrium expressed an immunohistochemical profile suggestive of myogenic differentiation (absence of vimentin, and expression of  $\alpha$ -SMA). The histodifferentiation of smooth muscle cells was clearly demonstrated by  $\alpha$ -SMA staining (although delayed), in both the intact and disrupted inner muscle layers, and in the outer myometrium. This argues against abnormal differentiation into various fibroblasts/myofibroblasts phenotypes.

The absence of vimentin immunostaining in the differentiating myometrial layers makes fibroblastic differentiation less likely. By contrast, those cells that were destined to form the endometrial stroma expressed vimentin. The absent myometrial expression of vimentin was not altered between control, tamoxifen, and estradiol-administered mice. The distribution and function of vimentin in the developing mouse myometrium is not well described in the literature. This suggests that vimentin may not be involved in the

differentiation and development of myometrial cells in the early stages mouse development. Similarly, vimentin reactivity could not be detected inside the myofibers of mice embryos or neonates (Parazzini et al., 1997).

This study observed reduced desmin expression in tamoxifen-administered mice.

Desmin is expressed in all muscle tissue. Its role in both cardiac and skeletal muscle has been widely described (Lazarides, 1980, Capetanaki et al., 1984, Parazzini et al., 1997).

However, little is known about its role and distribution in the myometrium. The fact that desmin is expressed very early in muscle development suggests that it may play a modulating role in myogenic differentiation (Lin et al., 1994, Parazzini et al., 1997).

Mice lacking desmin show severe disruption of the smooth muscle architecture, including loss of lateral alignment of myofibrils, perturbations of myofibrillar anchorage to the sarcolemma, abnormal mitochondrial number and organisation, and loss of nuclear shape and positioning (Milner et al., 1996).

These results are in agreement with the primary presence of desmin as an intermediate filament in myogenic cells. A reduced desmin in tamoxifen-administered mice might point to a perturbation or dysfunction of the myofibers, leading to weakness of its tensile strength and disruption with the resultant abnormal architecture. In skeletal muscles, desmin is essential for the tensile strength and integrity of myofibrils but not for myogenic commitment, differentiation and fusion (Shah et al., 2004, Milner et al., 1996, Park et al., 2000).

It is possible that disruption of the muscle layer allows invasion by the overlying endometrium. Adenomyosis development following tamoxifen treatment in CD-1 mice could also be due to an alteration in the composition of extracellular matrices, facilitating the “invasion” of the endometrial stroma and glands into the myometrium. Laminins and fibronectins are important glycoproteins components of the extracellular

matrix and basement membranes and are critically involved in cell differentiation in early development and in tissue formation and maintenance of mature tissues (Sasaki et al., 2004, Romberger, 1997). The findings in control mice are in agreement with previous reports (Brody and Cunha, 1989). The normal localisation of laminin and fibronectin observed following tamoxifen treatment suggests that these molecules are unlikely to be the primary target for tamoxifen effect.

The description of ER- $\alpha$  expression in control uteri is in agreement with previous studies (Kurita et al., 2001). Estrogen receptors have been identified in the epithelium, stroma, and myometrium of the developing uterus. In CD-1 mice, ER immunoreactivity was observed in stromal cells on day 1, and in epithelial cells by day 5 (Yamashita et al., 1989, Sato et al., 1992). The mode of action of tamoxifen is complex, but these results demonstrated that tamoxifen significantly downregulates ER- $\alpha$ . Tamoxifen is able to antagonize the action of calmodulin, protein kinase C and compete for membrane-binding sites for neurotransmitter substances (Lam, 1984, Horgan et al., 1986, Kroeger and Brandes, 1985, Batra, 1990). Myometrial strips from non-pregnant human myometrium showed a marked inhibition of spontaneous and vasopressin-induced contractions when tamoxifen was added to the bathing solution (Kostrzewska et al., 1997). This spasmolytic activity on smooth muscle was also demonstrated in the rat myometrium, where tamoxifen antagonised the contractions induced by exogenous calcium (Lipton and Morris, 1986). It is thus plausible that the myometrial abnormalities observed following tamoxifen treatment could be related to an underlying dysfunction in the active processes involved in the contractile machinery and the regulation of calcium metabolism.

In conclusion, these experiments demonstrated the development of adenomyosis in CD-1 mice as early as day 10, with over 80% of uteri being affected by day 15. The earliest

changes detected included discontinuity in the inner myometrial layer and in-growth of endometrial glands and stroma. The inner circular muscle layer exhibited marked thinning, lack of continuity and lack of orientation and bundling of the muscle cells. Desmin expression in these cells was markedly reduced. The findings suggest that abnormal development of the inner circular muscle layer resulting in its discontinuity may play a role in the development of uterine adenomyosis.

However, the prevalence of uterine adenomyosis in mice is strain-dependent. In CD-1 mice, spontaneous adenomyosis appears from about 6 months of age and by 12 months of age over 80% are affected with disease severity increasing thereafter (Greaves and White, 2006). In contrast, the C57/BL6J mouse strain is not known to develop spontaneous adenomyosis and is resistant to experimental adenomyosis (Irisawa and Iguchi, 1990, Mori et al., 1991, Mori et al., 1982). No research has been done on the effect of tamoxifen on C57/BL6J mice.

Whether the same inner myometrial changes and sequence of endometrial invasion can be demonstrated in a different mouse strain following tamoxifen administration is not known. To examine the possible strain (genetic) predisposition to tamoxifen induced adenomyosis, and to rule out the possibility that the the effect of tamoxifen on CD-1 mice is not strain specific, the following study will examine the effects of tamoxifen on the C57/BL6J mouse strain that is not known to develop spontaneous adenomyosis.

## **Chapter 3**

**The effects of tamoxifen on myometrial differentiation and organisation  
during early uterine development in the C57/BL6J mouse**

## **Chapter 3**

### **The effects of tamoxifen on myometrial differentiation and organisation during early uterine development in the C57/BL6J mouse**

#### **3.1 INTRODUCTION**

The previous experiment demonstrated the development of adenomyosis in CD-1 mice in response to tamoxifen. Whether the same inner myometrial changes and sequence of endometrial invasion can be demonstrated in a different mouse strain following tamoxifen administration is not known. This study will examine the effects of neonatal tamoxifen administration on the C57/BL6J mouse strain upon early uterine development and stromal / myometrial organisation and differentiation in order to examine the possible strain (genetic) predisposition to tamoxifen induced adenomyosis, the following study will examine the effects of tamoxifen on the C57/BL6J mouse strain that is not known to develop spontaneous adenomyosis.

#### **3.2 MATERIALS AND METHODS**

The study was conducted under the authority of the United Kingdom Home Office, Animals (Scientific Procedures) Act 1986. Pregnant time-mated C57/BL6J mice were obtained (Charles River Ltd, Margate, Kent, UK) and their female pups were divided into two groups. The first group (n=20) was orally dosed on days 1-5 after birth (day of birth being day 0) with 1mg/kg tamoxifen. The second control group received vehicle only (see chapter 2 for

preparation). Mice from the study group (n=5) and from the control group were culled on days 5, 10, 15 and 42. Uteri were collected and paraffin embedded cross sections were prepared and stained using the same technique as in chapter 2.

### **3.3 RESULTS**

Data on the uterine development in the control C57/BL6J mice is first presented, followed by the morphological changes observed in the tamoxifen group. Finally, the data on immunohistochemical markers is presented. The data is visually represented and summarised in tables 3.1 & 3.2, and figures 3.1 – 3.5.

#### **3.3.1 Morphology and uterine development**

##### **3.3.1.1 Normal uterine development of C57/BL6J mice**

**Day 5:** The uterine cavity had an oval-shaped lumen elongated in the mesometrial-antimesometrial axis. The luminal epithelium had tall columnar cells with elongated nuclei arranged in palisade with some multilayered areas. There was no evidence of gland formation. In the uterine wall, the mesenchymal cells started to segregate into three layers: endometrial stroma, inner circular and prospective outer longitudinal muscle layers. The prospective inner circular muscle layer was the most defined and densely staining. The cells were bundled, circularly orientated and tightly packed with elongated nuclei and minimal intercellular space. Vascular spaces started to appear, especially in the layer between the inner and outer myometrium (Figure 3.1A – 3.5A).

**Day 10:** Uterine sections had a more complex luminal epithelium invaginating the stroma to form simple tubular uterine glands. All layers of the uterine wall were more distinct. The stroma appeared more tightly packed and surrounded the endometrial glands. The inner

circular muscle layer was thicker compared to the outer myometrium and cells were organised into bundles. Longitudinally cut sections demonstrated elongated nuclei in the outer layer, confirming its longitudinal arrangement. Blood vessels were larger and observed in all layers of the uterine wall (Figure 3.1B – 3.5B)

**Day 15:** The adult configuration of the uterus was apparent. The endometrium had numerous simple tubular glands and a thick endometrial stroma. Stroma cells were randomly orientated, except around the individual glands where they appeared more circular. A distinct loose vascular layer separated the inner and outer myometrial layers. The outer myometrial cells became grouped in bundles connected by loose connective tissue sheaths and separated from the inner myometrium by a distinct loose vascular layer (Figure 3.1C – 3.5C).

**Day 42:** The adult uterus was larger and more complex, but had the same configuration as the uterus on day 15. The endometrial glands were more complex and branching, but were confined to the endometrial layer. The inner myometrium was quite distinct. The intervening vascular layer harboured most of the large blood vessels. The outer longitudinal muscle layer was composed of prominent bundles of cells with well-formed connective tissue sheaths (Figure 3.1D – 3.5D).

### **3.3.1.2 Uterine development following tamoxifen administration**

**Day 5:** The uterine epithelium was taller, with large pale elongated nuclei and prominent nucleoli. The uterine lumen was markedly dilated with prominent secretions, and the uteri were significantly heavier than controls. Blood filled spaces were seen throughout the uterine wall, which was thinner compared to controls. Some cells in the middle of the uterine wall

appeared to adopt circular orientation, but these were loosely bundled and only formed a thin patchy ring encircling about 25-40% of the uterus (Figure 3.2A – 3.5I).

**Day 10:** The uterine lumen was dilated and the endometrial stroma was highly cellular with ovoid nuclei. The luminal and glandular epithelium remained increased in height compared to controls. The myometrial layers were not distinct. Some cells had circular orientation but with no observable continuity. The interrupted bundles were surrounded by cellular stroma that appeared continuous with the endometrial stroma. The outer muscle layer was less obvious, with some bundles observed on the periphery (Figure 3.2B – 3.5J).

**Day 15:** The luminal and glandular epithelium was higher than controls. The circular muscle layer cells acquired darker staining cytoplasm and more obvious circular orientation. The outer myometrium showed signs of differentiation into bundles surrounded by thin loose connective tissue. The intervening vascular layer was not obvious although some prominent blood vessels were seen scattered in the uterine wall (Figure 3.2C – 3.5K).

**Day 42:** The uteri were smaller compared to controls. The endometrial stroma was highly cellular, and the glands developed normally, with the lining epithelium remaining higher than controls. The circular myometrium showed marked loosening and increased intercellular space. The outer myometrium was well developed with obvious bundling. Overall, the muscle integrity was more preserved on the anti-mesometrial border of the uterus. In summary, although the overall structure of the uterus was maintained and the outer longitudinal muscle layer developed normally, the development of the inner circular muscle layer was impaired, with marked dispersal of these cells. Overall, the muscle integrity was more preserved on the anti-mesometrial border of the uterus. Adenomyosis was not detected at any stage (Figure 3.2D, Figure 3.3 and 3.5L).

**Table 3.1: Comparison of the histological features measured at different stage of development of neonatal C57/BL6J mice after administration of tamoxifen or vehicle only, with reference to the similar CD-1 model (Chapter 2). Measurements are in  $\mu\text{m}$ : median (range).**

	C57/BL6J		CD-1 (Chapter 2)	
	Control	Tamoxifen	Control	Tamoxifen *
<b>Day 5</b>				
Epithelial height	10 (8-12)	12 (10-12)	18 (16-20)	25 (25-35)
Uterine wall thickness	75 (60-80)	80 (80-90)	110 (100-110)	70 (60-80)
Inner cellular layer (future stroma)	50 (45-55)	50 (45-60)	70 (60-80)	35 (35-40)
Inner circular muscle layer	15 (12-16)	9 (8-12)	30 (25-35)	20 (20-25)
Outer cellular layer (future outer myometrium)	10 (8-12)	10 (8-13)	12 (10-15)	12 (10-15)
<b>Day 10</b>				
Epithelium height	14 (12-14)	18 (18-20)	18 (16-20)	15 (12-20)
Uterine wall thickness	100 (90-110)	110 (90-115)	120 (110-130)	-
Inner cellular layer (future stroma)	55 (50-60)	-	90 (80-100)	-
Inner circular muscle layer	25 (20-26)	-	30 (25-35)	-
Outer cellular layer (future outer myometrium)	20 (18-22)	-	20 (15-25)	-

**Cont.**

**Table 3.1: Comparison of the histological features measured at different stage of development of neonatal C57/BL6J (Cont.)**

	C57/BL6J		CD-1 (Chapter 2)	
	Control	Tamoxifen	Control	Tamoxifen *
<b>Day 15</b>				
Epithelial height	12 (12-14)	14 (13-15)	18 (15-20)	18 (15-20)
Uterine wall thickness	115 (100-120)	100 (80-120)	170 (160-180)	-
Endometrial stroma	60 (55-70)	-	100 (90-110)	-
Inner circular myometrium	25 (22-28)	-	40 (35-40)	-
Intermediate vascular layer	10 (8-12)	-	10 (10-15)	-
Outer myometrium	20 (18-22)	20 (15-20)	25 (20-30)	25 (20-30)
<b>Day 42</b>				
Epithelial height	14 (12-16)	20 (15-20)	18 (15-20)	20 (15-20)
Uterine wall thickness	160 (150-170)	170 (160-180)	340 (320-360)	-
Endometrial stroma	70 (65-80)	-	120 (110-130)	-
Inner circular muscle layer	40 (30-45)	-	80 (75-90)	-
Intermediate vascular layer	20 (18-22)	-	50 (50-55)	-
Outer myometrium	30 (28-34)	35 (30-50)	90 (85-100)	50 (40-60)

\* The uteri in the CD-1 mice dosed with tamoxifen had wide irregular lumens and poorly defined layers characterised by penetrating stroma, markedly disrupted circular layer. The whole uterine structure was so disorganized with glands and surrounding stroma dispersed throughout the uterine wall, with few scattered muscle fibers and blood vessels. The wall thickness was measured from the luminal epithelium of the central lumen to the serosal edge. However, the central lumen was not identified in most CD-1 specimens treated with tamoxifen. Where the structures were intermingled and too indistinct to measure separately, some measurements were absent (-).

### **3.3.2 Immunohistochemical markers**

#### **3.3.2.1 $\alpha$ -Smooth Muscle Actin ( $\alpha$ -SMA) expression**

A narrow but distinct zone of variable staining intensity corresponding to the developing inner circular myometrium was seen in the middle of the uterine wall by day 5. On day 10, this layer strongly expressed  $\alpha$ -SMA. Expression in the outer longitudinal muscle layer was less intense. Uteri from day 15 onwards exhibited well-defined, intense staining of both the inner and outer muscle layers (Figure 3.1E-H and 3.5E-H).

In the tamoxifen group,  $\alpha$ -SMA expression was weaker, with fewer positive cells per area, reflecting disruption and loosening of the circular myometrium. Staining intensity was generally weaker in the inner circular as compared to the outer longitudinal muscle layers (Figure 3.2E-H and 3.5M-P).

#### **3.3.2.2 Desmin expression**

In control C57/BL6J mice, desmin expression followed a ‘wave’ of maturation from inside outwards. Initially, on day 5, the developing endometrial stroma strongly expressed desmin, whilst the myometrial uterine wall remained less intense. By day 10 and 15, as the inner and outer and longitudinal myometrium layers developed, they acquired and expressed stronger immunostaining to desmin compared to the endometrial stroma that reverted to be weakly positive. The blood vessel wall stained strongly positive, whilst endometrial epithelium was negative (Figure 3.1I-L). In pups receiving tamoxifen this “wave” of maturation was absent. The intensity of staining remained uniformly weak throughout the developmental phases (day 5 – 42) of the uterine wall structures. Generally, the intensity of staining was weaker than in controls. The endometrial epithelium remained negative (Figure 3.2I-L).

### **3.3.2.3 Vimentin expression**

Vimentin expression was observed in the endometrial stroma and blood vessels walls on day 15 and day 42, in both groups. No staining was seen in the myometrium. In some uteri, occasional staining was observed in the developing stroma on day 5 but this was not consistent. Blood vessels walls stained positive and were considered intrinsic quality control (Figure 3.1, Figure 3.2 M-P, and Figure 3.4).

### **3.3.2.4 Laminin and fibronectin expression**

On day 5, laminin expression was more localised to the middle third of the developing uterus i.e. the prospective inner circular muscle layer, while fibronectin was differentially expressed in the prospective endometrial stroma or the inner third of the developing uterus. The same expression pattern was observed on day 10 and subsequently. Laminin was exclusively expressed in the extracellular matrix surrounding the smooth muscle layers (inner circular and outer longitudinal). Fibronectin was exclusively expressed around the stromal cells and in the connective tissue sheaths separating the outer longitudinal muscle, and the intervening vascular layer. There was no difference in the localisation of laminin or fibronectin between the controls or tamoxifen groups. However, laminin expression was reduced in the tamoxifen group.

### **3.3.2.5 ER-alpha expression**

In the control mice, the whole thickness of the uterine wall expressed ER- $\alpha$  from day 2, while the epithelial lining remained negative till day 10, when the glandular epithelium in the glands necks exhibited some staining. As the various layers developed in the mesenchyme, ER- $\alpha$  immunostaining was more intense in the stroma as compared to the muscle layers. Staining intensity was more variable by day 42. This variation may or may not represent a reflection of

estrous cycle related changes. This cannot be ascertained, as vaginal smears were not performed (Figure 3.1Q-T, and Figure 3.4).

In tamoxifen treated mice, the overall ER- $\alpha$  expression was attenuated compared to control uteri. There was marked reduction of ER- $\alpha$  immunostaining, with no or very weak staining in all layers on days 5 and 10. However, by day 15, the ER- $\alpha$  staining has recovered in the endometrial layers (luminal epithelium and stroma), but was less obvious in the myometrium. On day 42, the glands and stroma were less positive, and both inner and outer muscle layers remained faintly immunopositive (Figure 3.2Q-T).

**Table 3.2: Immunohistochemical expression of desmin and vimentin in the uterus of C57/BL6J mice. All blood vessels wall stained strongly positive with vimentin.**

	Control		Tamoxifen	
	Desmin	Vimentin	Desmin	Vimentin
<b>Day 5</b>				
Inner layer	+++	-	++	-
Middle layer	++	-	+	-
Outer layer	++	-	+	-
<b>Day 10</b>				
Stroma	++	-	+	-
Inner myometrium	+++	-	+	-
Outer myometrium	++	-	+	-
<b>Day 15</b>				
Stroma	++	+	+	+
Inner myometrium	++	-	+	-
Outer myometrium	+++	-	+	-
<b>Day 42</b>				
Stroma	+	+	+	+
Inner myometrium	++	-	+	-
Outer myometrium	+++	-	+	-

**Figure 3.1: Control C57/BL6J mice. Hematoxylin & Eosin (A – D) and immunohistochemical staining patterns for alpha-smooth muscle actin (E – H), desmin (I – L), vimentin (M – P), and ER-alpha (Q – T). Magnification: Days 5, 10, and 15 micrographs (x20), day 42 (x10).**

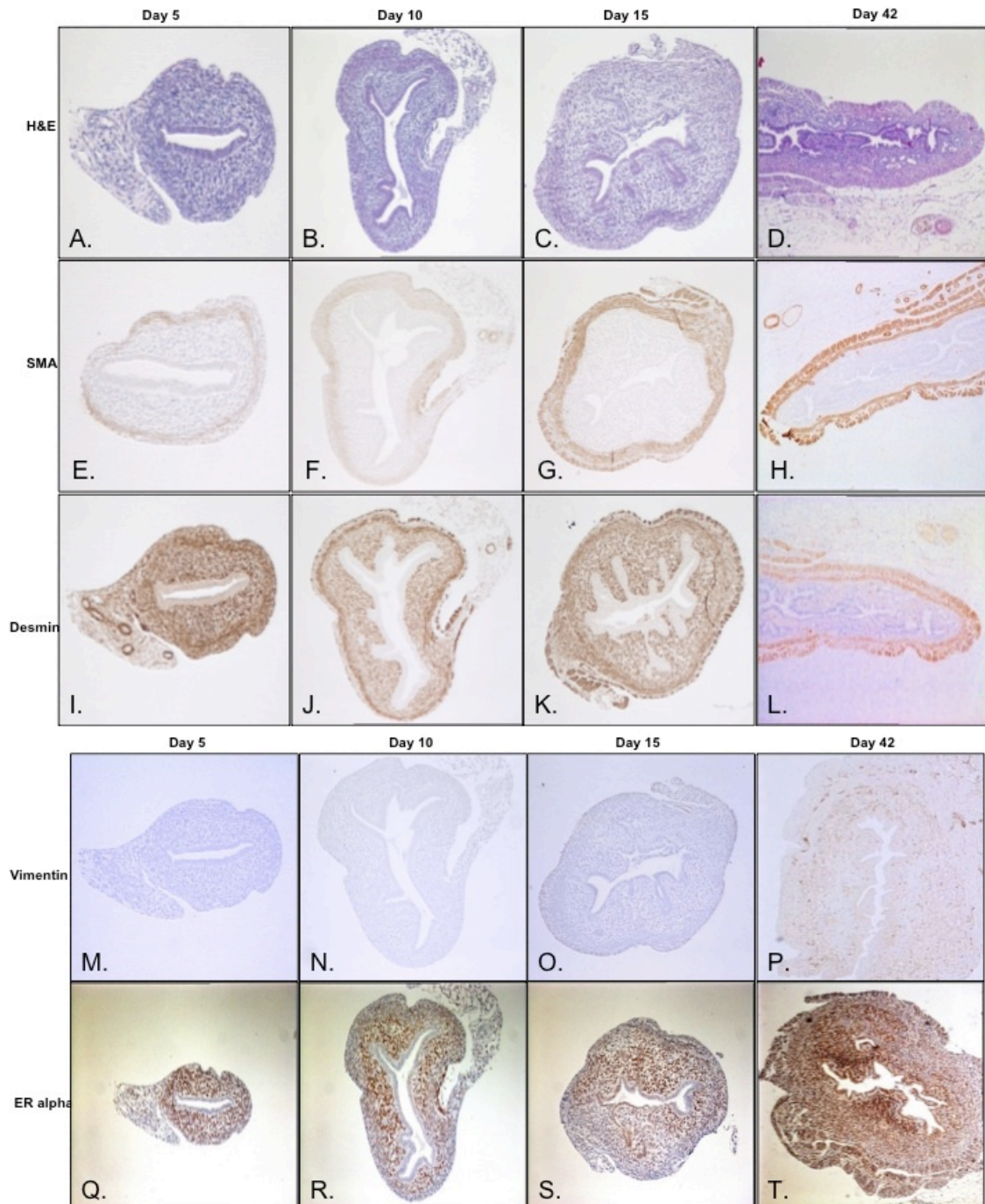


**Figure 3.2: Tamoxifen treated C57/BL6J mice. Hematoxylin & Eosin (A – D) and immunohistochemical staining patterns for alpha-smooth muscle actin (E – H), desmin (I – L), vimentin (M – P), and ER-alpha (Q – T). Magnification: Days 5, 10, and 15 micrographs (x20), day 42 (x10).**

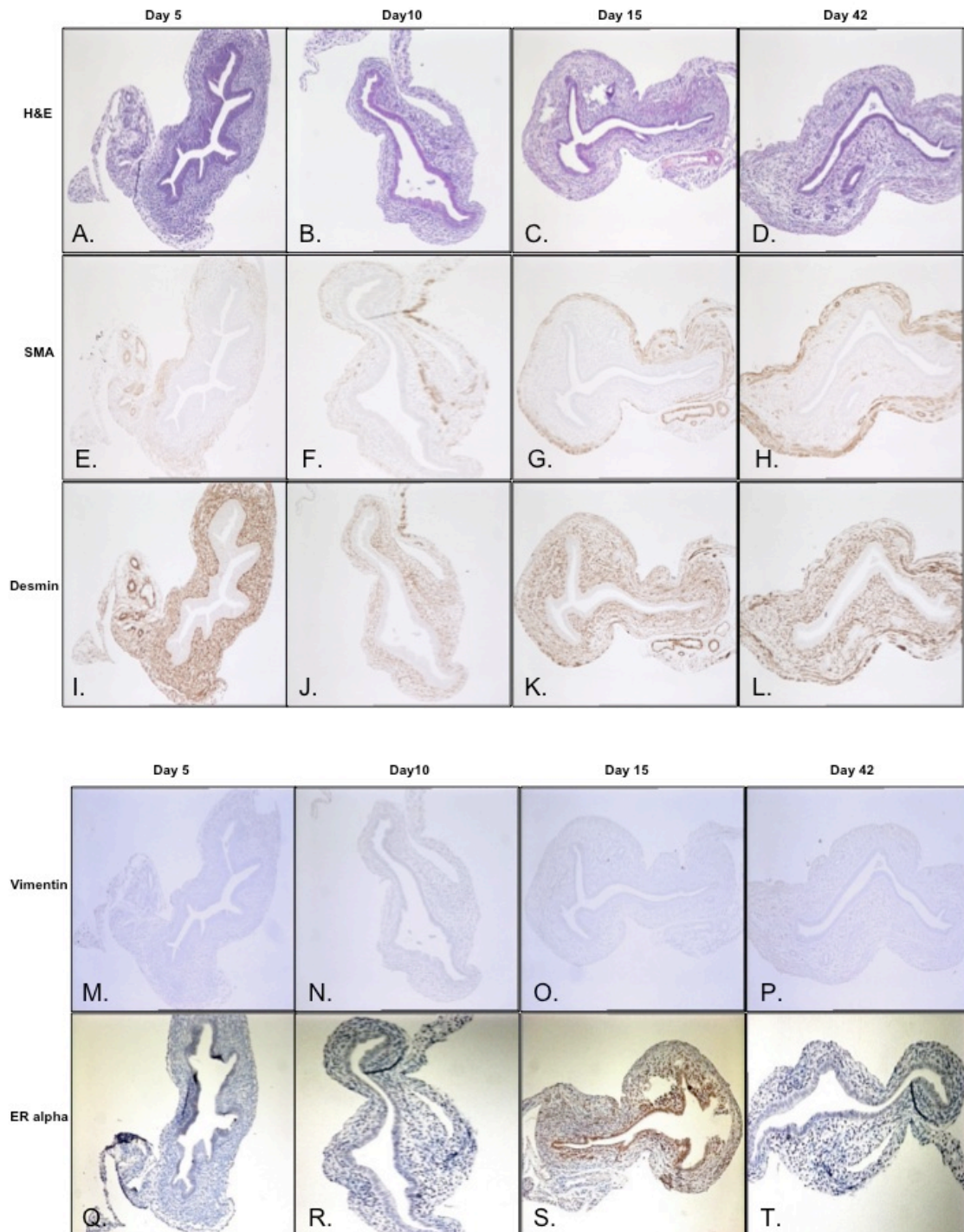


**Figure 3.3: Comparison between day 42 uteri of A: CD-1 mice treated with Tamoxifen and B: C57/BL6J mice treated with Tamoxifen. The inner myometrium (IM) is disrupted in both species, with the outer myometrium (OM) formed normally. The endometrium (endo) is well contained in the C57/BL6J uterus, but invades deeper to the inner myometrium in the CD-1 uterus, forming adenomyosis foci (Adeno). Some adenomyosis foci are subserosal, There is attenuation of the vascular layer in both uteri. Magnification: (x10).**

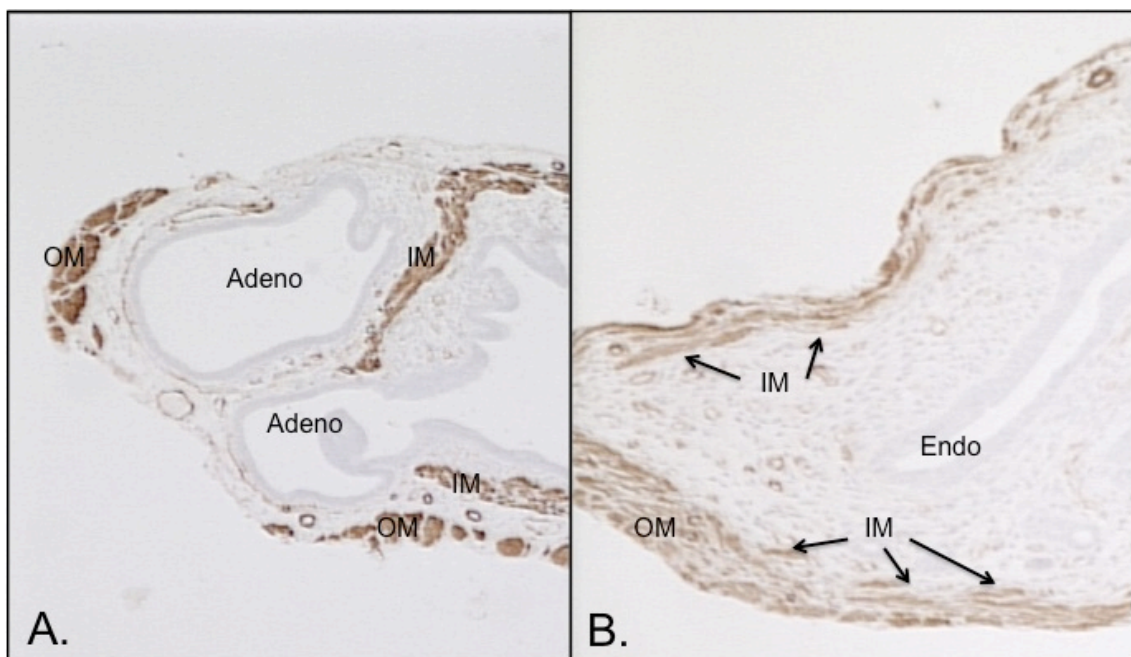


**Figure 3.4: Immunohistochemical staining of A: Vimentin, day 15, control C57/BL6J uterus; B: Vimentin, day 15, Tamoxifen treated C57/BL6J uterus; and C: Vimentin, day 42 Tamoxifen treated C57/BL6J uterus. Vimentin expression was observed in the endometrial stroma and blood vessels walls (arrows). No staining was seen in the myocytes. D: ER-alpha immunostaining, day 15, control uterus showing staining in the developing neck glands (arrow heads). Magnification: (x40).**

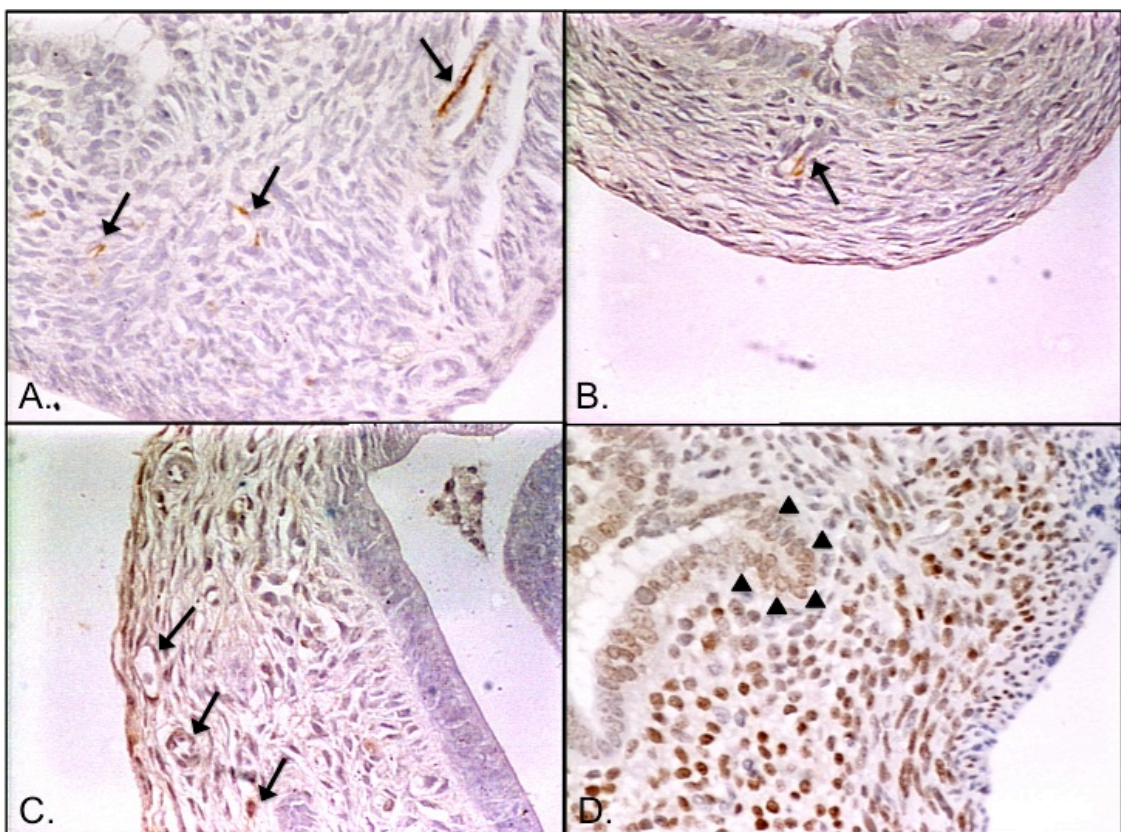
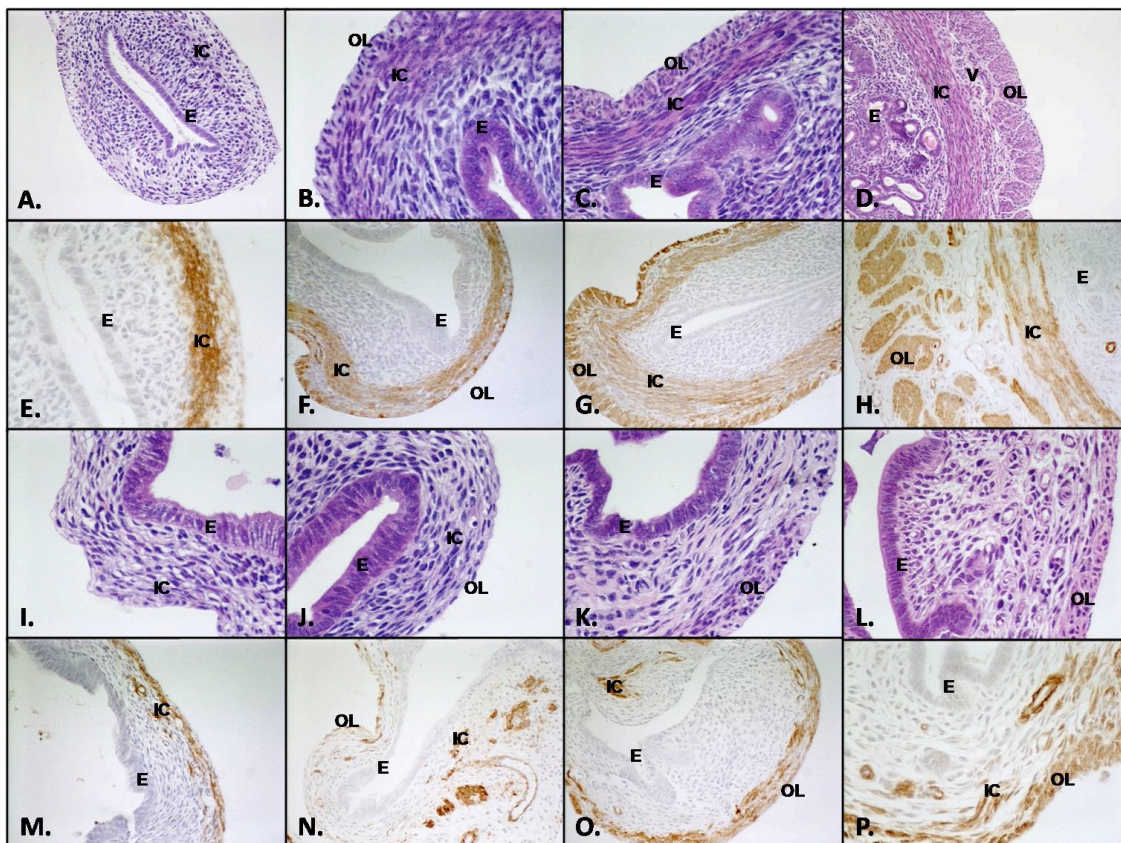


**Figure 3.5: A-D: Hematoxylin and Eosin stained section of control C57/BL6J mice (day 5, 10, 15 & 42). Mesenchymal cells appear to segregate into three layers: endometrium and endometrial stroma (E), inner circular (IC) and outer longitudinal (OL) muscle layers. A distinct loose vascular layer (V) separated the inner and outer myometrial layers from day 15 onwards. E-H (day 5, 10, 15 & 42): a-SMA immunostaining showing the progressive development of the IC and OL muscle layers. I-L: Hematoxylin and eosin stained and M-P (day 5, 10, 15 & 42): a-SMA immunostained uterine sections from tamoxifen treated mice. Note the dilated uterine lumen, prominent blood vessels, and thinner uterine walls. The IC muscle layer is poorly developed and fragmented. The myometrial layers are less distinct, and although the overall structure of the uterus was maintained and the OL muscle layer developed normally, the development of the IC muscle layer was impaired, with marked dispersal of these cells. Adenomyosis was not detected at any stage.**



### 3.4 DISCUSSION

Perinatal uterine development represents a critical phase for uterine morphogenesis and differentiation (Iguchi and Sato, 2000). In the previous experiment (chapter 2), it was demonstrated that neonatal exposure to tamoxifen in CD-1 mice, but not estradiol, resulted in failure of full differentiation and development of the inner circular myometrial layer. In-growth of endometrial glands and stroma was observed deep within the myometrium representing development of adenomyosis.

In the present study, in the C57/BL6J mice, which are constitutionally smaller than CD-1 mice but in which uterine developmental stages are similar (Cunha, 1976, Cunha et al., 1992, Brody and Cunha, 1989), exposure to tamoxifen also resulted in disruption of uterine myometrial development but unlike in CD-1 mice, not to the in-growth of the endometrium and development of adenomyotic changes. The similar effects upon myometrial development include that upon  $\alpha$ -SMA, desmin and vimentin expression in the inner myometrial and of extracellular matrix components. The effect upon the circular inner myometrial layer in the C57/BL6J mouse was maintained into the adult period without any indication of the development of adenomyosis.

Tamoxifen affected the morphological development of the inner circular muscle layer where normally muscle cells would be closely packed in circular orientation.

Additionally, there was some evidence that it was associated with a failure of full uterine smooth muscle cell differentiation. Thus, although developing myometrium expressed some immunohistochemical markers indicative of myogenic differentiation such as  $\alpha$ -SMA, expression of the latter was delayed and attenuated, and cells exhibited reduced desmin expression. This may indicate that tamoxifen exposure during this critical neonatal period may inhibit full differentiation of mesenchymal cells to smooth muscle cells and their phenotype may resemble a form of intermediate myofibroblasts

or immature smooth muscle cells. Reduced desmin in uterine muscle of tamoxifen-administered mice might also indicate a perturbation or dysfunction of their myofibers, leading to a reduction in tensile strength and disruption with the resultant abnormal architecture. Laminin is an important component of the basal lamina associated with smooth muscle and its expression being unaffected by tamoxifen may indicate normal smooth muscle differentiation; however its expression is also associated with myofibroblasts and immature forms of smooth muscle cells

Neonatal exposure to tamoxifen therefore interferes with subsequent uterine myometrial development, specifically the inner circular muscle coat. This does not appear to be strain specific. As tamoxifen effects are most likely to be mediated via estrogen receptors, it is interesting to note that they have been identified in the epithelium, stroma, and the myometrium of the developing uterus (Kurita et al., 2001). However, some strain dependent differences in expression in the uterus of neonatal mice have been reported. In CD-1 mice, ER immunoreactivity was observed in stromal cells on day 1, and in epithelial cells by day 5 (Yamashita et al., 1989, Sato et al., 1992). In BALB/c mice, ER expression was delayed till day 5 in the stroma and until day 14 in the epithelial cells (Yamashita et al., 1989, Li, 1994). Glandular development in the uteri of CD-1 mice has also been reported to be advanced by 3 days compared to BALB/c mice (Bigsby et al., 1990). In the absence of differences in the expression of ER- $\alpha$  distribution in C57/BL6J and CD-1 strains, it is unlikely that the different responses to tamoxifen are attributed to differences in ER- $\alpha$  expression in the myometrium.

The fact that in C57/BL6J mouse strain tamoxifen-induced changes were not associated with adenomyosis, per se suggests an additional factor is required. It may be of relevance that neonatal tamoxifen exposure caused early adenomyosis only in the CD-1

strain, which exhibits a high rate of spontaneous adenomyosis during late adult life. The presence of inner myometrial defects caused by tamoxifen may allow the constitutively 'invasive' endometrium to invade the inner muscle coat resulting in premature adenomyosis. This would suggest that in the 'predisposed' CD-1 strain the glandular and/or stromal components of the endometrium possess a higher invasive capacity. Thus, in the C57/BL6J strain, although tamoxifen produces the same circular muscle coat defect, the endometrium does not invade the disrupted muscle layer and does not present with adenomyosis.

It is interesting to note that in SHN strain which also exhibits age-related spontaneous adenomyosis the administration of the matrix metalloproteinase inhibitor ONO-4817 retarded the progression of uterine adenomyosis (Mori et al., 2002), which again suggests a role for an aggressive stromal invasion. The absence of differences in the extracellular matrix proteins laminin and fibronectin following tamoxifen administration (Romberger, 1997, Sasaki et al., 2004), also suggests that alterations in the myometrial layers is the primary cause of endometrial invasion into these tissues.

It seems that disruption of the inner myometrium cannot on its own explain the development of uterine adenomyosis and although these changes may be a prerequisite for the premature development of adenomyosis, additional genetic or epigenetic differences between strains expressed in the endometrium may be required. Elucidation of these strain-dependent mechanisms may contribute to the understanding of the pathology of adenomyosis in the human.

In conclusion, this section used a neonatal mouse model to examine the histogenesis of uterine adenomyosis, and to test whether adenomyosis is due to an abnormality in myometrial differentiation, or in extracellular matrix proteins expression. Data from the CD-1 mouse model (chapter 2) suggest that disruption of the inner myometrium may

play a role in the development of uterine adenomyosis. However, when the same experiment was repeated on the C57/BL6J mouse strain, the results suggest that adenomyosis development is not necessarily linked to the inner myometrial disruption on its own. Although tamoxifen induces inner myometrial changes in C57/BL6J neonatal mice similar to those induced in CD-1 mice, the C57/BL6J mice did not develop adenomyosis. It was also noted that the outer myometrium was not affected in either mouse strains, irrespective of the presence or absence of adenomyosis. These findings suggest that the inner and outer myometrial layers are different in their response to external stimuli and to the presence or absence of adenomyosis.

These results lead to the hypothesis that similar or other differences exist between the inner myometrium of uteri affected by adenomyosis and the inner myometrium of normal uteri. The following section will study the human uterus in order to detect if similar changes and differences exist between the inner and outer myometrial layers in the presence or absence of uterine adenomyosis in humans.

## **Section II**

### **Role of the myometrium and endometrial stroma in the development of human uterine adenomyosis**

## **Chapter 4**

### **Phenotypic characterization of the inner and outer myometrium in normal and adenomyotic uteri**

## Chapter 4

### Phenotypic characterization of the inner and outer myometrium in normal and adenomyotic uteri

#### 4.1 INTRODUCTION

The human myometrium is structurally different to that of the mouse uterus. Whereas in the mouse uterus the myometrium is organised in three distinct layers (inner circular, middle vascular, and outer longitudinal layers), the human myometrium seems at first sight to be homogenous under light microscopy, with no obvious layering. However, MRI has defined a structurally different “junctional zone” or subendometrial myometrium that forms the outer boundary of the EMI (Brosens et al., 1998).

The uterine junctional zone (JZ) is seen in T2-weighted magnetic resonance imaging (MRI) as a distinct low intensity inner band in the myometrium (Brosens et al., 1998). The same layer is often seen as a subendometrial halo using high resolution ultrasound (Kunz et al., 2000). The junctional zone was shown to be hormonally dependent; being indistinct before puberty and after the menopause, and showing maximum increase in thickness in the second half of the proliferative phase (Wiczuk et al., 1988, Demas et al., 1986). The normal JZ as seen in MRI or ultrasound is defined as being regular and  $\leq 5\text{mm}$  thick (Mark et al., 1987), and a  $\text{JZ} \geq 12\text{mm}$  is highly predictive of adenomyosis (Reinhold et al., 1998). The diffuse homogenous low-signal-intensity seen in adenomyosis is attributed to smooth muscle hyperplasia; a recognised feature of the disease (Fusi et al., 2006).

Studies using video-sonography have demonstrated peristaltic waves confined to the JZ myometrium. These waves vary during the cycle (Ijland et al., 1997). JZ contractions during the late proliferative phase may have a role in sperm transport, whilst quiescence during the secretory phase may facilitate implantation (Fanchin et al., 1998).

The reason for the distinct MRI appearance remains uncertain. In the normal uterus, differences between the JZ and outer myometrium are not well characterised (Lee et al., 1985). The MRI appearance may be related to different water content (McCarthy et al., 1989b). Differences in blood flow have been proposed, but these are unlikely to account for the zonation which is also noted in uterine specimens following hysterectomy (Scoutt et al., 1991). The distinct zonation seen on MRI may be related to a three-fold increase in the percentage of nuclear area - reflecting an increase in both size and number of nuclei - at the JZ compared to the outer myometrium (Scoutt et al., 1991). The density of the extracellular matrix components collagen, laminin and fibronectin, did not vary between the inner and outer myometrium of uteri without adenomyosis (Scoutt et al., 1991). But other components such as laminin  $\beta$ 2 and elastin were shown to be less abundant in the inner compared to the outer myometrium (Campbell et al., 1998, Metaxa-Mariatou et al., 2002).

In the previous chapter, tamoxifen was shown to cause disruption of the inner myometrium in CD-1 and C57/BL6J even though the latter species did not develop adenomyosis. The outer myometrium appeared unaffected. There were differences in mesenchymal markers, mainly a reduction in desmin expression following tamoxifen administration compared to controls. Together with the presence of a disrupted inner myometrium, this suggests that the myometrium from uteri with adenomyosis may exhibit different features compared to unaffected uteri. It also suggests that the inner

and outer myometrial layers are different in their response to external stimuli and to the presence or absence of adenomyosis.

In order to detect whether similar changes exist in the human myometrium, this study will examine the histological structure and immunohistochemical characteristics of the inner and outer myometrium of human uteri affected with adenomyosis compared to controls.

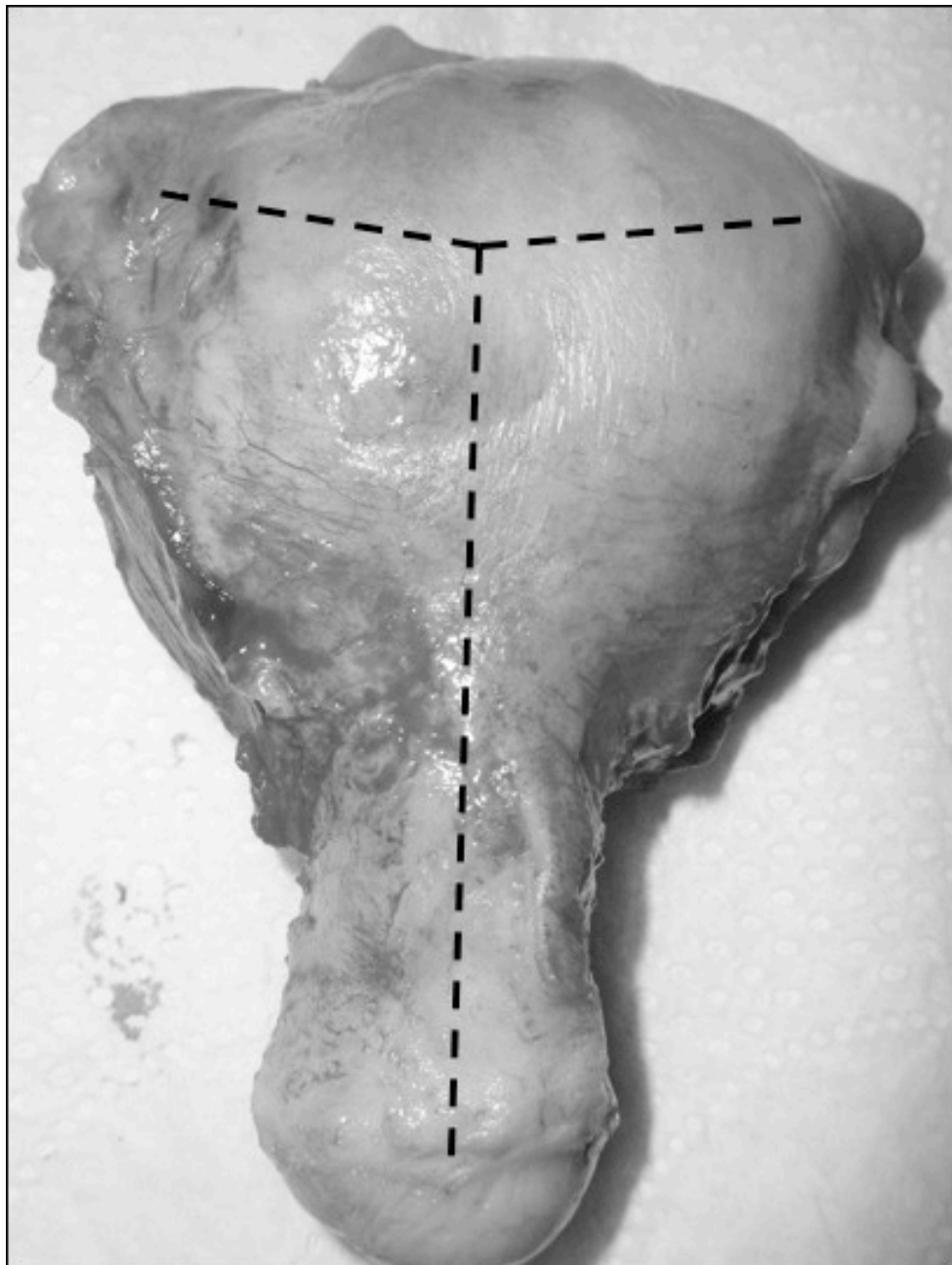
## **4.2 MATERIALS AND METHODS**

### **4.2.1 Samples**

The study was approved by the Leicestershire Research Ethics Committee. All samples from premenopausal women were obtained from hysterectomy specimens where menorrhagia was the main indication for the operation. Postmenopausal uteri were removed by vaginal hysterectomy for prolapse. Histological sections encompassing the full uterine wall thickness from endometrium to the serosa were used for this study. All samples were obtained from the anterior wall of the uterus near the fundus (Figure 4.1). For the purpose of this experiment, a cut-off point of >2.5mm for glandular extension below the endometrial-myometrial interface (EMI) has been used to define adenomyosis (Uduwela et al., 2000). Menstrual cycle specimens were classified according to the phase of the menstrual cycle into early, mid-, late-proliferative (EP, MP, LP) and early, mid-, late-secretory (ES, MS, LS), using histological criteria (Noyes and Haman, 1953). Postmenopausal specimens had atrophic endometrium (AT). The study included 45 control uteri with no endometrial or myometrial pathology (i.e. no fibroids, endometrial hyperplasia, malignancy, or polyps) (EP=5; MP=6; LP=5;

ES=8;MS=6; LS=5; AT=10) and 64 uteri with adenomyosis as the sole pathology (EP=10; MP=11; LP=6; ES=8; MS=9; LS=10; AT=10).

**Figure 4.1: Figure illustrating the way the anterior uterine wall was incised in the midline, and towards the cornual ends. The area sampled was at the intersection of the three lines (i.e. the anterior wall of the uterus near the fundus).**



#### **4.2.2 Immunohistochemistry**

Serial sections were immunohistochemically stained for the mesenchymal markers:  $\alpha$ -smooth muscle actin ( $\alpha$ -SMA), desmin, and vimentin, and for marker of proliferation (Ki-67). In summary, sections were dewaxed in xylene, and rehydrated in graded alcohols and water. Epitope antigen retrieval for Ki67 was performed using microwave and citrate buffer (pH = 6.0). Endogenous peroxidase activity was blocked with 6% (v/v) hydrogen peroxide ( $H_2O_2$ ). Sections were incubated overnight at 4°C with the primary antibodies against  $\alpha$ -SMA (mouse monoclonal, clone 1A4, 1:50 (v/v), Dako, Cambridge, UK); desmin (mouse monoclonal, clone DR33, 1:50 (v/v), Dako, Cambridge, UK); vimentin (mouse monoclonal, clone V9, 1:2300 (v/v), Sigma, UK); and Ki-67 (mouse monoclonal, clone NCL-KI-MM1, 1:150 (v/v), Novocastra, Newcastle upon Tyne, UK). Biotinylated rabbit anti-mouse was used (Dako, Cambridge, UK) at a concentration of 1:400 (v/v) as secondary antibody. Immunoreactivity was demonstrated with 3,3'-diaminobenzidine/  $H_2O_2$  (DAB solution) (Vector labs, Peterborough, UK). Sections were lightly counterstained with haematoxylin, then dehydrated and cleared in graded alcohol and xylene.

#### **4.2.3 Image analysis & validation**

Image capture and analysis was performed using Axioplan® 2 light microscope (Carl Zeiss, Germany) and an image capture system, based on a single chip colour video camera (Sony DXC-151P, Sony Inc., Japan), a camera adapter (Sony CMA-151P, Sony Inc., Japan), and a Meteor 2 MMC graphics display. Digital image analysis was performed using Axiovision image analysis software (version 4.0, Carl Zeiss, Germany). Standardisation was performed by maintaining the same illumination and settings through the experiment. Acquired images were optimized by correcting for image border artefacts and non-uniform illumination. The areas of interest were selected

through image segmentation in true color followed by thresholding and watershed correction. Desired features were measured after visual confirmation of each section. The measurements were exported into datasheets for further analysis. A programmed workflow maintained the settings for all experiments. After capture, microscopic images were analysed blind of the histological diagnosis.

Manual counts were performed on random sections, and were found to agree with the automated measurement functions within 5% margin of error. As an additional validation, Feulgen nuclear staining (Scoutt et al., 1991) was performed on duplicate sections and the results were found to correlate with the results obtained from examination of H&E slides (Lin's concordance correlation coefficient = 0.88) (Lin, 1989, Lin, 2000).

#### **4.2.4 Measurements**

Sequential high-power fields (hpf x200;  $124,403 \mu\text{m}^2$ ) of the whole myometrial thickness from the endometrium to the serosa were examined. Sequential measurements avoided any glandular tissue, large blood vessels, or any sectioning artefact. In each captured field, the following parameters were measured: the number of nuclei (nuclear count = n/hpf) to reflect cell density, the total nuclear area i.e. area of the image occupied by nuclei (expressed as percentage), and the average nuclear size ( $\mu\text{m}^2$ ).

The muscle mass was calculated as percentage positive area expressing  $\alpha$ -SMA per hpf using image analysis. The same method was used to examine desmin expression.

Vimentin immunostaining was examined and expressed as Staining Index (SI) (Tuxhorn et al., 2002). The percentage of positive cells was graded on a scale of 0 – 3 (0 = 0% positive cells, 1 = 1 – 33% positive cells, 2 = 34 – 66% positive cells; and 3 = 67 – 100% positive cells), and multiplied by the score for staining intensity (0 = no staining,

1 = weak staining, 2 = moderate staining; and 3 = intense staining), to give the Staining Index (range 0 – 9) (Tuxhorn et al., 2002). The Proliferation Index (PI) was calculated as the percentage of Ki67 positive cells.

#### **4.2.5 Statistical analysis**

The minimum number of cases (34 per group) was calculated in order to satisfy a two-sided *t*-test with 80% power, and  $\alpha = 0.05$  to detect difference between the two groups means. Based on pilot calculation the effect size was = 0.7. Samples were collected till an adequate representation of all phases of the menstrual cycle was obtained. Graphpad Instat<sup>®</sup> 3 and Graphpad Prism<sup>®</sup> 5 software were used for statistical analysis (GraphPad Software, San Diego California USA, [www.graphpad.com](http://www.graphpad.com)). Data were tested for normality using the Kolmogorov-Smirnov test and comparisons were made using Student's *t*-test for continuous data and Mann-Whitney U-test for non-continuous data. One-way analysis of variance (ANOVA) with Tukey's correction for multiple testing was used to compare the data across the menstrual cycle.

### **4.3 RESULTS**

In premenopausal women, with or without adenomyosis, cell density, nuclear size, total nuclear area and muscle mass were significantly greater ( $p < 0.01$ ) in the IM compared to OM (Table 4.1).

**Table 4.1: Overall characteristics of the inner (IM) and outer myometrium (OM) in control and adenomyotic uteri in premenopausal uteri. Values expressed as mean  $\pm$  SEM.**

	Control group (n=35)		Adenomyosis group (n=54)	
	IM	OM	IM	OM
<b>Cell density, nuclear count (n/hpf)</b>	1171 $\pm$ 52 <sup>a</sup>	801 $\pm$ 43	970 $\pm$ 36 <sup>a,b</sup>	625 $\pm$ 25 <sup>b</sup>
<b>Nuclear size (<math>\mu\text{m}^2</math>)</b>	24.81 $\pm$ 0.47 <sup>a</sup>	23.44 $\pm$ 0.52	26.38 $\pm$ 0.27 <sup>a,b</sup>	25.15 $\pm$ 0.33 <sup>b</sup>
<b>Total nuclear area (%)</b>	23.12 $\pm$ 1.17 <sup>a</sup>	14.83 $\pm$ 0.8	20.54 $\pm$ 0.77 <sup>a,b</sup>	12.76 $\pm$ 0.57
<b>Muscle mass (%/hpf)<sup>c</sup></b>	65.01 $\pm$ 0.76 <sup>a</sup>	42.6 $\pm$ 1.39	65.01 $\pm$ 0.76 <sup>a</sup>	46 $\pm$ 1.25

<sup>a</sup> Statistically significant compared to the outer myometrium ( $p < 0.01$ ) in the same group (control and adenomyosis).

<sup>b</sup> Statistically significant compared to the corresponding zone in the control group ( $p < 0.05$ )

<sup>c</sup> Expressed as percentage area expressing  $\alpha$ -SMA per high power field

The same was noted in postmenopausal women, but the difference in nuclear size did not reach statistical significance. In premenopausal uteri with adenomyosis, both the IM and OM featured lower cell density and larger nuclear size compared to controls ( $p < 0.05$ ), and the total nuclear area was lower in adenomyosis compared to controls, but the difference was statistically significant in the IM but not the OM ( $p = 0.013$  and  $0.09$  respectively). Although they did not reach statistical significance, similar differences were noted in the postmenopausal uteri. None of the measured parameters varied with the phase of the cycle in the IM or OM of control uteri. In adenomyosis, there was a statistically significant ( $p < 0.05$ ) reduction in cell density and total nuclear area during the mid-secretory phase in the IM, but not the OM (Table 4.2 and Figure 4.2).

**Table 4.2: Characteristics of the inner (IM) and outer (OM) myometrium in control and adenomyotic uteri of post-menopausal women. Data expressed as mean  $\pm$  SEM.**

	Control group (n=10)		Adenomyosis group (n=10)	
	IM	OM	IM	OM
<b>Cell density, nuclear count (n/hpf)</b>	1374 $\pm$ 53 <sup>a</sup>	813 $\pm$ 55	1106 $\pm$ 44 <sup>a</sup>	778 $\pm$ 61
<b>Nuclear size (<math>\mu\text{m}^2</math>)</b>	24.6 $\pm$ 0.89	24.5 $\pm$ 0.59	26.2 $\pm$ 0.72	25.6 $\pm$ 0.84
<b>Total nuclear area (%)</b>	26.7 $\pm$ 1.51 <sup>a</sup>	16.3 $\pm$ 1.23	23.4 $\pm$ 0.74 <sup>a</sup>	16.2 $\pm$ 1.49
<b>Muscle mass (%/hpf)<sup>b</sup></b>	57.27 $\pm$ 3.85 <sup>a</sup>	39.35 $\pm$ 1.85	62.78 $\pm$ 2.45 <sup>a</sup>	44.54 $\pm$ 5.61

<sup>a</sup> Statistically significant compared to the outer myometrium ( $p < 0.01$ ).

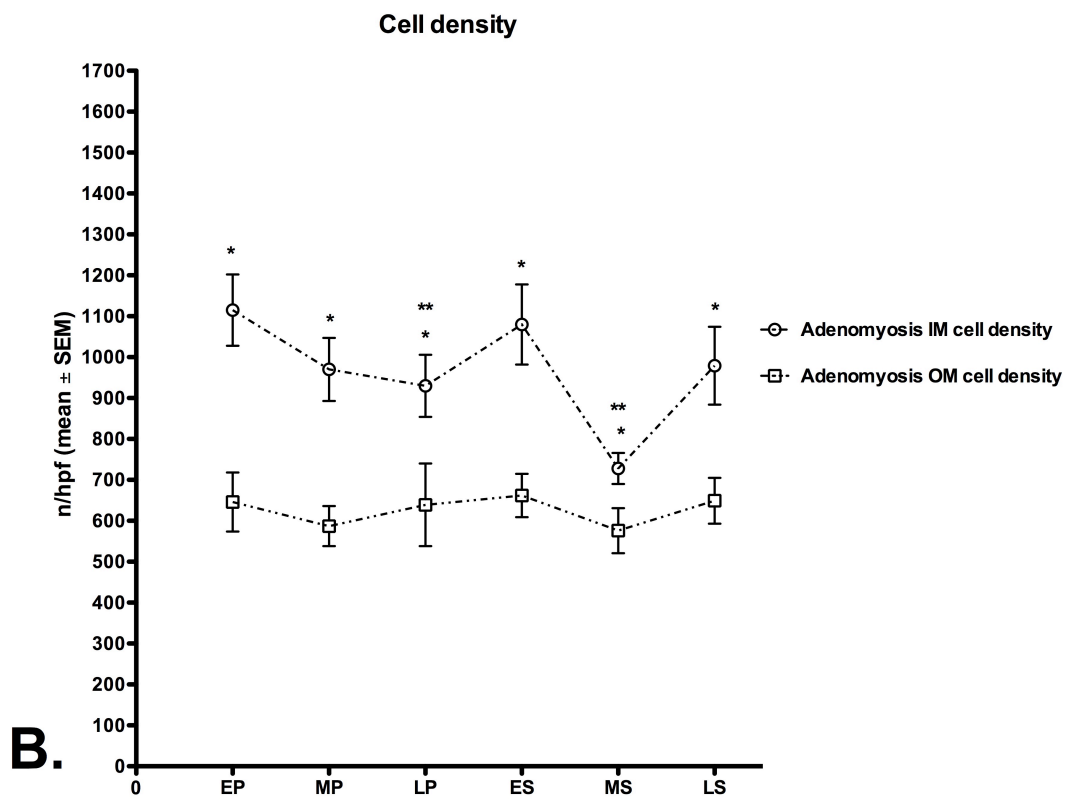
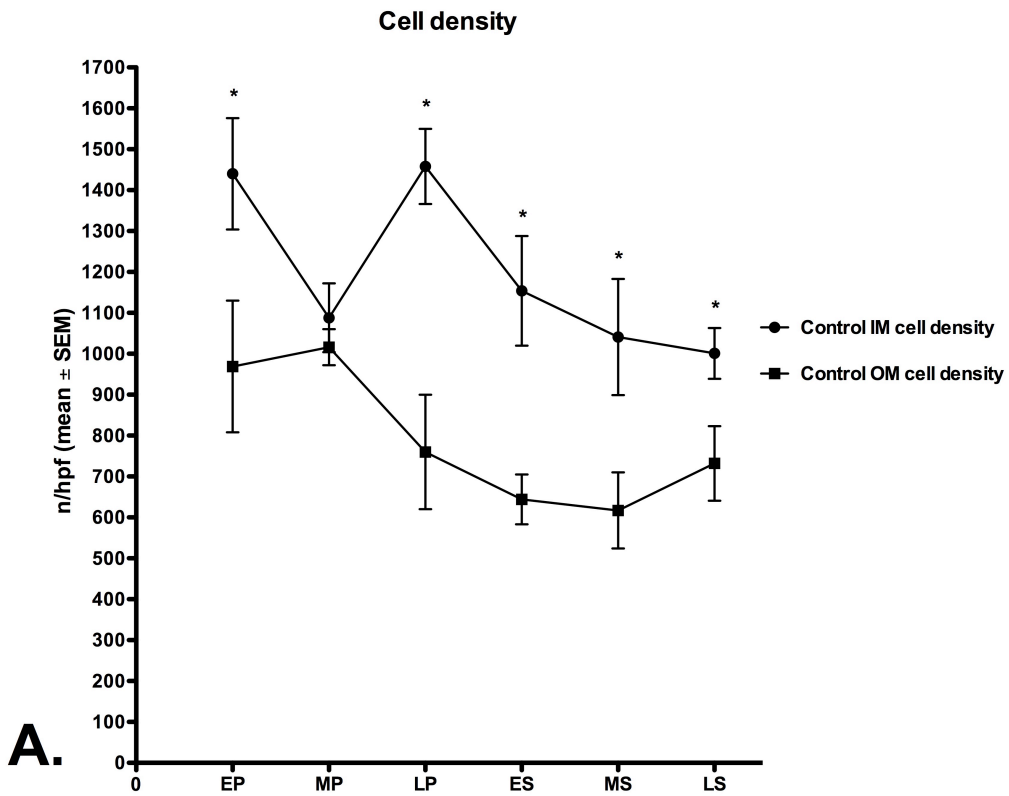
<sup>b</sup> Expressed as percentage area expressing  $\alpha$ -SMA per high power field.

**Figure 4.2: Characteristics of the IM and OM in control (A, C, E, G) and adenomyotic (B, D, F, H) uteri, during the different phases of the menstrual cycle. Cell density, nuclear size, and total nuclear area are expressed as mean  $\pm$  SEM.**

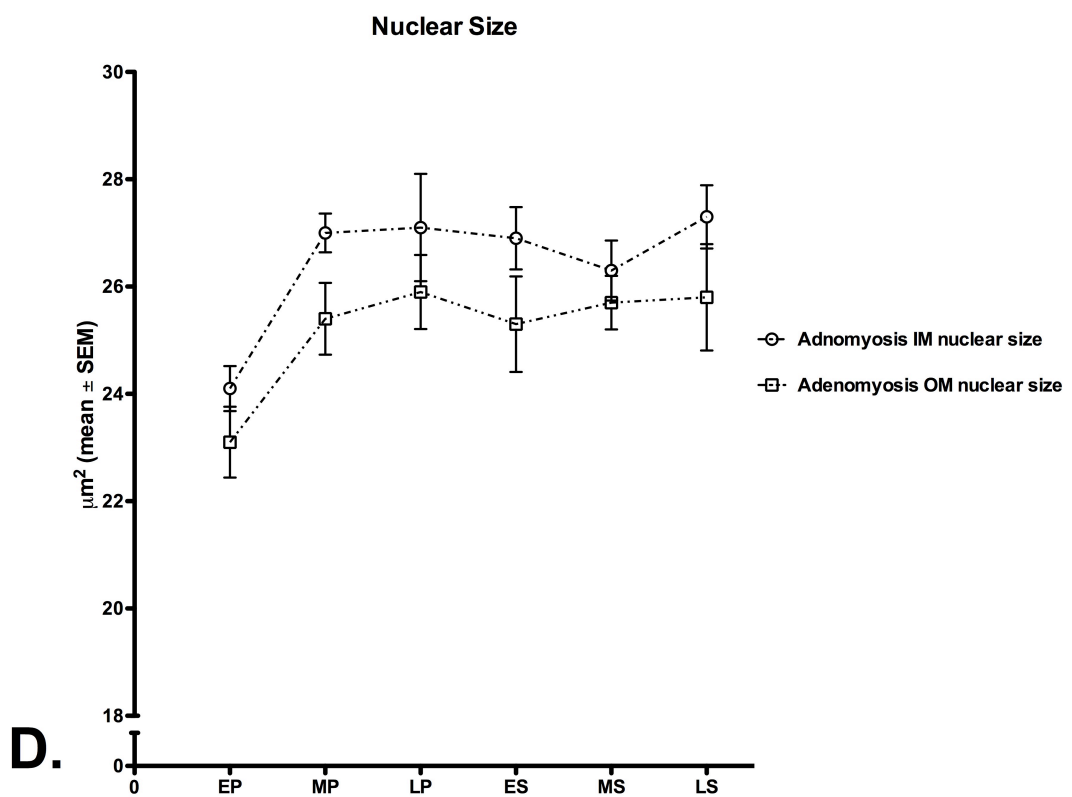
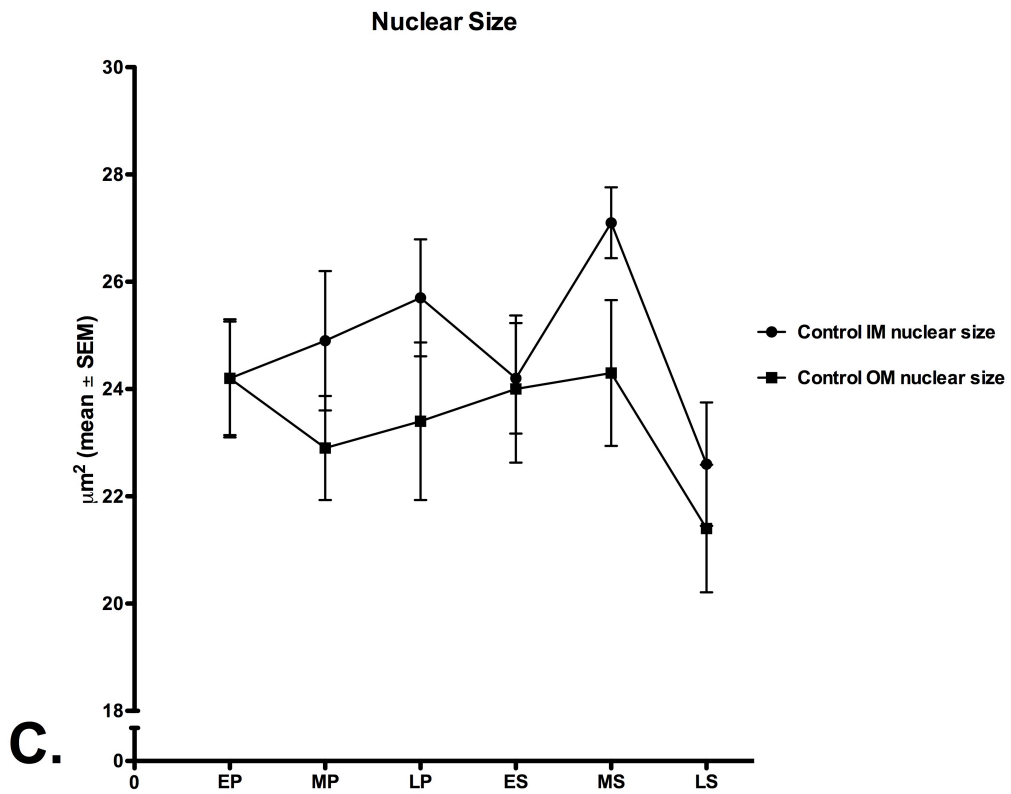
**\* Statistically significant compared to the outer myometrium ( $p < 0.01$ ) in the same group (control and adenomyosis).**

**\*\* Statistically significant compared to the corresponding zone in the control group ( $p < 0.05$ )**

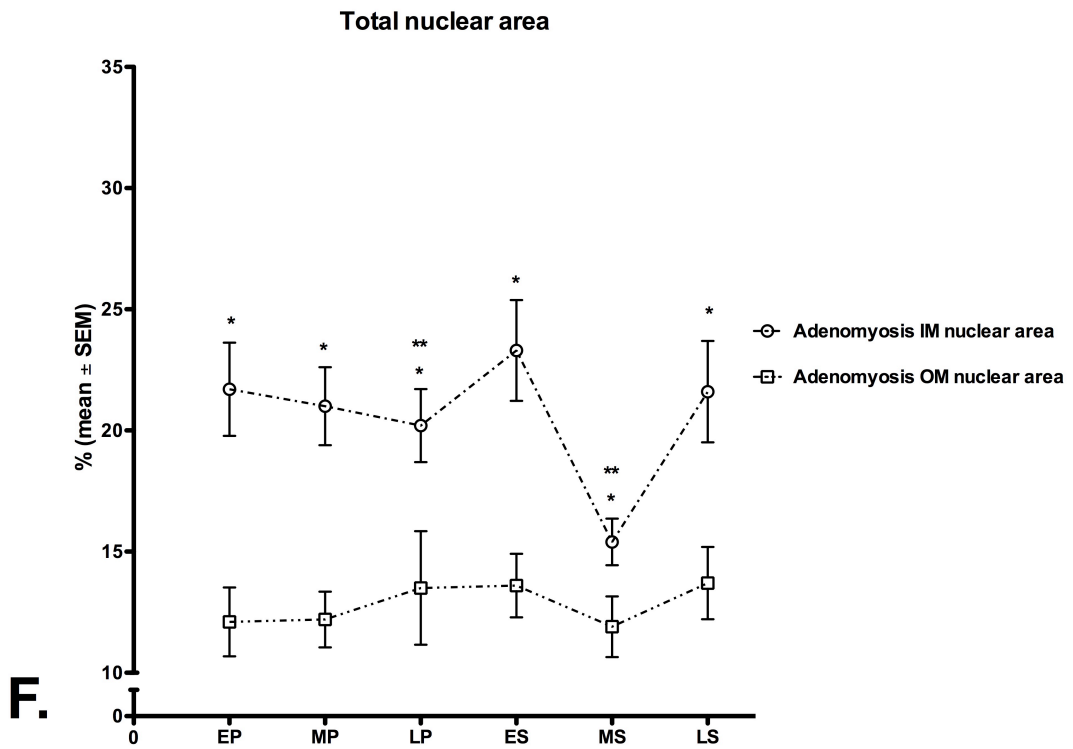
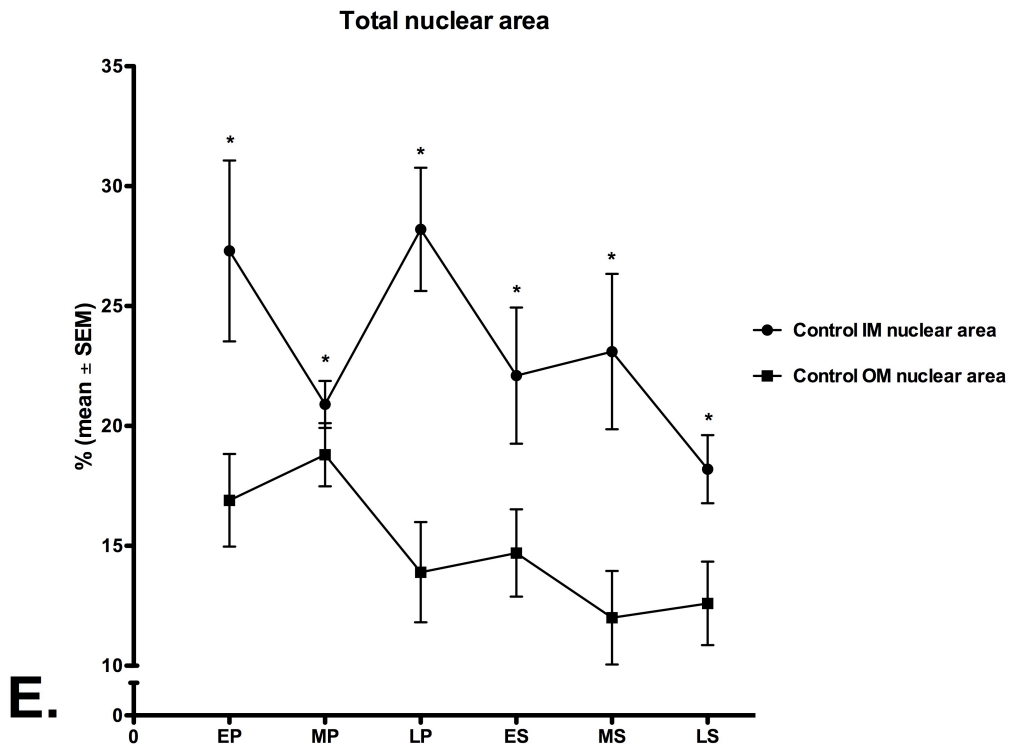
**(see next page)**



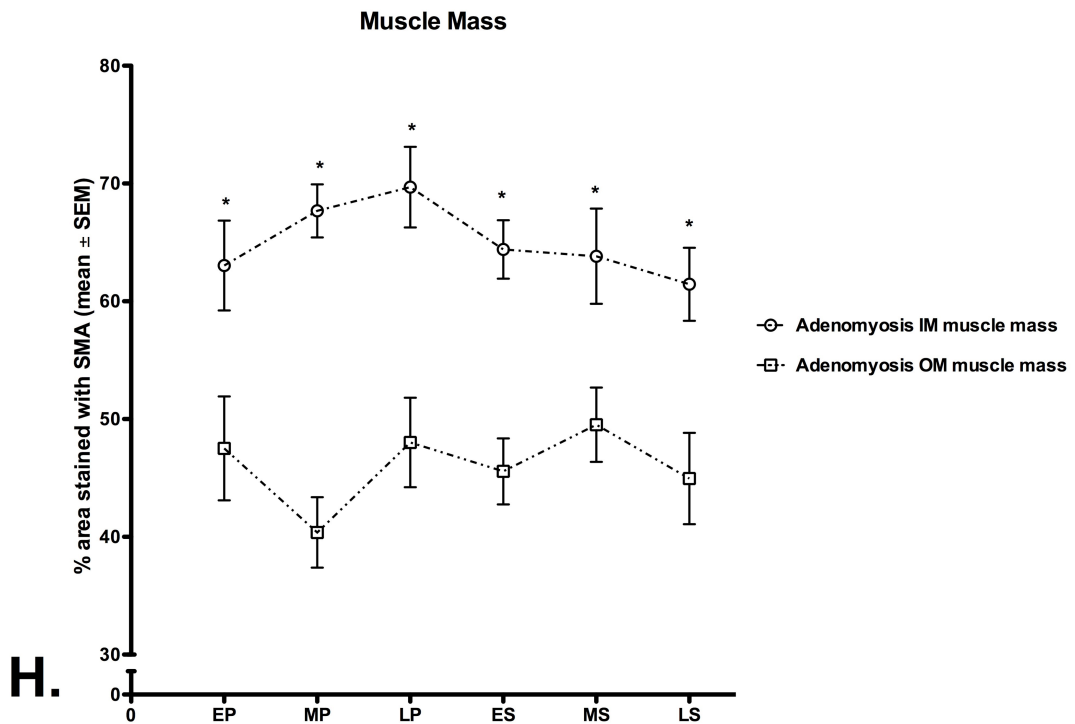
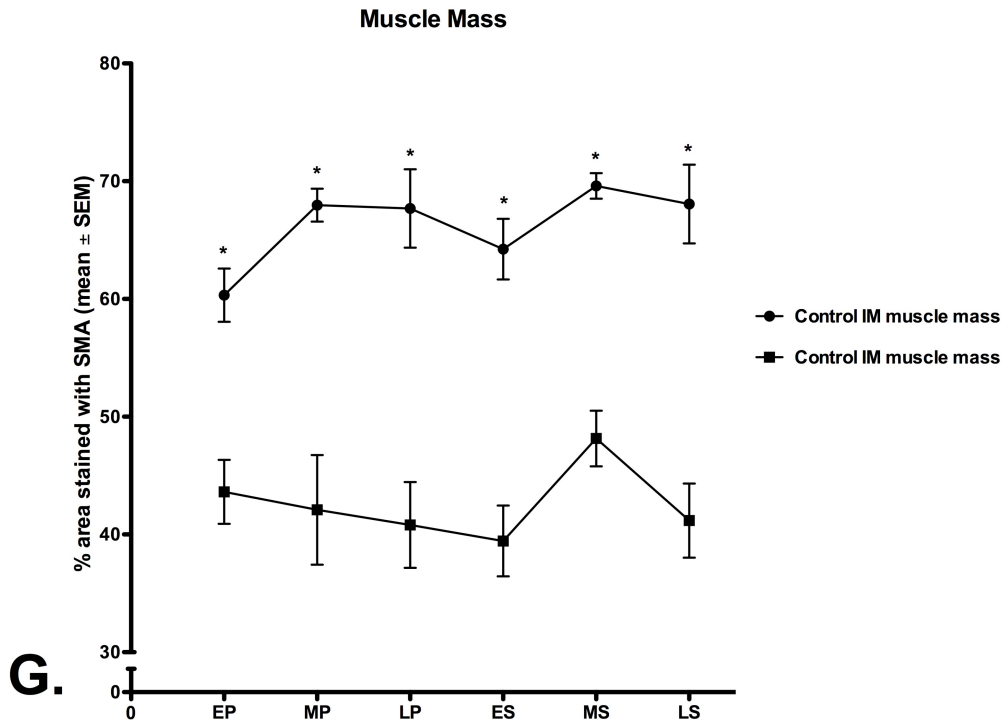
(cont.)



(cont.)



(cont.)



\* Statistically significant compared to the outer myometrium ( $p < 0.01$ ) in the same group (control and adenomyosis).

\*\* Statistically significant compared to the corresponding zone in the control group ( $p < 0.05$ )

Examination of sequential high-power fields of full myometrial thickness showed that the reduction in cell density and total nuclear area from the IM to the OM in both adenomyosis and controls was gradual with no distinct zonation (Figure 4.3).

In control uteri, the nuclei appeared morphologically similar in the IM and OM. In adenomyosis, the nuclei in the IM were significantly larger, paler and exhibited a clear nuclear ground vesicular interface (Figure 4.4 and 4.5). Areas away from the adenomyotic foci were examined to ascertain the uniformity of the findings, and this nuclear phenotype was also present in areas remote from the adenomyotic lesions.

$\alpha$ -SMA expression (muscle mass) did not vary significantly across the menstrual cycle or between adenomyotic and control uteri (Table 4.1, Figure 4.2).

Figure 4.3: Total nuclear area examined in a full thickness myometrium from the endometrial-myometrial junction to the serosa, in a midproliferative control (60 readings) and adenomyotic (53 readings) uterus. Data were normalised and averaged to compensate for differences in wall thickness between uteri.

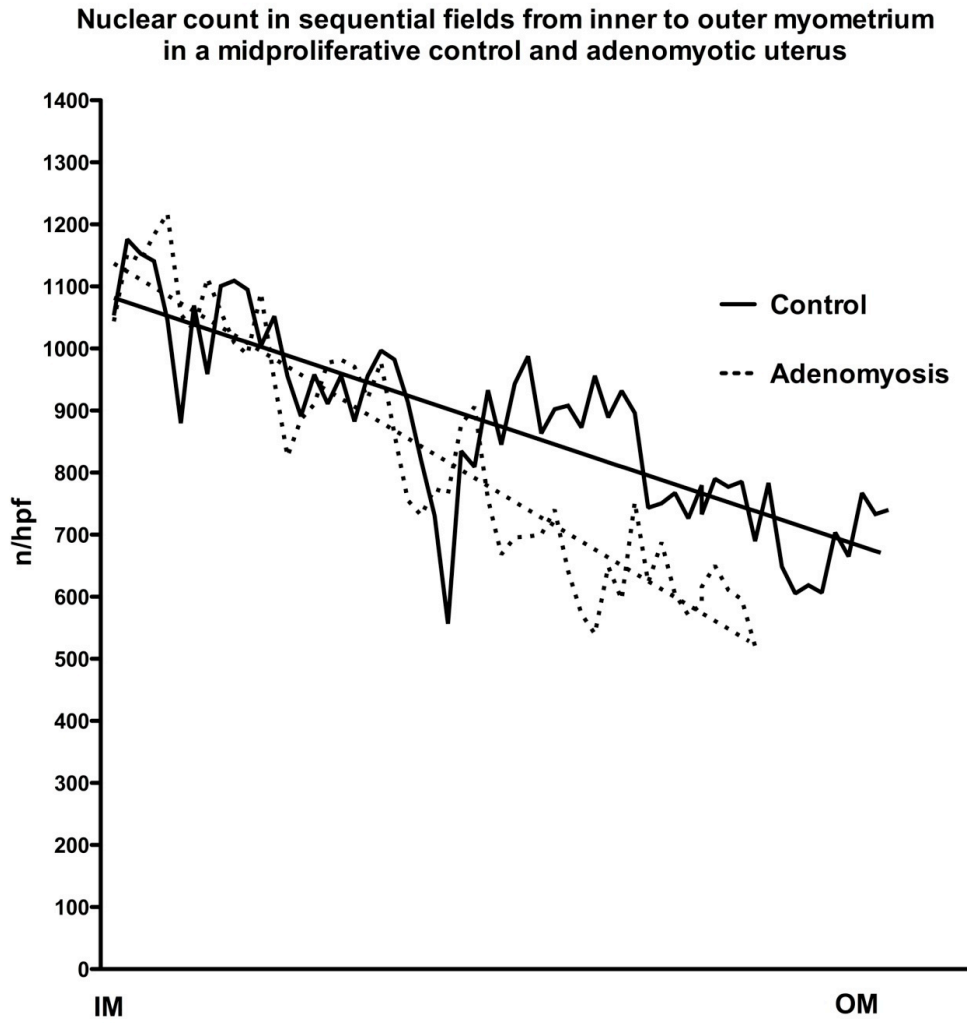


**Figure 4.4: Histological section of mid-secretory (A) Control inner myometrium (B) Control outer myometrium, (C) Adenomyotic inner myometrium, and (D) Adenomyotic outer myometrium layers illustrating the differences in total nuclear area (count) and cell density (x20).**

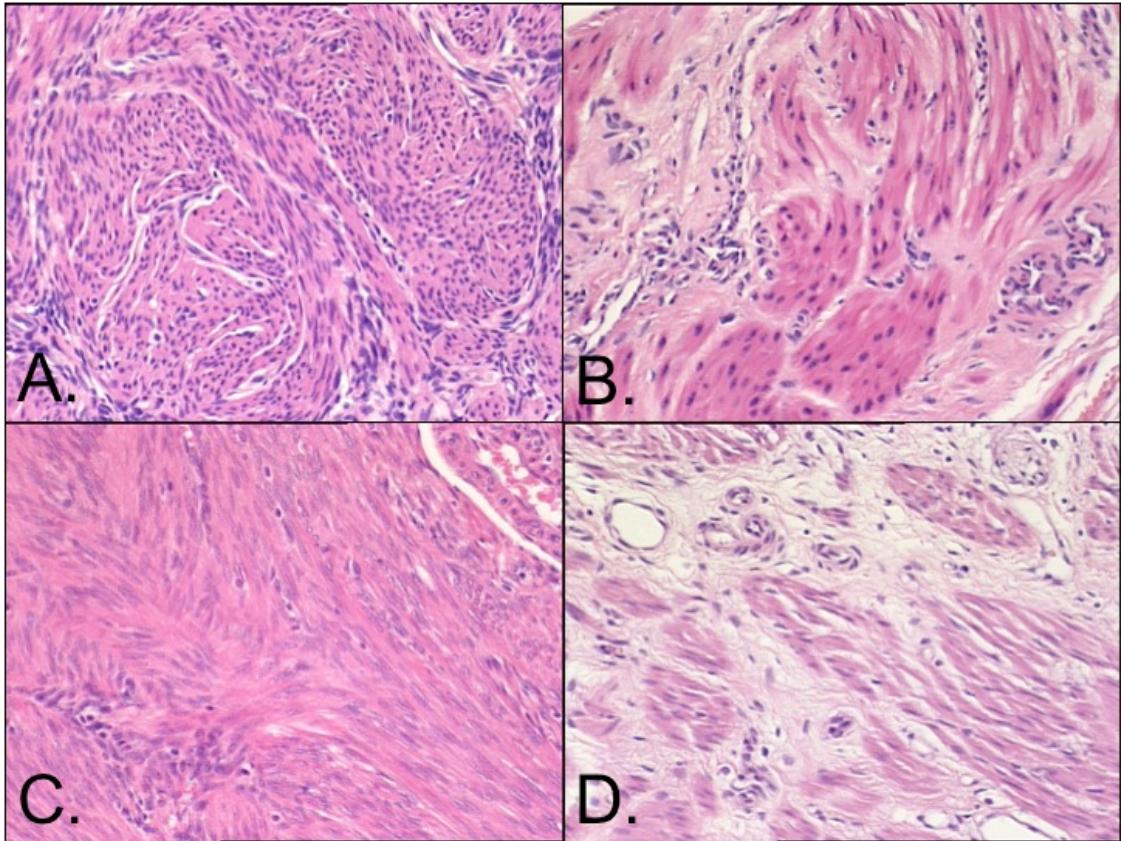
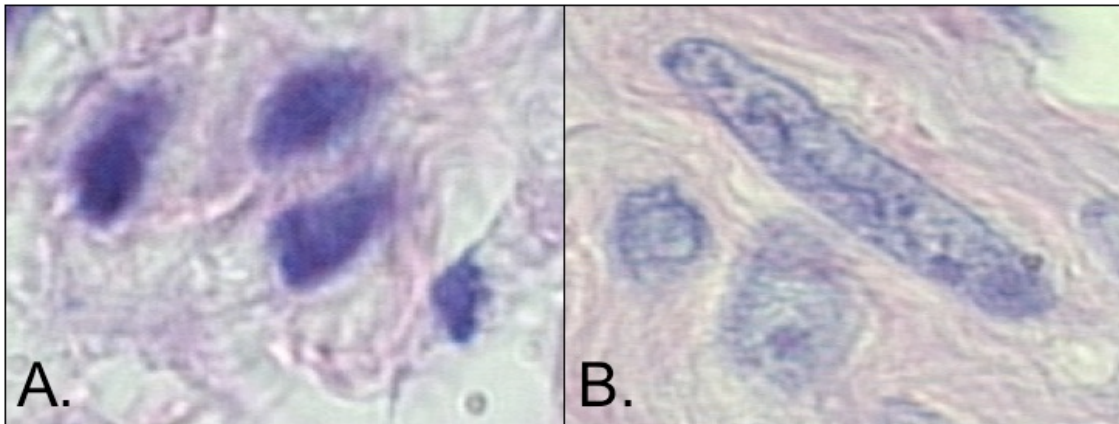


**Figure 4.5: Nuclear morphology in inner myometrium of (A) normal and (B) adenomyotic uteri. (Oil immersion lens, x100)**



Desmin expression was confined to the myocytes, with no staining of extracellular or connective tissue. Desmin diffuse intracellular immunostaining followed a similar pattern to that of  $\alpha$ -SMA, uniformly staining the myometrium, both in the IM and OM. Desmin immunostaining in the IM and OM did not vary significantly across the menstrual cycle or between adenomyotic and control uteri. Staining intensity did not vary according to proximity to adenomyotic foci. There was no distinct zonation between the IM and OM. Both desmin and  $\alpha$ -SMA staining revealed that the muscle layer was organised into thinner, less well-defined bundles. Vimentin immunostaining was more intense in connective tissue cells surrounding the muscle bundles. The muscle cells stained weakly positive for vimentin.

In controls, IM and OM myocytes exhibited weak diffuse cytoplasmic staining (SI = 1) with vimentin and there were no cyclic changes. Vimentin SI was significantly higher in the IM in adenomyosis compared to control in all phases of the menstrual cycle except the EP phases (SI = 2-3,  $p < 0.05$ ) (Figure 4.6 and 4.7). Vimentin staining in adenomyosis IM showed significant cyclical variation, being higher in the LP and ES phases. Vimentin expression in the OM was similar in adenomyosis and controls.

**Figure 4.6: Vimentin SI in the junctional zone of control and adenomyotic uteri, showing higher SI in adenomyotic IM, together with variation within the menstrual cycle, compared to control. In controls, IM and OM showed weak diffuse cytoplasmic vimentin staining (SI = 1) with no cyclic variation. Vimentin expression in the OM was similar in adenomyosis and controls (\* significant difference,  $p < 0.05$ ).**

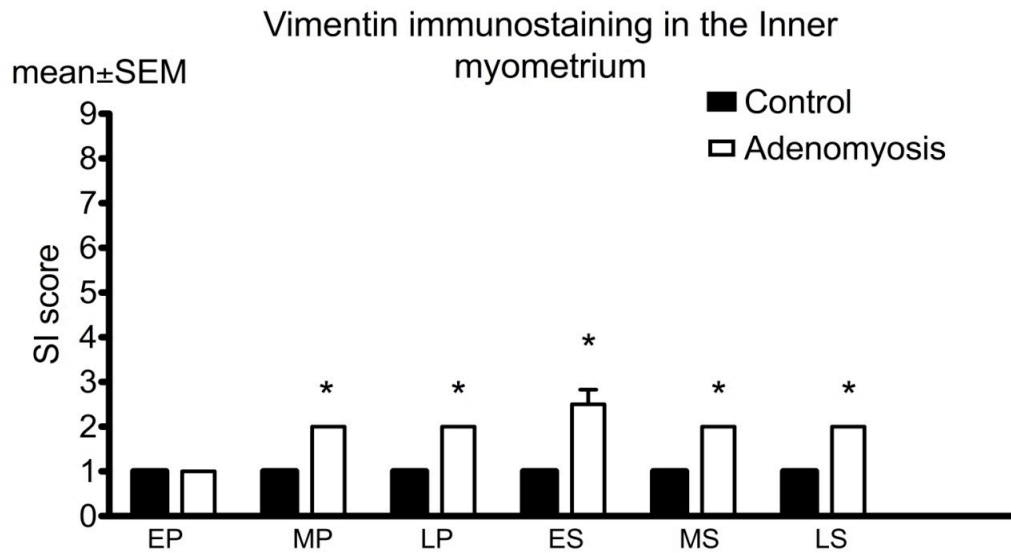
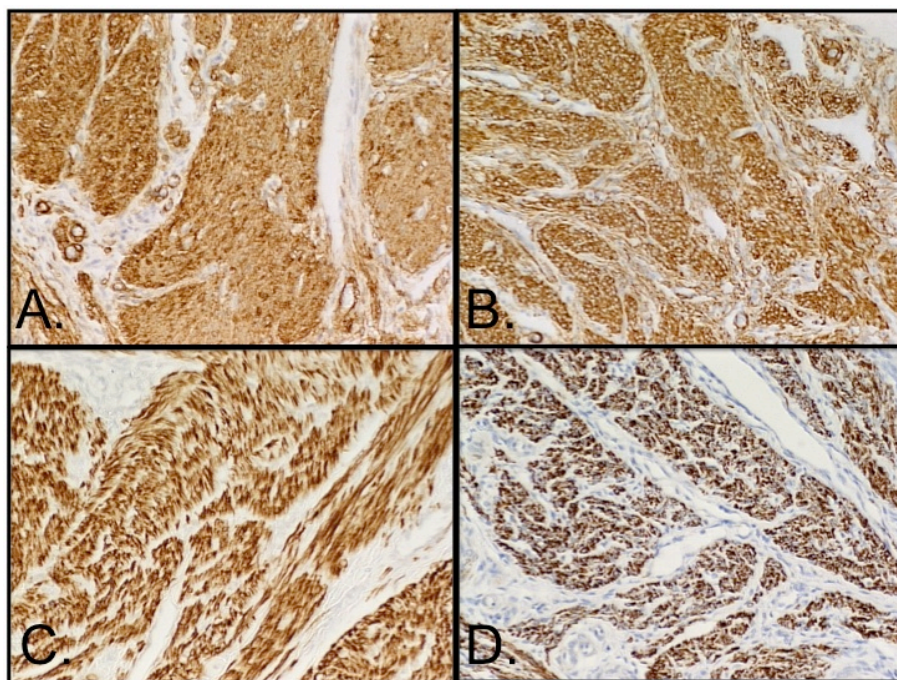
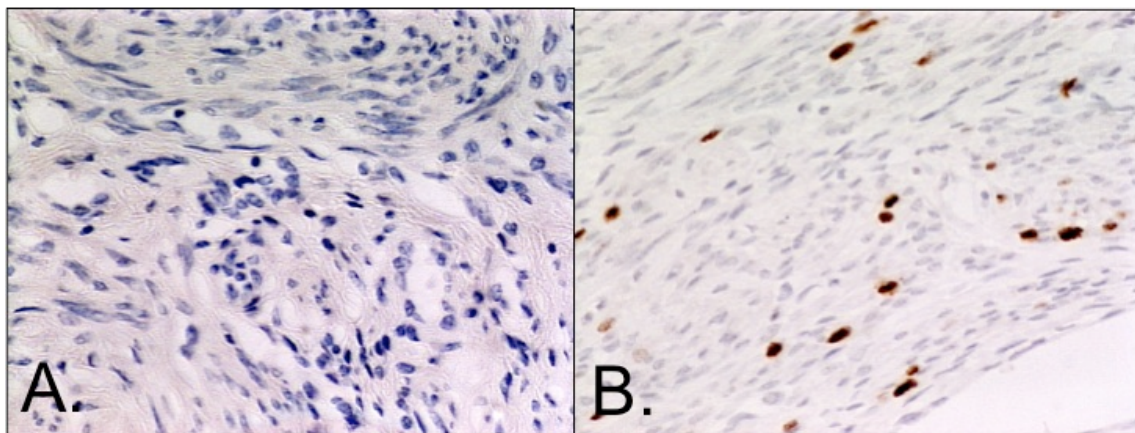


**Figure 4.7: Desmin immunostaining of A. inner and B. outer control myometrium, compared to adenomyotic C. inner and D. outer myometrium demonstrating the fragmentation and loss of architecture of the muscle fibers (x20).**



The myometrium in adenomyosis weakly expressed Ki-67 (PI: IM==0.8%, and OM=0.4%). Control uteri did not express Ki-67 in the myometrium (Figure 4.8).

**Figure 4.8: Ki-67 immunostaining of the inner myometrium in A. control and B. adenomyotic uterus, demonstrating the increased in ki-67 expression in diseased uteri (x20).**



#### 4.4 DISCUSSION

MRI imaging identifies the uterine JZ as a distinct hypodense layer (Scoutt et al., 1991, Brown et al., 1991). The reported increased nuclear area in the inner myometrium (Scoutt et al., 1991), different water content (McCarthy et al., 1989a), and distribution of laminin  $\beta 2$  (Campbell et al., 1998) suggest that local anatomical differences may account for the zonation seen on MRI. Magnetic resonance imaging features suggestive of adenomyosis are indirect and include increased JZ thickness (Hauth et al., 2007, Brown et al., 1991, Reinhold et al., 1998). The results demonstrated that the IM of normal uteri, has higher cell density and total nuclear area compared to the outer myometrium (1.6-1.8 folds), but importantly, that the change in cell density is gradual throughout the uterine thickness. This supports the finding of gradual increase in elastin expression from the inner to the outer myometrium (Metaxa-Mariatou et al., 2002).

This contrasts with the clearly defined JZ as seen on MRI. The maximum change in cell density from the IM to OM observed in this experiment is less than the 3-fold change reported by *Scoutt et al.* (Scoutt et al., 1991). The current experiment used true colour image analysis without gray-scale transformation, which allowed accurate definition of cellular structures. It remains possible that the distinct MRI features are due to lower water content in the inner myometrium reflecting a reduction in intercellular space between more tightly packed cells. It has been suggested that water content is lower in the subendometrial compared to the outer myometrium (McCarthy et al., 1989a). This suggests that the in-vivo difference in cell density between the IM and OM may in fact be larger than the differences noted in formalin fixation tissue. It is also possible that the subendometrial halo seen on MRI reflects a transitional point of cell count or water content, but it remains unclear why this zone is not seen in all uteri (Hauth et al., 2007). On the other hand, the finding of similar expression of the intracellular components  $\alpha$ -SMA and desmin supports reduced extracellular fluid content in adenomyosis, thus the reason for increased JZ thickness in affected uteri remains unclear.

The lack of a clear distinction between the inner and outer muscle layers does not rule out a functional distinction as demonstrated in studies using ultrasound (Kunz and Leyendecker, 2002, Kunz et al., 1996, Kunz et al., 2000), as differences may exist in steroid receptors expression (Noe et al., 1999) or in innervation (Quinn, 2007).

In summary, the JZ of adenomyotic uteri exhibited reduced cell density and larger nuclear size compared to normal uteri. The OM exhibited similar changes, suggesting a diffuse uterine defect rather than an effect localised to the inner myometrium.

$\alpha$ -SMA (and desmin) expression (measured as staining per unit area) did not vary between adenomyosis and controls, which indicate cellular hypertrophy rather than increased extra-cellular components. Indeed, hypertrophy is a characteristic histologic

feature of adenomyosis, and may reflect a compensatory mechanism or arrested maturation. The increased expression of Ki-67 in the myometrium affected by adenomyosis compared to controls supports myometrial hyperplasia.

Both desmin and  $\alpha$ -SMA staining in adenomyosis revealed that the muscle layer was organised into thinner, less well-defined bundles. The disruption of normal geometry of the muscle bundles and fascicles observed on desmin and  $\alpha$ -SMA staining, with widening of the intercellular space and rearrangement of the myocytes may influence uterine function. Myometrial cell density did not vary significantly with the phases of the cycle in normal uteri. The reduction in cell density in the IM in adenomyosis during the MS phase suggests increased tissue oedema, perhaps in response to progesterone.

In contrast with the mouse experimental model described in section 1 of this thesis, this experiment confirmed the presence of morphological changes in the myometrium of uteri affected by adenomyosis, these changes were not localised to the inner myometrium. Whether these changes are responsible for - or the effect of - the invasion of endometrial glands and stroma, is not known. But the fact that these changes are present in the OM, which is not invaded by adenomyosis, suggests that the defect is primarily myometrial.

The ultrastructural features underlying the observed microscopical changes will be examined by electron microscopy in the following experiment.

## **Chapter 5**

### **Ultrastructural study of the inner and outer myometrium in uteri with and without adenomyosis**

## Chapter 5

### Ultrastructural study of the inner and outer myometrium in uteri with and without adenomyosis

#### 5.1 INTRODUCTION

In the first section of this thesis, the data from the animal model suggested that the development of adenomyosis could be related to the presence of a myometrial defect that could allow a constitutively ‘invasive’ endometrium to penetrate the underlying muscle coat, in a *predisposed* uterus.

Although the gross and ultrastructure of the myometrium have been previously described in normal (Lowy and Small, 1970, Gompel and Silverberg, 1994) and leiomyomatous uteri (Ferency, 1979, Richards et al., 1998), there is no literature describing the myometrial structure in uterine adenomyosis.

In the previous experiment (chapter 4), microscopic examination of the inner and outer myometrium of human uteri showed the presence of myometrial changes such as larger nuclei, and myometrial hypertrophy in the presence of uterine adenomyosis. These changes were not localised to the inner myometrium.

In this experiment, using electron microscopy, the ultrastructure of the junctional zone and the outer myometrium will be examined in the presence and absence of uterine adenomyosis, in order to identify the potential underlying ultrastructural changes responsible for these myometrial differences observed on light microscopy.

## 5.2 PATIENTS AND METHODS

The study was approved by the local Research and Ethics Committee, and all participants provided written consent. Hysterectomy specimens from premenopausal women not using exogenous hormones were selected for this study. The uteri were removed by abdominal or laparoscopic assisted vaginal hysterectomy for menorrhagia with or without dysmenorrhea (Table 5.1). None of the participants had fibroids or endometrial abnormalities on preoperative ultrasound or hysteroscopy.

**Table 5.1: Clinical characteristics of participants (TAH: Total abdominal hysterectomy, LAVH: Laparoscopic assisted vaginal hysterectomy, NVD: Normal vaginal delivery, SH: Subtotal hysterectomy).**

No	Group	Age (years)	Parity	Indication for hysterectomy	Phase of cycle	Route of hysterectomy
1	Adenomyosis	39	0	Menorrhagia, dysmenorrhea	Secretory	TAH
2	Adenomyosis	49	4, NVD	Menorrhagia, dysmenorrhea	Proliferative	TAH
3	Normal	34	3, NVD	Menorrhagia, dysmenorrhea	Proliferative	LAVH
4	Normal	54	3, NVD	Menorrhagia	Proliferative	TAH
5	Normal	43	2, NVD	Menorrhagia	Secretory	LAVH
6	Normal	36	2, NVD	Menorrhagia	Secretory	TAH
7	Normal	47	4, NVD	Menorrhagia	Secretory	TAH
8	Normal	35	2, NVD	Menorrhagia	Proliferative	TAH
9	Adenomyosis	39	3, NVD	Menorrhagia	Proliferative	SH
10	Adenomyosis	45	6, NVD	Menorrhagia, dysmenorrhea	Proliferative	TAH

Histopathological examination proved normal endometrium and absence of fibroids, and confirmed adenomyosis (glands >2.5mm below EMI). None of the participants had endometriosis. All participants were parous except one woman in the adenomyosis group. None had a history of curettage, caesarean section or uterine surgery. There was no significant difference in mean age between the adenomyosis group (43 years) and the control group (40.4 years).

Uteri were obtained within 10 minutes of surgical removal and opened in the sagittal plane. Multiple 3mm<sup>3</sup> samples were immediately obtained from the junctional zone (the first 5-8 mm underneath the endometrial/myometrial junction) and outer myometrium (the outer third of the myometrium). All samples were obtained from the anterior wall of the uterus near the fundus (as described in chapter 4, figure 4.1). Samples were primarily fixed in 2% glutaraldehyde in 0.1M Sörensen's phosphate buffer for 48 hours at 4 degrees Celsius. Then, the samples were washed, post-fixed in buffered 1% Osmium Tetroxide for 30 minutes, re-washed, dehydrated in ethanol series, and treated with propylene oxide. The samples were then infiltrated with propylene oxide / LR white resin before final embedding and polymerisation in LR White resin. Ultrathin 80 nanometre sections were cut from each sample using a Reichert Ultracut S ultramicrotome, collected on copper mesh grids, counter stained with 2% Uranyl Acetate and Reynolds' lead citrate and examined using a JEOL 1220 transmission electron microscope using an accelerating voltage of 80 kV. Digital Images were recorded using a SIS Megaview III Digital Camera with Analysis Software.

Parallel full uterine thickness samples were prepared for light microscopy, stained with hematoxylin and eosin, and used to confirm the menstrual cycle phase (proliferative or secretory), the presence or absence of adenomyosis, and to ensure that the samples are obtained from representative areas. A total of 10 uteri were examined: 4 with and 6

without adenomyosis. Measurement of the sarcolemmal dense bands (attachment plaques) length and the average nuclear size was made in 10 random fields from each area. Comparisons of means were made using Student's T-test for non-paired samples, and differences were considered significant if  $p < 0.05$ .

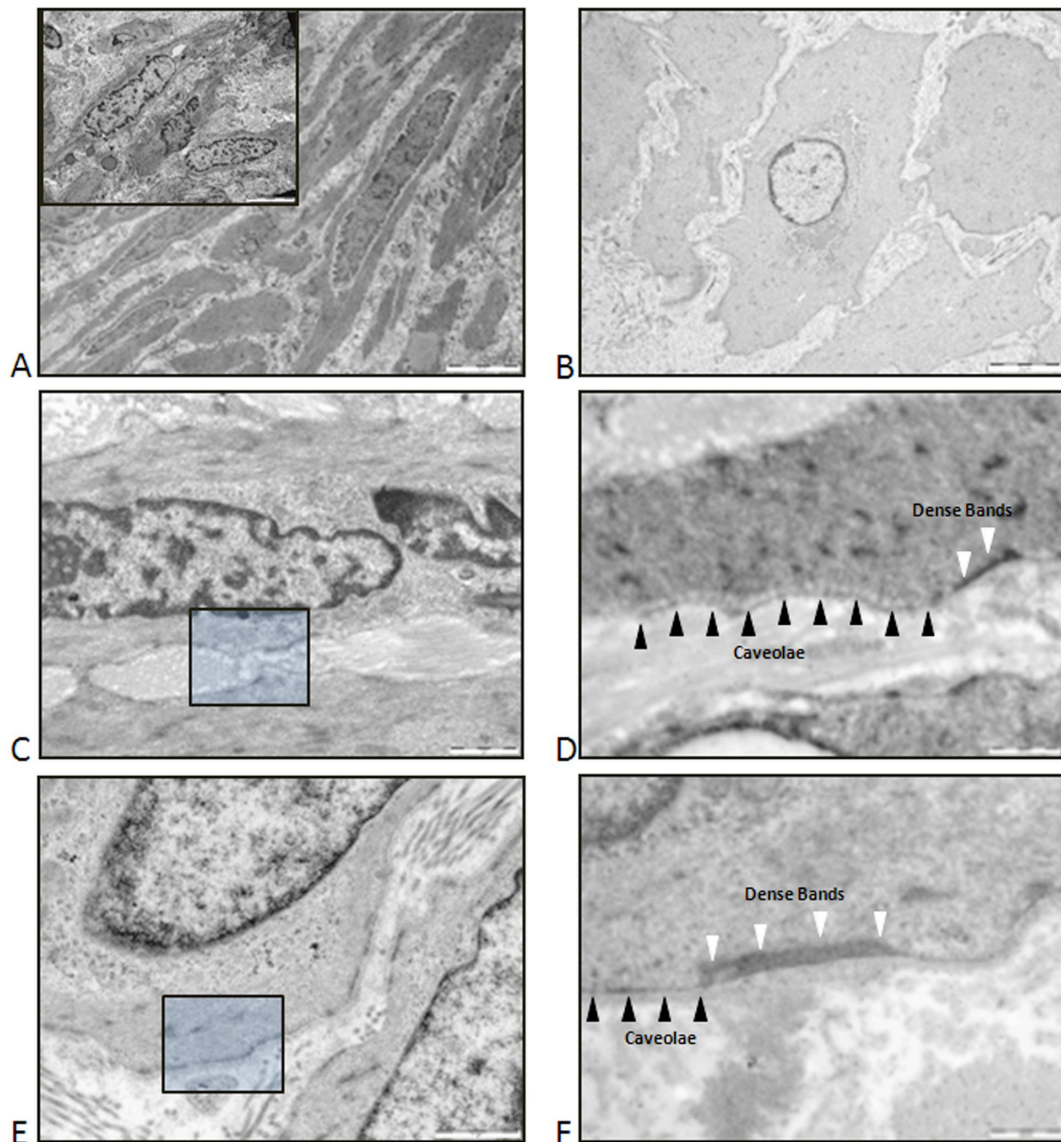
## **5.3 RESULTS**

### **5.3.1 Myometrium ultrastructure in the absence of adenomyosis**

The junctional zone was rich in myocytes closely interwoven in a dense connective tissue matrix with prominent collagen fibrils (Figure 5.1A). The connective tissue-to-myocytes ratio was about 40/60. The cytoplasm was sparse and the typical trilaminar sarcolemmal (cell surface) membrane showed an even distribution of short dense plaques (sarcolemmal bands or attachment plaques), alternating with numerous prominent caveolae (Figure 5.1C and 5.1D). The length of the sarcolemmal bands was measured in random fields from each specimen (Table 5.2), and the average was  $0.81 \pm 0.1$  micrometers (mean  $\pm$  SEM). The cytoplasm contained an abundance of myofilaments, with their associated dense bodies, which were peripherally distributed in tight bundles, parallel to the sarcolemmal membrane. The nuclei were fusiform in shape with blunt ends, centrally placed in the myocyte and with crenated nuclear envelope (irregular outline) (Figure 5.1A and 5.1C). The chromatin material was dense and finely dispersed in the nuclear ground substance. The average nuclear size was  $24.75 \pm 0.41 \mu\text{m}^2$  (mean  $\pm$  SEM) (Table 5.2). The cells contained a normal prominent complement of perinuclear organelles (Figure 5.2A), with no discernible structural abnormalities. In the normal outer myometrium, the myocytes were arranged in well-defined bundles, with narrow intercellular space, rich in collagen fibrils (Figure 5.3). The individual bundles

were widely spaced, separated by connective tissue, with a reversed connective tissue-to-myocytes ratio (60/40). Overall, the individual myocytes appeared similar to the junctional zone, with sparse cytoplasm rich in myofilaments lying parallel to the cell membrane. Numerous cytoplasmic aggregates of intermediate filaments and myelin bodies (lipolysosomes) were seen (Figure 5.3B). The arrangement, frequency and length of the attachment plaques ( $0.66\pm 0.06\ \mu\text{m}$ ) and caveolae were comparable to the JZ. The nuclei maintained their elongated shape and size ( $23.66\pm 0.43\ \mu\text{m}^2$ ), with a crenated nuclear envelope, dense ground substance and finely dispersed chromatin material. No differences were observed between myometrial samples from different phases of the cycle (proliferative vs. secretory).

**Figure 5.1 A -F: Ultrastructure of the myocytes at the Junctional zone in normal and adenomyotic uteri: A (and inset): Normal architecture of the JZ and the close proximity of the myocytes with no distinct bundle formation. The collagen fibers are prominent in the extracellular matrix. B: The myocytes in adenomyotic uteri are more separated with less dense collagen. Nuclei have a smooth outline with a clear nuclear ground and peripherally arranged chromatin. C and D: Attachment plaques (sarcolemmal bands) (white arrows) and caveolae (black arrows) on the sarcolemmal membrane of normal myocytes. E, F: Long sarcolemmal bands and sparse caveolae in adenomyotic myocytes (Scale bars are shown on individual images).**



### 5.3.2 Myometrial ultrastructure in the presence of uterine adenomyosis

In the presence of uterine adenomyosis, the JZ myocytes were widely separated by a loose connective tissue matrix, with less prominent collagen fibrils. The cytoplasm was abundant, denoting cellular hypertrophy. The cytoplasmic myofilaments were less abundant, with less distinct bundling, but there was an abundance of intermediate filaments with a tendency to form cytoplasmic aggregates (Figure 5.2E). Myelin bodies (lipolysosomes) were similarly more frequently observed (Figure 5.2F). Compared to the normal JZ, the nuclei were more round and significantly enlarged (average nuclear size  $26 \pm 0.24 \mu\text{m}^2$ ,  $p=0.001$ ), and the nuclear envelope lost its corrugated appearance exhibiting a smooth outline. The nuclei showed a clear ground substance with prominent nucleoli. The nuclear chromatin was peripherally arranged under the smooth nuclear envelope (Figure 5.1B). Occasional infolding of the nuclear envelope with entrapment of cytoplasmic organelles was seen (Figure 5.2C). The sarcolemmal bands were significantly longer ( $1.33 \pm 0.14 \mu\text{m}$ ,  $p<0.01$ ) (Table 5.2) with less prominent caveolae (Figure 5.1E and 5.1F).

With an abundant cytoplasm, the perinuclear cell organelles were more distinct. The mitochondria exhibited unfolding of the internal cristae (Figure 5.2D). The rough endoplasmic reticulum and Golgi apparatus were more prominent, denoting active protein synthesis, consistent with the observed cellular hypertrophy (Figure 5.2B).

The outer myometrium showed features similar to the junctional zone. The bundle structure was preserved, but with increased intercellular space and less dense collagen fibrils. The nuclei were significantly larger than controls ( $24.71 \pm 0.32 \mu\text{m}^2$ ,  $p=0.03$ ), with abundant cytoplasm and the attachment plaques were significantly longer ( $1.3 \pm 0.08 \mu\text{m}$ ,  $p<0.01$ ).

**Figure 5.2 A - H: Myocytes abnormalities detected in the presence of adenomyosis. A (and inset): Perinuclear organelles in normal myocytes compared to B: Prominent cell organelles and endoplasmic reticulum in adenomyotic myocytes. C: Abnormal invagination of the nuclear envelope entrapping organelles. D: Abnormal mitochondria (M) with unfolded cristae. E and F: Intermediate filaments aggregates (IF) and myelin bodies (MB) (scale bars shown on individual images).**

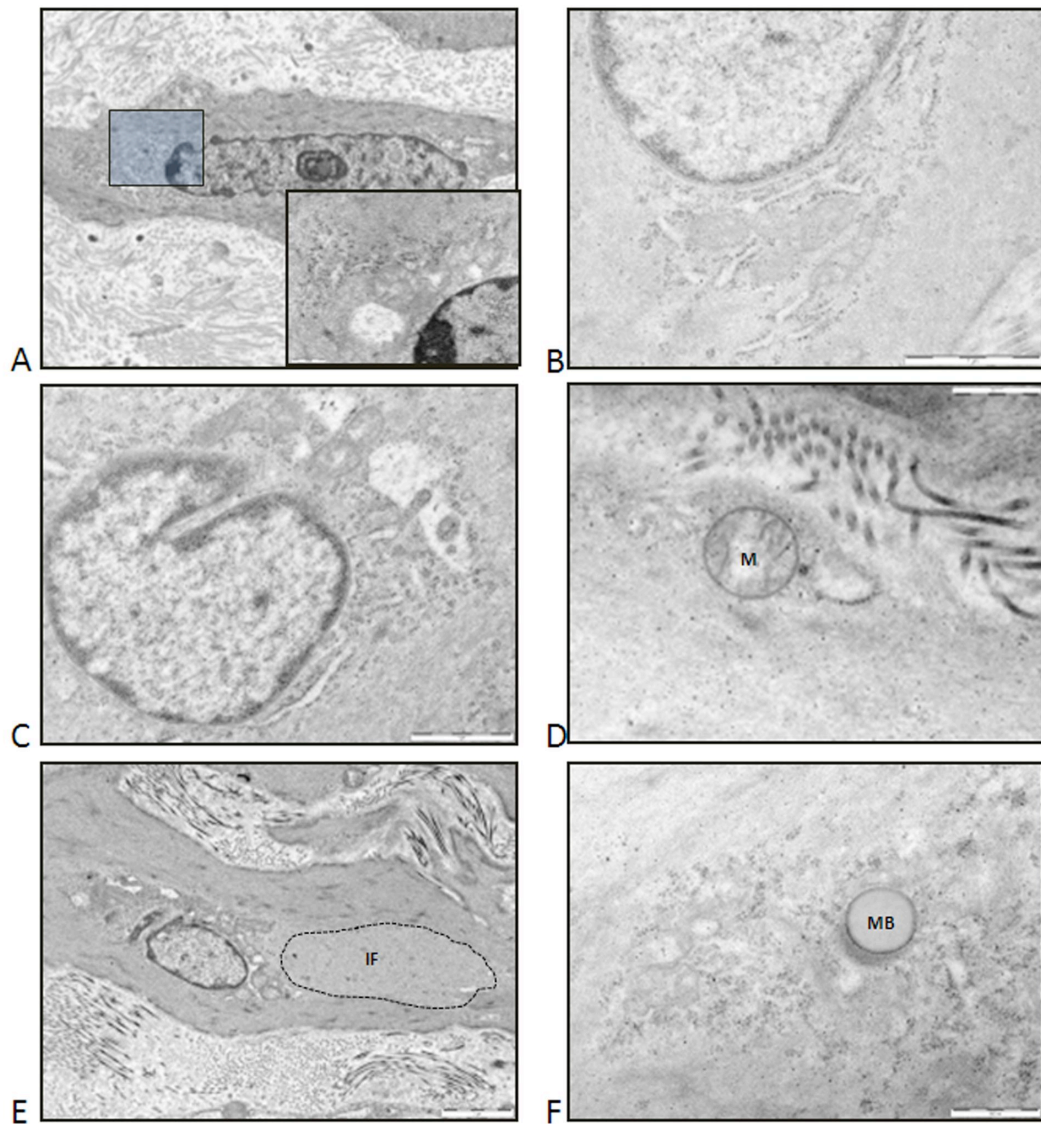


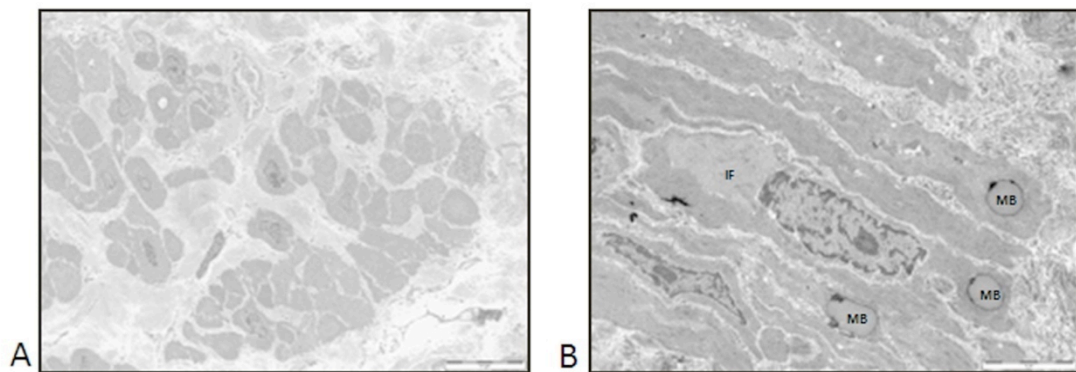
**Table 5.2: Myocytes attachment plaques length ( $\mu\text{m}$ , mean  $\pm$  SEM) and nuclear size ( $\mu\text{m}^2$ , mean  $\pm$  SEM). Measurements were based on 10 measurements per patient. JZ = Junctional zone, OM = Outer myometrium.**

	Sarcolemmal plaques length		Nuclear size	
	JZ	OM	JZ	OM
<b>Normal group (n=6)</b>	0.81 $\pm$ 0.1	0.66 $\pm$ 0.06	24.75 $\pm$ 0.41	23.66 $\pm$ 0.34
<b>Adenomyosis group (n=4)</b>	1.33 $\pm$ 0.14*	1.3 $\pm$ 0.08**	26.34 $\pm$ 0.24*	24.71 $\pm$ 0.32**

\* Significantly greater than normal junctional zone ( $p < 0.01$ )

\*\* Significantly greater than normal outer myometrium ( $p < 0.05$ )

**Figure 5.3 A and B: Normal outer myometrium bundle arrangement and high collagen-to-myocytes ratio. Note the intermediate filaments aggregates (IF) and the myelin bodies (MB) (scale bars shown on images).**



## 5.4 DISCUSSION

This study describes a range of ultrastructural abnormalities in the junctional zone and outer myometrial layers in women with uterine adenomyosis. As the lack of variation in ultrastructure of myocytes with the normal cycle has been described in the literature (Richards et al., 1998), and confirmed at a histologic level in the previous chapter, there was no need to study each phase of the cycle separately. The co-existence of fibroids could have an effect on the host myometrium (e.g. compression effect, hyperplasia) (Richards et al., 1998). To avoid confounding, only uteri where fibroids have been excluded by ultrasound, macroscopic and microscopic assessment were studied. The inner and outer myometria are believed to be functionally and structurally distinct layers, based on magnetic resonance imaging (MRI) (Brosens et al., 1998), anatomic and histologic studies (Wetzstein, 1965, Noe et al., 1999). No significant ultrastructure differences were found between the inner and outer layer myocytes. However, the junctional zone had higher cellular density, with decreased extracellular space and no clear bundle arrangement. Overall, this description of the normal myometrium is in agreement with the previous studies examining the histology ultrastructure of the normal human myometrium (McCarthy et al., 1989a, Scutt et al., 1991, Brown et al., 1991, Mark, 1956, Hashimoto et al., 1960, Fujii et al., 1989, Fujii et al., 1990, Cole and Garfield, 1989).

The presence of myelin bodies (lipolysosomes) is suggested to be linked to cell injury, particularly ischaemia (Cotran et al., 1989). Nevertheless, the observation that outer myometrial cells from normal uteri contained an abundance of myelin bodies is unlikely to be explained by ischaemia because of the rich uterine blood supply. Thus; the cause of these myelin bodies in normal uteri remains speculative, but could possibly be related to postpartum involution.

In the presence of adenomyosis, the observed loose connective tissue matrix, with less prominent collagen fibrils may be explained by intercellular space expansion. Further research is needed to characterise the extracellular matrix components.

In line with the observations made by light microscopy in the previous chapter (Loud et al., 1983, Owens et al., 1981), the findings of enlarged nuclei and increased cytoplasm are consistent with cellular hypertrophy. In the presence of adenomyosis, the junctional zone showed cellular and nuclear hypertrophy, abnormal nuclear and mitochondrial shape, abundant myelin bodies and intermediate filaments aggregates, extensive endoplasmic reticulum, and lengthening of sarcolemmal plaques with reduced caveolae. The outer myometrium was similarly affected. The absence of localised changes indicates the presence of a uterus-wide pathology both in the JZ and outer myometrium. It is more plausible that these changes represent a primary myometrial defect rather than a phenomenon secondary to the presence of adenomyosis, as these changes were equally present in the outer myometrium, which does not contain adenomyosis foci.

The increase in intracellular aggregates suggest an increase in intermediate filaments (Richards et al., 1998), as demonstrated by vimentin and desmin immunohistochemical staining (Eyden et al., 1992). It is plausible that these filament aggregates could be related to an increased synthetic activity in the myocyte, as evidenced by the observed cellular hypertrophy, expanded cytoplasm, and by the increase in ribosomes and rough endoplasmic reticulum. The net effect can be an imbalance between the production and turnover of the cytoskeletal components.

The contractile filaments of the cytoplasm can affect the shape of the nucleus. Contracted intestinal smooth muscle cells exhibited exaggerated nuclear envelope invaginations when examined using electron microscopy (Lane, 1965). Similarly, alterations of the intracellular ionic environment (especially bivalent cations e.g.

calcium) cause changes to the nuclear shape (Davies and Spencer, 1962) and to the appearance of the chromatin material (Barnicot, 1967). Increased intracellular calcium is associated with nuclear envelope indentations and a condensed chromatin. Thus, the nuclear abnormalities in uteri with adenomyosis could potentially be explained by abnormal contractility.

The sarcolemma of smooth muscle cells is divided into two structurally distinct regions: those bearing submembranous dense plaques and intervening zones which bear many vesicular invaginations or caveolae. The dense bands are junctions of the adherens type, and serve as anchorage sites for actin cytoskeleton and are typically marked by antibodies to vinculin (North et al., 1993).

Caveolae have been implicated in a wide range of cellular functions. Caveolae contain a host of receptors, second messenger generators, G proteins, kinases, and ion channels in close proximity. Caveolae are often in close proximity to sarcoplasmic reticulum or mitochondria, and have been proposed to organize signalling molecules (Fujimoto, 1993, Goto et al., 1993). The increased length of the dense bands which anchor intracellular myofilaments could reflect an increase in cytoskeletal filaments (Richards et al., 1998). Abnormally shaped mitochondria with unfolded cristae suggest an abnormality in active cellular processes or the initiation of a degenerative process (Cotran et al., 1989, Richards et al., 1998).

It is plausible that the main function of the junctional zone is concerned with preparation of the endometrium for implantation, sperm transport as well as haemostasis during menstruation; with the outer myometrium being primary involved with parturition. It is also possible that the ultrastructural abnormalities observed with the sarcolemmal bands and caveolae may cause a disturbance in the normal calcium cycling in the affected myocytes, with a subsequent loss of normal rhythmic contractions.

Chronic uterine dysfunctional peristalsis and hyperperistalsis have been proposed as causal factors for adenomyosis and endometriosis, as this result in dislocation of the basal endometrium both in the underlying myometrium and peritoneal cavity. Women with endometriosis displayed marked uterine hyperperistalsis that differs significantly from the peristalsis in unaffected women during the early and mid-follicular and mid-luteal phases (Kunz et al., 2000). This study demonstrates that the myocytes of uteri harbouring adenomyosis are ultrastructurally different from those of normal uteri. These ultrastructural changes suggest a possible defect in myometrial contractility. Dysfunctional contractility could be the result of the presence of adenomyosis or could contribute to its pathogenesis.

Although there is no clear evidence of an impaired systemic hormonal milieu, local hyperestrogenaemia has been suggested to be involved in the development of uterine adenomyosis. Similar to uterine leiomyomata, estrogen was found to be synthesized and secreted by adenomyotic tissue (Yamamoto et al., 1993). In normal uteri, estrogen and progesterone receptors were suggested to show cyclic changes in the subendometrial myometrium but not in the overlying basalis endometrium (Leyendecker et al., 1998). Immunohistochemistry studies of estrogen and progesterone receptors in adenomyosis foci and surrounding myometrium showed that ER was always present but in a reduced quantity when compared to the corresponding normal myometrium. In contrast, progesterone receptors (PR) were not always present (Tamaya et al., 1979).

The current study described an enlargement of the endoplasmic reticulum and an increase in myofilament content and hypertrophy in the myometrium of uteri affected with adenomyosis. In previous electron microscopy studies, enlargement of endoplasmic reticulum and an increase in free ribosomes have been described with supraphysiologic doses of estrogen (Friederici and DeCloux, 1968), and an increase in

myofilament content and hypertrophy have been observed with synthetic progestogens (Dito and Batsakis, 1961).

Similar changes were observed in this current study, and given the potential role of gonadal steroid hormones and the conflicting reports on estrogen and progesterone receptors expression, the next experiment will examine the steroid hormones receptors expression (i.e. ER- $\alpha$ , ER- $\beta$ , PR-A, PR-B) in the myometrium of uteri with adenomyosis.

## **Chapter 6**

**Estrogen and Progesterone receptors distribution in uteri with and without adenomyosis through the menstrual cycle**

## Chapter 6

### **Estrogen and Progesterone receptors distribution in uteri with and without adenomyosis through the menstrual cycle**

#### **6.1 INTRODUCTION**

Ovarian steroid hormones play a crucial role in the maintenance and function of the uterine endometrium during the menstrual cycle, with phenotypical changes in the stromal and glandular epithelial compartments being regulated by the interaction of the ovarian steroid hormones with their receptors. Using immunohistochemistry, the distribution of estrogen receptors (ER) and progesterone receptors (PR) expression has been described in the normal human endometrium, fallopian tube, myometrium and cervix (Snijders et al., 1992, Lessey et al., 1988, Amso et al., 1994, Fung et al., 1994, Tseng and Zhu, 1997, Garcia et al., 1988, Prentice et al., 1992), through the menstrual cycle. When specified, these studies examined the subendometrial (inner) myometrium assuming that there were no differences between the inner and outer myometrial layers (Snijders et al., 1992, Lessey et al., 1988, Amso et al., 1994). Little attention has been paid to the outer myometrium, which may display varying functions during different phases of the reproductive process.

The junctional zone (JZ) was shown to be hormonally dependent. On MRI, it is indistinct before puberty and after the menopause, and showing maximum increase in thickness in the second half of the proliferative phase (Wiczzyk et al., 1988, Demas et al., 1986). Studies using video-sonography have demonstrated peristaltic waves

confined to the JZ myometrium. These waves vary during the cycle (Ijland et al., 1997). JZ contractions during the late proliferative phase may have a role in sperm transport, whilst quiescence during the secretory phase may facilitate implantation (Fanchin et al., 1998).

Uterine peristaltic activity is under the control of the ovarian steroid hormones.

Adenomyosis has been linked to hyperestrogenic states, in common with other uterine pathologies such as endometrial hyperplasia and fibroids. Although there is no clear evidence of an impaired systemic hormonal milieu in patients with adenomyosis, local hyperestrogenism may be involved in the development of uterine adenomyosis (Leyendecker et al., 1998). *Leyendecker et al.* (1998) suggested a model for the development of adenomyosis, where a key event appears to be an increase in the local production of estrogen secondary to an increased expression of the P<sub>450</sub> aromatase enzyme. Locally increased levels of estrogen could up-regulate the endometrial oxytocin mRNA, increasing levels of oxytocin and resulting in uterine hyperperistalsis. Increased peristalsis, with and endometrial proliferation could lead to detachment of the endometrium and infiltration of the underlying myometrium resulting in adenomyosis (Leyendecker et al., 1998). This remains speculative.

In the mouse model (chapters 2 and 3), there was an attenuation of ER- $\alpha$  expression in both in C57BL/6J mice (that did not develop adenomyosis) and in CD-1 mice (that did develop adenomyosis) following tamoxifen administration. It is thus unlikely that the different responses to tamoxifen are attributed to differences in ER- $\alpha$  expression. In addition, tamoxifen (an anti-estrogen) was administered to neonatal pups not exposed to estrogen, suggesting that the mechanism of action involves other receptors. As mentioned earlier, adenomyosis is frequently observed in women on tamoxifen (chapter 1), and again the mechanism and link are not clear.

The aim of this study was to examine the expression and distribution of estrogen and progesterone receptors in the uteri with or without adenomyosis, during the menstrual cycle. Layers examined are the functionalis and basalis endometrium (glands and stroma), inner and outer myometrium. In addition, adenomyosis foci glandular epithelium and stroma were examined in affected uteri. In the literature, there is no such description of the distribution of estrogen and progesterone receptors in the individual layers of the uteri affected by adenomyosis.

## **6.2 MATERIALS AND METHODS**

### **6.2.1 Patients and samples**

Hysterectomy specimens from premenopausal women not using exogenous hormones were selected for this study. The uteri were removed by abdominal or laparoscopic assisted vaginal hysterectomy (LAVH) for menorrhagia with or without dysmenorrhea. None of the participants had fibroids or endometrial abnormalities on preoperative ultrasound or hysteroscopy, and none had endometriosis. Histological sections encompassing the full uterine wall thickness from endometrium to the serosa were used. All samples were obtained from the anterior wall of the uterus near the fundus as previously described. Adenomyosis was defined by the presence of endometrial glands and stroma deeper than 2.5mm below the endometrial-myometrial interface (Uduwela et al., 2000). Histopathological examination proved normal endometrium and absence of fibroids, and confirmed adenomyosis. The specimens were classified according to the phase of the menstrual cycle into early, mid-, late-proliferative (EP, MP, LP) and early, mid-, late-secretory (ES, MS, LS), using established histological criteria (Noyes and Haman, 1953). The study included 35 control uteri with no endometrial or myometrial

pathology (i.e. no fibroids, endometrial hyperplasia, malignancy, or polyps) (EP=5; MP=6; LP=5; ES=8;MS=6; LS=5) and 54 uteri with adenomyosis as the sole pathology (EP=10; MP=11; LP=6; ES=8; MS=9; LS=10).

### **6.2.2 Immunohistochemistry**

Serial 5 µm sections were immunohistochemically stained for ER-α, ER-β, PR-A and PR-B. In summary, sections were dewaxed in xylene, and rehydrated in graded alcohols and deionised water. Epitope antigen retrieval was done using microwave and citrate buffer (pH = 6.0). Endogenous peroxidase activity was blocked with 6% (v/v) hydrogen peroxide (H<sub>2</sub>O<sub>2</sub>) before endogenous avidin and biotin-binding sites were blocked (Avidin-Biotin blocking kit, Vector Laboratories, Peterborough, UK). Non-specific binding was blocked with 3% Bovine serum albumin (BSA) (Sigma-Aldrich, Poole, Dorset, UK) in phosphate buffer saline (PBS) for 30 minutes. Sections were incubated overnight at 4°C with the primary monoclonal antibodies against ER-α (NCL-L-ER-6F11, 1:50 (v/v), Novocastra, Newcastle upon Tyne, UK); ER-β (MS-ERB13-PX1, 1:500 (v/v), Genetex, Abcam, Cambridge, UK); PR-A (NCL-PGR-312, 1:200 (v/v), Novocastra, Newcastle upon Tyne, UK); and PR-B (NCL-PGR-B, 1:200 (v/v), Novocastra, Newcastle upon Tyne, UK). Biotinylated rabbit anti-mouse (Dako, Cambridge, UK) at a concentration of 1:400 (v/v) was used as secondary antibody. Immunoreactivity was demonstrated with 3,3'-diaminobenzidine/ H<sub>2</sub>O<sub>2</sub> (DAB solution) (Vector labs, Peterborough, UK). Sections were lightly counterstained with haematoxylin, then dehydrated and cleared in graded alcohol and xylene. This methodology has been previously validated and described in details (Taylor and Al-Azzawi, 2000, Thornton et al., 2003). Negative control slides were run in parallel by using iso-type IgG (Vector) at the same concentration and dilutions as the respective

primary antibody counterparts. Positive tissue controls were used to validate the assay as per manufacturer's recommendation. No staining for Fc-region antibody binding was found with any of the primary antibodies tested (data not shown).

### **6.2.3 Images capture and analysis**

Image capture and analysis was performed using Axioplan® 2 light microscope (Carl Zeiss, Germany) and an image capture system, based on a single chip colour video camera (Sony DXC-151P, Sony Inc., Japan), a camera adapter (Sony CMA-151P, Sony Inc., Japan), and a Meteor 2 MMC graphics display. Digital image analysis was performed using Axiovision image analysis software (version 4.0, Carl Zeiss, Germany). Standardisation was performed by maintaining the same illumination and settings throughout the experiment.

The pattern of distribution of the positively stained cells was recorded and the percentage of positively stained cells per high power field assessed by the capture of 10 randomly selected fields per layer at x400 magnification. The layers evaluated were functionalis and basalis endometrium (glands and stroma), innermost myometrium and outermost myometrium, in addition to the adenomyosis foci glandular epithelium and stroma in affected uteri. The percentage of positively stained immunoreactive cell nuclei or cytoplasm was obtained by counting the number of positive (brown-stained) and negative (blue- stained) cells in the field. Endothelial and neural cells were omitted from the count. Each specimen provided a mean score and the average and standard error of the mean calculated for each phase of the menstrual cycle.

#### **6.2.4 Statistical analysis**

Graphpad Instat<sup>®</sup> 3 and Graphpad Prism<sup>®</sup> 5 software were used for analysis (GraphPad Software, San Diego California USA, www.graphpad.com). Data were tested for normality using the Kolmogorov-Smirnov test and comparisons were made using Student's *t*-test for continuous data and Mann-Whitney U-test for non-continuous data, with  $p < 0.05$  accepted as statistically significant. One-way analysis of variance (ANOVA) with Tukey's correction for multiple testing was used to compare the data across the menstrual cycle. Similar studies have previously demonstrated the validity of these methods for the study of antigen staining by immunohistochemistry (Wahab et al., 1999b, Wahab et al., 1999a).

### **6.3 RESULTS**

#### **6.3.1 Estrogen receptor alpha (ER- $\alpha$ ) distribution**

The results are summarized in Table 6.1. Figures 6.1 – 6.7 (Appendix 1) show representative sections of the different uterine layers throughout the menstrual cycle, with respective comparisons between adenomyosis and control uteri.

ER- $\alpha$  immunostaining was confined to the nucleus of the cells examined. In the epithelial component of the control functionalis, ER- $\alpha$  immunoreactivity was 96-98% in the proliferative phases, and dropped to 63-69% in the secretory phases. In adenomyotic uteri, the functionalis glands followed the same pattern but expression was significantly lower in the MS phase (11.2%). In the functionalis stroma, the ER- $\alpha$  expression was lower in adenomyosis in EP, MP, and MS (Figure 6.1 and 6.2, Appendix 1).

Likewise, in the basalis glands and stroma, comparable differences were observed.

However, there was some cyclical fluctuation in ER- $\alpha$  expression in the basalis glands

and stroma, but this did not reach statistical significance (Figure 6.3 and 6.4, Appendix 1). Adenomyosis foci ER- $\alpha$  expression was similar to the basalis in intensity and lack of significant cyclical changes, both in glandular and stromal components (Figure 6.29 and 6.30, Appendix 1).

There was no cyclical variation in the inner or outer myometrium of control or adenomyotic uteri. With adenomyosis, the inner myometrium showed higher ER- $\alpha$  expression in LP and LS phases. Such differences were not seen in the outer myometrium (Figure 6.5 – 6.7, Appendix 1).

**Table 6.1: Estrogen receptor alpha distribution in different uterine layers in the different phases of the menstrual cycle. Immunohistochemical staining expressed as percentage of positively stained cells per high power field (mean ± SEM).**

	FG		FS		BG		BS		IM		OM		Adenomyosis	
	<u>Control</u>	<u>Adeno</u>	<u>Control</u>	<u>Adeno</u>	<u>Control</u>	<u>Adeno</u>	<u>Control</u>	<u>Adeno</u>	<u>Control</u>	<u>Adeno</u>	<u>Control</u>	<u>Adeno</u>	<u>Glands</u>	<u>Stroma</u>
<b>EP</b>	97.6	98.8	<b>85.2</b>	<b>68.1</b>	99.2	98.8	<b>90.7</b>	<b>78.3</b>	88.3	81.4	81.6	71.1	94.2	83
	± 0.4	± 0.7	± <b>2.6</b>	± <b>5.4*</b>	± 0.1	± 0.4	± <b>0.7</b>	± <b>3.2*</b>	± 1.6	± 4.6	± 7.2	± 5.6	± 1	± 7.3
<b>MP</b>	98.4	94.5	<b>90</b>	<b>72.1</b>	99.4	90.8	<b>88.1</b>	<b>63.1</b>	84.5	83.7	80.8	77	93	76.9
	± 0.2	± 1.5	± <b>2</b>	± <b>3.6*</b>	± 0.1	± 4.9	± <b>1.4</b>	± <b>10.9*</b>	± 2.2	± 1.9	± 2.9	± 4	± 2.6	± 3.8
<b>LP</b>	95.8	98.6	87.2	83.7	97.8	98.7	73.6	75.1	<b>66.8</b>	<b>89.6</b>	54.8	77.8	91.8	77.6
	± 2.9	± 0.5	± 2.9	± 3	± 1.2	± 0.4	± 12.7	± 2.3	± <b>8.6</b>	± <b>0.5*</b>	± 15	± 3.4	± 3.1	± 6.2
<b>ES</b>	68.8	62.6	52.8	64.4	84.8	87.7	<b>80.7</b>	<b>53.9</b>	76.7	84.7	62.2	71.6	93.1	79.6
	± 10.7	± 8.9	± 13	± 4.5	± 12.9	± 5.4	± <b>4.9</b>	± <b>8.7*</b>	± 1.8	± 3.9	± 7.4	± 7.1	± 3.1	± 4.7
<b>MS</b>	<b>61.2</b>	<b>11.2</b>	<b>63.2</b>	<b>20.8</b>	<b>96</b>	<b>60.1</b>	<b>86.2</b>	<b>57.6</b>	81.3	78.8	72.9	71.2	81.5	80.7
	± <b>6.9</b>	± <b>3.5*</b>	± <b>7.9</b>	± <b>5.9*</b>	± <b>1.9</b>	± <b>16*</b>	± <b>1.6</b>	± <b>15.8*</b>	± 3.4	± 4.7	± 3.4	± 2.4	± 13.6	± 5.7
<b>LS</b>	62.8	66.2	67.4	66.2	98	91.4	83.3	75.8	<b>83.2</b>	<b>90.9</b>	75	76.7	93.8	77.6
	± 11.1	± 13.1	± 5.2	± 10.3	± 0.6	± 1.1	± 1.2	± 3.9	± <b>1.9</b>	± <b>1.7*</b>	± 8.4	± 7.7	± 1.8	± 5.2

\* Significant difference between adenomyosis and control ( $p < 0.05$ ) uteri

EP=Early Proliferative, MP=Mid-Proliferative, LP=Late Proliferative, ES=Early Secretory, MS=Mid-Secretory, LS=Late Secretory

FG= functionalis glands, FS= functionalis stroma, BG= basalis glands, BS= basalis stroma, IM= inner myometrium, OM= outer myometrium.

### **6.3.2 Estrogen receptor beta (ER- $\beta$ ) distribution**

Results are summarized in table 6.2. Respective sections and analyses are illustrated in Figures 6.8 – 6.14 (Appendix 1). ER- $\beta$  staining was both nuclear and cytoplasmic in most cells, with the majority of cells predominantly showing nuclear staining.

In the functionalis, ER- $\beta$  staining in the glandular epithelial cells was significantly higher in the early secretory (ES) phase when compared to the proliferative phases. This pattern was reversed in the adenomyotic uteri functionalis glands (i.e. lowest levels observed in ES phase compared to the rest of the cycle). In addition, ER- $\beta$  expression was significantly higher compared to control functionalis in EP, MP and LP phases. The functionalis stroma showed minimal cyclical fluctuation in controls (statistically non-significant) and levels were not significantly different compared to adenomyosis functionalis stroma (Figure 6.8 and 6.9, Appendix 1).

In control basalis, the peak glandular expression was in LP and ES phases. In adenomyosis group, the expression pattern was similar to functionalis glands, and was significantly different from controls in EP phases. Basalis stroma showed significantly higher expression levels in adenomyotic samples in EP, LP, MS, LS phases compared to controls (Figure 6.10 and 6.11, Appendix 1). Adenomyotic foci ER- $\beta$  expression was similar to the basalis in intensity and lack of cyclical changes, both in glandular and stromal components (Figures 6.29 and 6.31, Appendix 1).

Similar to ER- $\alpha$ , the myometrium did not show minimal statistically non-significant cyclical variation of ER- $\beta$  expression. However, both inner and outer myometrial layers of adenomyotic uteri showed significantly higher ER- $\beta$  levels in MP, LP, and MS cycle phases. There was no difference between the inner and outer myometrium both in control or adenomyosis groups (Figure 6.12 – 6.14, Appendix 1).

**Table 6.2: Estrogen receptor beta distribution in different uterine layers in the different phases of the menstrual cycle. Immunohistochemical staining expressed as percentage of positively stained cells per high power field (mean  $\pm$  SEM).**

	FG		FS		BG		BS		IM		OM		Adenomyosis	
	<u>Control</u>	<u>Adeno</u>	<u>Glands</u>	<u>Stroma</u>										
<b>EP</b>	<b>51.6</b>	<b>84.4</b>	11.6	12.9	<b>42.9</b>	<b>90.3</b>	<b>1.8</b>	<b>8.6</b>	0.6	4.7	0.2	10.4	98.5	5.6
	$\pm 4.9$	$\pm 11.4^*$	$\pm 4.7$	$\pm 4.3$	$\pm 10.1$	$\pm 7.2^*$	$\pm 1$	$\pm 1.6^*$	$\pm 0.1$	$\pm 2.8$	$\pm 0.1$	$\pm 6.2$	$\pm 0.3$	$\pm 1.7$
<b>MP</b>	<b>52.7</b>	<b>85.7</b>	27.2	24.7	76.9	84.6	3.5	7.3	<b>1.4</b>	<b>22</b>	<b>0.2</b>	<b>33.3</b>	93.9	6.9
	$\pm 5.6$	$\pm 5.1^*$	$\pm 7.6$	$\pm 13.5$	$\pm 12.7$	$\pm 12.5$	$\pm 1.4$	$\pm 1.3$	$\pm 0.4$	$\pm 5.7^*$	$\pm 0.1$	$\pm 12.2^*$	$\pm 3.6$	$\pm 1.7$
<b>LP</b>	<b>51.6</b>	<b>94.8</b>	15.2	48.5	85.1	87.5	<b>3.3</b>	<b>41.3</b>	7.7	20.5	<b>6.8</b>	<b>45.6</b>	88.3	25.9
	$\pm 9.2$	$\pm 3.2^*$	$\pm 10.2$	$\pm 19.8$	$\pm 9.1$	$\pm 11.6$	$\pm 2.3$	$\pm 14.2^*$	$\pm 7.1$	$\pm 4.9$	$\pm 6.1$	$\pm 15.5^*$	$\pm 9.5$	$\pm 6.4$
<b>ES</b>	74.1	51.9	16.8	20	84.5	46.9	1.1	7	2.4	6.7	2.9	12.9	53.1	4.3
	$\pm 13.2$	$\pm 20$	$\pm 5.1$	$\pm 12$	$\pm 12.7$	$\pm 19.8$	$\pm 0.5$	$\pm 4.2$	$\pm 1.8$	$\pm 4.4$	$\pm 1.8$	$\pm 5.1$	$\pm 19.8$	$\pm 1.8$
<b>MS</b>	70.6	77.3	23.2	44.3	71.9	66.4	0.6	18.6	<b>6.9</b>	<b>23.6</b>	<b>5.6</b>	<b>43</b>	90	10.1
	$\pm 10.5$	$\pm 12.4$	$\pm 5.6$	$\pm 14.3$	$\pm 10.2$	$\pm 7$	$\pm 0.2$	$\pm 4.9$	$\pm 5.2$	$\pm 3.1^*$	$\pm 3.8$	$\pm 9.4^*$	$\pm 4.8$	$\pm 2.7$
<b>LS</b>	55.2	71	17.8	29.2	42.2	71.3	0.2	25.3	<b>0.9</b>	<b>19.2</b>	0.3	20.9	97	9.4
	$\pm 12.7$	$\pm 15.7$	$\pm 3$	$\pm 29.3$	$\pm 18.9$	$\pm 10.4$	$\pm 0.1$	$\pm 8.8$	$\pm 0.2$	$\pm 4.5^*$	$\pm 0.1$	$\pm 9.4$	$\pm 1.6$	$\pm 3.2$

\* Significant difference between adenomyosis and control ( $p < 0.05$ ) uteri

EP=Early Proliferative, MP=Mid-Proliferative, LP=Late Proliferative, ES=Early Secretory, MS=Mid-Secretory, LS=Late Secretory

FG= functionalis glands, FS= functionalis stroma, BG= basalis glands, BS= basalis stroma, IM= inner myometrium, OM= outer myometrium.

### **6.3.3 Progesterone receptors (PR-A and PR-B) distribution**

The results are summarized in tables 6.3 and 6.4. The pattern of both PR-A and PR-B immunoreactivity was confined to the nucleus of all cells examined. Both receptors showed similar changes through the menstrual cycle in all examined layers. Figures 6.15 – 6.28 (Appendix 1) show representative sections of the different uterine layers throughout the menstrual cycle, with respective comparisons between adenomyosis and control uteri.

In the functionalis and basalis control glandular epithelial cells, both PR-A and PR-B showed a steep decline in expression levels in the secretory phases from an almost 100% expression earlier in the proliferative phases. In adenomyosis group, the glands expressed lower levels of PR-A in the EP in functionalis and basalis, and MP in functionalis. The endometrial stromal expression of PR-A and PR-B showed no cyclical variability in control uteri. In adenomyotic uteri, the expression of PR-A was lower in proliferative and late secretory phases, while PR-B was lower in MP and secretory phases in the functionalis stroma. In the basalis stroma, the expression of both PR-A and PR-B was lower in all phases of the menstrual cycle (Figures 6.15 – 6.18 for PR-A and figures 6.22 – 6.25 for PR-B, Appendix 1). Once more, adenomyosis foci PR-A and PR-B expression was similar to the basalis in intensity and lack of cyclical changes, both in glandular and stromal (Figures 6.29, 6.32 and 6.33, Appendix 1).

There was minimal, statistically non-significant cyclical fluctuation in the expression of PR-A and PR-B in the inner or the outer myometrium of control uteri. In adenomyotic uteri, PR-A immunoreactivity was significantly lower in all phases of the cycles (except ES) both in the inner and the outer myometrium, while PR-B immunostaining was lower in EP, MP, MS and LS phases (Figures 6.18 – 6.21 for PR-A and figures 6.26 – 6.28 for PR-B, Appendix 1).

**Table 6.3: Progesterone receptor A distribution in different uterine layers in the different phases of the menstrual cycle. Immunohistochemical staining expressed as percentage of positively stained cells per high power field (mean  $\pm$  SEM).**

	FG		FS		BG		BS		IM		OM		Adenomyosis	
	<u>Control</u>	<u>Adeno</u>	<u>Glands</u>	<u>Stroma</u>										
EP	98.6	62.3	86.6	53.1	99.5	70.7	91.7	49.6	91.8	51.9	89.1	59.9	89.5	45.5
	$\pm 0.3$	$\pm 19.4^*$	$\pm 1.3$	$\pm 13.1^*$	$\pm 0.1$	$\pm 14.3^*$	$\pm 1.5$	$\pm 16.3^*$	$\pm 1.2$	$\pm 9.2^*$	$\pm 3.3$	$\pm 8.8^*$	$\pm 5.9$	$\pm 12.6$
MP	99.6	82.7	88.7	59.1	99.6	81	92.5	45.4	90	68.1	88.4	55.1	93.2	73.3
	$\pm 0.2$	$\pm 5.5^*$	$\pm 1.5$	$\pm 10.5^*$	$\pm 0.1$	$\pm 13.3$	$\pm 1.2$	$\pm 12.1^*$	$\pm 1.1$	$\pm 3.9^*$	$\pm 1.6$	$\pm 7.7^*$	$\pm 4.7$	$\pm 5.5$
LP	99.4	98.6	89.4	81.7	99.8	99.2	94.2	76.8	90	74.1	84	66.1	99.1	75.9
	$\pm 0.3$	$\pm 1.2$	$\pm 2.3$	$\pm 1.6^*$	$\pm 0.1$	$\pm 0.5$	$\pm 0.7$	$\pm 3.1^*$	$\pm 1.5$	$\pm 2.3^*$	$\pm 3.2$	$\pm 5.5^*$	$\pm 0.1$	$\pm 4.6$
ES	99.9	94.1	88.3	78.4	99.9	91.7	93.3	72.7	86.9	77.7	86.7	74.1	90.1	79.4
	$\pm 0.1$	$\pm 3.8$	$\pm 3.2$	$\pm 7.5$	$\pm 0.1$	$\pm 7.8$	$\pm 0.7$	$\pm 7.9^*$	$\pm 2.7$	$\pm 3.8$	$\pm 4$	$\pm 4.6$	$\pm 9.1$	$\pm 4.6$
MS	44.2	30.6	77.1	72.9	58.5	34.6	91.7	63.4	91	69.6	88.3	62.1	88.8	64.5
	$\pm 13.6$	$\pm 16.5$	$\pm 4.1$	$\pm 5.8$	$\pm 13.3$	$\pm 13$	$\pm 1.4$	$\pm 4.1^*$	$\pm 0.9$	$\pm 2.3^*$	$\pm 2.3$	$\pm 8.8^*$	$\pm 3.6$	$\pm 7.3$
LS	8.5	6.3	79.6	45.2	57.4	37	89.5	53	88.2	78.8	88	61.8	60.5	71.6
	$\pm 4.1$	$\pm 1.8$	$\pm 3.7$	$\pm 15^*$	$\pm 15.3$	$\pm 11.9$	$\pm 1.4$	$\pm 8.8^*$	$\pm 2$	$\pm 3.8^*$	$\pm 2.4$	$\pm 10.6^*$	$\pm 16.5$	$\pm 7.7$

\* Significant difference between adenomyosis and control ( $p < 0.05$ ) uteri

EP=Early Proliferative, MP=Mid-Proliferative, LP=Late Proliferative, ES=Early Secretory, MS=Mid-Secretory, LS=Late Secretory

FG= functionalis glands, FS= functionalis stroma, BG= basalis glands, BS= basalis stroma, IM= inner myometrium, OM= outer myometrium.

**Table 6.4: Progesterone receptor B distribution in different uterine layers in the different phases of the menstrual cycle. Immunohistochemical staining expressed as percentage of positively stained cells per high power field (mean ± SEM).**

	FG		FS		BG		BS		IM		OM		Adenomyosis	
	<u>Control</u>	<u>Adeno</u>	<u>Control</u>	<u>Adeno</u>	<u>Control</u>	<u>Adeno</u>	<u>Control</u>	<u>Adeno</u>	<u>Control</u>	<u>Adeno</u>	<u>Control</u>	<u>Adeno</u>	<u>Glands</u>	<u>Stroma</u>
<b>EP</b>	99.5	98.5	<b>79.7</b>	<b>74.6</b>	99.4	98.5	<b>88.1</b>	<b>60.3</b>	<b>88</b>	<b>62.2</b>	85.8	66.2	90	47.1
	± 0.1	± 0.4	± <b>5.2</b>	± <b>8.6*</b>	± 0.1	± 0.7	± <b>2</b>	± <b>10*</b>	± <b>1.9</b>	± <b>10.3*</b>	± 3.3	± 9.9	± 6.4	± 9.7
<b>MP</b>	99.5	99.8	<b>89</b>	<b>76.1</b>	99.3	97.6	<b>85.8</b>	<b>61</b>	<b>81.1</b>	<b>66.4</b>	<b>82.9</b>	<b>58.4</b>	98.4	56.8
	± 0.8	± 0.1	± <b>0.2</b>	± <b>3.4*</b>	± 0.1	± 1.8	± <b>1.9</b>	± <b>6.7*</b>	± <b>2.7</b>	± <b>5.4*</b>	± <b>2.2</b>	± <b>4.7*</b>	± 0.5	± 6.7
<b>LP</b>	98.8	99.2	86	84.9	98.5	99.1	<b>85.2</b>	<b>58.6</b>	77.9	62.5	68.6	58.1	99	63.1
	± 0.5	± 0.4	± 2.4	± 4.6	± 0.7	± 0.5	± <b>3.3</b>	± <b>11.2*</b>	± 5.6	± 6.3	± 8.5	± 13.1	± 0.3	± 7.8
<b>ES</b>	99.8	75.3	<b>88.6</b>	<b>47.8</b>	99.7	74.7	<b>88.3</b>	<b>37.2</b>	84.6	61.1	73.2	55.8	94.5	44.6
	± 0.1	± 17.5	± <b>1.1</b>	± <b>15.4*</b>	± 0.1	± 17.4	± <b>0.8</b>	± <b>12.1*</b>	± 2.9	± 14.3	± 7.6	± 9	± 4.5	± 12
<b>MS</b>	34.3	31.8	<b>67.7</b>	<b>32</b>	55.1	44.8	<b>87.2</b>	<b>36.4</b>	<b>77.2</b>	<b>59.4</b>	69.7	49.6	89.6	36.1
	± 12.6	± 19.2	± <b>9.4</b>	± <b>14.7*</b>	± 10.6	± 17.6	± <b>2.1</b>	± <b>12*</b>	± <b>4.4</b>	± <b>6.2*</b>	± 4.3	± 9.3	± 5.5	± 10.4
<b>LS</b>	4.3	1.2	<b>74</b>	<b>12.2</b>	48.8	17.1	<b>79</b>	<b>19.6</b>	<b>82.1</b>	<b>29.4</b>	<b>76.7</b>	<b>57.4</b>	4.9	12.7
	± 3.1	± 0.9	± <b>4.2</b>	± <b>12.1*</b>	± 16.9	± 11.5	± <b>10</b>	± <b>15.1*</b>	± <b>0.9</b>	± <b>17.2*</b>	± <b>3.9</b>	± <b>5.1*</b>	± 4.8	± 12.7

\* Significant difference between adenomyosis and control ( $p < 0.05$ ) uteri

EP=Early Proliferative, MP=Mid-Proliferative, LP=Late Proliferative, ES=Early Secretory, MS=Mid-Secretory, LS=Late Secretory

FG= functionalis glands, FS= functionalis stroma, BG= basalis glands, BS= basalis stroma, IM= inner myometrium, OM= outer myometrium.

## 6.4 DISCUSSION

This study describes the receptor distribution of ER- $\alpha$ , ER- $\beta$ , PR-A and PR-B in the endometrium (functionalis and basalis) and the myometrium (inner and outer) of uteri with or without adenomyosis, through the menstrual cycle. Immunocytochemistry with the use of specific monoclonal antibodies allowed the visualization of estradiol and progesterone receptors in individual cells of the uterus as a target organ for ovarian steroids. With respect to the distribution of estradiol and progesterone receptors in the glandular and stromal part of the functionalis and basalis endometrium in control uteri and their cyclical changes throughout the menstrual cycle, this study largely confirms previous results (Garcia et al., 1988, Lessey et al., 1988, Snijders et al., 1992, Amso et al., 1994, Shiozawa et al., 1996, Taylor and Al-Azzawi, 2000, Mylonas et al., 2004), indicating that the samples used were representative of a well-defined menstrual cycle, and ensuring the validity of the methodology.

The pattern of ERs and PRs distribution in the endometrium of uteri affected by adenomyosis was different from control uteri. In adenomyotic uteri, all layers examined showed abnormal expression of steroid hormones receptors. The expression of both ERs and PRs in the uterine layers and the cyclic changes (when present) of the receptor expression is, in addition to up-regulation by estradiol, primarily a matter of down-regulation by changing progesterone concentrations in the luteal phases (Kraus and Katzenellenbogen, 1993, Iwai et al., 1995, Graham and Clarke, 1997). The functional significance of cell-specific differential receptor regulation may be viewed in a suppression of hormone action in the respective tissue in the presence of high circulating concentrations of this hormone required for continuing action in another tissue (King et al., 1981, McCormack and Glasser, 1980, Lessey et al., 1988, Shiozawa et al., 1996).

In the functionalis glands, ER- $\alpha$  was significantly lower in the MS phase, while ER- $\beta$  was significantly higher in all the proliferative phases. PR-A expression was lower in EP and MP phases. PR-B was no different. In the functionalis stroma, ER- $\alpha$  expression was lower in EP, MP and MS; PR-A was lower in EP, MP, LP and LS; while PR-B was lower in all phases of the cycle except EP and LP. ER- $\beta$  was not different. Examining the basalis glands, minimum differences were observed mainly in the EP for PR-A and ER- $\beta$ , and MS for ER- $\alpha$ . No difference in PR-B distribution was observed.

Interestingly, the basalis stroma was the layer showing most of the differences between adenomyosis and controls. PR-A and PR-B were significantly lower in all phases of the cycle in basalis stroma of uteri affected by adenomyosis. ER- $\alpha$  was equally lower in all phases except LP and LS. On the opposite, ER- $\beta$  expression was higher in all phases except in MP and ES phases.

The presence of higher expression of ER- $\beta$  in the endometrium of adenomyotic uteri might equally contribute to the presence of the commonly associated endometrial hyperplasia (Sapino et al., 2006b, Natoli et al., 2005, Trapido et al., 1984).

The expression of steroid receptors expression in adenomyosis foci glands and stroma was comparable to the overlying basalis endometrium. This is in agreement with previous studies that suggested that the endometrial glands and stroma in adenomyosis resemble the basalis endometrium (Ferenczy, 1998), possibly explaining the limited changes with the menstrual cycle. This is also in agreement with previous studies where steroid receptors in adenomyosis were examined using Scatchard plot analysis. ER were detected in all cases, while PR was not detected in some cases and, when detected, the content seemed to be lower (Tamaya et al., 1979), corresponding to the delayed “dating” of ectopic foci of endometrium compared to the overlying eutopic endometrium suggested by the authors.

There was no significant cyclical fluctuation in estrogen or progesterone receptors distribution or immunostaining across the myometrial wall (i.e. in the inner or outer myometrium). The distribution and cyclical changes in steroid receptors in the normal myometrium have been inconsistently reported in the literature. While Noe et al (1999) (Noe et al., 1999) showed that the expression of steroid receptors in the subendometrial myometrium paralleled the cyclic pattern of the endometrial epithelium and stroma, this was not shown in the current study. The reason for the discrepancy between these two immunohistochemical studies is not readily apparent but may be related to the site of the uterine biopsy or more likely to the quantitative methodology used. In this thesis, the percentage of positively staining cells was used as an objective measurement of the receptors expression to avoid the introduction of the subjective notion of intensity of staining and the area stained. In addition, the presence of positively stained nuclei indicates the expression of receptor in this cells, allowing subsequent biological activity and effect of its ligand, irrespective of the intensity of staining which might be more linked to the absolute number of receptors in the nucleus.

The observed lack of cyclicity of steroid receptors in the inner myometrium is in agreement with other studies that used a similar methodology (Mertens et al., 2001, Scharl et al., 1988). The lack of cyclical changes and absence of differences between the inner and outer myometrium in estrogen or progesterone receptors expression was equally confirmed by myometrial tissue cDNA microarrays (chapter 7). In conclusion, the findings of this thesis do not support the idea that the inner myometrium behaves and cycles in a way similar to the functionalis endometrium.

Another observation of this study is that the pattern of ERs and PRs distribution in uteri affected by adenomyosis was very different from control uteri. In adenomyotic uteri, all layers examined showed abnormal expression of steroid hormones receptors. The

expression of both ERs and PRs in the uterine layers and the cyclic changes (when present) of the receptor expression is, in addition to up-regulation by estradiol, primarily a matter of down-regulation by changing progesterone concentrations in the luteal phases (Kraus and Katzenellenbogen, 1993, Iwai et al., 1995, Graham and Clarke, 1997). There is cell-type specific differential receptor regulation to allow for differential tissue action in the presence of high circulating concentrations of this hormone (i.e. the same ligand levels will lead to different actions in different tissues due to different cell specific expression levels of its receptors) (King et al., 1981, McCormack and Glasser, 1980, Lessey et al., 1988, Shiozawa et al., 1996).

There was no difference in ERs or PRs distribution between the inner and outer myometrium of uteri with adenomyosis. However, when compared to controls, adenomyotic myometrium showed generally higher expression of ER- $\alpha$  and ER- $\beta$ , while the expression of PR-A and PR-B was generally lower.

Higher expression of ER- $\beta$  was observed in the myometrium of adenomyotic uteri. ER- $\beta$  expression was found to correlate with the expression of smooth muscle markers (smooth muscle actin and calponin), suggesting a role of ER- $\beta$  in the myofibroblastic differentiation of stromal cells in the breast (Sapino et al., 2006b). ER- $\beta$  is equally involved in elastin and collagen homeostasis either through transcriptional effects on their genes or through regulation of some of the proteases involved in the degradation of these proteins (Natoli et al., 2005, Trapido et al., 1984). The presence of higher expression of ER- $\beta$  in the myometrium of adenomyotic uteri might equally contribute to the presence of the classically described myometrial hyperplasia. Indeed, hypertrophy is a characteristic histologic feature of adenomyosis, and has been demonstrated and supported earlier in chapter 4.

In conclusion, this work demonstrated that adenomyotic uteri show abnormal steroid receptors expression, mainly PRs. The reduction in PRs expression might explain the poor response of adenomyosis-associated menstrual symptoms to progestational agents. These results do not support previous findings of cyclical variation in receptors levels in the inner myometrium previously described in the literature.

## **Chapter 7**

### **Microarray analysis comparison of the inner and outer myometrium in uteri with and without adenomyosis**

## **Chapter 7**

### **Microarray analysis comparison of the inner and outer myometrium in uteri with and without adenomyosis**

#### **7.1 INTRODUCTION**

This work has suggested the presence of a possible underlying myometrial defect in the pathogenesis of adenomyosis. Using electron microscopy, there were significant differences between the myometrium of normal and adenomyotic uteri (chapter 4). The development of adenomyosis in the CD-1 mouse following neonatal exposure to tamoxifen was associated with thinning, lack of continuity and disorganisation of the inner myometrium (chapter 2). Similar changes were observed in the C57/BL6J mouse (chapter 3) although adenomyosis did not develop, suggesting an additional role for the endometrium. Characterization of the myometrium in uteri affected by adenomyosis suggested the presence of myometrial defects both in the inner and outer myometrial layers (chapters 4 and 5).

There is no literature describing the gene expression of the myometrium in uteri affected by adenomyosis. In this study, an RNA microarray experiment is conducted in order to further characterize the myometrial defects observed in the inner and outer myometrium of uteri with adenomyosis.

## **7.2 METHODS**

### **7.2.1 Patients and samples**

The study was approved by the local Research and Ethics Committee, and all participants provided written consent. Hysterectomy specimens from premenopausal women not using exogenous hormones were selected for this study. The uteri were removed by abdominal or laparoscopic assisted vaginal hysterectomy for menorrhagia with or without dysmenorrhea. None of the participants had fibroids or endometrial abnormalities on preoperative ultrasound or hysteroscopy, and this was confirmed on subsequent histological examination. None of the participants had endometriosis.

A total of 24 uteri were examined: 12 affected by adenomyosis (6 in proliferative and 6 in secretory phase) and 12 uteri without adenomyosis (controls) (6 in proliferative and 6 in secretory phase). Uteri were obtained immediately after surgical removal and opened in the sagittal plane. Myometrial samples were obtained from the inner (IM) and outer (OM) parts of the myometrium, from areas not grossly affected by adenomyosis, giving a total of 48 samples to analyse. All samples were obtained from the anterior wall of the uterus near the fundus. Samples were immediately snap-frozen in liquid nitrogen and stored at -80°C until processed for microarray analysis.

Parallel full uterine thickness samples were fixed in 10% formalin and paraffin embedded for light microscopy, stained with hematoxylin and eosin, and used to confirm the menstrual cycle phase (proliferative or secretory), to confirm/establish the diagnosis of uterine adenomyosis.

## **7.2.2 Sample size calculation:**

Sample size was calculated according to previously published literature (Liu and Hwang, 2007), considering a power of 0.8 and a false discovery rate (FDR) of 0.05. The sample size was estimated to be 6 samples per group.

## **7.2.3 RNA preparation, array hybridization and scanning**

### **7.2.3.1 Total RNA extraction**

Total RNA extraction was performed using standard Trizol reagent technique, according to manufacturer's instructions (Invitrogen, UK). In summary, myometrial tissue was thawed to room temperature on ice using 1ml Tri reagent (Sigma, Dorset, UK) per 100mg of tissue, and homogenised. Samples were allowed to stand at room temperature (RT) for 5 min to ensure complete dissociation of nucleoprotein complexes. Chloroform (200 $\mu$ L/ml) was added to each sample and shaken vigorously for 15 seconds. After standing at RT for 3 min, the samples were centrifuged at 7500 RPM at 4°C for 15 min. The aqueous phase from each sample was transferred to a fresh tube. Isopropanol (0.5 ml) was added and the mixture was left to stand at RT for 10 min and centrifuged at 13000 RPM at 4°C for 10 minutes. The supernatant was discarded and the remaining RNA pellet was washed with 1ml of 75% ethanol in DEPC treated water. This was again centrifuged at 13000 RPM at 4°C for 5 minutes and the supernatant discarded. The pellet was air dried, re-suspended in 100 $\mu$ L of DEPC water and heated to 55°C for 5 minutes. The RNA preparations were DNase treated and further purified using RNeasy Mini KIT (Quiagen, Crawley, UK).

### **7.2.3.2 RNA Quantification and Quality Assessment**

The total RNA purity and concentration were analysed by both the 260/280 absorbance ratio using the NanoDrop™ 8000 spectrophotometer (Thermo Scientific, Wilmington, USA), as well as the Agilent 2100 Bioanalyzer (Agilent Technologies, Berkshire, UK). The RNA samples were then stored in RNase-free water at -80 ready for use.

### **7.2.3.3 Microarray**

First-strand and second-strand cDNA were prepared using the Illumina TotalPrep RNA Amplification Kit (Ambion, Applied biosystems, Warrington, UK). In summary, the RNA samples were thawed and adjusted to contain 250ng of RNA in 11µL of Nuclease-free water. A 'Reverse Transcription Master Mix' was prepared containing a T7 Oligo(dT) Primer to synthesise cDNA containing a T7 promoter sequence. The Master Mix was added to each RNA sample and incubated at 42°C for 2 hours. Second strand master mix containing DNA polymerase and RNase H was prepared and added to each sample in order to convert the single stranded cDNA into double-stranded cDNA and to simultaneously degrade the RNA. Samples were incubated at 16°C for 2 hours.

cDNA purification was carried out to remove RNA, primers, enzymes and salts. A cDNA Binding Buffer was added to each sample and then each sample was passed through a cDNA filter cartridge. In Vitro Transcription (IVT) was done to generate multiple copies of biotinylated cRNA from the double-stranded cDNA templates. An 'IVT Master Mix' was added to each sample. Samples were then incubated for 14 hrs at 37°C. The IVT reaction was stopped and the resulting cRNA purified to remove enzymes salts and un-incorporated nucleotides with the use of a cRNA filter cartridge.

The concentration of cRNA was assessed using the NanoDrop™ 8000 spectrophotometer (Thermo Scientific, Wilmington, USA). cRNA quality was assessed using the Agilent 2100 Bioanalyzer (Agilent Technologies, Berkshire, UK).

#### **7.2.3.4 cRNA Direct Hybridisation Assay**

The microarray was carried out using an Illumina® HT-12 v3 Expression BeadChip (Illumina, Essex, UK). The BeadChip contains 12 high-density microarrays, which allows for simultaneous analysis of 12 samples. Each microarray on the BeadChip contains about 48,000 50-mer probes that target more than 25,000 annotated genes.

The cRNA samples were dispensed onto the BeadChip and incubated for 16 hours overnight to allow for hybridisation. The BeadChip was then washed and stained with Streptavidin-Cy3 and scanned using the Illumina Beadstation 500 (Illumina, Essex, UK).

#### **7.2.3.5 Data Analysis**

Raw scanned images were saved and the intensity values of different probe sets (genes) generated were exported directly to Illumina BeadStudio (Version 3, Illumina, Essex, UK) for grouping, differential expression analysis and quality control. The probe-level expression data was converted into gene-level expression data then normalized. After identifying sample replicates, normalization steps were taken to ensure that the distribution of expression values was comparable across the chips, to remove outlier genes, and to subtract background noise. This resulted in a working gene list of 37,804 genes.

Differential gene expression between inner and outer myometrium was examined for each phase of the cycle, using Benjamin-Hochberg multiple testing correction for FDR at 0.05. Fold changes were calculated for genes with statistically significant differential expression ( $P < 0.05$  in the ANOVA analysis test, equivalent to a differential expression score of  $\pm 13$  in Beadstudio) and then exported for further pathways analysis using Pathvisio v 2.0, Wikipathways (van Iersel et al., 2008, Pico et al., 2008) and KEGG library of pathway maps and modules (Kyoto Encyclopaedia of Genes and Genomes) (Kanehisa and Goto, 2000, Kanehisa et al., 2009, Kanehisa et al., 2006). Further analysis identified pathways that were most significantly linked to the genes in the data set. The significance of the association and the over- or under-representation of the genes in the pathways were measured in two ways: (1) the ratio of the number of genes from the data set that map to the pathway divided by the total number of genes that map to the canonical pathway, and (2) Z-score which indicates the probability that the association between the genes in the dataset and the pathway is explained by chance alone. A Z-score of  $\pm 1.96$  represents a significant P-value of  $< 0.05$  on a Fisher's exact test. Functional hierarchies (ontologies) of the identified pathways are presented with reference to the KEGG library.

#### **7.2.4 Validation of the microarray data by Real-Time polymerase chain reaction (RT-PCR)**

Genes of different expression fold changes were selected for validation by real-time polymerase chain reaction (PCR), using standard techniques. Briefly, RNA was thawed on ice; quantified spectrophotometrically at 260 and 280 nm and RNA quality assessed using ethidium-stained gels. RNA with a 260/280 ratio of 1.8 and above was reverse-transcribed using avian myeloblastosis reverse transcriptase (Promega Corp.

Southampton, UK) as described previously (Stevenson et al., 2008). For quantitative PCR, 10 pmol of human GAPDH RNA specific primers (sense 5'-AGAACATCATCCCTGCCTC-3'; antisense 5'-GCCAAATTCGTTGTCATACC-3') (Hall et al., 1998) or human Wnt5a primers (sense 5'-ATTCTTGGTGGTCGCTAGG-3'; antisense 5'-CTGTCCTTGAGAAAGTCCTG-3') (Tulac et al., 2003) were used in a SYBR green system (Roche Diagnostics, Lewes, UK) with 1 µl of cDNA as template in a Roche Lightcycler 1.2. The PCR conditions were, in all cases, initiated with a denaturation step at 95°C for 10 min, followed by up to 40 cycles of denaturation 95°C, 30 sec; annealing 60°C, 30 sec and primer extension 72°C, 30 sec. Standard curves of diluted cDNA pools from normal myometrium were constructed for each gene target and the expression levels corrected for the levels of human GAPDH using the  $2^{-\Delta\Delta Ct}$  method (Livak and Schmittgen, 2001) with the data normalised to the levels in control inner or outer myometrium. Product sizes were confirmed both by agarose gel electrophoresis (Habayeb et al., 2008) and melting point analyses (Ririe et al., 1997).

## **7.3 RESULTS**

### **7.3.1 Comparison of inner myometrium in uteri with and without adenomyosis, in the proliferative phase**

In the proliferative phase, when the inner myometrium was compared in the adenomyotic and control uteri, a total of 27,552 genes were identified. 184 genes were significantly differentially expressed ( $P < 0.05$ ), of these 65 genes were down-regulated and 119 genes were up-regulated. With a cut-off value 2 fold change, 69 genes were differentially expressed, of which 30 were down-regulated and 39 genes were up-regulated (Table 7.1 and 7.2, Appendix 2). Pathways analysis considering only a  $P < 0.05$

and a 2-fold change, identified 8 pathways only with significant over-representation of genes (Table 7.3, Appendix 2).

### **7.3.2 Comparison of inner myometrium in uteri with and without adenomyosis, in the secretory phase**

In the secretory phase, a total of 28,811 genes were identified. 77 genes were significantly differentially expressed ( $P < 0.05$ ), of these 33 genes were down-regulated and 44 genes were up-regulated, in the inner myometrium of adenomyotic uteri compared to controls. When a 2-fold change cut-off was used, 44 genes were differentially expressed, of which 28 were down-regulated and 16 genes were up-regulated (Table 7.4 and 7.5, Appendix 2). Pathways analysis considering only a  $P < 0.05$  and a 2-fold change, identified 15 pathways with significant over-representation and 12 pathways with under-representation of genes (Table 7.6, Appendix 2).

### **7.3.3 Comparison of outer myometrium in uteri with and without adenomyosis, in the proliferative phase**

Differences in gene expression were compared between the outer myometrium of adenomyotic and control uteri in the proliferative phase. A total of 32,161 genes were identified, with 1,312 genes that were significantly differentially expressed ( $P < 0.05$ ), of which 460 were down-regulated and 852 were up-regulated. When a 2-fold change cut-off was used, 395 genes were differentially expressed, of which 144 were down-regulated and 251 genes were up-regulated (Table 7.7 and 7.8, Appendix 2). The 10 and 8 pathways with significant over- and under-representation of genes respectively, are shown in table 7.9, Appendix 2.

#### **7.3.4 Comparison of outer myometrium in uteri with and without adenomyosis, in the secretory phase**

In the secretory phase, the OM in the uteri with adenomyosis showed 243 genes that were significantly differentially expressed ( $P < 0.05$ ) compared to controls (out of 32,957 genes identified), of these 223 genes were down-regulated and 20 genes were up-regulated. When a 2-fold change cut-off was used, 34 genes were differentially expressed, of which 20 were down-regulated and 14 were up-regulated (Table 7.10 and 7.11, Appendix 2). The 19 pathways with significant over-representation and the 12 pathways with significant under-representation of genes are shown in table 7.12, Appendix 2.

#### **7.3.5 Overall comparison of the myometrium in uteri with and without adenomyosis**

Comparing the myometrium of uteri with and without adenomyosis, irrespective of the layer (i.e inner or outer) or the menstrual phase (i.e proliferative or secretory), *Wnt5a* was identified as the sole gene commonly down-regulated. The processes and pathways affected by *Wnt5a* gene are shown in figures 7.1 and 7.2.

Figure 7.1: Wnt signalling pathway (simple view)

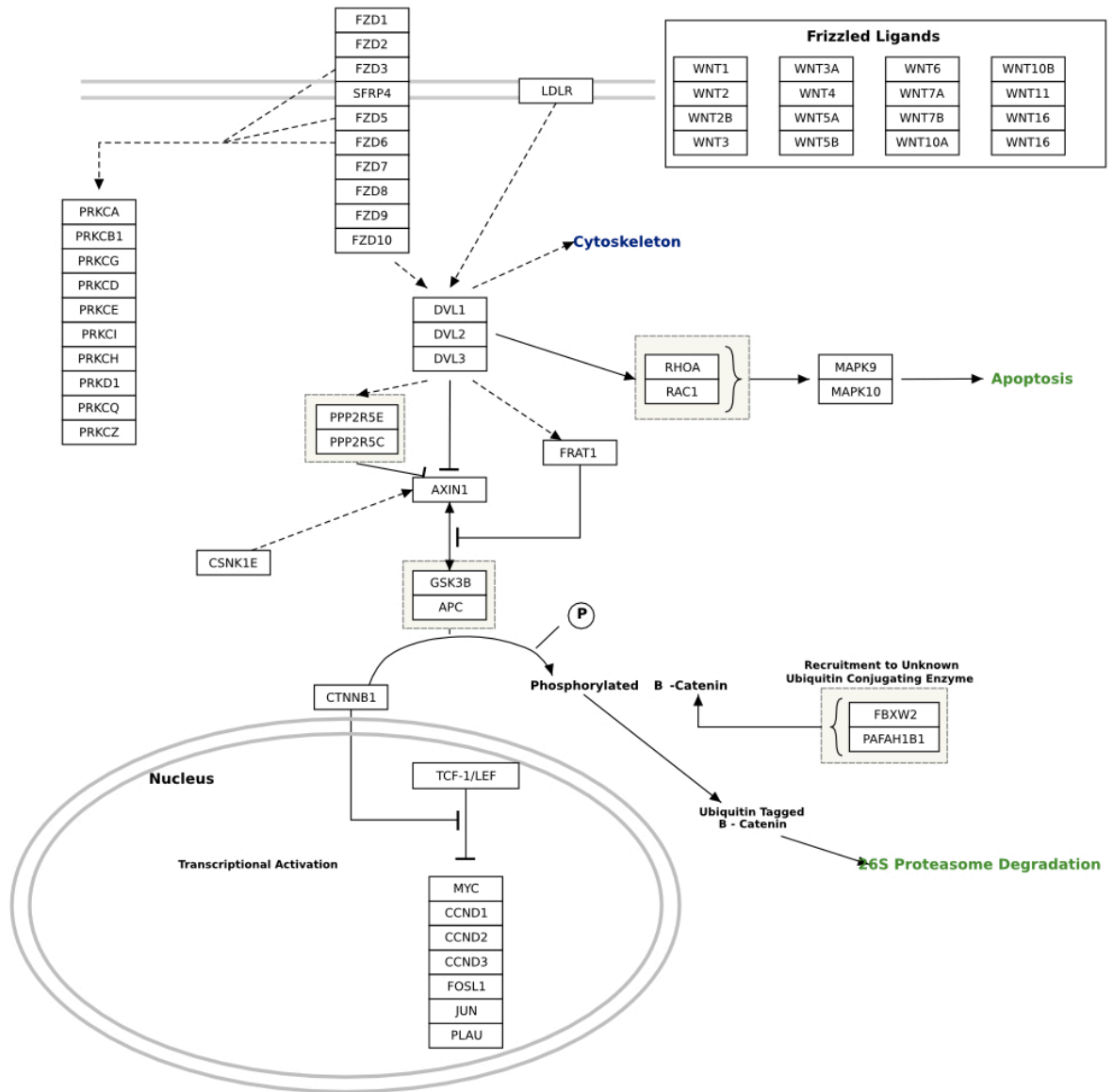
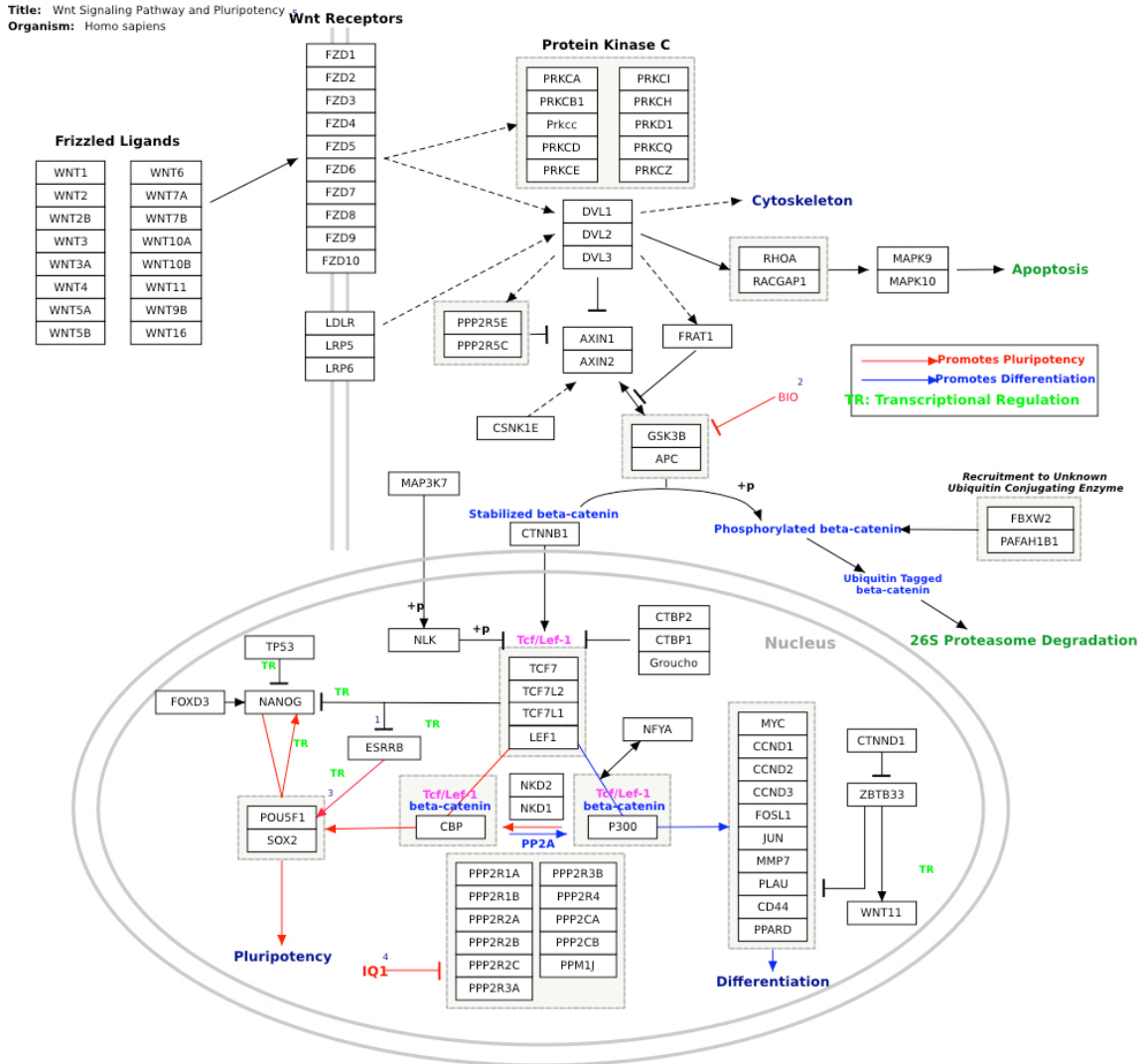


**Figure 7.2: Wnt signalling pathway (detailed view)**



### **7.3.6 Validation of microarray data by Quantitative Real-Time PCR (QT-PCR) and correlation with steroid receptors immunohistochemistry data (chapter 6)**

Quantitative real-time PCR analysis of Wnt5a and GAPDH gene expression confirmed the microarray data. The qPCR data showed that all conditions resulted in up-regulated Wnt5a expression using the delta:delta Ct method, although the inner myometrium secretory phase was only just so (Table 7.13 & 7.14 and figure 7.3). The microarray data for estrogen and progesterone receptors are shown in table 7.15.

**Table 7.13: Wnt5a differential expression in the myometrium using microarray analysis and quantitative RT-PCR expressed as fold changes (adenomyosis vs control). IM: inner myometrium, OM outer myometrium (Special acknowledgement goes to Mrs Muna Abbas and Dr Anthony Taylor for conducting the RT-PCR experiment and helping in analysis of data).**

<b>Layer and phase</b>	<b>Microarray fold changes</b>	<b>q-PCR fold changes</b>
<b>IM proliferative</b>	-2.260	-1.414
<b>IM secretory</b>	-2.271	-1.162
<b>OM proliferative</b>	-3.056	-1.655
<b>OM secretory</b>	-2.478	-1.486

**Table 7.14: GAPDH and Wnt5a Ct values (mean  $\pm$  SEM) results using quantitative RT-PCR (adenomyosis vs control). IM: inner myometrium, OM outer myometrium (Special acknowledgement goes to Mrs Muna Abbas and Dr Anthony Taylor for conducting the experiment and helping in analysis of data).**

<b>Layer and phase</b>	<b>GAPDH Ct (mean <math>\pm</math> SEM)</b>	<b>Wnt5a Ct (mean <math>\pm</math> SEM)</b>	<b>Mean delta:delta Ct</b>
<b>Control IM proliferative</b>	23.23 $\pm$ 0.14	26.55 $\pm$ 0.21	3.32
<b>Control OM proliferative</b>	23.57 $\pm$ 0.09	27.44 $\pm$ 0.08	3.88
<b>Adenomyosis IM proliferative</b>	23.01 $\pm$ 0.3	26.82 $\pm$ 0.31	3.82
<b>Adenomyosis OM proliferative</b>	23.03 $\pm$ 0.07	27.12 $\pm$ 0.15	4.09
<b>Control IM secretory</b>	22.57 $\pm$ 0.19	25.98 $\pm$ 0.21	3.42
<b>Control OM secretory</b>	22.93 $\pm$ 0.14	26.58 $\pm$ 0.17	3.65
<b>Adenomyosis IM secretory</b>	22.86 $\pm$ 0.11	27.00 $\pm$ 0.31	4.14
<b>Adenomyosis OM secretory</b>	22.19 $\pm$ 0.13	26.41 $\pm$ 0.41	4.22

**Figure 7.3: Graph of Wnt5a Gene fold changes in inner (IM) and outer myometrium (OM) in proliferative and secretory phase from microarray and RT q-PCR data (Special acknowledgement goes to Mrs Muna Abbas and Dr Anthony Taylor for conducting the RT q-PCR experiment and helping in analysis of data).**

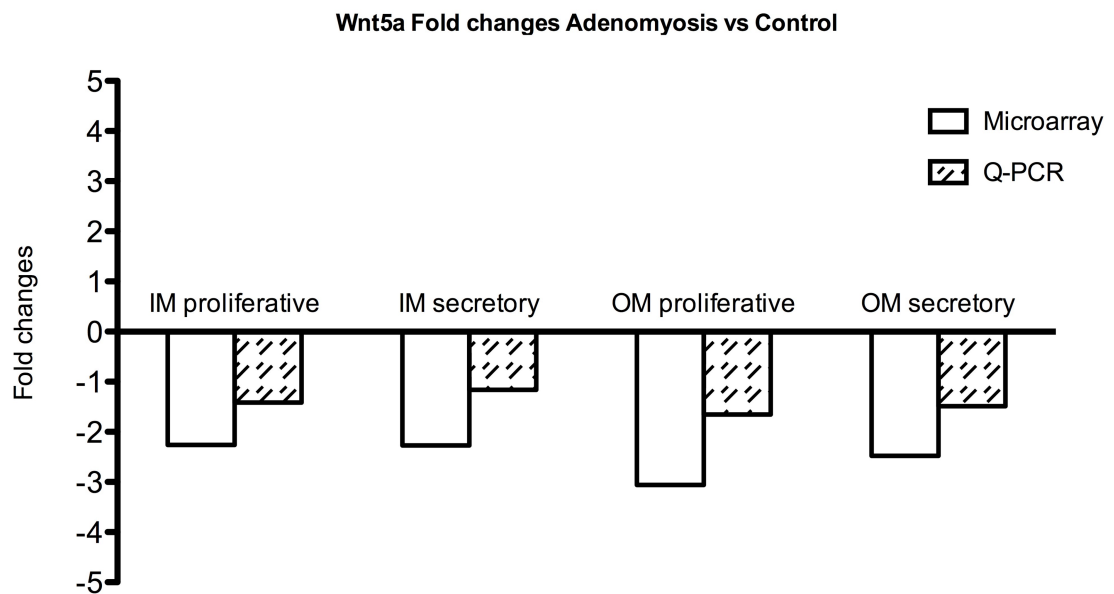


**Table 7.15: Estrogen and Progesterone receptors differential expression in the myometrium using microarray analysis expressed as fold changes (adenomyosis vs control). IM: inner myometrium, OM outer myometrium.**

Layer and phase	ER-alpha	ER-beta	PR (not differentiated on microarray)
IM proliferative	-1.12	3.81	-1.14
IM secretory	-1.36	1.77	1.03
OM proliferative	-1.60	7.33	-1.06
OM secretory	-1.14	3.14	-1.45

## 7.4 DISCUSSION

Microarrays studies of the human myometrium in the literature mainly describe the differences between normal myometrium and uterine fibroids (Dimitrova et al., 2009, Litovkin et al., 2008, O'Brien et al., 2008, Peng et al., 2009, Pan et al., 2008, Marsh et al., 2008, Zaitseva et al., 2007, Roth et al., 2007, Hever et al., 2006, Breuiller-Fouche and Germain, 2006, Luo et al., 2005a, Luo et al., 2005b, White et al., 2004, Havelock et al., 2005, Wang et al., 2003), or between pregnant and non-pregnant uteri (Breuiller-Fouche et al., 2007, Esplin et al., 2005a, Esplin et al., 2005b). There are no published comparisons between the myometrium of human uteri with and without adenomyosis.

Microarray analysis of adenomyotic uteri has been described in animal studies. Parrott *et al.* (2001) investigated experimentally induced adenomyosis of mice using cDNA arrays containing a limited set of genes and identified nerve-growth factor- $\alpha$  (NGF), pre-adipocyte factor-1 and insulin-like growth factor II as differentially regulated genes in adenomyosis (Parrott et al., 2001). Green *et al.* (2005) also performed cDNA microarray analysis of tamoxifen-induced adenomyosis in mice (Green et al., 2005).

Up-regulated genes included those for nerve growth factor (NGF), cathepsin B (CTSb), transforming growth factor beta induced (TGFbi) and collagens (Colla1, Colla2). The authors suggested these genes to provide a basis for understanding the mechanism for tamoxifen induced tissue remodelling and the development of adenomyosis.

The main objective of this study was to survey the gene expression patterns in uteri with adenomyosis to gain insight into the potential role of the myometrium in the disease and attempting to identify potential markers for adenomyosis. Gene expression profiles differences were observed between uteri with and without adenomyosis, depending on the myometrial layer and the phase of the cycle examined.

First, comparing the inner myometrium of uteri with and without adenomyosis showed multiple differences, both in the proliferative and secretory phases. Dysregulated pathways involved antigen processing and presentation, contraction pathways (skeletal, cardiac and GPCRs), cellular immunity (natural killer cytotoxicity, complement and coagulation cascades, interleukin signalling pathways), transcription and energy metabolism regulatory pathways, metabolic and cancer development pathways. Cellular invasion and control of cell growth genes were commonly found to be dysregulated in the current analysis. The functional ontology of the identified genes is described in the tables and include morphogenesis; cell-cell signalling; signal transduction, cytoskeleton organisation and biogenesis, disturbance in cell death, regulation of transcription, cell-cell signalling, cell cycle, cellular assembly and organisation, cellular movement, DNA replication and recombination and repair, and immune responses.

A possible limitation of these observed differences would be the possibly unavoidable contamination of the inner myometrium by the invading glands and stroma in uteri affected by adenomyosis. Laser-capture microdissection separation of myometrial and glandular tissue from fixed slides could be a potential solution. However, this technique yields a minimal amount of RNA and requires amplification of the RNA material potentially introducing errors in transcription.

Second, comparing the outer myometrium of uteri with and without adenomyosis confirmed the presence of numerous differences, both in the proliferative and secretory phases. Pathways similar to the ones affected in the inner myometrium were equally involved (i.e. immunity, contraction, metabolism, and cancer pathways). The differences observed in the outer myometrium are less likely to be related to endometrial contamination. The presence of such differences in the outer myometrium indicates that the adenomyosis-related defects exist in both myometrial layers (i.e. not

restricted to the inner myometrium) confirming the earlier findings of this thesis.

G proteins coupled receptors (GPCRs) regulated pathways were commonly identified in the analysis and are of particular interest. GPCRs are actively involved in intracellular signalling in the myometrium and play important roles in regulating myometrial contraction and relaxation (Sanborn et al., 1998).

Wnt5a was identified as a key under-expressed gene in adenomyotic myometrium, irrespective of the layer or phase examined. Other members of the Wnt family were equally involved to different degrees (e.g. Wnt2 and Wnt4). Some studies identified that epithelial-mesenchymal interactions are crucial in the correct development of the mammalian female reproductive tract. Three members of the Wnt family of growth factors (Wnt4, Wnt5a, Wnt7a) were identified to play an important role in this context, in mice (Mericksay et al., 2004).

In order to identify candidate genes and gene networks that regulate postnatal uterine development, Hu et al (2004) collected uteri from CD-1 mice on postnatal days (PND) 3, 6, 9, 12 and 15, and gene expression profiling was conducted on whole uteri and on uterine epithelium enzymatically separated from underlying stroma/myometrium. Of the approximately 12,000 genes analyzed, 9,002 genes were expressed in the uterus, and expression of 3,012 genes increased or decreased 2-fold during uterine development. Results from this study demonstrated that uterine development is a complex process involving overlapping positive and negative changes in uterine epithelial and stromal/myometrial gene expression. Candidate genes regulating uterine development included secreted factors (Wnt5a, Wnt7a), transcription factors (Hoxa10, Hoxa11, Hoxd10, MSX-1), enzymes (matrix metalloproteinases, cathepsin, carbonic anhydrase), growth factors (IGF-II, IGF binding proteins), and components of the extracellular matrix (osteopontin) to name a few (Hu et al., 2004).

During smooth muscle formation in the mouse uterus, Wnt4 and 5a are normally downregulated and eventually excluded from regions of smooth muscle differentiation (Miller et al., 1998). Whether such mechanism is operational in the human uterus development is unknown. However, the absence of inner myometrium development in tamoxifen induced adenomyosis in CD-1 mice (chapter 2) and the down-regulation of Wnt5a in this current study, might possibly suggest a role in the development of myometrial defects and adenomyosis in human uteri. Supporting the role of Wnt5a in coordinated female reproductive tract development in the mouse, it was found that Wnt5a-deficient females have coiled and shortened uteri with poorly defined cervix and vagina (Mericksay et al., 2004). Genetic analysis revealed that Wnt5a is closely linked to Wnt7a and AbdB Hoxa genes during female reproductive tract development (Mericksay et al., 2004). Wnt genes are particularly interesting regulators of tissue differentiation and interactions between neighbouring cells. A key component of their signalling pathway is  $\beta$ -Catenin, which also functions as a component of the Cadherin complex, controlling cell-cell adhesion and cell migration (Nelson and Nusse, 2004). Wnt signalling acts as a positive regulator of  $\beta$ -Catenin by inhibiting its degradation, causing its accumulation (Nelson and Nusse, 2004). Wnt signalling leads to the translocation of  $\beta$ -Catenin from the cytoplasm to the nucleus and transcription of target genes (Mikels and Nusse, 2006). Dysregulated Wnt signalling through  $\beta$ -Catenin is a well-established mechanism for tumourigenesis (Tanwar et al., 2009). *Tanwar et al.* used a mouse model that expresses constitutively activated  $\beta$ -Catenin in uterine mesenchyme. These mice showed myometrial hyperplasia, and developed mesenchymal tumours. Additionally, adenomyosis and endometrial hyperplasia were observed in some mice (Tanwar et al., 2009). Thus, down-regulated Wnts and subsequently down-regulated  $\beta$ -Catenin could play a role in the development of human adenomyosis

although to date there is no direct evidence for this theory and there is no published data describing the involvement of the Wnt genes in the human uterine development and morphogenesis.

In conclusion, the microarray analysis data in this study confirms the presence of myometrial defects both in the inner and outer layers, and points toward s a possible role for Wnt5a and other members of the Wnt family in the pathogenesis of uterine adenomyosis. The role played by the endometrium – as suggested by the data from the C57/BL6J mouse model (chapter 3) – and its interaction with the underlying myometrium will be examined in the next chapter.

## **Chapter 8**

**Study of stromal – myometrial interaction in a three-dimensional co-culture model and proteomic analysis**

## Chapter 8

### Study of stromal – myometrial interaction in a three-dimensional co-culture model and proteomic analysis

#### 8.1 INTRODUCTION

So far, this work has suggested the presence of myometrial defects in uteri affected by adenomyosis, both in animal model and in human uteri, both on the microscopic and ultrastructural levels. In chapter 5, a range of ultrastructural abnormalities was described in the junctional zone and outer myometrial layers in women with uterine adenomyosis. These included fewer cytoplasmic myofilaments, cytoplasmic aggregates, smooth nuclear outline with a clear ground substance, prominent nucleoli, peripherally arranged nuclear chromatin with occasional infolding of the nuclear envelope and entrapment of cytoplasmic organelles. It was also demonstrated that the development of adenomyosis in the CD-1 mouse following neonatal exposure to tamoxifen is associated with a thinning, a lack of continuity and disorganisation of the inner myometrium (chapter 2). However, a different mouse strain (C57/BL6J) treated in the same manner did not develop adenomyosis following tamoxifen exposure, despite similar myometrial defects (chapter 3). Thus, the findings from the C57/BL6J mouse model suggest that muscle changes are not enough on their own to explain the development of adenomyosis, which may also be dependent upon an interaction with stromal factors.

A characteristic feature of the normal endometrial-myometrial interface (EMI) is the lack of an intervening basement membrane or submucosa, which allows the endometrial

stroma to come into direct contact with the underlying junctional zone myometrium. Abnormal stromal cell differentiation and invasion has been proposed in the aetiology of adenomyosis (Uduwela et al., 2000, Parrott et al., 2001), but the features in the microenvironment that limit myometrial penetration by the overlying endometrium and the changes that precede or trigger the development of uterine adenomyosis are unknown (Parrott et al., 2001).

In this study, the potential role played by the endometrial stroma and its interaction with the underlying myometrium will be examined in this chapter. A novel three-dimensional co-culture model is used to compare the invasive properties of endometrial stromal cells from women with adenomyosis compared to those obtained from women without adenomyosis, and how myometrial cells influence that invasion. A proteomic analysis is conducted to detect the factor(s) that may influence this interaction/invasion.

## **8.2 MATERIALS AND METHODS**

### **8.2.1 Samples**

Primary myometrial and stromal cells were obtained from uteri with and without adenomyosis (designated control muscle: CM, control stroma: CS, adenomyosis muscle: AM, adenomyosis stroma: AS). All hysterectomies were performed for heavy periods. Histopathological examination confirmed the absence or presence of adenomyosis (glands >2.5mm below endometrial-myometrial interface). Steroid responsive endometrial stromal and inner myometrial cells were isolated as described previously (Arnold et al., 2001). Isolated cells were cultured in Dulbecco's Modified Eagle's Medium (DMEM) Glutamax<sup>+</sup>™ (Invitrogen, Paisley, UK) supplemented with 10% fetal calf serum (FCS) (Sigma-Aldrich, Dorset, UK) and 5% Penicillin /

Streptomycin / Fungizone<sup>TM</sup> mixture (Gibco, Invitrogen, Paisley, UK). No exogenous steroids were added to the media. The cells were incubated at 37°C in 5% CO<sub>2</sub>. Cultures were assessed for morphology and pattern of growth, and maintained until 70-90% confluent. Cells were harvested for co-culture using standard trypsin-EDTA (Gibco) protocol. The study was approved by the Local Research Ethics Committee.

### **8.2.2 Construction of the in-vitro cell-culture model**

During the optimisation and the development phases, all experimental and analytical techniques, used in the current experiment were tested, practised and tuned according to the requirements of the experiment.

#### **Growth and Maintenance of Cell Lines**

Tissue culture flasks containing made-up culture medium were used for cell growth. For ideal growth conditions, the cells were incubated in a humidified atmosphere of 5% CO<sub>2</sub> at 37°C and their medium was renewed every few days. Cultured cells were examined daily for the purpose of checking their morphology and density until they become 70-90% confluent (stationary or constant growth phase).

#### **Passaging and storage of cells**

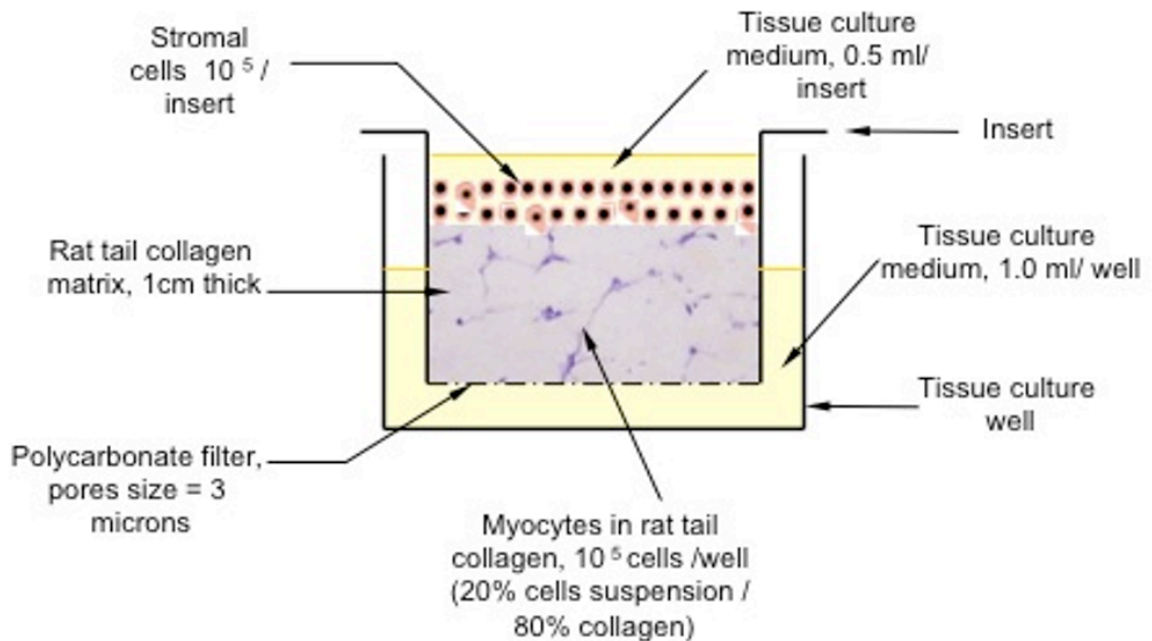
All cultured cells were harvested when they reached a confluent population density. The first step involved removing the medium and washing the growth surface with 5ml of PBS (pre-warmed at 37°C) twice. Cells were then detached from the growth surface by using trypsin (pre-warmed at 37°C). After the second PBS wash, 5ml of trypsin was added and left to act on the cells for 5 minutes at 37°C. When the majority of cells detached from the growth surface, they were washed with 10ml of fresh culture medium (pre-warmed at 37°C) to neutralise the trypsin. The cellular suspension was then

aspirated and centrifuged at 1000 rpm for 5 minutes at room temperature. The supernatant was carefully removed and the pellet of cells was resuspended in a suitable amount of DMSO/BSA (Dimethyl Sulfoxide / Bovine serum albumin) and stored at -80°C till further use, when the stored cells were allowed to thaw at 37°C then resuspended in culture medium. Cell concentration was estimated using a standard haemocytometer.

### **Description of the cell co-culture model used for the experiment**

Eight parts of rat-tail collagen type I (3.11mg/ml solution containing 0.02M acetic acid) (Becton Dickinson, BD Biosciences, Oxford, UK), was mixed with 1 part 10 × Hank's Balanced Salt Solution (HBSS), 2M sodium hydroxide (pH neutraliser) and 1 part FCS on ice. Myocytes were then added at a concentration of 100,000 cells/ml of prepared gel and gently mixed. Next, 1 ml of collagen gel, with or without suspended myocytes, was used to fill an insert placed within 12-well culture plates (BD Falcon™ cell culture inserts and plates, BD Biosciences, Oxford, UK) (Figure 8.1). Gel inserts were then polymerised at 37°C in the incubator for 30 minutes. At this point, 1 ml of culture medium (DMEM- Glutamax<sup>+</sup>™ with 10% FCS, and 5% Antibiotics) was added on top of the inserts and to the bottom of the wells. Stromal cells (100,000 cells/insert) were seeded as a monolayer on the top of the collagen insert. Culture medium from the inserts and the wells was replaced every 48h, and culture supernatant from wells and inserts stored separately at -80°C. After 10 days, 1 ml of melted agarose gel (3% agarose in HBSS boiled and allowed to cool to room temperature) was added on top of the inserts and the collagen matrix-agarose block carefully removed using forceps. The collagen matrix was fixed in 10% neutral buffered formalin for 24 hrs and embedded in paraffin wax for histology and immunohistochemistry.

**Figure 8.1: Schematic representation of the co-culture model used in the study. The experiments were conducted in 12-well/insert plates, each replicating this design.**



### **Development of the cell co-culture model**

In the course of the current work different configurations were constructed and examined. Different collagen gel matrices were tried. It was attempted to reach an optimal mixture of collagen gel that contains myocytes within its structure that closely mimics the normal myometrial conditions. Matrigel® (BDbiosciences, Oxford, UK) basement membrane matrix was originally used. However, it did not withstand paraffin fixation to prepare the blocks, because of its high aqueous consistency. Rat-tail collagen type I was subsequently used and was found to withstand all the experimental conditions. As high as possible a concentration of cells was used in the gel. Different cell concentrations were embedded into the collagen matrix. The 10<sup>5</sup> cell concentration was found to be optimal as higher concentration of cells was found to be associated with excessive cell death and contraction of the gel.

The general idea was to maintain the development of the models until they require harvesting and formalin fixation after a number of specified days. The relatively short-term survival of embedded myocytes and the disintegration and contraction of the collagen gel after 12-14 days did not allow for longer incubation periods.

Alpha smooth muscle actin was used to identify the smooth muscle cells in the gels. Using specific stromal cells antibody (CD-10) was not possible, as it required microwave heating antigen retrieval, which led to the destruction of the gels.

### **8.2.3 Histology and immunohistochemistry**

Cross sections (8 $\mu$ m) were mounted on silane-coated glass slides for haematoxylin and eosin staining, and  $\alpha$ -smooth muscle actin ( $\alpha$ -SMA) immunohistochemistry (chapter 2), using mouse monoclonal anti-human SMA antibody (clone SMM1, Vector labs, Peterborough, UK). Endometrial stromal cells were  $\alpha$ -SMA negative, and this was confirmed in all sections. Image capture and analysis was performed using a single chip colour video camera (Sony DXC-151P, Japan), Axioplan microscope (Carl Zeiss, Germany) and Axiovision software (version 4.0, Carl Zeiss, Germany). The whole section was examined and the maximum depth of invasion measured in five fields per section. Measurements were taken perpendicular to the surface down to the deepest invading cell. Ten sections were examined per experiment and the measurements averaged (Figure 1B). Data were found to approximate to a Gaussian distribution (Shapiro-Wilk test; GraphPad PRISM version 5.0, GraphPad Software Inc., San Diego, USA) and means were compared using Student's unpaired t-test.

## **8.2.4 Proteomic analysis**

### **8.2.4.1 Samples and arrays preparation**

The cell culture fluid supernatants were analyzed on ProteinChip® arrays (Bio-Rad Laboratories, Hertfordshire, UK). Optimisation experiments were performed using weak anion exchange (CM10), strong anion exchange (Q10), and reverse-phase hydrophobic (H50) array chips. Stepwise dilutions were tested using appropriate binding buffers: 100 mM sodium acetate (pH 4.0) for the CM10 arrays; 100 mM Tris-HCl (pH 9.0) for the Q10 arrays; and 10% acetonitrile / 0.1% trifluoroacetic acid (TFA) for the H50 arrays, and a sample to buffer dilution of 1:16 was chosen to achieve maximal definition. Preparation of the arrays was performed according to the manufacturer's standard protocols and samples were allowed to bind to the array surfaces for 30 min at room temperature, on a shaking bed. The arrays were washed 3 times in buffer and rinsed twice with HPLC-grade water. Sinapinic acid (SPA) matrix was prepared in the saturated energy-absorbing molecule solution of 50% acetonitrile and 0.5% TFA (Bio-Rad Laboratories) according to the manufacturer's instructions. This was added to the arrays and allowed to dry overnight. A reference standard cell culture medium sample was included as control. All array preparations were produced using a ProteinChip® Cassette-Compatible Bioprocessor (Bio-Rad Laboratories) and all array preparations including binding and processing were performed on the same day. Each sample was prepared in duplicate on the separate arrays.

#### **8.2.4.2 Surface Enhanced Laser Desorption/Ionization – Time of Flight – Mass Spectrometry (SELDI-TOF-MS) Analyses**

All arrays were analyzed using the ProteinChip® SELDI, Enterprise Edition (Ciphergen Biosystems, Surrey, UK). Each sample was examined using low and high laser intensities to focus on proteins of relative molecular masses lower and higher than 30,000 Daltons, respectively. Protein profile spectra were generated in which individual proteins were displayed as unique peaks based on their mass-to-charge ( $m/z$ ) ratio. Spectral data were collected using ProteinChip® Ciphergen Express data manager software (Ciphergen Biosystems), which was also used for data processing and univariate statistical analysis. After baseline subtraction, the spectra were internally mass calibrated and peak intensities normalized using total ion current. Peak clustering was performed in a range that excluded the very low mass region, which is dominated by SPA peaks. Automatic peak detection was then performed using a signal-to-noise ratio of five for the first pass of peak detection, and two times the signal-to-noise ratio for the second pass. The two passes were combined and from the detected peaks, a list of peak clusters was created. In this study, a peak cluster was created if the given peak was found in 20% of all spectra for an individual condition above the first-pass cutoff. Following identification of the  $m/z$  ratio values, the potential candidate proteins were identified using the UniProtKB/Swiss-Prot database of proteins. The database search was performed using the ExPASy (Expert Protein Analysis system) proteomics system and the TagIdent search tool ([www.expasy.ch/tools/tagident.html](http://www.expasy.ch/tools/tagident.html)). The search parameters used were an isoelectric point range of 4 to 10 and a molecular weight range of  $\pm 0.1\%$  (Wilkins et al., 1996, Wilkins et al., 1998, Gasteiger et al., 2005).

## 8.3 RESULTS

### 8.3.1 Co-culture invasion assay

The maximum depth of invasion was almost three times higher for AS compared to CS when grown on plain collagen, and the difference was statistically significant ( $p=0.0005$ ) (Table 8.1 and Figure 8.2A). Co-culture with CM or AM increased the depth of invasion of both AS and CS. The depth of invasion of AS grown on CM was statistically significantly higher compared to CS grown on CM ( $p=0.0092$ ). The depth of invasion of AS grown on AM was statistically significantly higher compared to CS grown on AM ( $p=0.02$ ). Growth on AM also enhanced the invasion of CS compared to CS grown on CM ( $p=0.001$ ) (Figure 8.2B). The invasion of AS when grown on AM was also statistically significantly higher compared to AS grown on CM ( $p=0.0331$ ) (Figure 8.2C).

**Table 8.1: The maximum depth of endometrial stromal cell invasion when grown on plain collagen alone or with the addition of myometrial cells from control or adenomyosis**

Wells containing	Depth of invasion ( $\mu\text{m}$ ) <sup>a</sup>	
	Inserts containing	
	Control stroma (CS)	Adenomyotic stroma (AS)
Plain collagen	339.12 $\pm$ 66.36	1090.61 $\pm$ 173.78 <sup>b</sup>
Myocytes from controls (CM)	829.15 $\pm$ 69.16	1321.09 $\pm$ 157.72 <sup>b</sup>
Myocytes from adenomyosis (AM)	1310.30 $\pm$ 110.23 <sup>c</sup>	1701.04 $\pm$ 117.34 <sup>b,c</sup>

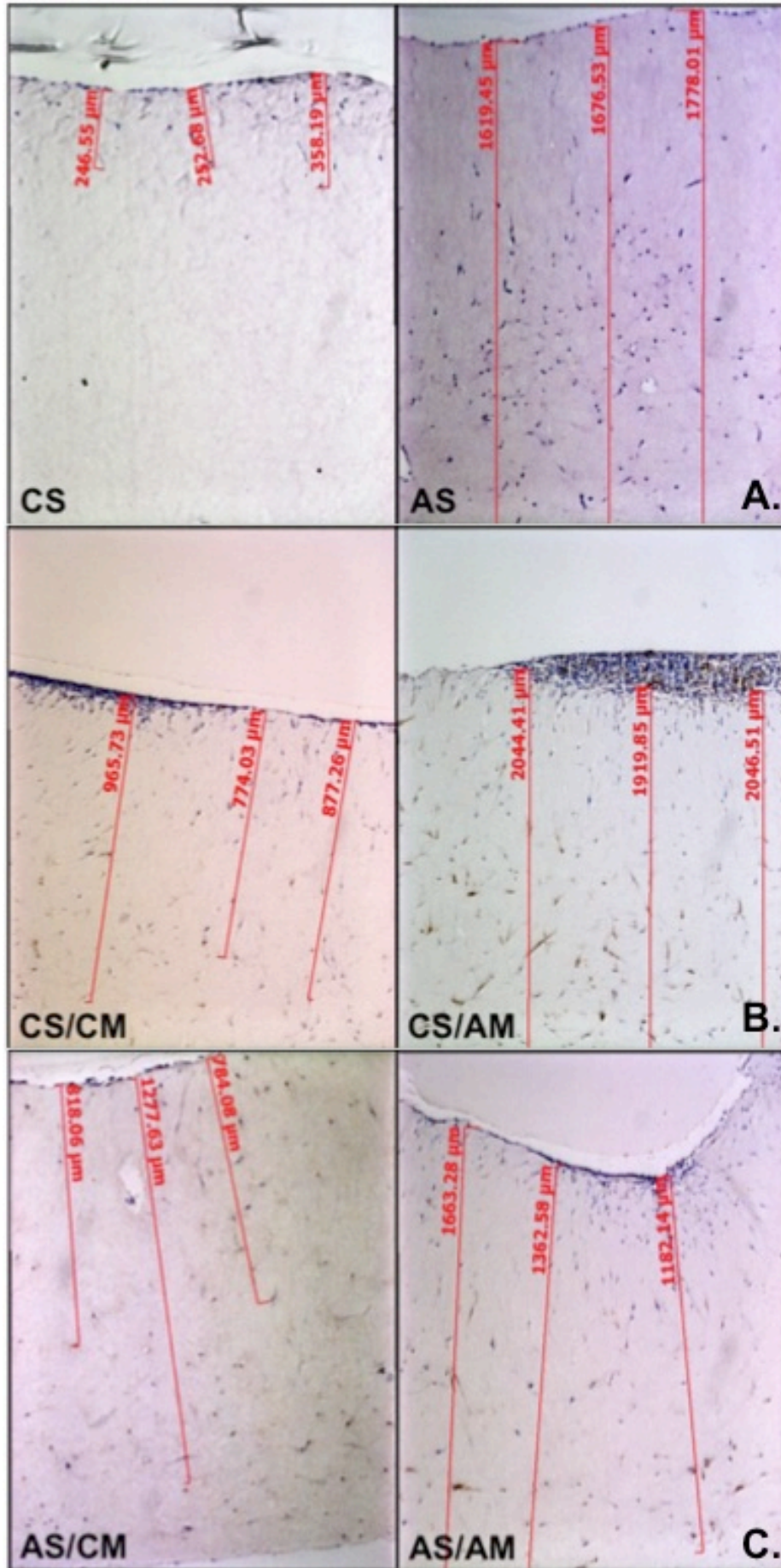
<sup>a</sup> Determinations are mean  $\pm$  SEM; N=12 for each combination.

<sup>b</sup> Statistically significant ( $p < 0.05$ ) compared to control stroma.

<sup>c</sup> Statistically significant ( $p < 0.05$ ) compared to plain collagen or control myometrium; Student's unpaired t-test.

**Figure 8.2: A: Haematoxylin and eosin staining of a plain collagen insert with control (CS) or adenomyosis stroma (AS) cultured on top. The maximum depth of invasion was almost three times higher for AS compared to CS. B: Histologic slide immunostained with alpha smooth muscle actin ( $\alpha$ -SMA) showing control stroma (CS) cultured on top of collagen inserts containing control (CM) or adenomyotic myometrium (AM). Negatively stained cells are the stromal cells. Growth on AM enhanced the invasion of CS compared to CS grown on CM. C: as for panel B but showing adenomyosis stroma (AS) cultured on top of collagen inserts containing control (CM) or adenomyotic myometrium (AM). The invasion of AS when grown on AM was significantly higher compared to AS grown on CM.**

**(See next page)**



### 8.3.2 Protein expression analysis:

Culture supernatants obtained separately from culture fluid from inserts (representing diffusion products from stromal cells) and from wells (representing diffusion products from myometrial cells and invading stromal cells) produced proteins of similar and dissimilar molecular masses. Representative traces for stromal and myometrial compartments of normal and adenomyotic co-cultures are shown in Figure 8.3.

Analysis of diffusion products obtained from adenomyotic and control stromal cells (comparison 1), allowing for a 0.1% margin of error in estimating the m/z ratio of protein clusters, revealed there to be 28 common peak clusters differentially expressed between control and adenomyosis stromal cells under the three different experimental conditions (i.e. on plain collagen, or on collagen containing control or adenomyotic myocytes) (Figure 8.4A). Examination of the diffusion products obtained from adenomyotic and control myometrial cells (comparison 2) revealed there to be 9 common peak clusters differentially expressed between control and adenomyosis myometrial cells under the three different experimental conditions (i.e. in plain collagen, or when co-cultured with control or adenomyotic stromal cells) (Figure 8.4A). Contrasting the common peaks from comparisons 1 and 2 revealed that 6 peaks were common to both ‘adenomyotic stromal cells’ and ‘adenomyotic myometrial cells’. The average m/z ratios and the list of corresponding candidate proteins are presented in Table 8.2.

When the analysis was repeated allowing a 0.2% and 0.25% range of possible error in m/z ratio, 7 common peaks were found at the 0.2% margin of error, and 27 common peaks at the 0.25% margin of error (Figure 8.4B, 8.4C and Table 8.2).

**Figure 8.3: Representative traces for protein expression profiles produced by SELDI-TOF analysis. Graphs represent analysis of cell culture fluid supernatant from inserts of CS/CM and AS/AM (CS = control stroma, AS = adenomyosis stroma, CM = control myometrium, AM = adenomyotic myometrium). Shown are the m/z ratio spectrum and peak intensity analysis at low laser intensity.**

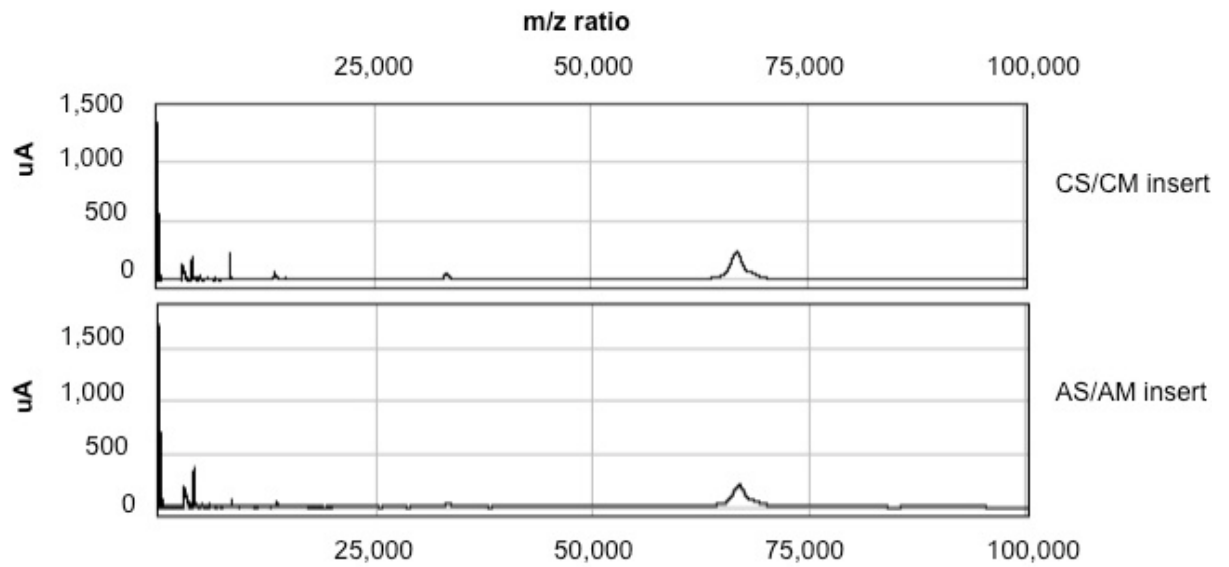


**Figure 8.4: Venn diagrams representing the number of differentially expressed protein peaks observed in adenomyosis and control stromal and myometrial supernatants under different experimental conditions and at different margins of error (A: 0.1%, B: 0.2%, C: 0.25%). The cell type used is designated as follows: CS = control stroma, AS = adenomyosis stroma, CM = control myometrium, AM = adenomyotic myometrium.**

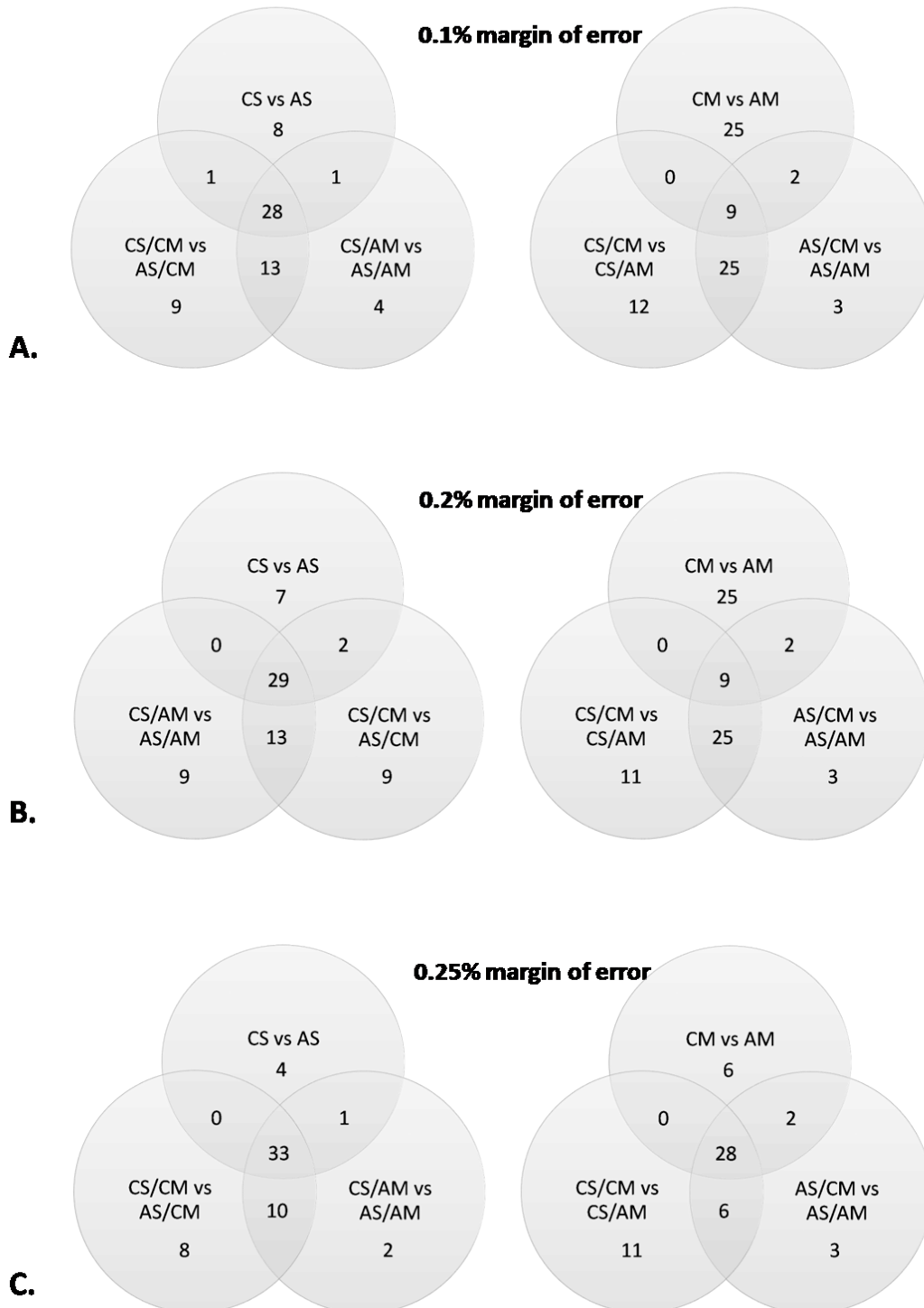


**Table 8.2: Adenomyosis-specific soluble proteins**

<b>m/z ratio</b> <b>(± 0.1%)</b>	<b>Candidate proteins <sup>a</sup></b>
<b>2987</b>	Intestinal peptide PHM-27
<b>4080*</b>	Thrombin light chain; Peptide YY(3-36); Histatin-3
<b>4211*</b>	Glucagon-like peptide 1; Pancreatic hormone; Dolichyl-diphosphooligosaccharide-protein glycosyltransferase; ER-37; Big PEN-LEN (By similarity)
<b>5978*</b>	NADH dehydrogenase [ubiquinone] 1 subunit C1, mitochondrial; Gastrin-52; Metallothionein-1E; Minor histocompatibility protein HMSD variant form; Elafin; Granulin-3; Adrenomedullin; Progressive rod-cone degeneration protein; Mitochondrial import receptor subunit TOM5 homolog; Beta-defensin 123; Uncharacterized protein C21orf109; Beta-defensin 104; Small nuclear protein PRAC; Putative uncharacterized protein C1orf217; Putative transcript Y 14 protein
<b>6841</b>	Gamma-secretase C-terminal fragment 59; Guanine nucleotide-binding protein G(I)/G(S)/G(O) subunit
<b>10208</b>	Putative uncharacterized protein ENSP00000347057; Glycoprotein hormones alpha chain; Uncharacterized protein C18orf18; Interferon alpha-inducible protein 27- like protein 2

<sup>a</sup> Proteins were identified within a 0.1% range of the average m/z ratio value of the identified adenomyosis-specific proteins peaks (i.e. this commonly expressed by stromal and myometrial cells under different experimental conditions). The names of candidate proteins were obtained from the UniProtKB/Swiss-Prot database using the TagIdent search tool.

In addition to the above, one additional common peak (m/z = 5102) was identified using a 0.2% range in average m/z, and 20 additional common peaks (m/z ratios: 7452, 8380, 8552, 8768, 11640, 13548, 13678, 13885, 14914, 15882, 16122, 22304, 27631, 33446, 39293, 44741, 67015, 78609, 89784, 100111) were identified using a 0.25% range in average m/z.

\* Candidate proteins detected using a 1% range in average m/z.

## 8.4 DISCUSSION

Three dimensional co-culture models have been previously used for the study of cancer invasion (Jones et al., 1997, Jones et al., 2003) where tumour cell invasion was shown to be modulated by the presence of normal myoepithelial cells (Jones et al., 2003). Co-cultures have also been used to examine the invasive properties of trophoblasts (Cohen and Bischof, 2009). A three-dimensional co-culture model was modified to examine the interactions between endometrial stromal cells and inner myometrial cells derived from uteri with or without adenomyosis. Endometrial stromal cells from women with uterine adenomyosis exhibited greater invasion compared to stromal cells from women without adenomyosis (controls). This observation supports the hypothesis that adenomyosis results from invasion of the endometrial stroma into the myometrium. It also suggests that increased invasiveness is an innate property of stroma from adenomyosis. On the other hand, the addition of myocytes from women with adenomyosis to the collagen matrix increased the depth of invasion of stromal cells from both control and adenomyosis affected uteri. This suggests that adenomyotic muscle might produce a soluble factor(s) that enhances the migration of stromal cell, regardless of origin. The exact agent(s) involved is not known but a list of potential proteins and factors were identified through proteomic analysis in this experiment (e.g. Intestinal peptide PHM-27, Thrombin light chain, Peptide YY (3-36); Histatin-3, Glucagon-like peptide 1, Pancreatic hormone, Dolichyl-diphosphooligosaccharide-protein glycosyltransferase, ER-37, mitochondrial NADH dehydrogenase). The exact nature and role of these proteins require further characterisation.

The in-vitro model showed clear stromal cell invasion, but some limitations are acknowledged. The endometrium is a complex 3D structure with glandular and other components including the extracellular matrix (ECM). The influence of these (if any)

cannot be assessed in this model. The in-vitro co-culture is nevertheless a simplification that allows examination of invasiveness. Equally, the ECM of the myometrium consists of a variety of collagen fibers and embedded structural glycoproteins that mediate the interaction between adjacent cells, and some of these extracellular factors may be involved in adenomyosis. On the other hand, glandular epithelial cells are not in direct contact with myometrial cells but are surrounded by intervening stroma, suggesting that adenomyosis may be mediated through an interaction between stromal and muscular compartments. Type I collagen gel, with or without embedded myocytes, which was used in the study is a component of the myometrial ECM, making it an appropriate constituent in this model.

The relatively short-term survival of embedded myocytes and the disintegration and contraction of the collagen gel after 12-14 days did not allow for longer incubation periods. A similar problem was reported by Zhu *et al.* (Zhu et al., 2001) who showed a vast increase in apoptosis among fibroblasts embedded in collagen gels after 14 compared with 7 days in culture. Nevertheless, 10 days incubation allowed migration of stromal cells deep within the collagen or collagen-myometrial suspension, and demonstrated different depth of migration over this period. Another limitation of the model is the number of myocytes that could be embedded in the collagen matrix. It would have been theoretically advantageous to have a higher myocyte concentration, but this was hampered by cell clumping and death at the higher density.

This study provides new insights into the aetiology of uterine adenomyosis. This study provides evidence for the role of the myometrium in facilitating this process. The differential effect of myometrium from adenomyosis suggests an innate predisposition. Stromal cells and myometrial cells from women with adenomyosis had a distinct proteomic profile compared to stromal and myometrial cells from controls.

Furthermore, some of the distinct features of adenomyosis derived cells are shared between stromal and myometrial cells. This suggests that adenomyosis may be characterised by a soluble secreted protein profile, at least in co-culture. This supports the hypothesis that adenomyosis is a disease of both the myometrium and the endometrial stroma. This is perhaps not surprising given the common paramesonephric duct embryological origin of the endometrial stroma and the inner myometrium. The research by Fujii *et al.* (1989), shows that stromal and myometrial cells exhibit some level of plasticity because the cells at the stromal-myometrial interface morphologically resemble follicular phase myofibroblasts and differentiate into cells morphologically resembling smooth muscle cells often found in the luteal phase and in early pregnancy (Fujii *et al.*, 1989). In support of this is the research by Konishi *et al.* (1984) on human abortuses and stillborn fetuses. They observed that the outer part of the mesenchyme of the uterus gives rise to the myometrium and that the inner part corresponds to the endometrial stroma (Konishi *et al.*, 1984).

In conclusion, using a novel three-dimensional co-culture model, this study demonstrated that endometrial stromal and muscle cells derived from adenomyotic uteri influence stromal cell invasion. The study provides supportive evidence that adenomyosis is a disease of both the stroma and the myometrium and that there are some soluble proteins common to both cell types. Further research is needed to identify those proteins, and to understand the pathways involved in the cross talk between the myometrium and stroma.

## **Chapter 9**

### **Discussion**

## Chapter 9

### Discussion

#### 9.1 GENERAL DISCUSSION

The exact aetiology and pathogenesis of adenomyosis are not clear. In the literature three theories have been proposed for the development of intra-myometrial endometrium. However there is no conclusive evidence for any of these models.

The first theory explains adenomyosis by a metaplastic process, where the intra-myometrial foci would originate and ultimately develop through metaplasia from de novo ectopic intra-myometrial endometrial tissue, possibly from multipotent pericytes along blood vessels. Hormonal, genetic, immunological and growth factors might possibly play a role in the initiation of this metaplastic process (Mai et al., 1997). This theory derives from the observation that the endometrium and underlying inner myometrium have a common Mullerian embryological origin. The Mullerian duct tissue is pluripotent, and forms two components - epithelium and stroma - that are characterised by positive cytokeratin filaments staining in the epithelial tissue and by positive vimentin staining in the stromal/mesenchymal tissue. The same profile can be found in adenomyosis (Moll et al., 1983). There is some evidence that metaplasia can occur in the endometrium. Some decidual and endometrial stromal cells express  $\alpha$ -smooth muscle actin and show ultrastructural similarities with myofibroblasts, and smooth muscles (Oliver et al., 1999, Fujii et al., 1989). This suggests that smooth muscle differentiation possibly occurs from multi-potential mesenchymal cells in the endometrial stroma (Fujii et al., 1989). It is unknown if the same phenomenon occurs

around the endometrium of adenomyotic foci, contributing to the myometrial hypertrophy and hyperplasia surrounding the ectopic endometrium. It is equally not known if the reverse metaplasia from myocytes to stroma and glands can occur.

The second theory suggests that the basalis endometrium invagination occurs along the intra-myometrial lymphatic system, rather than by disruption and “invasion “ of the muscle bundles. This is supported by the occasional finding of endometrial tissue in the intra-myometrial lymphatics in hysterectomy specimens (Sahin et al., 1989). *Mai et al.* (1997) characterized isolated nodules of endometrial stromal cells without endometrial glands, along blood or lymphatic vessels – what they called type 1 nodules. The authors suggested that due to the proliferative nature of the endometrial glands, the newly enlarged area of stroma serves as “new soil”, facilitating further downward growth of the endometrial glands (Mai et al., 1997). However, this expansion and growth may represent a type of stromatosis or endometrial stromal sarcoma (endolymphatic stromal myosis), both of which are characterized by endometrial stroma without endometrial glands (as opposed to adenomyosis that consists of both endometrial stroma and glands) (Goldblum et al., 1995).

The third and commonest theory proposes that adenomyosis originates from basalis endometrium that invaginates deep within the myometrium. This is supported by the observation of histological continuity between the basal endometrium and underlying adenomyosis in some tissue sections (Leyendecker et al., 2002). This endometrial invasion is possibly facilitated by the loss of cohesion of myometrial bundles caused by specific enzymes such as matrix metalloproteinases (Devlieger et al., 2003, Uduwela et al., 2000). Endometrial stromal fibroblasts produce tenascin, a fibronectin inhibitor that in turn facilitates epithelial migration. Tenascin mediates epithelial-mesenchymal interactions by inhibiting cell attachment to fibronectin, an action stimulated by

hormonally regulated epidermal growth factors. Whether this interaction plays a role in the development of uterine adenomyosis or endometriosis is unclear (Chiquet-Ehrismann et al., 1989) (Ferenczy, 1998). Adenomyosis has long been thought to share a common pathogenesis with endometriosis (Leyendecker et al., 2002, Leyendecker et al., 1998, Leyendecker et al., 1996). Endometriotic cells have also been shown in vitro to have an invasive potential (Gaetje et al., 1995).

The endometrial-myometrial interface (EMI) characteristically lacks a distinct, intervening basement membrane (Uduwela et al., 2000). As a result the endometrial stroma is in direct contact with the underlying myometrium, allowing a special free type of communication and interaction. This situation may facilitate endometrial invagination/invasion of either a structurally weakened myometrium or by the influence of ovarian hormones via their respective sex-steroid receptors. During periods of regeneration, healing and re-epithelialization, the endometrium could invade a predisposed myometrium or a traumatized EMI (Ferenczy, 1998). Mechanical damage to and/or physical disruption of the EMI by dysfunctional uterine hyperperistalsis and/or dysfunctional contractility of the sub-endometrial myometrium (Kunz et al., 2000, Leyendecker et al., 2002) or by sharp curettage during pregnancy (Curtis et al., 2002) may allow for the dislocation of basal endometrium into the myometrial wall and the development of adenomyosis. The latter is supported by the association of adenomyosis with a history of intra-uterine procedures such as pregnancy termination (Levgur et al., 2000), as well as by animal experiments where transplantation of the anterior pituitary in the uterine lumen of adult SHN and SLN mice strains induced adenomyosis (Mori and Nagasawa, 1983). The EMI is also disturbed by the intra-myometrial penetration of trophoblast during early pregnancy and this may underlie the higher incidence in parous patients. Disturbance of the junctional zone - either directly by endometrial factors or

indirectly by an altered immune response (Ota et al., 1998) - may be involved as triggering 'invasive' factors.

However, the early stages and sequence of events of the development of adenomyosis is unclear and is subject to speculation. There are rare reports of adenomyosis in neonates/children. *Lewinski* (1931) reported an incidence of 54% in 54 autopsies (*Lewinski*, 1931). In one series, 7 cases were reported in which mothers and daughters were affected (*Emge*, 1962). It is not known which component of the EMI (i.e. basal endometrium or subendometrial myometrium) plays the key role in the development of adenomyosis. Whether the endometrium in adenomyosis has a higher invasive potential and penetrates a normal subendometrial myometrium, or alternatively, the subendometrial myometrium in cases of adenomyosis is more permissive to invasion by a normal basal endometrium is not known. This thesis was undertaken to examine the hypothesis that the primary pathology in uterine adenomyosis is an *abnormal development or behaviour of the endometrial-myometrial interface (EMI) (basal endometrium / subendometrial myometrium)*, postulating that this zone behaves differently in adenomyosis compared to normal uteri and as compared to the deeper myometrium. Experimental work was done to identify which component of the EMI (i.e. basal endometrium or subendometrial myometrium) played the key role in the development of adenomyosis. The thesis tested two possibilities: (i) that the *subendometrial myometrium* is permissive to invasion by a normal basal endometrium, or (ii) that *the basal endometrium* has a higher invasive potential and penetrates a normal subendometrial myometrium.

In order to examine this hypothesis, the thesis followed two experimental approaches. In the first section, an experimental (murine) model of adenomyosis was used. This

work examined the sequence of early uterine development changes and aberrations that lead to uterine adenomyosis, and the effect of tamoxifen on the differentiation of the different muscle layers and the development of adenomyosis in the uteri of CD-1 mice, and concluded that abnormal development and disruption of the inner circular muscle layer may play a role in the development of uterine adenomyosis. To examine the possible strain predisposition in response to these hormonally active agents, this work equally examined the effects of tamoxifen on the C57/BL6J mouse strain that is not known to develop spontaneous adenomyosis, and concluded that disruption of the inner myometrium cannot on its own explain the development of uterine adenomyosis and although these changes may be a prerequisite for the development of adenomyosis, additional genetic or epigenetic differences between strains expressed in the endometrium may be required.

The second section examined the disease in human uteri. This work described the phenotypic and genotypic characteristics of the human myometrium in uteri affected by adenomyosis. The gross and ultrastructure of the myometrium were examined, together with the differences in genes expression between control and affected myometrium. Subsequently, the characteristics of the endometrium / stroma in uteri with and without adenomyosis were examined. The invasive properties of the stroma and its interaction with the underlying myometrium were further studied.

The thesis showed that the phenotype and the expression of steroid receptors in adenomyosis foci glands and stroma were comparable to the overlying eutopic basalis endometrium, both in levels of expression and lack of cyclicity. This is in agreement with previous studies that suggested that the endometrial glands and stroma in adenomyosis foci resemble the overlying basalis endometrium (Ferency, 1998), possibly explaining the limited changes with the menstrual cycle. This may support the

hypothesis that the adenomyosis foci and glands arise from the deep penetration of the overlying basalis endometrium, although active penetration and invasion could not be ascertained from this finding on its own.

The endometrial stroma of the basalis endometrium of uteri with adenomyosis showed differences in its immunohistochemistry staining profiles compared to controls' basalis. There was a higher expression of estrogen receptors in particular ER- $\beta$  (chapter 6), associated with an increased in Ki-67 expression. This entails an increased proliferation in this layer and potentially explains the commonly associated endometrial hyperplasia without atypia and endometrial polyps. An increased ER- $\beta$  expression and proliferation, may also explain the penetration of the endometrium deep in the myometrium and the development of adenomyosis foci. These results are in agreement with the literature. It has been reported that ER expression in the adenomyotic foci is greater than in the normal endometrium and is associated with expression of the apoptosis-suppressing gene product, bcl-2, throughout the menstrual cycle (Ueki et al., 2004). Bcl-2 is expressed in a cyclic fashion in the normal endometrium, with a peak occurring during the proliferative phase of the menstrual cycle (Otsuki et al., 1994). It is therefore conceivable that constant expression of bcl-2 together with increased expression of ER and Ki-67, with a hyperestrogenic metabolic state may promote both the invagination process and the development of adenomyosis into the myometrium.

There was a reduction in progesterone receptors (PR-A and PR-B) expression (chapter 6) in the endometrial stromal cells and glands of uteri with adenomyosis, both in the functionalis and the basalis, and in the adenomyotic foci. Progesterone induces its anti-proliferative activity through its receptors. This reduction in receptors expression might explain the poor response to progestational agents used in treatment of menstrual

symptoms in these women. The lack of progestational activity may also contribute to the common presence of endometrial hyperplasia in association with adenomyosis.

The potential role of the myometrium in the development of adenomyosis has not been described in the literature. Myometrial hyperplasia and hypertrophy are recognized features of adenomyosis, The precise reason for myometrial hypertrophy located around deep foci of endometrium is not known but may indicate either an attempt at controlling endometrial invagination of the myometrium or may be a reaction to the presence of invading endometrium. This myometrial abnormality may equally be the cause behind adenomyosis i.e. abnormally developed myometrium is more permissive to invasion by the endometrium. However, It has never been proposed that the myometrium may play a role in the pathogenesis of adenomyosis. This work presents evidence for the presence of unique myometrial defects in uteri affected by adenomyosis. In the neonatal CD-1 mouse model (chapter 2), and following neonatal tamoxifen exposure, all uteri showed adenomyosis by 6 weeks of age. The inner myometrium showed marked thinning, lack of continuity and orientation, disorganisation and bundling, as early as day 10, and preceding the downgrowth of endometrium to form adenomyosis. Desmin expression in the myometrial cells was markedly reduced. These findings suggest that abnormal development of the inner circular muscle layer may play a role in the development of uterine adenomyosis.

Microscopic examination of the human myometrium (chapter 4) demonstrated that the inner myometrium of normal uteri, has higher cell density and total nuclear area compared to the outer myometrium (1.6-1.8 folds), and that the change in cell density is gradual throughout the uterine thickness. The inner myometrium of adenomyotic uteri exhibited reduced cell density and larger nuclear size compared to normal uteri, suggesting a less compact myometrium that could be less resistant to penetration by the

overlying endometrium. Interestingly, the outer myometrium of uteri affected with adenomyosis, exhibited similar reduced density, suggesting a diffuse uterine defect rather than an effect localised to the inner myometrium.

Another defect observed in the adenomyotic uteri was the presence of myometrial cellular hypertrophy. The reduction in cell density with normal  $\alpha$ -SMA (and desmin) expression indicates cellular hypertrophy rather than increased extra-cellular components. This is further supported by an increase in cellular proliferation evidenced by an increased expression of Ki-67 in the adenomyotic myometrium.

In association with adenomyosis, the myocytes were organised into thinner, less well-defined bundles, with a disruption of normal geometry of the muscle bundles and fascicles, with widening of the intercellular space and rearrangement of the myocytes could influence uterine function. The morphological changes described in chapter 4 support a further role for the myometrium in the development of adenomyosis, possibly facilitating endometrium penetration.

Electron microscopic examination of the human myometrium confirmed the presence of ultrastructural changes (chapter 5) in the myocytes of uteri affected with adenomyosis. The nuclei had a smooth outline with a clear ground substance, prominent nucleoli and peripherally arranged nuclear chromatin. There was occasional infolding of the nuclear envelope with entrapment of cytoplasmic organelles. The sarcolemmal bands were significantly longer and there were fewer caveolae. The perinuclear cell organelles were more distinct. The rough endoplasmic reticulum and Golgi apparatus were more prominent, denoting active protein synthesis, consistent with the observed cellular hypertrophy. Abundant intermediate filaments formed cytoplasmic filaments aggregates and myelin bodies. All these changes were present both in the inner and the outer myometrium. These distinct features suggest a possible effect on myometrial

contractility, together with hypertrophy. Dysfunctional contractility could be the result of the presence of adenomyosis or could contribute to its pathogenesis. This supports the idea that the myometrium shows distinct changes in cases of adenomyosis, and that these changes are not limited to the inner myometrium, i.e. adenomyosis is a disease of the whole uterus.

The hypothesis that the myometrium plays a role in the development of adenomyosis is further supported by the abnormal expression of estrogen and progesterone receptors in the myometrium of uteri affected by adenomyosis (chapter 6). The observed increased expression of estrogen receptors (ER- $\alpha$  and in ER- $\beta$ ) may contribute to the development of adenomyosis-associated myometrial hyperplasia, while a reduced expression of progesterone receptors (PR-A and PR-B) observed in the inner and outer myometrium of diseased uteri may explain the poor response of these women to progestational agents. Both the inner and outer myometrium showed comparable abnormal expression of ERs and PRs.

RNA microarray analysis of the inner and outer myometrium (chapter 7) confirmed the presence of numerous differences in genes expression profiles and pathways in the myometrium of uteri affected by adenomyosis. Wnt5a was one of the key down-regulated genes in adenomyosis uteri. The presence of unique differences in gene expression profile in the muscle of affected uteri, suggests an inherent predisposition to the disease. Thus, the thesis provides substantial evidence for the presence of unique myometrial defects associated with adenomyosis both in the animal model, and in the affected human uteri at the phenotypic, ultrastructural, immunohistochemical and gene expression levels.

Although the literature suggests endometrial stromal invasion for the pathogenesis of adenomyosis, this has not been previously demonstrated in any model. This thesis

provides evidence for a role of endometrial stroma in the development of adenomyosis and conclusive evidence for increased invasiveness. As described, findings from the CD-1 mouse experiment suggest a role for a predisposed myometrium in the development of adenomyosis (chapter 2). Tamoxifen induced inner myometrial disruption and organisation in the C57/BL6J mice (chapter 3) similar to those observed in the CD-1 mice. However, the C57/BL6J mice did not develop adenomyosis. Thus, it seems that disruption of the inner myometrium cannot on its own explain the development of uterine adenomyosis and although these changes may be a prerequisite for the development of adenomyosis, additional genetic or epigenetic differences between strains expressed in the endometrium may be required. This suggests the presence of specific endometrial / stromal factors that are mandatory for the development of adenomyosis. It equally suggests the presence of an inherent predisposition to the disease (as spontaneous adenomyosis is known to develop in the CD-1 but not the C57/BL6J mice). The presence of a unique gene expression profile in the myometrium of human uteri with adenomyosis, confirms this view.

An increased invasion and penetration potential of endometrial stromal cells from uteri with adenomyosis was clearly demonstrated in the three-dimensional co-culture model described in this thesis (chapter 8). Adenomyotic stromal cells were three times more invasive to the underlying gels compared to controls. This confirms the original hypothesis that the endometrial stroma plays a role in the development of adenomyosis through increased invasion. In addition, this experiment provides evidence for the role of the myometrium from adenomyosis in facilitating this process, as the described increased endometrial stromal invasion was further enhanced in the presence of adenomyotic myocytes in the co-culture. The differential effect of myometrium from adenomyosis suggests once more an innate predisposition to the disease.

Thus, this thesis confirms the presence of endometrial stromal cells phenotypic abnormalities as well as an increased invasive potential in uteri with adenomyosis. But more importantly, this work proposes that adenomyosis is a disease of both the myometrium and endometrial stroma, given the unique myometrial changes described earlier. The co-culture model also provides evidence for the role of the myometrium in facilitating the endometrial invagination process, as the described increased endometrial stromal invasiveness was further enhanced in the presence of adenomyotic myocytes in the co-culture. The differential effect of myometrium from adenomyosis suggests once more an innate predisposition to the disease. Stromal cells and myometrial cells from women with adenomyosis had a distinct proteomic profile compared to stromal and myometrial cells from controls (chapter 8). Furthermore, some of the distinct features of adenomyosis derived cells are shared between stromal and myometrial cells. This suggests that adenomyosis may be characterised by a soluble secreted protein profile, at least in co-culture. This also supports the hypothesis that adenomyosis is a disease of both the myometrium and the endometrial stroma. Further research is needed to identify those proteins, and to understand the pathways involved in the cross talk between the myometrium and stroma. Findings from the RNA microarray analysis of the inner and outer myometrium (chapter 7) further confirms the presence of numerous differences in genes expression profiles and pathways in the myometrium of uteri affected by adenomyosis, with *Wnt5a* being a key down-regulated gene.

Epithelial-mesenchymal transition (EMT) has been recently identified as a critical step for appropriate embryonic development. EMT is also engaged in wound healing, tissue regeneration, organ fibrosis and cancer progression (Kalluri, 2009). During embryogenesis, epithelia are considered to be highly plastic and able to switch back and forth between epithelia and mesenchyme, via the processes of EMT and its reverse

mesenchymal-epithelial transition (MET) (Thiery, 2002, Kalluri and Neilson, 2003). It has been traditionally believed that upon completion of organ development epithelia typically serve specialised functions, with a state of terminal differentiation. This has been recently challenged by observations that terminally differentiated epithelia can change their phenotype under the influence of repair-associated or pathological stresses (Boyer et al., 2000, Nieto, 2002, Tsai et al., 2002). However, pathologists still debate the relevance of EMT/MET to human conditions such as fibrosis and cancer progression (Kalluri, 2009). Whether EMT/MET could be operational in the pathogenesis of uterine adenomyosis, with the reversibility of the processes observed during embryonic development, when migratory mesenchyme gives rise to secondary epithelia, is only highly speculative. Although this has not been the direct focus of the thesis, but the possibility of EMT/MET cannot be ruled out. There is cumulative evidence for specific phenotypic and genotypic changes associated with uterine adenomyosis presented through the thesis and summarised in this discussion makes EMT/MET a possibility, although this needs further testing.

In conclusion, this thesis demonstrated that the endometrial – myometrial interface behaves differently in uteri with adenomyosis compared to control. These findings generate hypotheses that adenomyosis is a uterine disease characterized by both increased invasiveness and myometrial defects that play a facilitative role for this invasion. Both the myometrium and endometrial stroma of diseased uteri show a unique phenotype, gene expression and protein expression profiles.

## **9.2 SUGGESTED MODEL FOR THE PATHOGENESIS OF UTERINE ADENOMYOSIS**

This model is in agreement with the literature about pathogenesis of uterine adenomyosis (endometrial-myometrial interface disruption, invasion, disordered proliferation and regeneration, a role for endometrial stromal cells, an impaired hormonal milieu, the presence of biochemical abnormalities, and a genetic predisposition) reviewed in chapter 1. This model highlights the role played by the myometrium in the development of the disease and the potential proteins, genes and pathways involved in the pathogenesis of adenomyosis.

## **9.3 FUTURE RESEARCH**

Following from this thesis, other suggested areas for investigation are:

- 1- Examining the reproductive performance and pregnancy outcomes of CD-1 mice following the experimental induction of adenomyosis, to answer a fundamental question related to the effects of adenomyosis on human reproduction.
- 2- Further characterization and localisation of the Wnt genes family in the human female reproductive tract.
- 3- The examination of the contractile properties of the myometrium of diseased uteri.
- 4- Further characterisation and isolation of the potential proteins identified in the endometrial stroma and myometrium from adenomyosis.
- 5- The manipulation of the cell culture medium and environment in the co-culture medium to examine the effect of different hormones and therapeutic agents on the stromal invasiveness.

## **APPENDIX 1**

### **Additional figures and plates for Chapter 6**

**Estrogen and Progesterone receptors distribution in uteri with and without adenomyosis through the menstrual cycle**

**Figure 6.1: Estrogen receptor alpha distribution in the functionalis (glands and stroma) in the different phases of the menstrual cycle. Immunohistochemical staining expressed as percentage of positively stained cells per high power field (mean  $\pm$  SEM) (\* significant difference between adenomyosis and controls,  $P < 0.05$ ).**

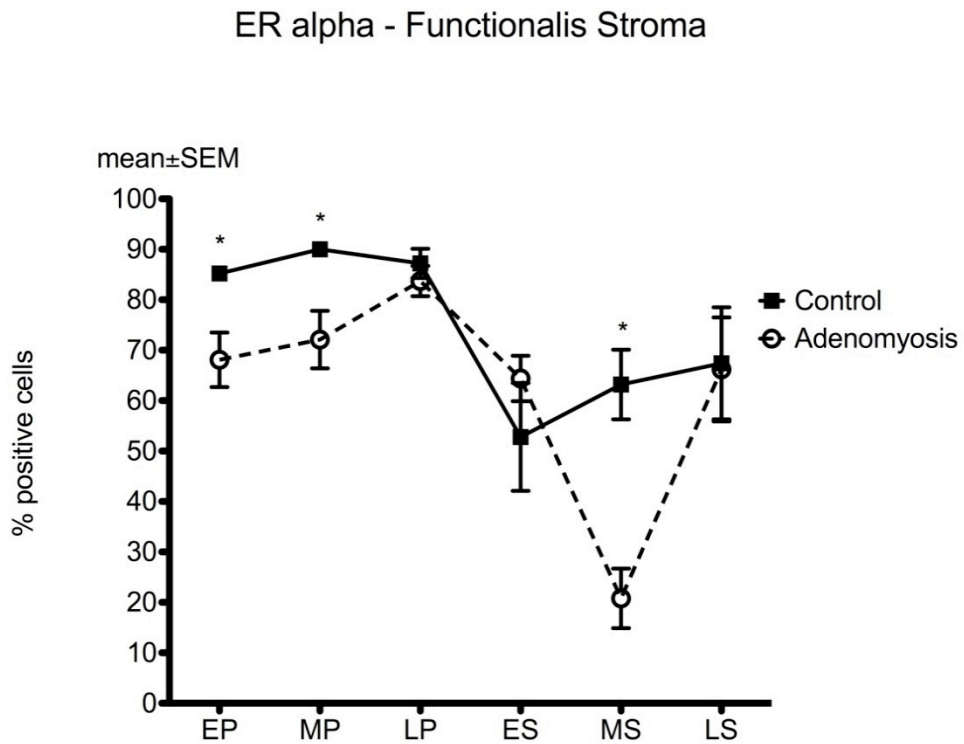
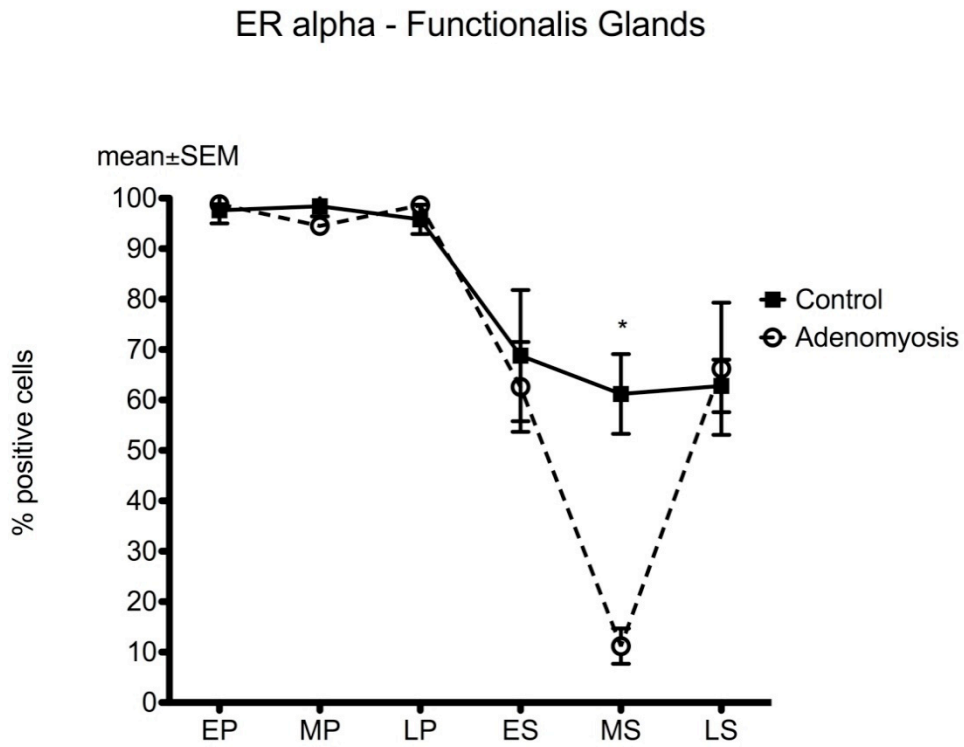
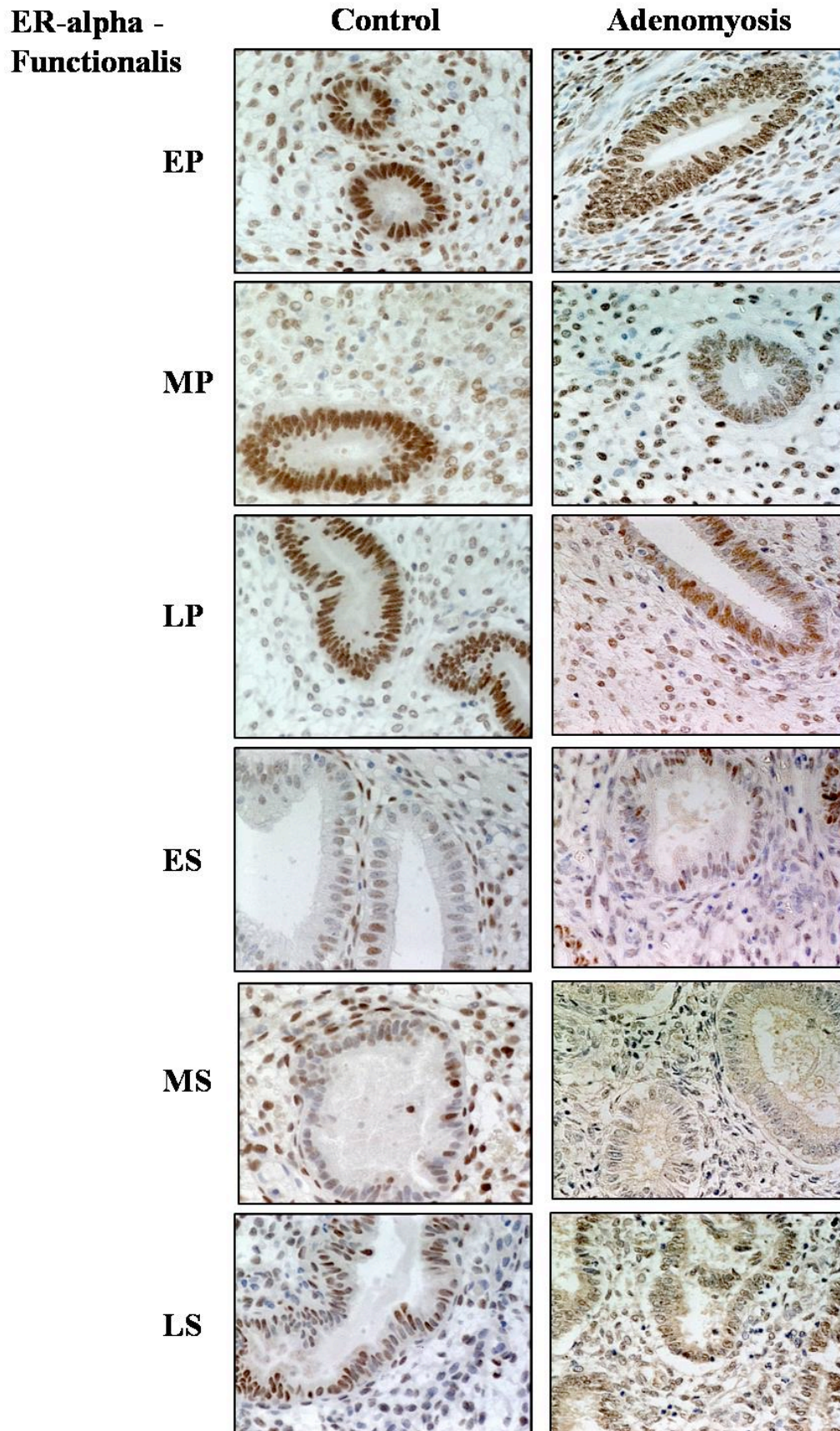


Figure 6.2: Estrogen receptor alpha distribution in the functionalis (glands and stroma) in the different phases of the menstrual cycle (magnification x20).



**Figure 6.3: Estrogen receptor alpha distribution in the basalis (glands and stroma) in the different phases of the menstrual cycle. Immunohistochemical staining expressed as percentage of positively stained cells per high power field (mean  $\pm$  SEM) (\* significant difference between adenomyosis and controls,  $P < 0.05$ ).**

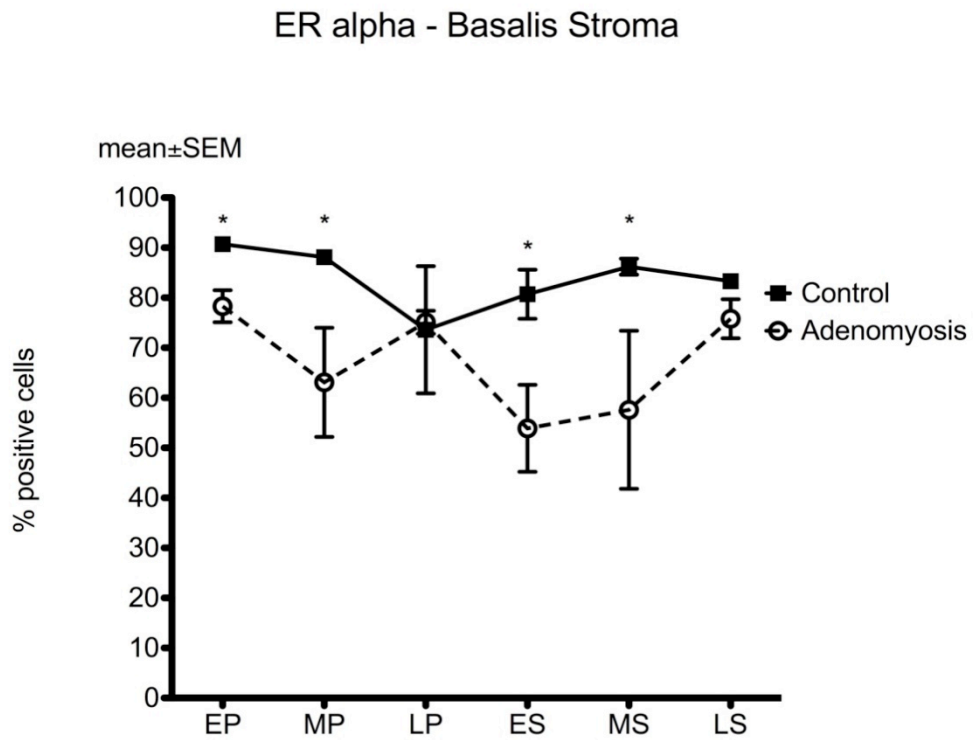
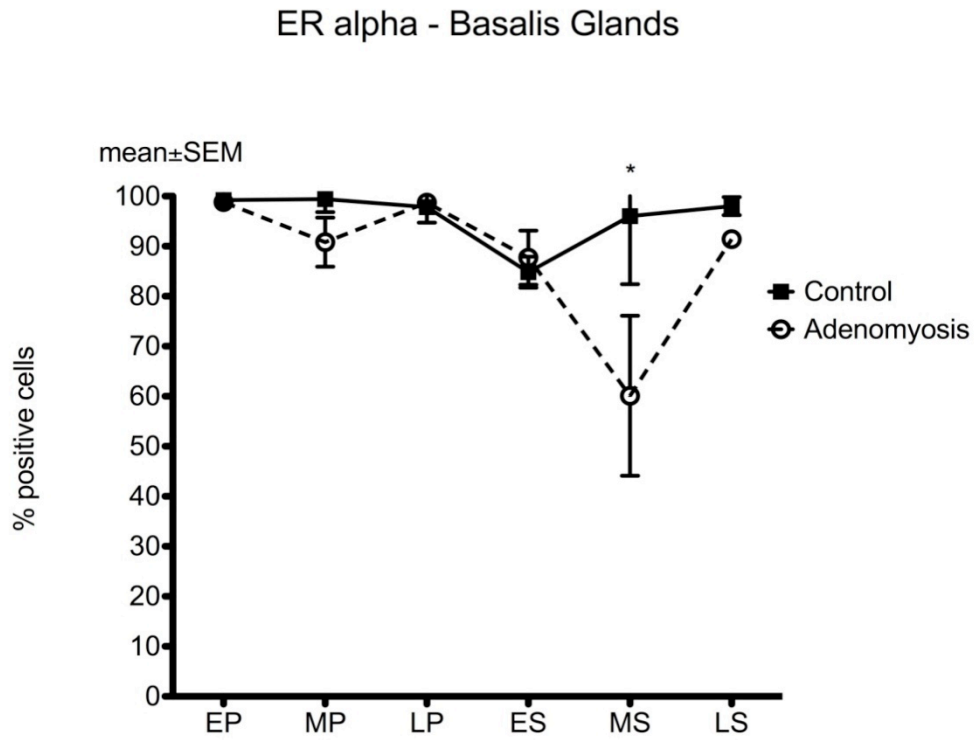
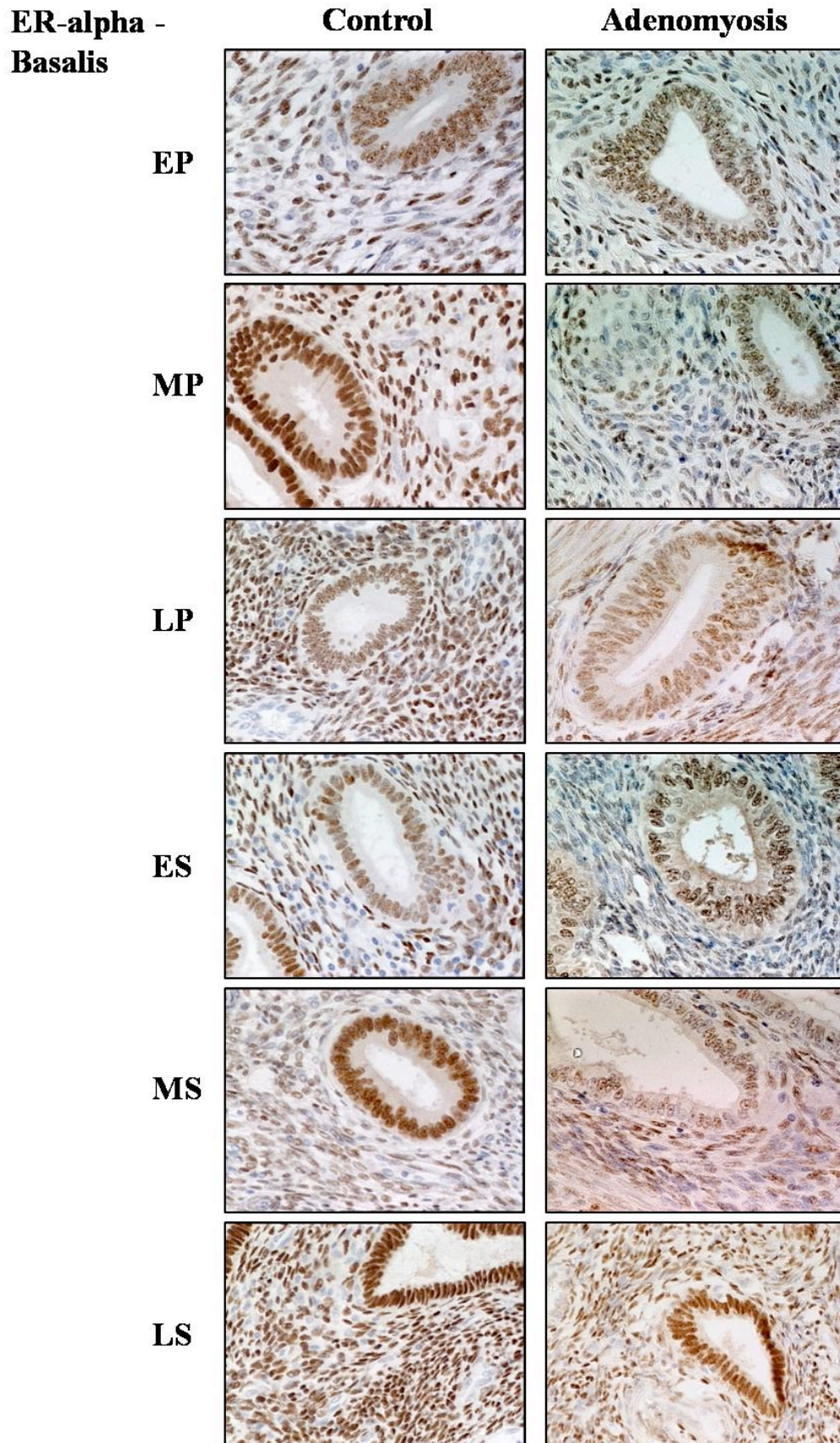


Figure 6.4: Estrogen receptor alpha distribution in the basalis (glands and stroma) in the different phases of the menstrual cycle (magnification x20).



**Figure 6.5: Estrogen receptor alpha distribution in the myometrium (inner and outer) in the different phases of the menstrual cycle. Immunohistochemical staining expressed as percentage of positively stained cells per high power field (mean  $\pm$  SEM) (\* significant difference between adenomyosis and controls,  $P < 0.05$ ).**

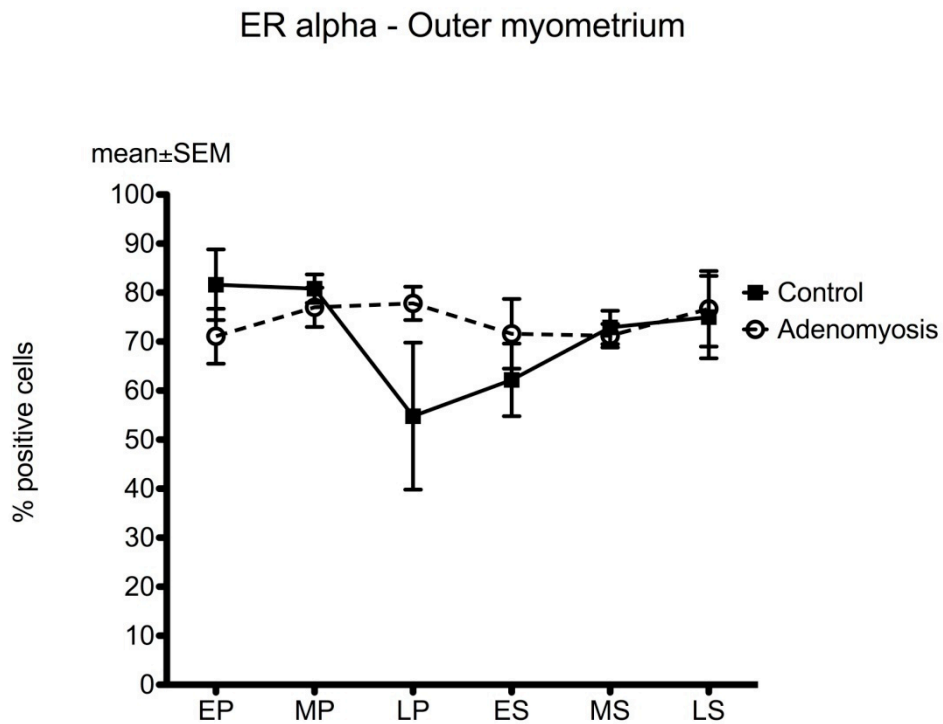
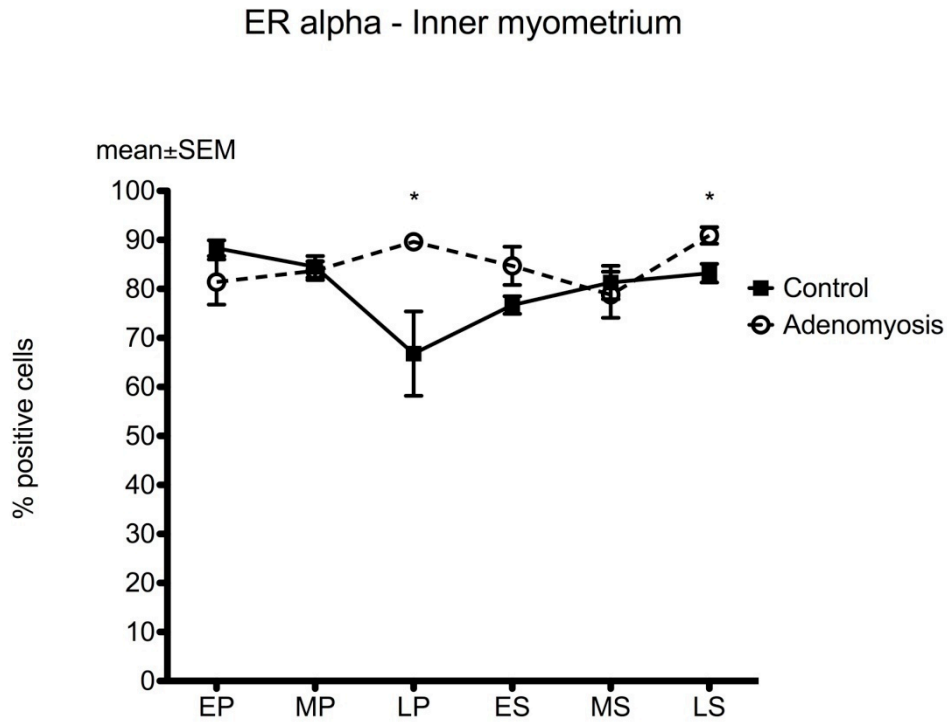


Figure 6.6: Estrogen receptor alpha distribution in the inner myometrium in the different phases of the menstrual cycle (magnification x20).

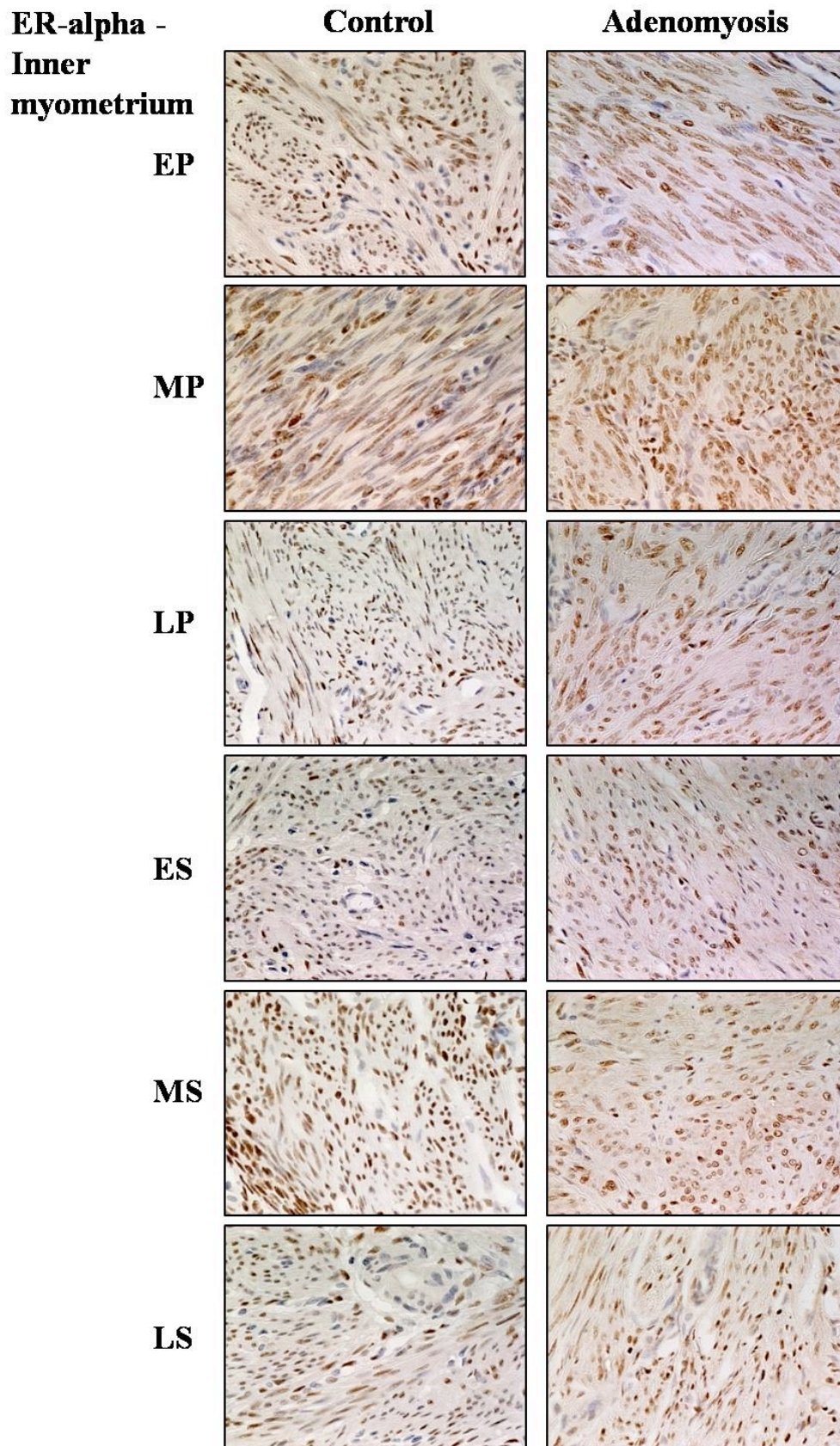
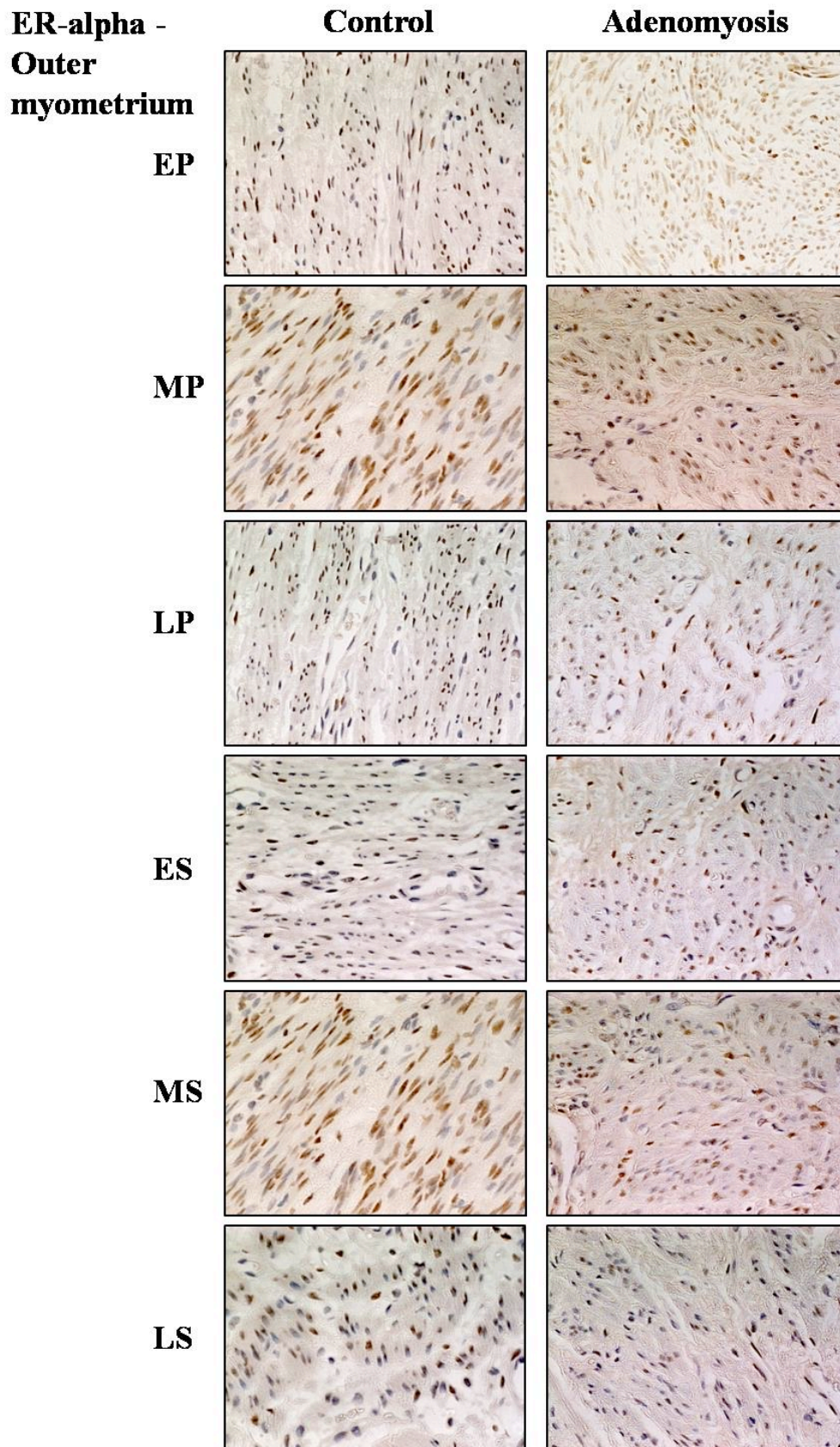


Figure 6.7: Estrogen receptor alpha distribution in the outer myometrium in the different phases of the menstrual cycle (magnification x20).



**Figure 6.8: Estrogen receptor beta distribution in the functionalis (glands and stroma) in the different phases of the menstrual cycle. Immunohistochemical staining expressed as percentage of positively stained cells per high power field (mean  $\pm$  SEM) (\* significant difference between adenomyosis and controls,  $P < 0.05$ ).**

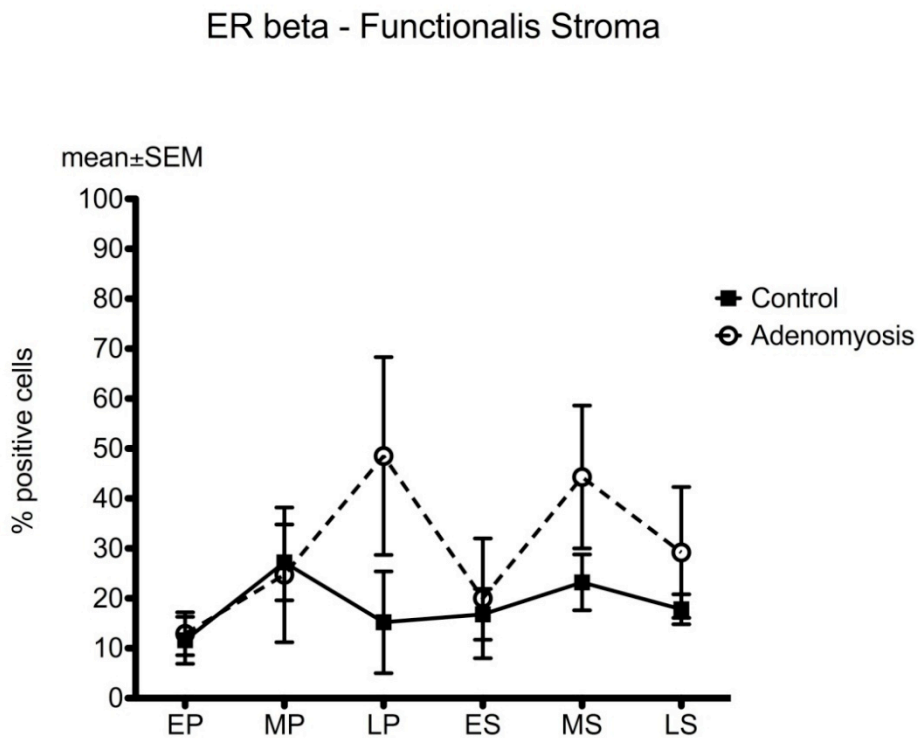
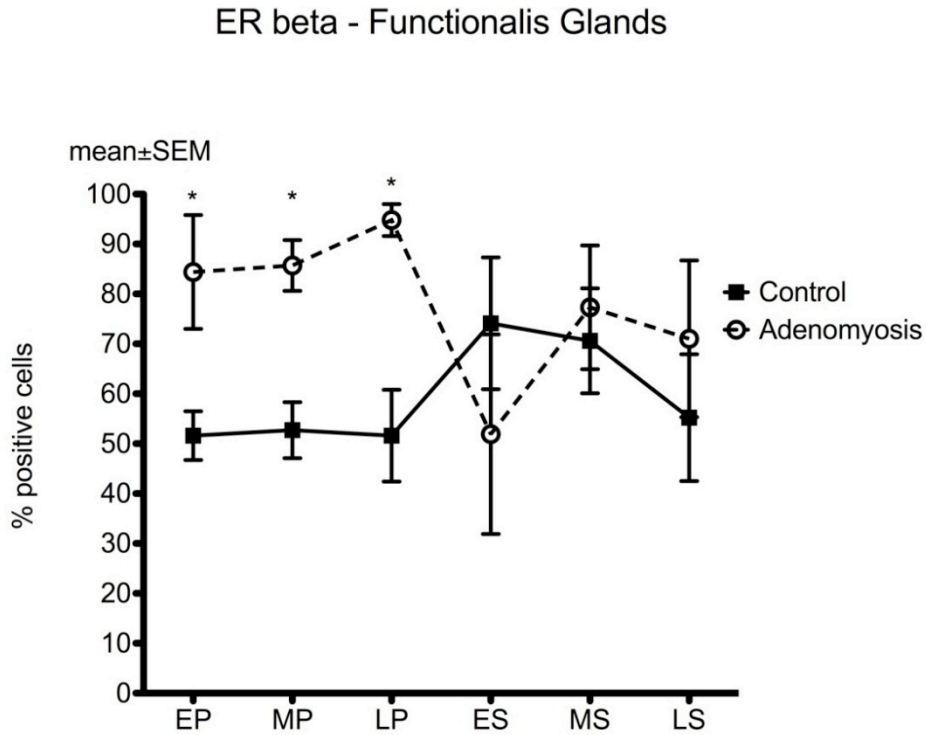
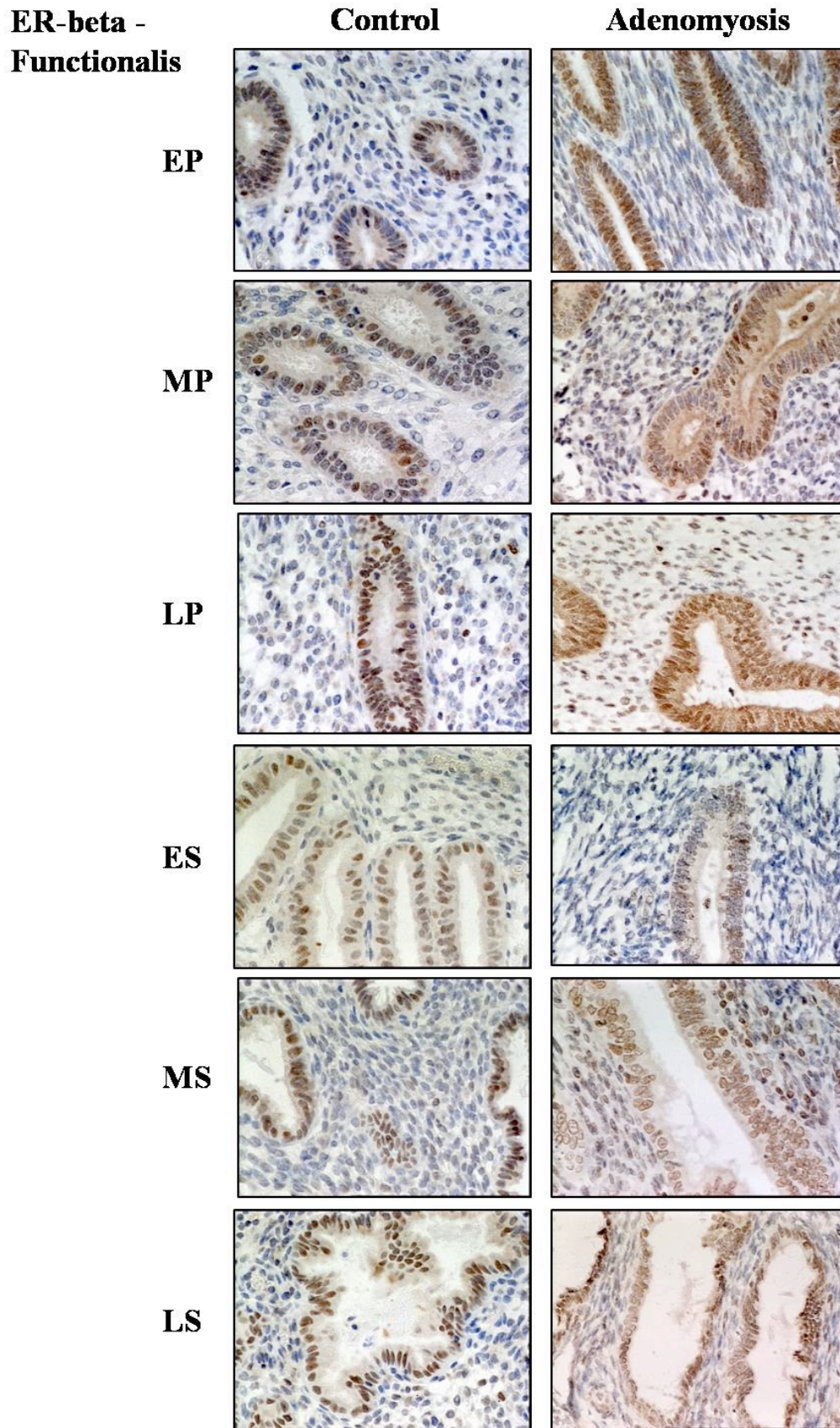


Figure 6.9: Estrogen receptor beta distribution in the functionalis (glands and stroma) in the different phases of the menstrual cycle (magnification x20).



**Figure 6.10: Estrogen receptor beta distribution in the basalis (glands and stroma) in the different phases of the menstrual cycle. Immunohistochemical staining expressed as percentage of positively stained cells per high power field (mean  $\pm$  SEM) (\* significant difference between adenomyosis and controls,  $P < 0.05$ ).**

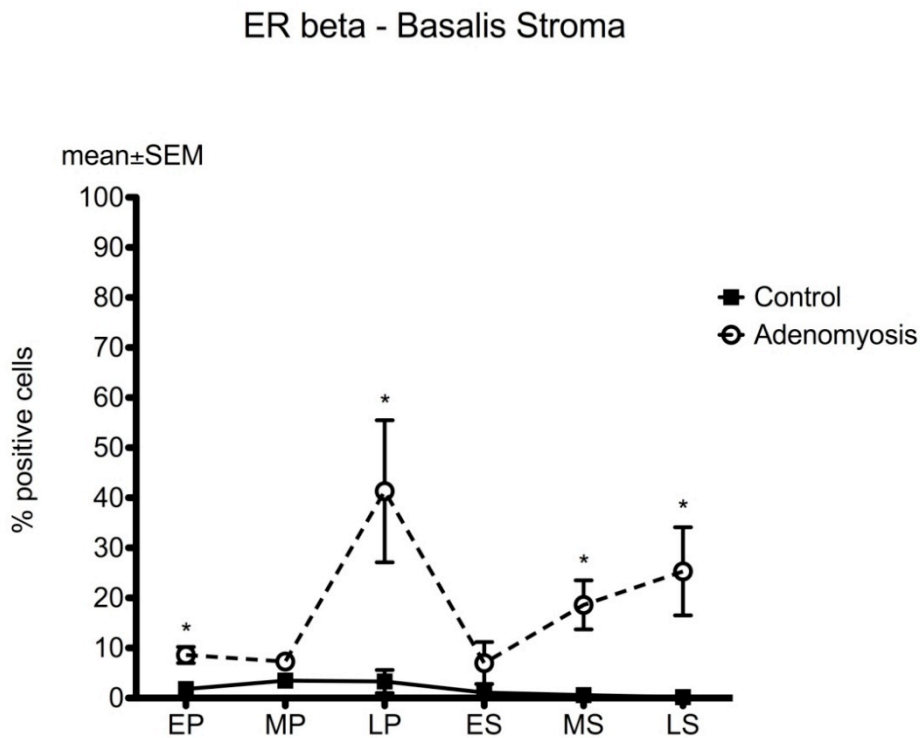
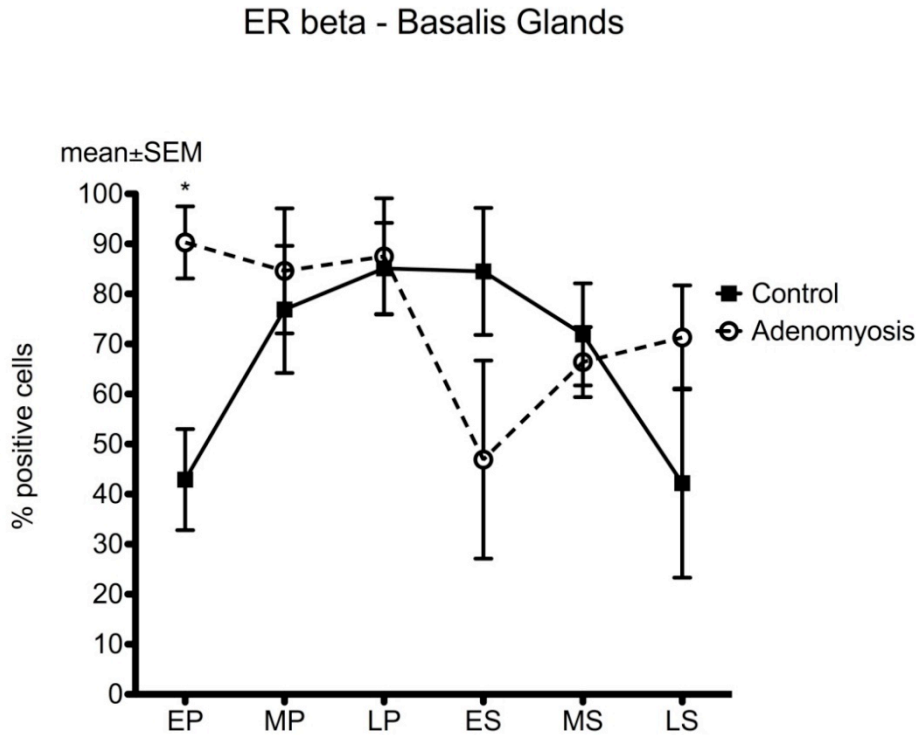
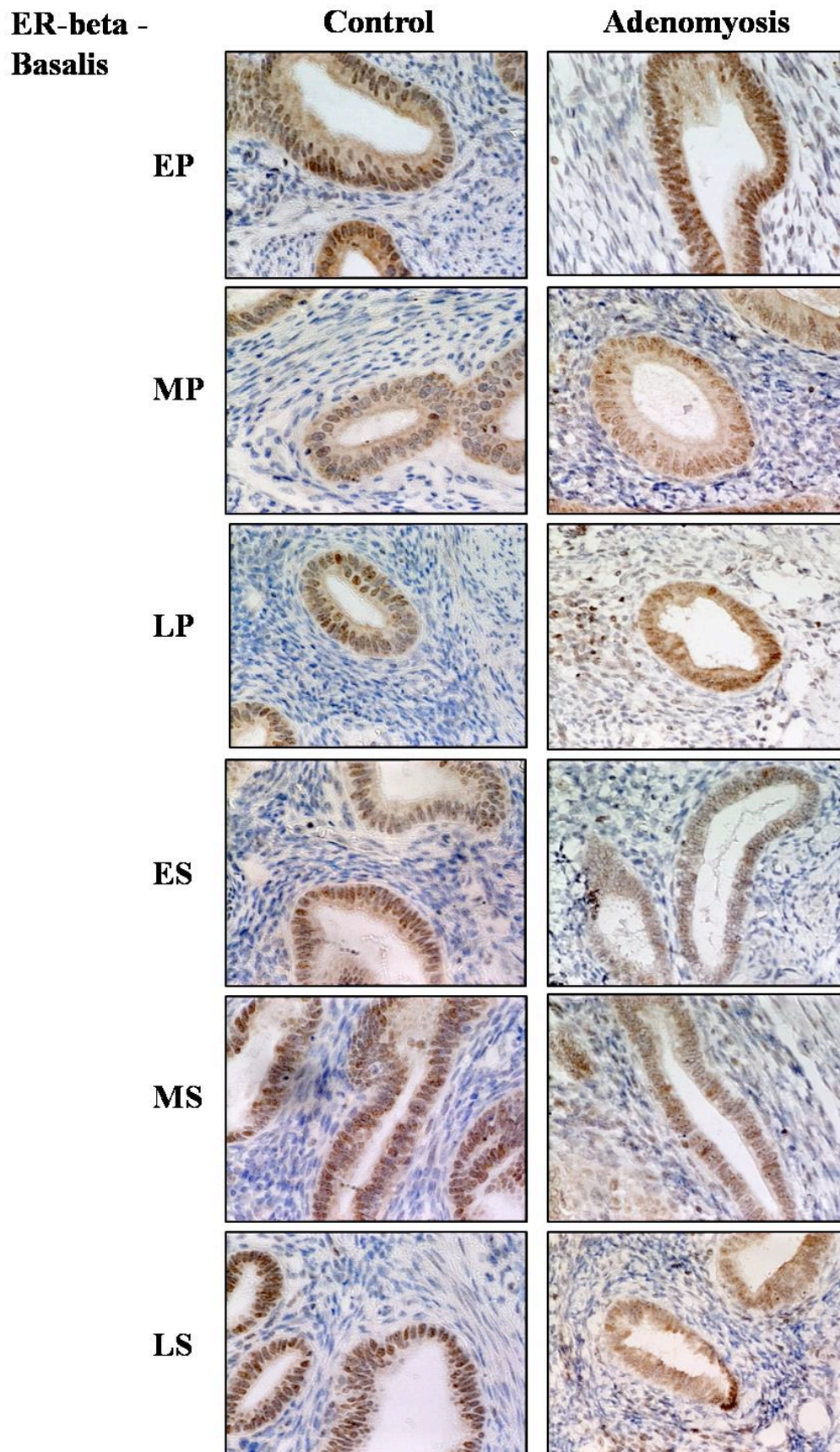
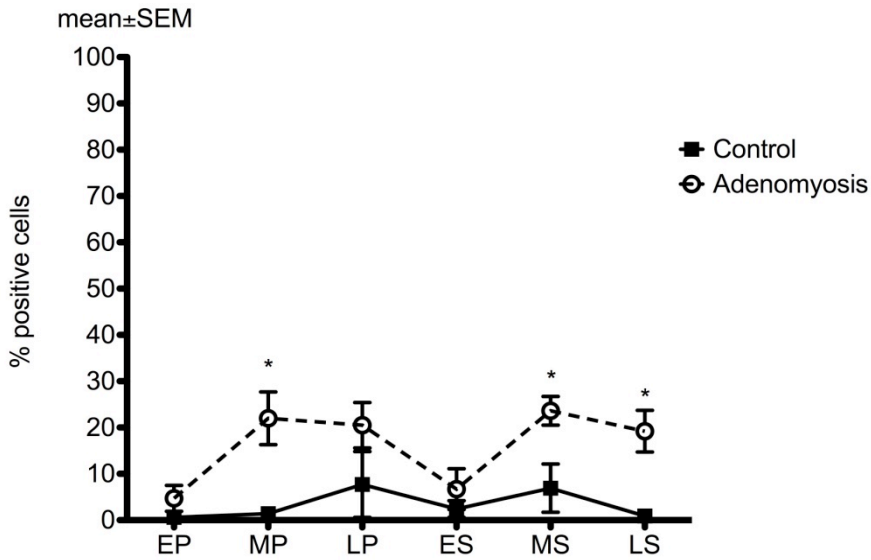


Figure 6.11: Estrogen receptor beta distribution in the basalis (glands and stroma) in the different phases of the menstrual cycle (magnification x20).



**Figure 6.12: Estrogen receptor beta distribution in the myometrium (inner and outer) in the different phases of the menstrual cycle. Immunohistochemical staining expressed as percentage of positively stained cells per high power field (mean  $\pm$  SEM) (\* significant difference between adenomyosis and controls,  $P < 0.05$ ).**

ER beta - Inner myometrium



ER beta - Outer myometrium

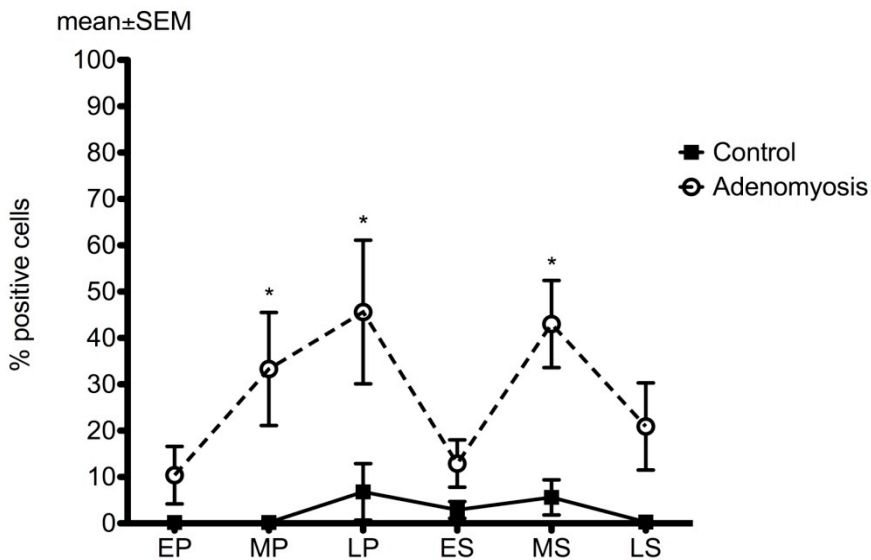


Figure 6.13: Estrogen receptor beta distribution in the inner myometrium in the different phases of the menstrual cycle (magnification x20).

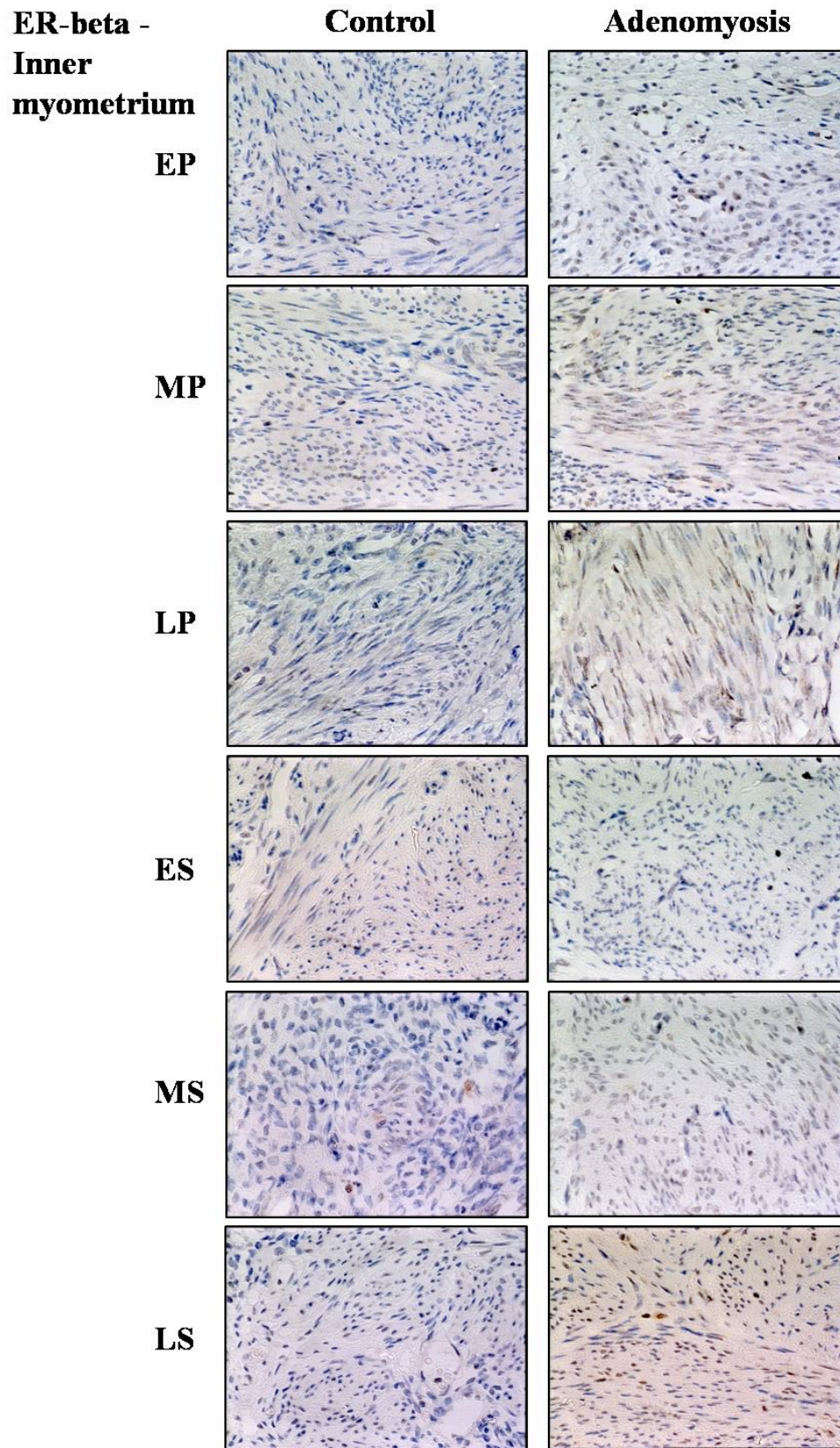
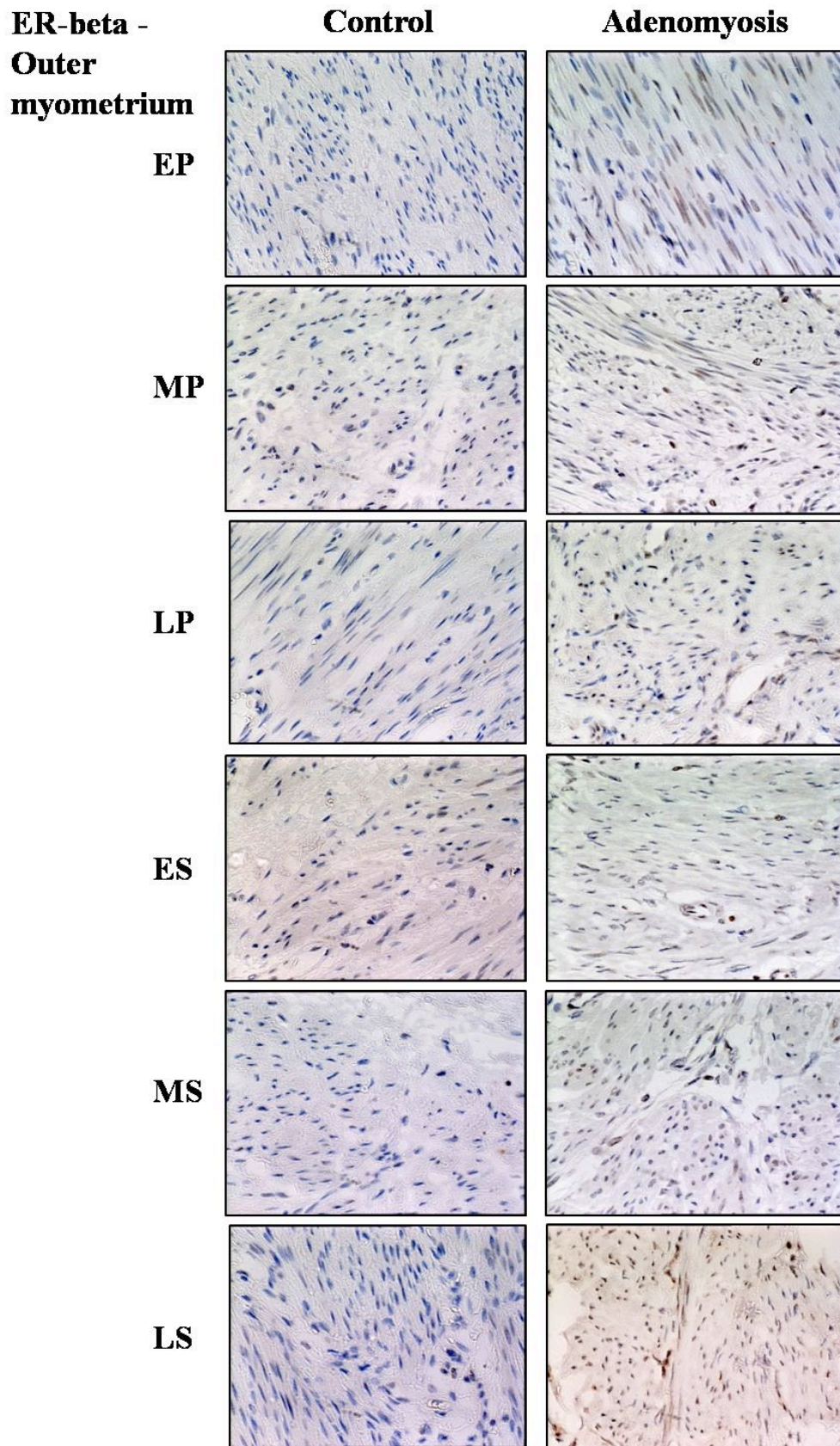


Figure 6.14: Estrogen receptor beta distribution in the outer myometrium in the different phases of the menstrual cycle (magnification x20).



**Figure 6.15: Progesterone receptor A distribution in the functionalis (glands and stroma) in the different phases of the menstrual cycle. Immunohistochemical staining expressed as percentage of positively stained cells per high power field (mean  $\pm$  SEM) (\* significant difference between adenomyosis and controls,  $P < 0.05$ ).**

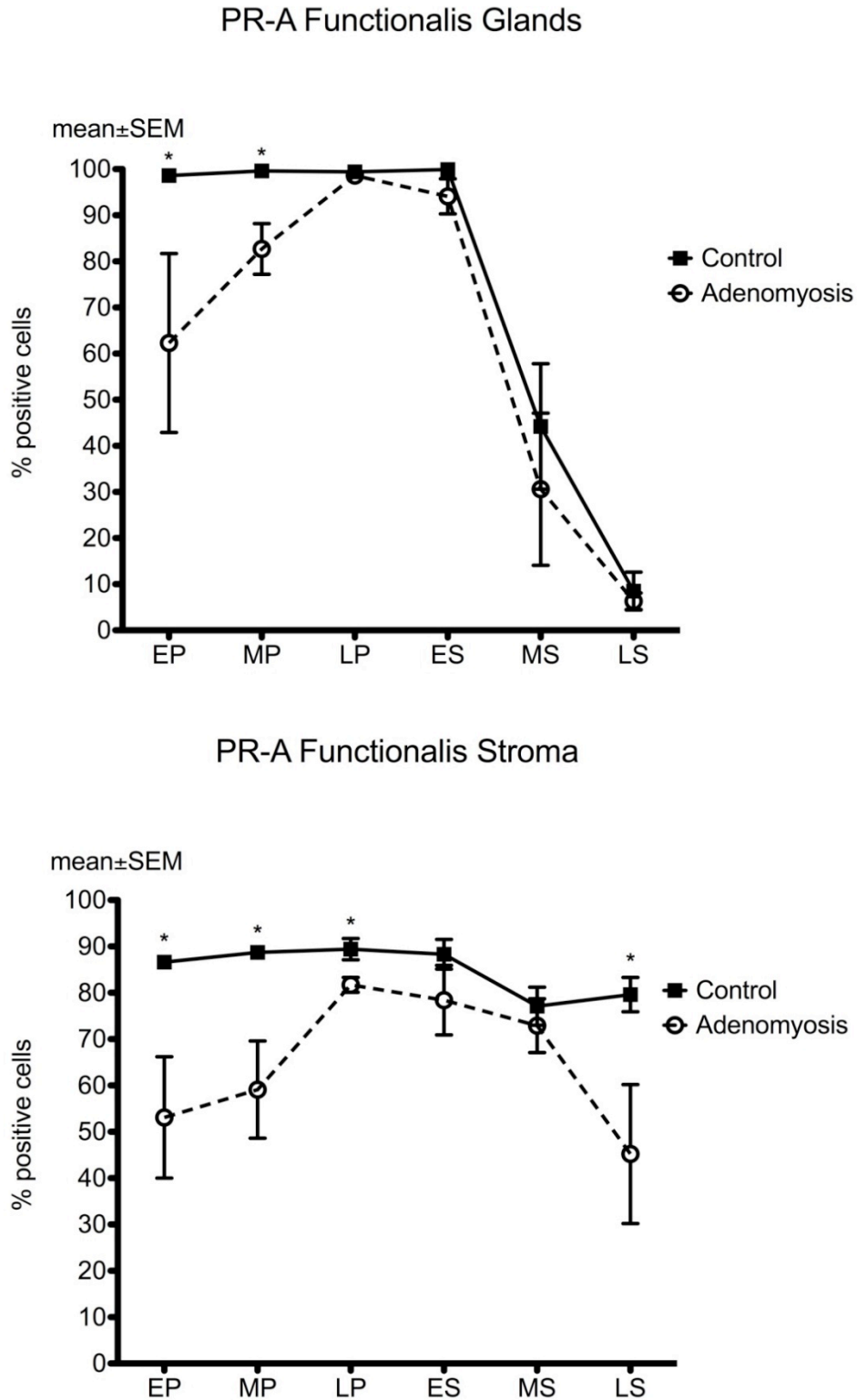
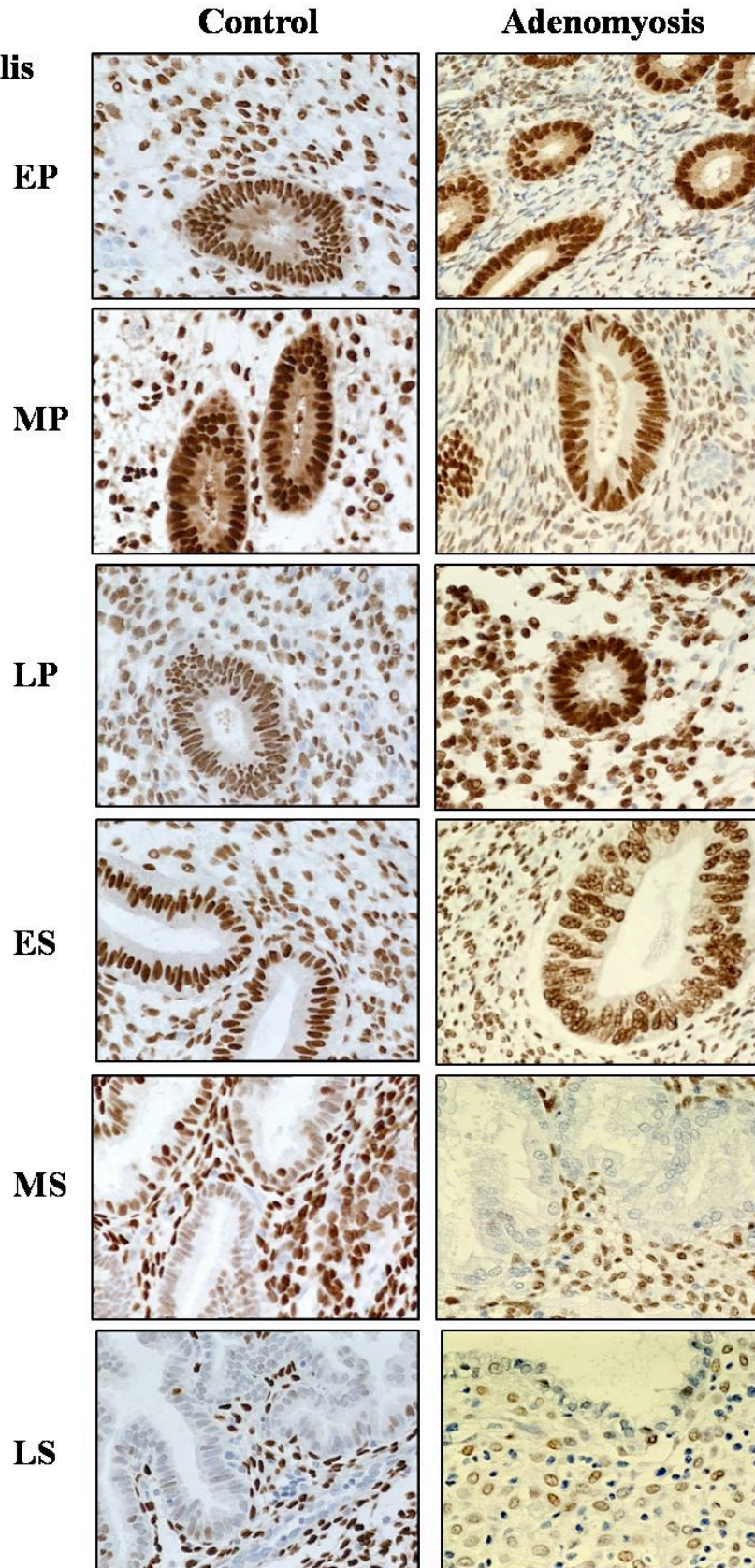


Figure 6.16: Progesterone receptor A distribution in the functionalis (glands and stroma) in the different phases of the menstrual cycle (magnification x20).

**PR-A -  
Functionalis**



**Figure 6.17: Progesterone receptor A distribution in the basalis (glands and stroma) in the different phases of the menstrual cycle. Immunohistochemical staining expressed as percentage of positively stained cells per high power field (mean  $\pm$  SEM) (\* significant difference between adenomyosis and controls,  $P < 0.05$ ).**

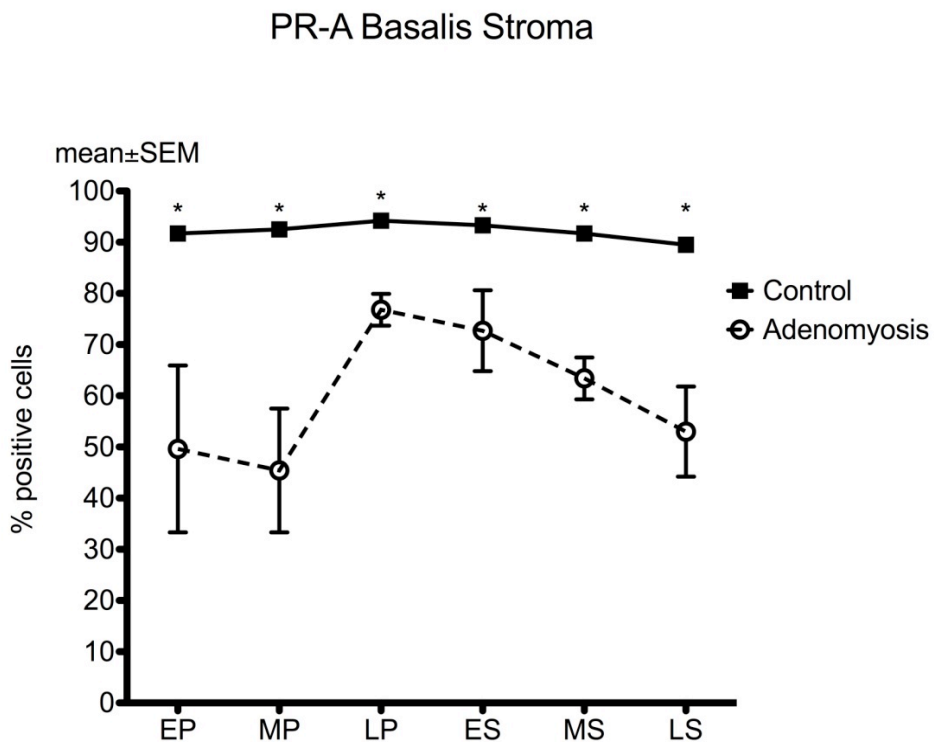
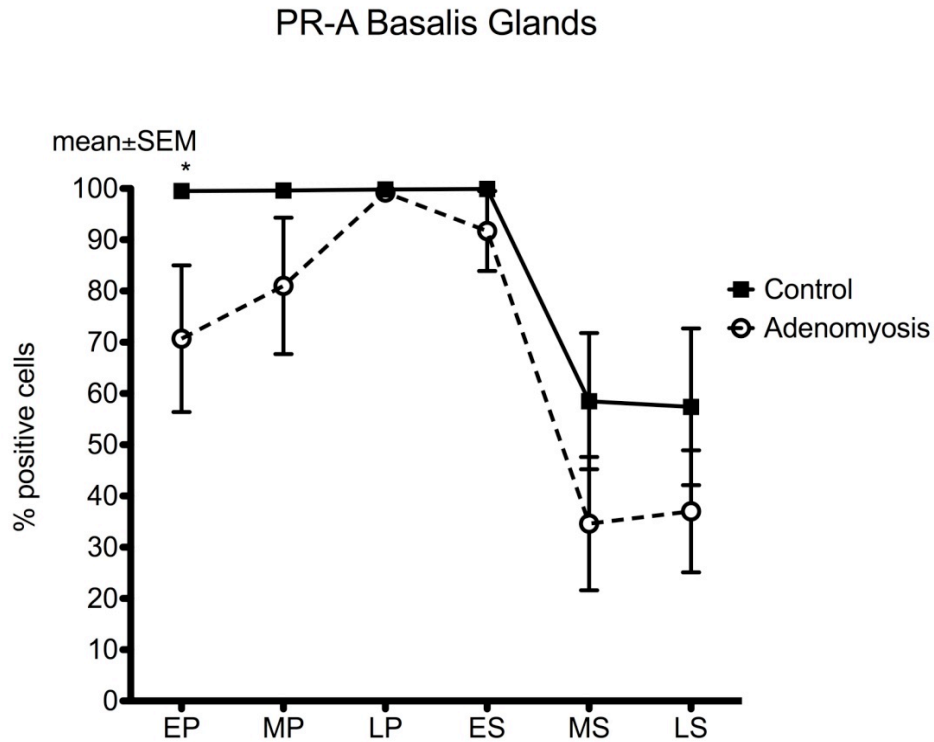
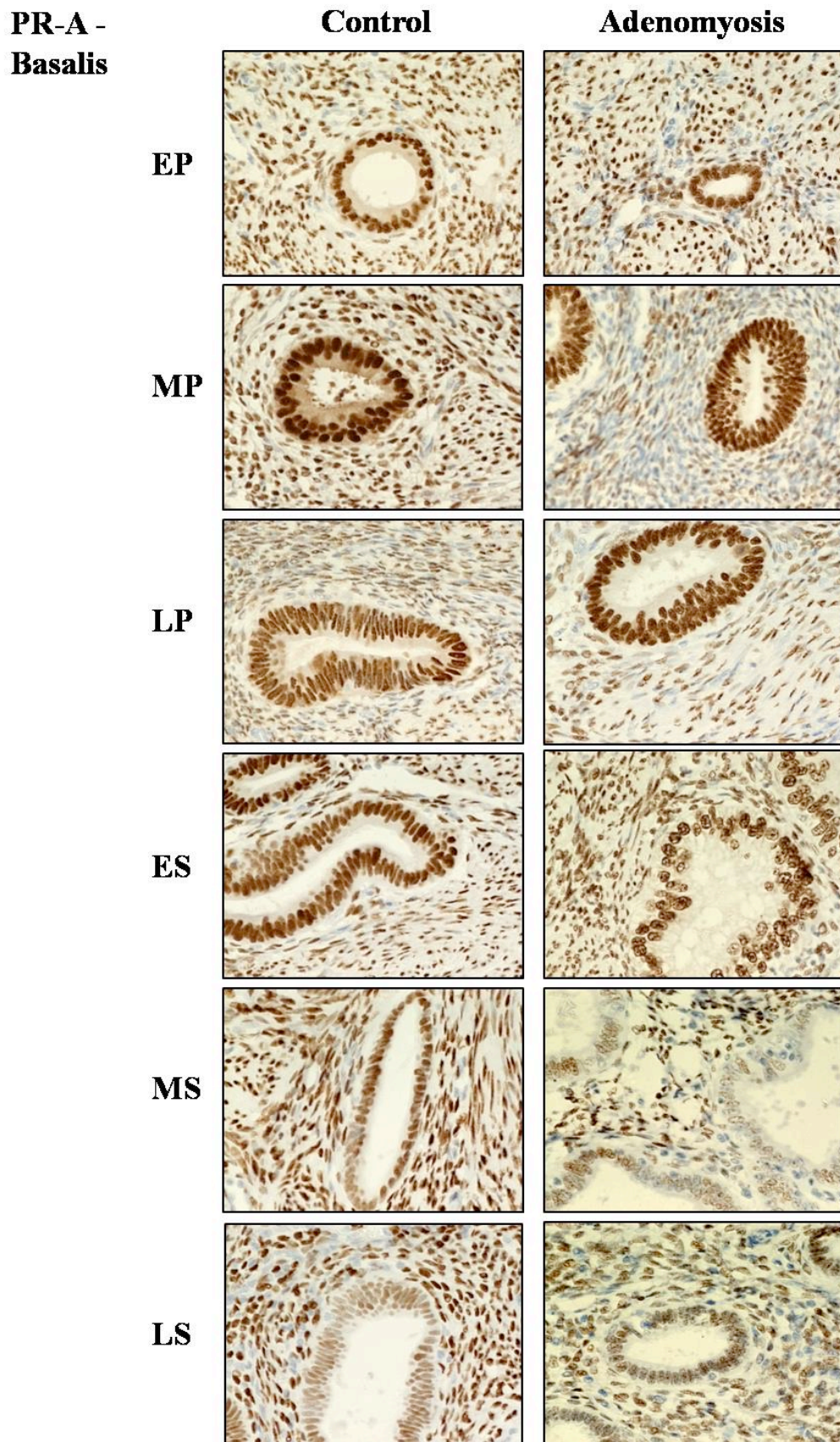


Figure 6.18: Progesterone receptor A distribution in the basalis (glands and stroma) in the different phases of the menstrual cycle (magnification x20).



**Figure 6.19: Progesterone receptor A distribution in the myometrium (inner and outer) in the different phases of the menstrual cycle. Immunohistochemical staining expressed as percentage of positively stained cells per high power field (mean  $\pm$  SEM) (\* significant difference between adenomyosis and controls,  $P < 0.05$ ).**

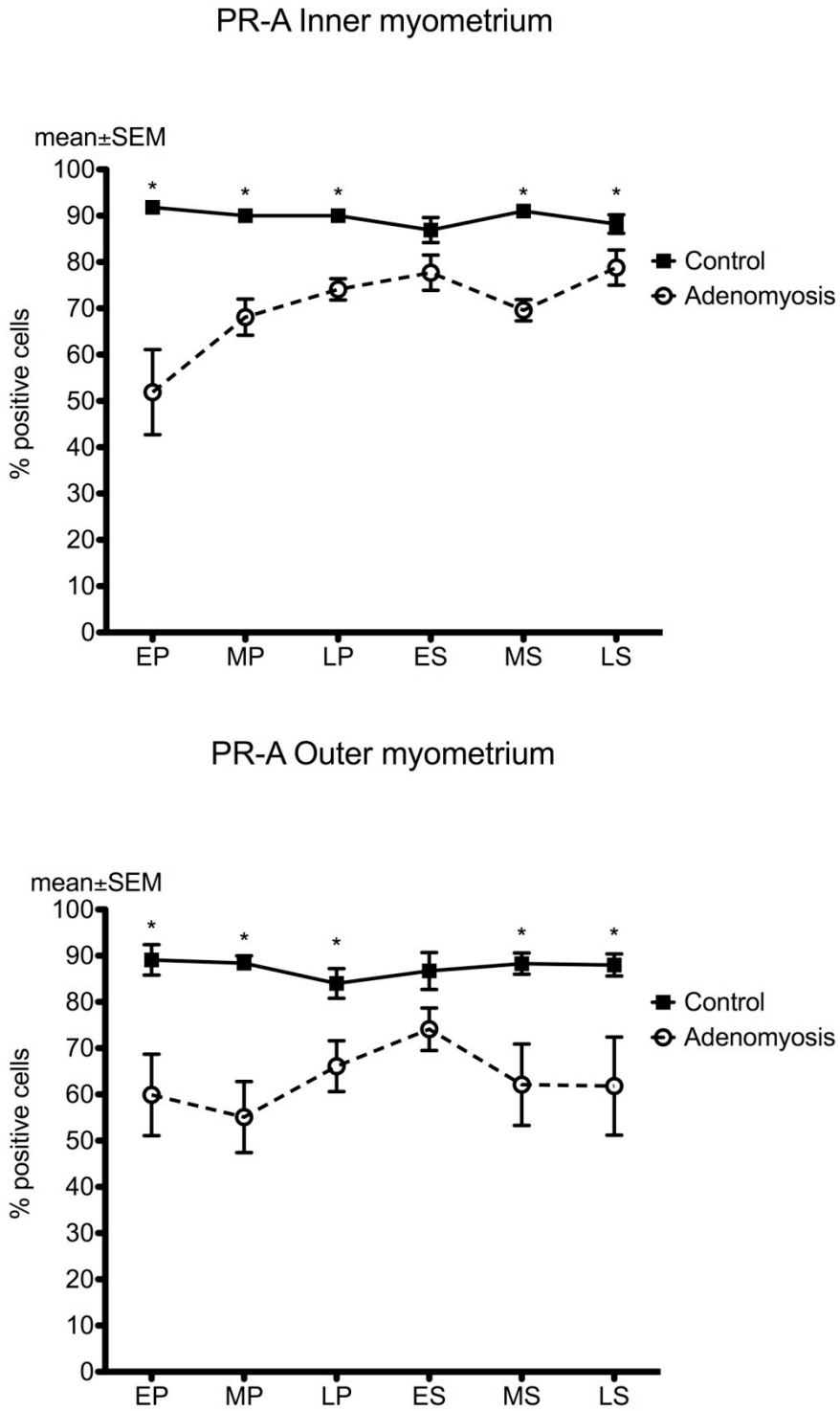


Figure 6.20: Progesterone receptor A distribution in the inner myometrium in the different phases of the menstrual cycle (magnification x20).

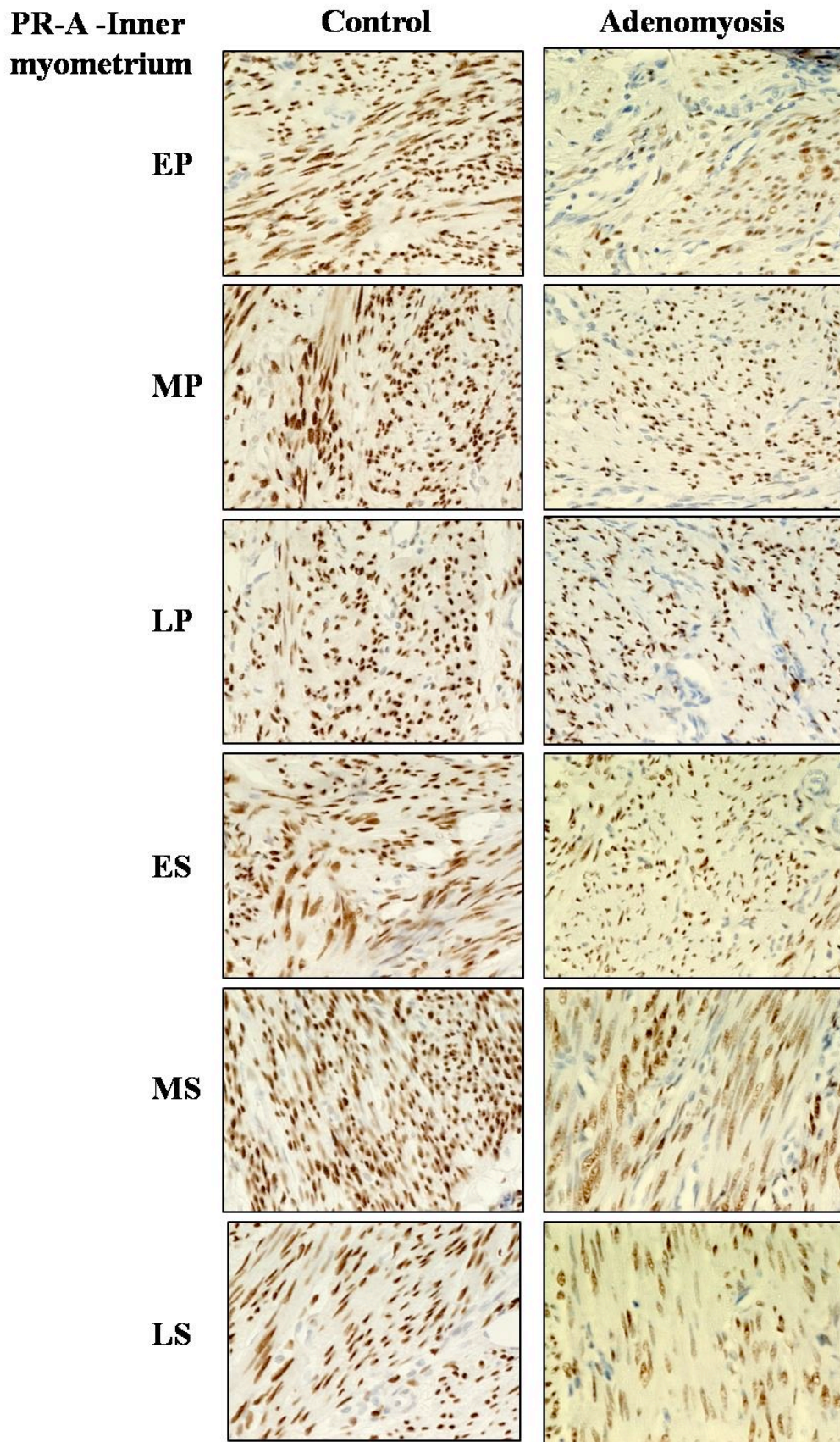
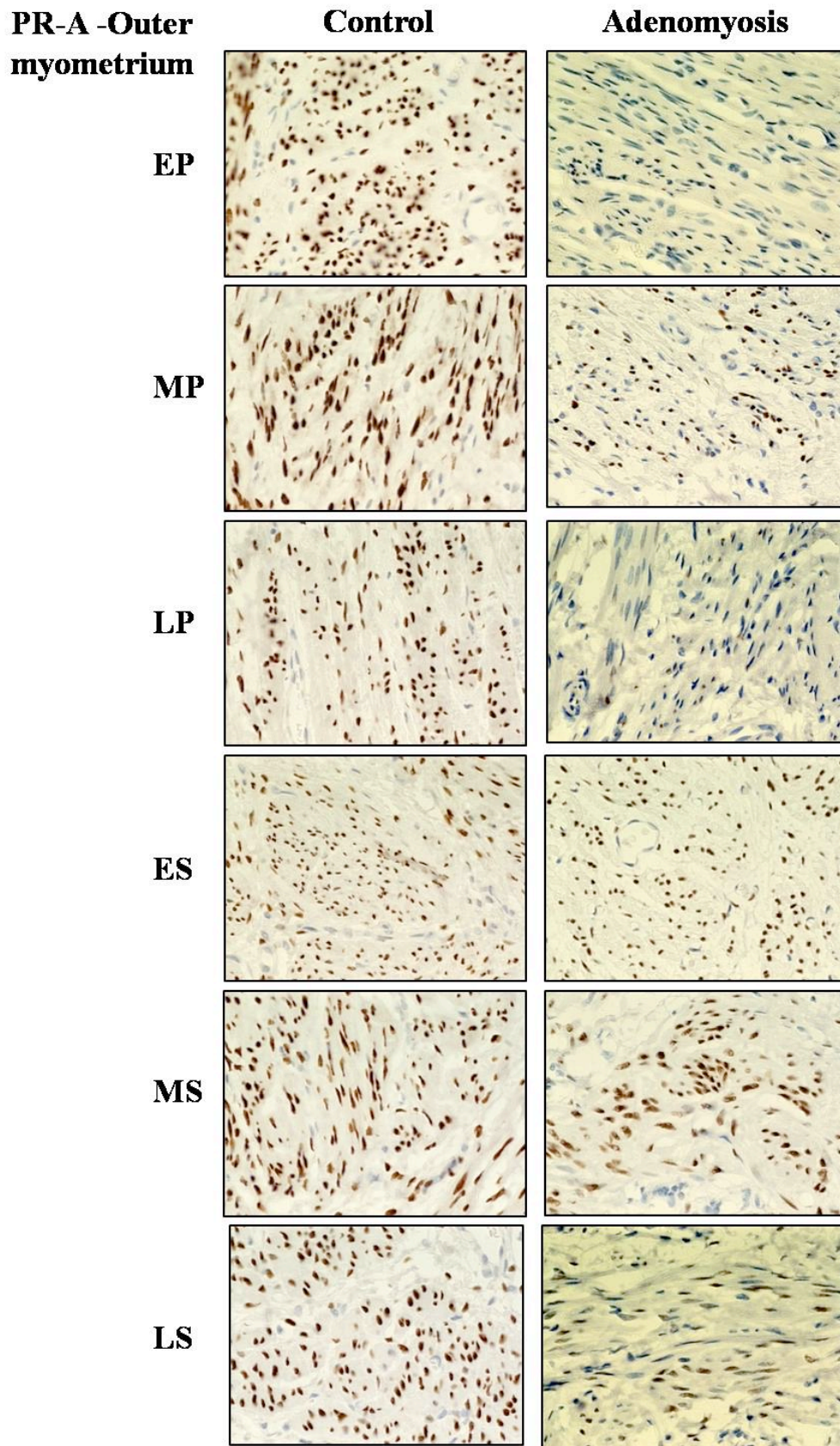


Figure 6.21: Progesterone receptor A distribution in the outer myometrium in the different phases of the menstrual cycle (magnification x20).



**Figure 6.22: Progesterone receptor B distribution in the functionalis (glands and stroma) in the different phases of the menstrual cycle. Immunohistochemical staining expressed as percentage of positively stained cells per high power field (mean  $\pm$  SEM) (\* significant difference between adenomyosis and controls,  $P < 0.05$ ).**

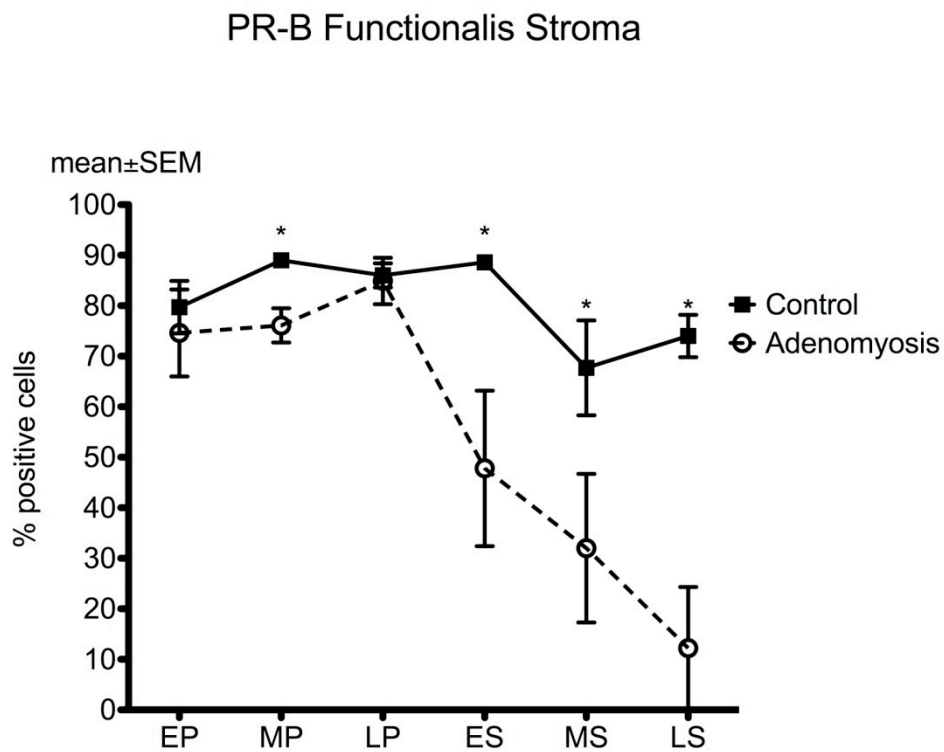
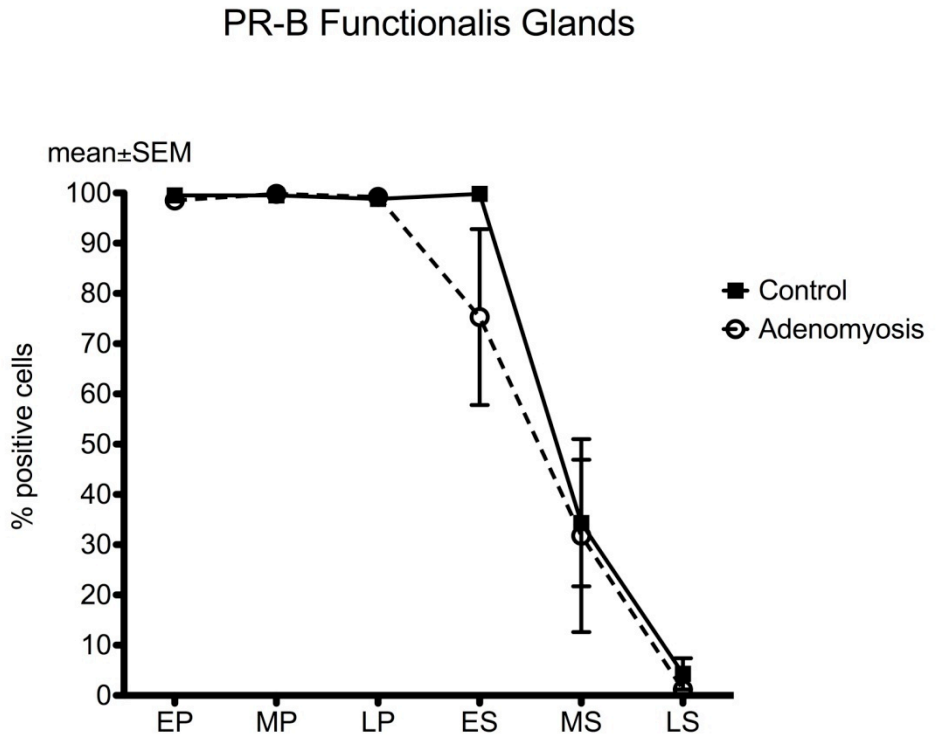
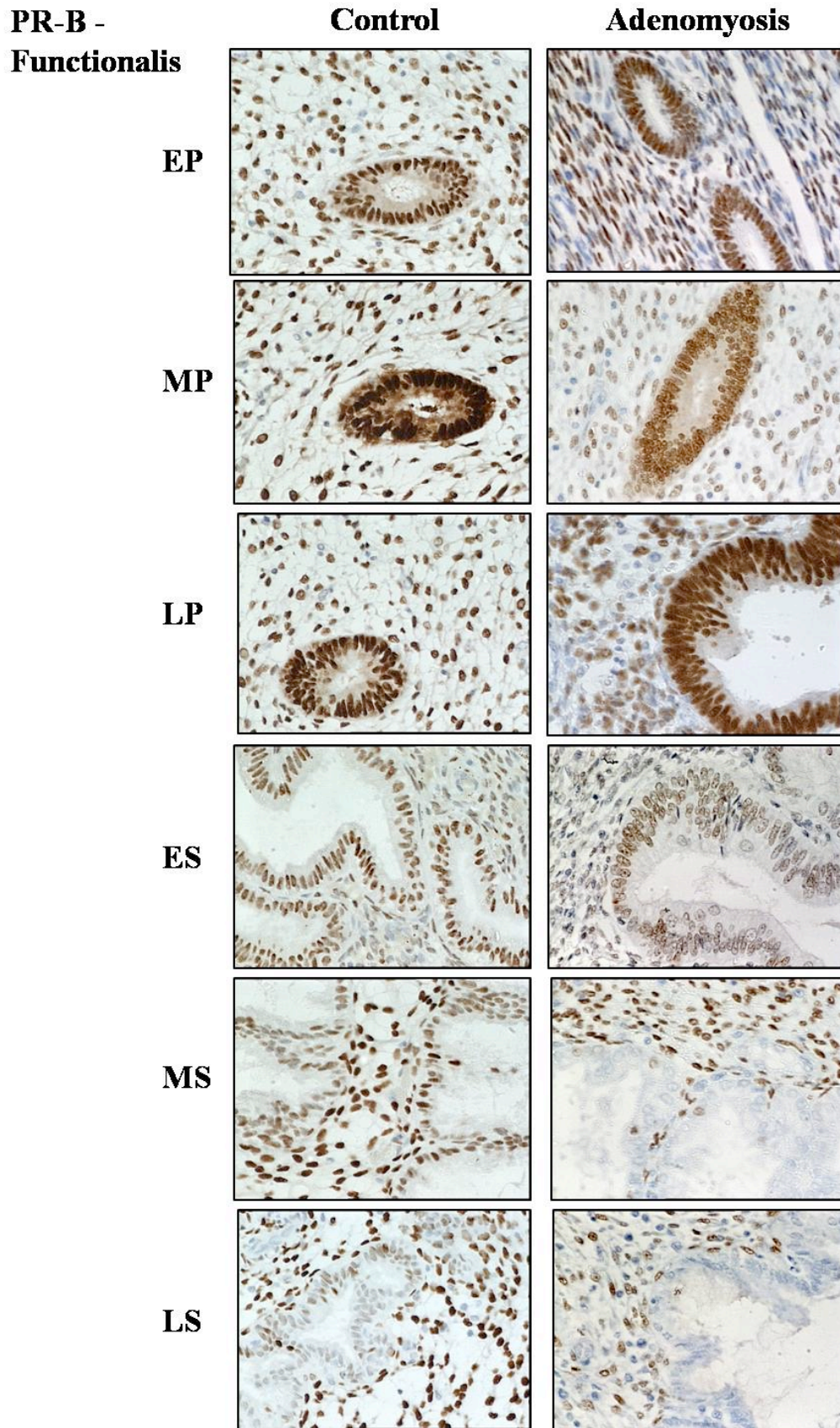


Figure 6.23: Progesterone receptor B distribution in the functionalis (glands and stroma) in the different phases of the menstrual cycle (magnification x20).



**Figure 6.24: Progesterone receptor B distribution in the basalis (glands and stroma) in the different phases of the menstrual cycle. Immunohistochemical staining expressed as percentage of positively stained cells per high power field (mean  $\pm$  SEM) (\* significant difference between adenomyosis and controls,  $P < 0.05$ ).**

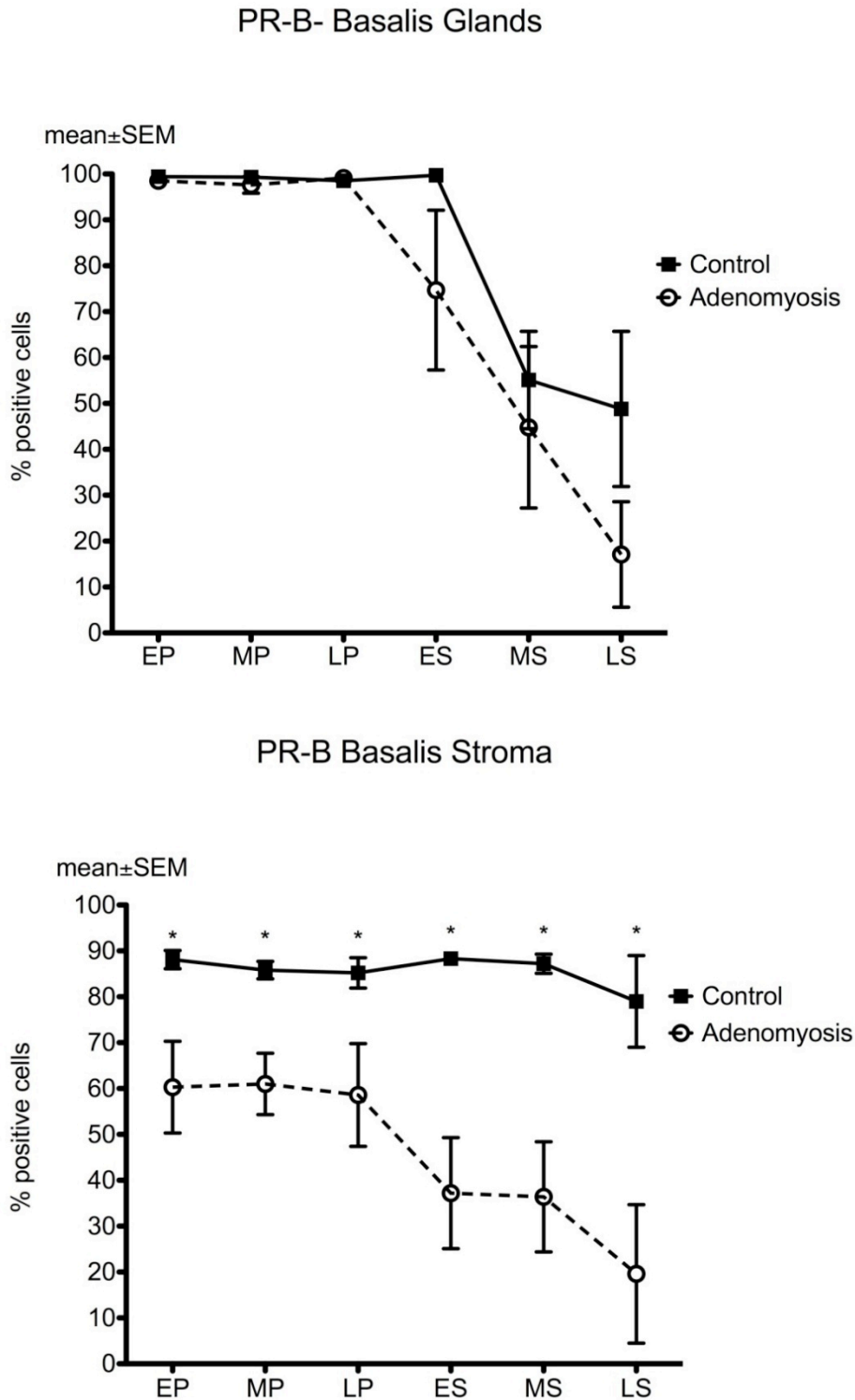


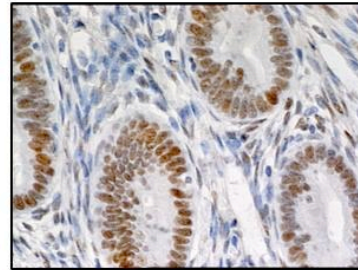
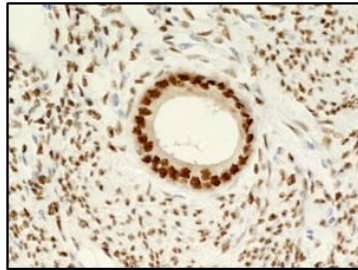
Figure 6.25: Progesterone receptor B distribution in the basalis (glands and stroma) in the different phases of the menstrual cycle (magnification x20).

**PR-B -  
Basalis**

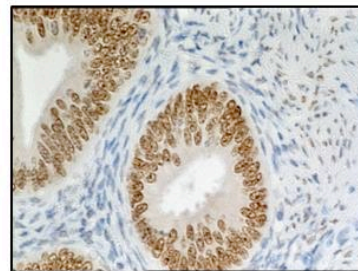
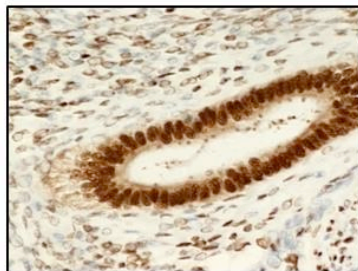
**Control**

**Adenomyosis**

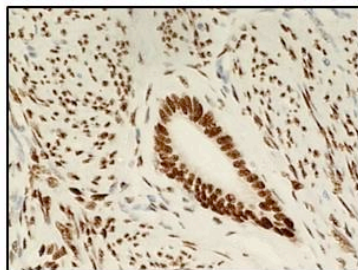
**EP**



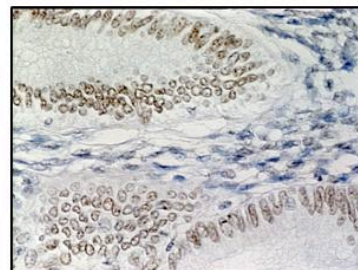
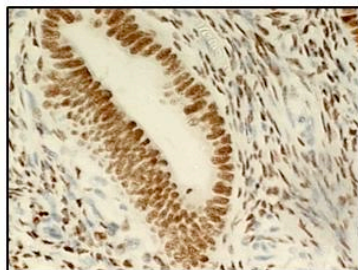
**MP**



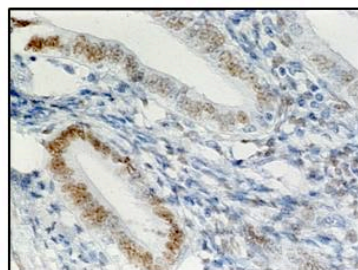
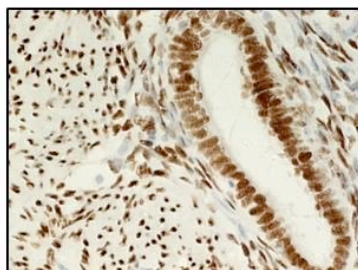
**LP**



**ES**



**MS**



**LS**

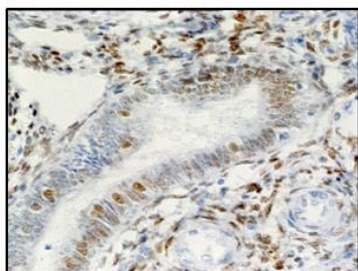
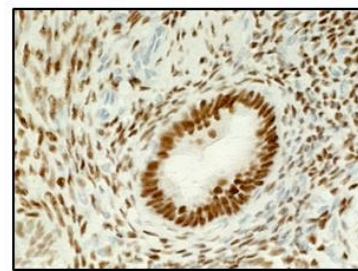


**Figure 6.26: Progesterone receptor B distribution in the myometrium (inner and outer) in the different phases of the menstrual cycle. Immunohistochemical staining expressed as percentage of positively stained cells per high power field (mean  $\pm$  SEM) (\* significant difference between adenomyosis and controls,  $P < 0.05$ ).**

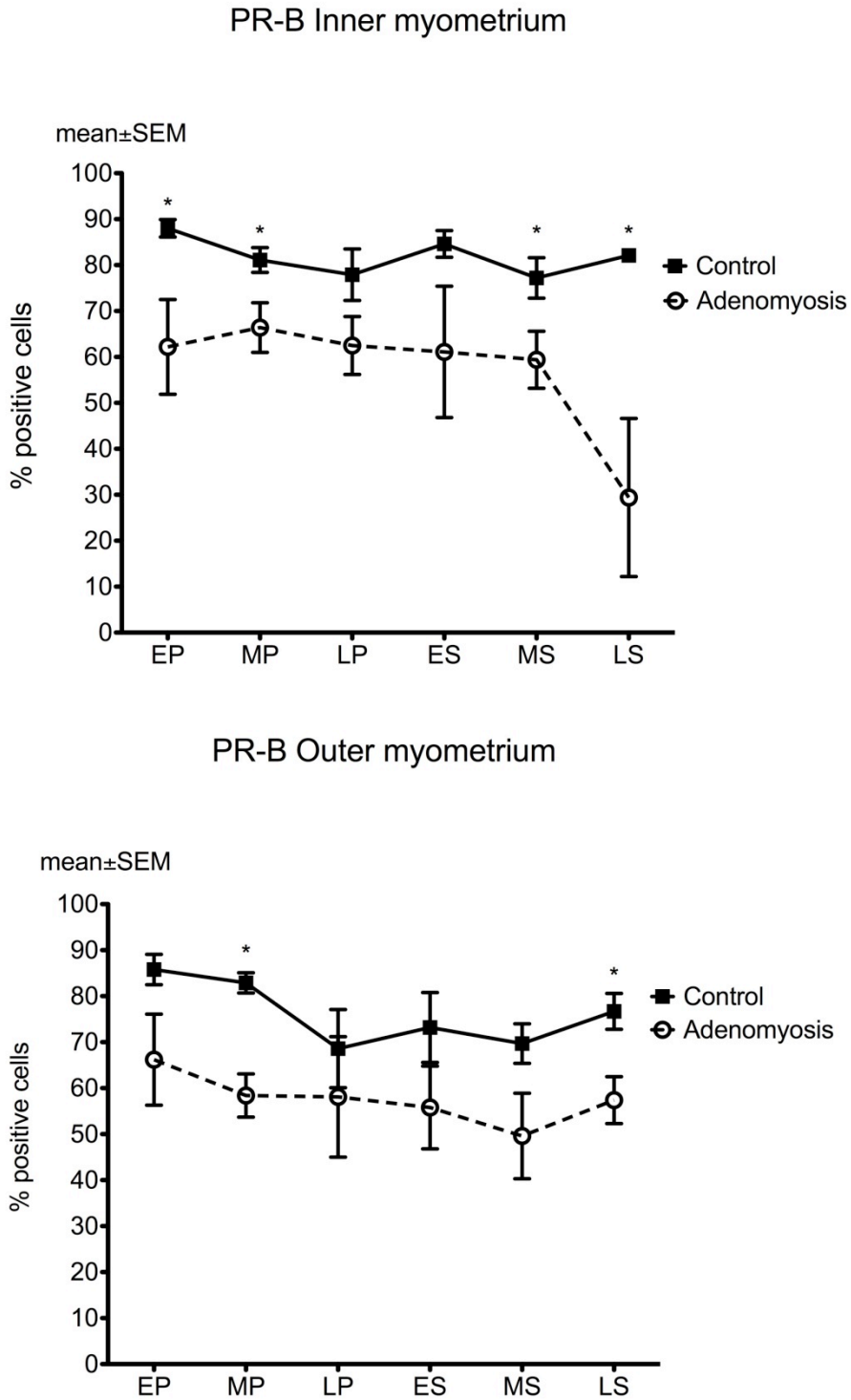


Figure 6.27: Progesterone receptor B distribution in the inner myometrium in the different phases of the menstrual cycle (magnification x20).

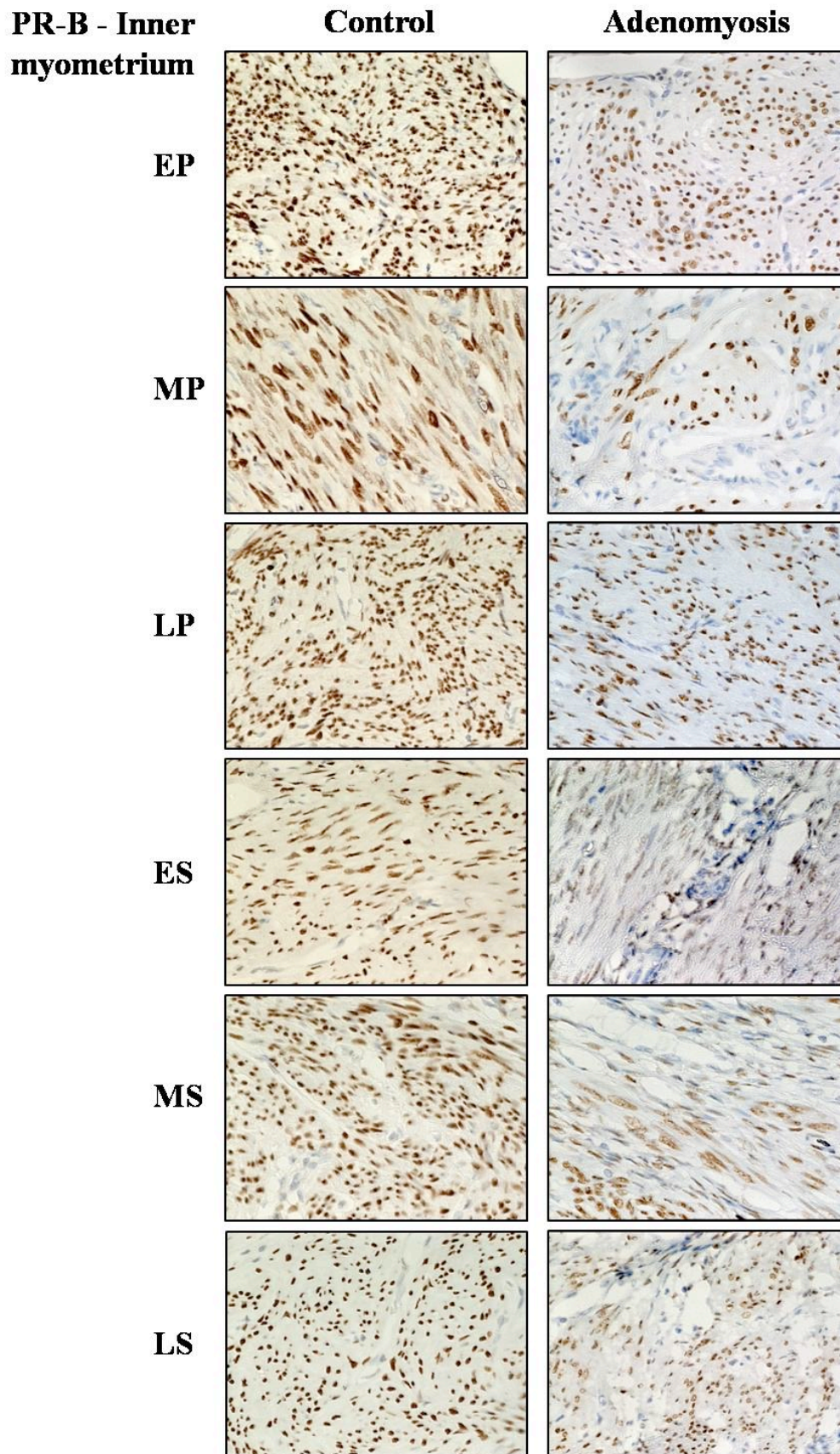
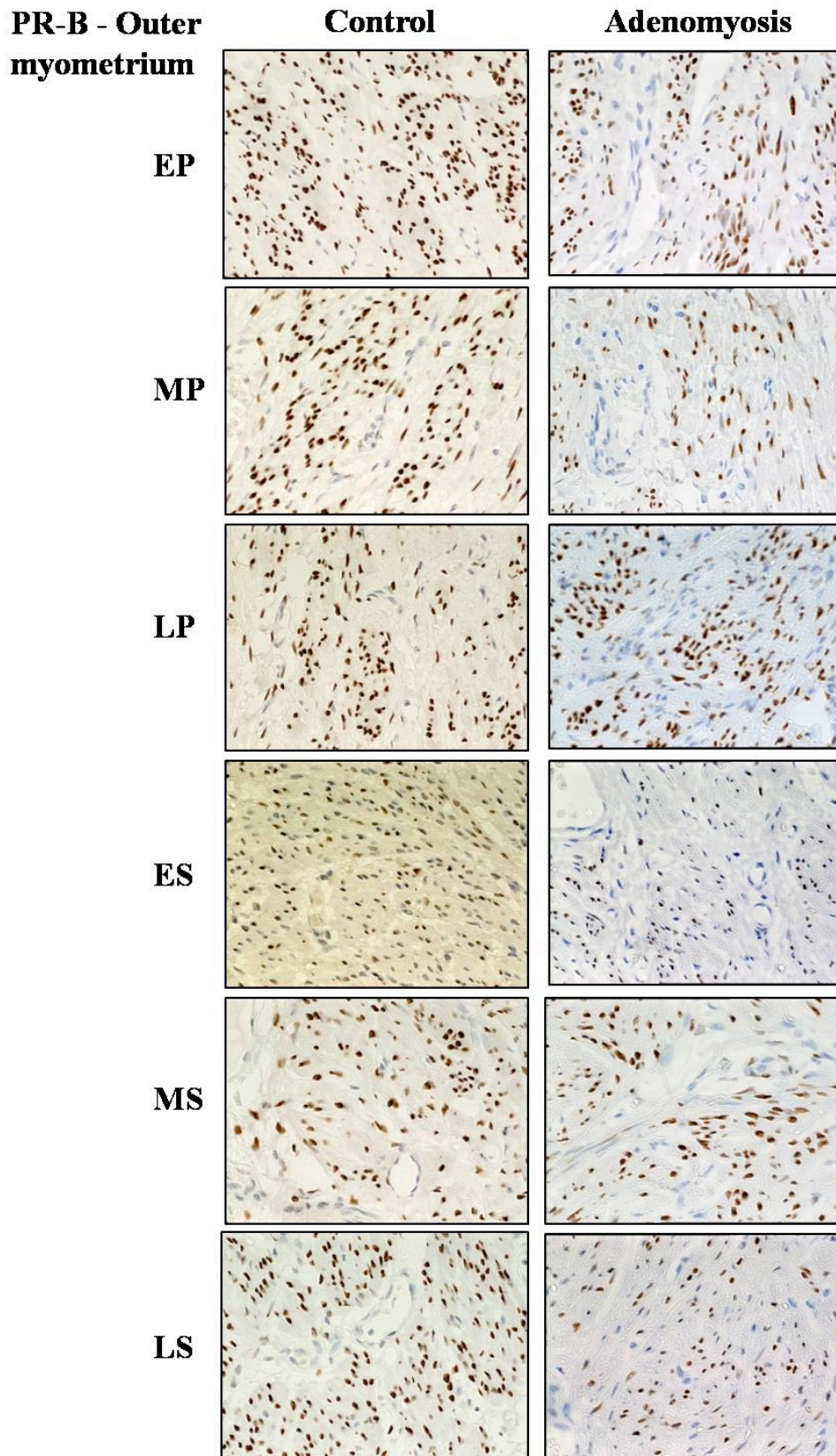
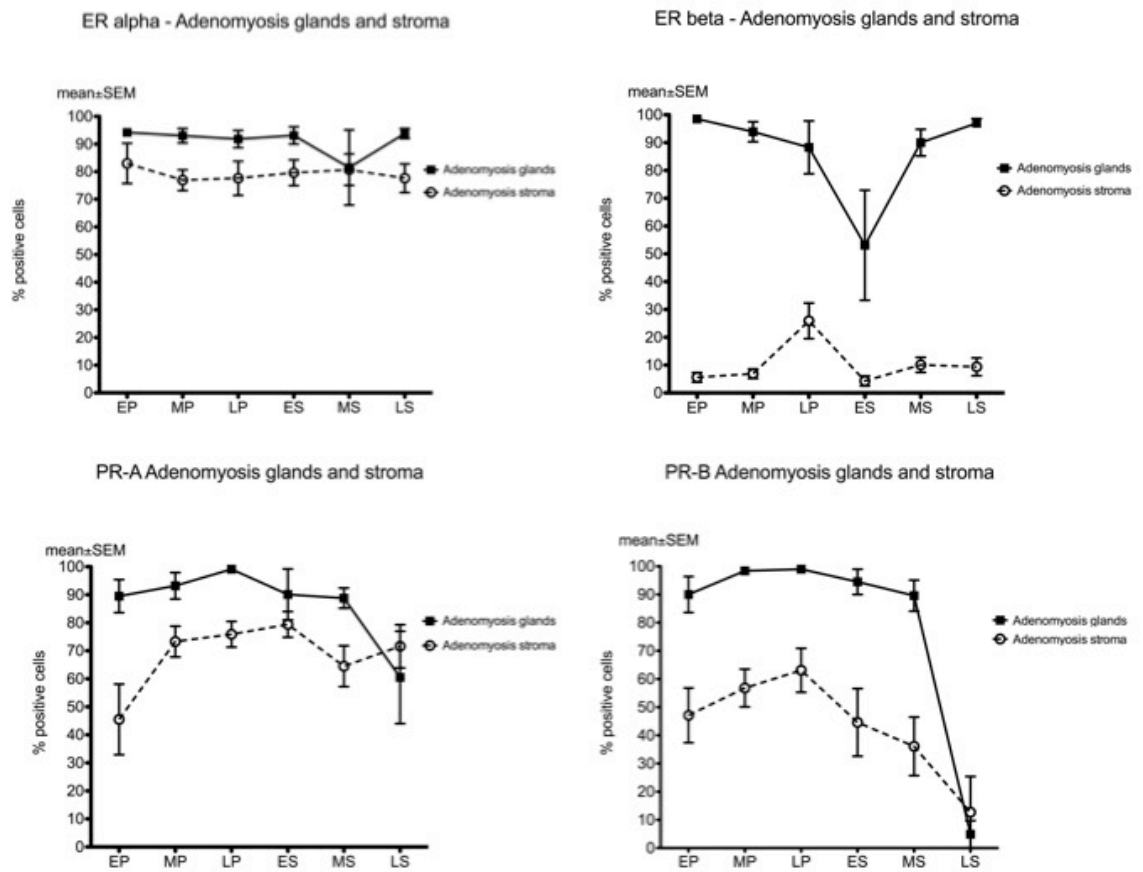


Figure 6.28: Progesterone receptor B distribution in the outer myometrium in the different phases of the menstrual cycle (magnification x20).



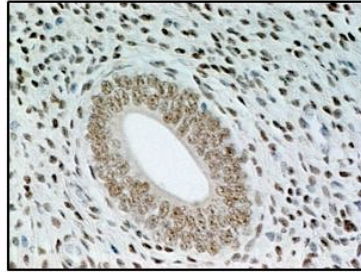
**Figure 6.29: Estrogen and Progesterone receptors distribution in the adenomyosis foci (glands and stroma) in the different phases of the menstrual cycle. Immunohistochemical staining expressed as percentage of positively stained cells per high power field (mean  $\pm$  SEM).**



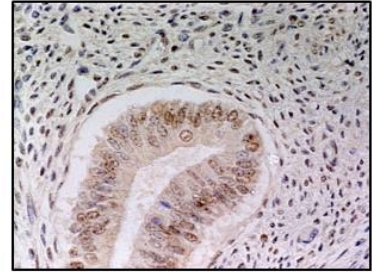
**Figure 6.30: Estrogen receptor alpha distribution in the adenomyosis foci (glands and stroma) in the different phases of the menstrual cycle (magnification x20).**

**ER-alpha -  
Adenomyosis  
foci**

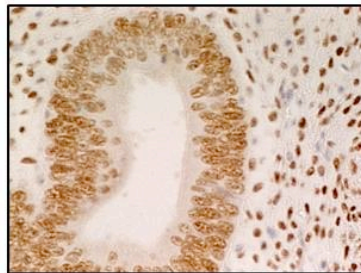
**EP**



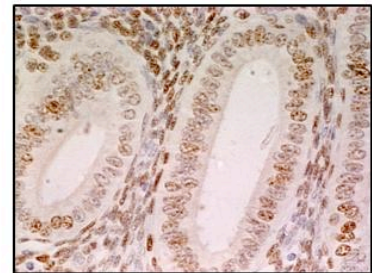
**ES**



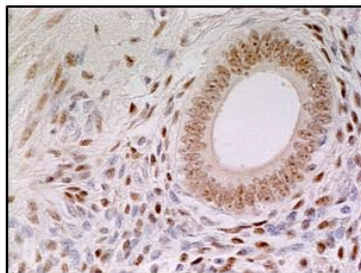
**MP**



**MS**



**LP**



**LS**

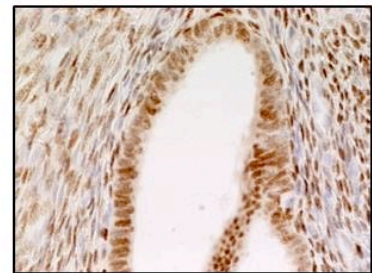
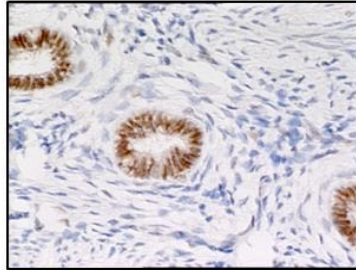


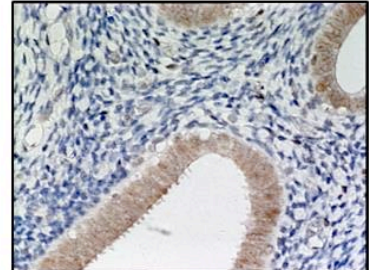
Figure 6.31: Estrogen receptor beta distribution in the adenomyosis foci (glands and stroma) in the different phases of the menstrual cycle (magnification x20).

**ER-beta -  
Adenomyosis  
foci**

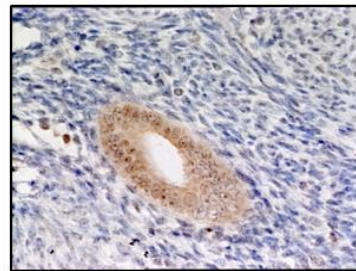
**EP**



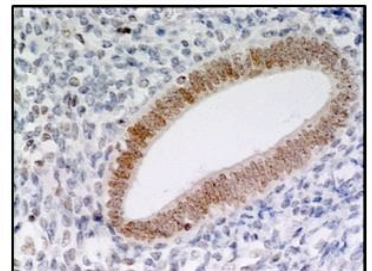
**ES**



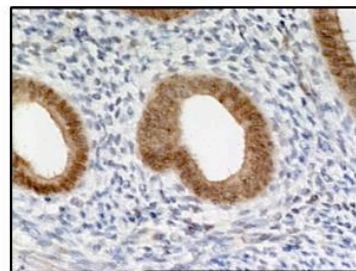
**MP**



**MS**



**LP**



**LS**



**Figure 6.32: Progesterone receptor A distribution in the adenomyosis foci (glands and stroma) in the different phases of the menstrual cycle (magnification x20).**

**PR-A -  
Adenomyosis  
foci**

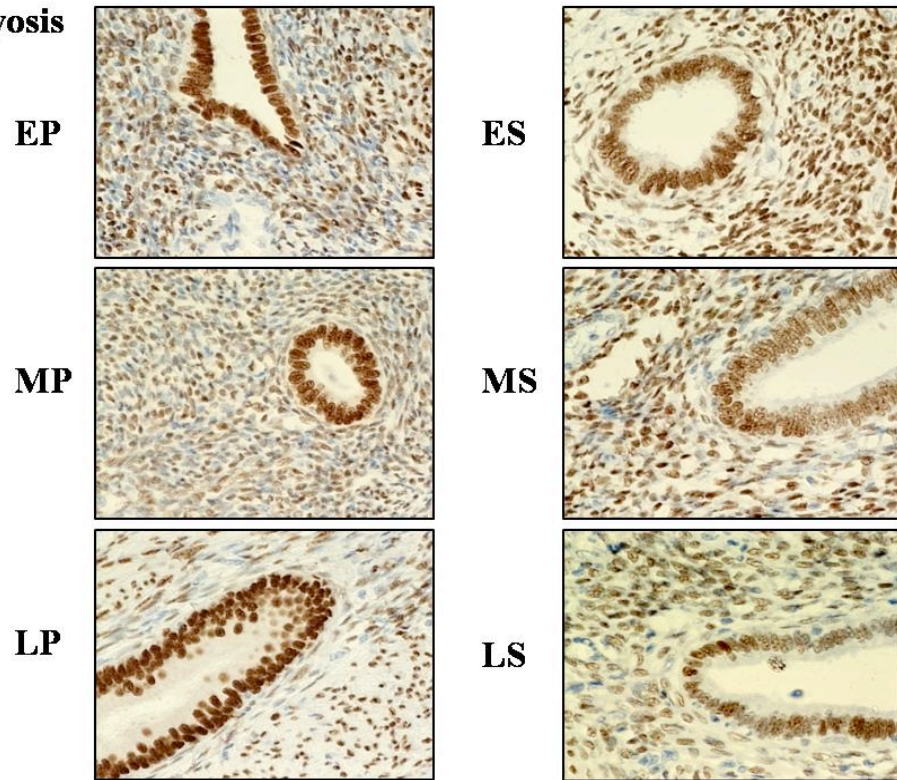
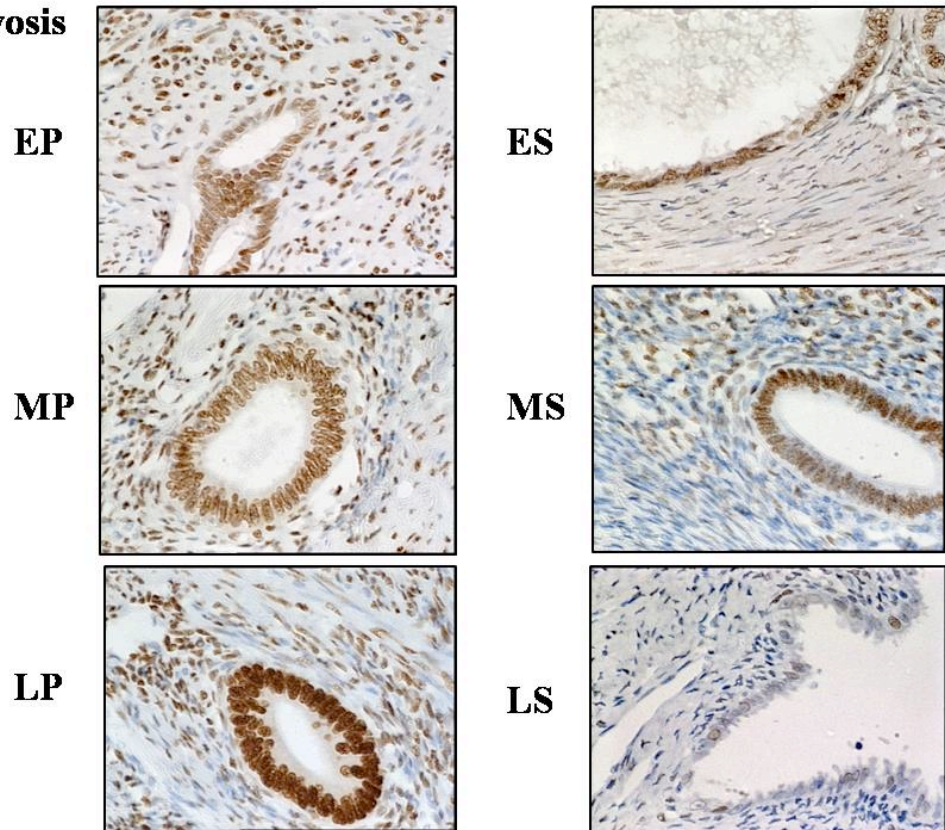


**Figure 6.33: Progesterone receptor B distribution in the adenomyosis foci (glands and stroma) in the different phases of the menstrual cycle (magnification x20).**

**PR-B -  
Adenomyosis  
foci**



## **APPENDIX 2**

### **Additional tables for Chapter 7**

#### **Microarray analysis comparison of the inner and outer myometrium in uteri with and without adenomyosis**

**Table 7.1: Top 25 down-regulated genes in the inner myometrium of adenomyotic uteri (compared to controls), in the proliferative phase, with associated gene ontology**

Symbol	Gene ID	Fold changes	Chromosome	Definition	Synonyms	Ontology Component	Ontology process	Ontology function
<b>ELMOD1</b>	55531	-8	11	ELMO/CED-12 domain containing 1 (ELMOD1)	DKFZp547C176	Cytoskeleton	Phagocytosis	
<b>FOXL2</b>	668	-7	3	Forkhead box L2 (FOXL2)	BPES1; PINTO; BPES; POF3; PFRK	Nucleus	Ovarian follicle development; positive regulation of apoptosis; DNA fragmentation during apoptosis; positive regulation of transcription, DNA-dependent; transcription; cell differentiation	Sequence-specific DNA binding; transcription factor activity; protein binding
<b>SH3GL3</b>	6457	-6	15	SH3-domain GRB2-like 3 (SH3GL3)	SH3D2C; EEN-2B-L3; HsT19371; CNSA3; EEN-B2; SH3P13	Cytoplasm	Central nervous system development; signal transduction	
<b>LOC401089</b>	401089	-5	3	FLJ43329 protein (LOC401089)				
<b>TFAP2C</b>	7022	-5	20	Transcription factor AP-2 gamma (activating enhancer binding protein 2 gamma) (TFAP2C)	AP2-GAMMA; TFAP2G; hAP-2g; ERF1	Nucleus	Transcription; cell-cell signaling; regulation of transcription from RNA polymerase II promoter	Protein dimerization activity; transcription factor activity
<b>KRT8</b>	3856	-4	12	Keratin 8 (KRT8)	CYK8; KO; K8; K2C8; CK8; CARD2	Intermediate filament	Cytoskeleton organization and biogenesis	Structural molecule activity; protein binding
<b>NELL2</b>	4753	-4	12	NEL-like 2 (chicken) (NELL2)	NRP2	Extracellular region	Cell adhesion	Structural molecule activity; calcium ion binding; protein binding
		-4		full length insert cDNA clone ZB55F04				

**Cont.**

**Table 7.1: Top 25 down-regulated genes in the inner myometrium of adenomyotic uteri in the proliferative phase (cont.)**

Symbol	Gene ID	Fold changes	Chromosome	Definition	Synonyms	Ontology Component	Ontology process	Ontology function
<b>PSD</b>	5662	-4	10	pleckstrin and Sec7 domain containing (PSD)	KIAA2011; TYL	Intracellular	Signal transduction	ARF guanyl-nucleotide exchange factor activity; signal transducer activity
		-3		BX089019 Soares_testis_NHT cDNA clone IMAGp998K243513 ; IMAGE:1391375, mRNA sequence				
		-3		PREDICTED: LOC440151 (LOC440151), mRNA				
<b>CCL21</b>	6366	-3	9	Chemokine (C-C motif) ligand 21 (CCL21)	MGC34555; 6Ckine; TCA4; SLC; ECL; CKb9; SCYA21	Extracellular region; extracellular space	Immune response; cell-cell 232ignalling; chemotaxis; signal transduction; inflammatory response 6954] [pmid 9235955]	Chemokine activity
<b>WNT2</b>	7472	-3	7	Wingless-type MMTV integration site family member 2 (WNT2)	IRP; INT1L1	Extracellular region	Development; frizzled-2 signaling pathway	Extracellular matrix structural constituent; signal transducer activity
<b>KCNN2</b>	3781	-3	5	Potassium intermediate/small conductance calcium-activated channel, subfamily N, member 2 (KCNN2), transcript variant 1	Kca2.2; SKCA2; SK2; hSK2	Membrane; integral to membrane	Ion transport; potassium ion transport	Calmodulin binding; small conductance calcium-activated potassium channel activity; ion channel activity; calcium-activated potassium channel activity
<b>AGMAT</b>	79814	-3	1	Agmatine 232ignalling232ses (agmatinase) (AGMAT)	FLJ23384	Mitochondrion	Arginine catabolism; putrescine biosynthesis; spermidine biosynthesis	Hydrolase activity; arginase activity; manganese ion binding; metal ion binding; agmatinase activity
<b>IGFBP2</b>	3485	-3	2	Insulin-like growth factor binding protein 2, 36kDa (IGFBP2)	IGF-BP53; IBP2	Extracellular region; extracellular space	Regulation of cell growth	Insulin-like growth factor binding
<b>OLFML2B</b>	25903	-3	1	olfactomedin-like 2B (OLFML2B)	RP11-227F8.1; MGC51337	Membrane		latrotoxin receptor activity
<b>LOC389457</b>	389457	-3	7	PREDICTED: hypothetical protein LOC389457 (LOC389457)				

**Cont.**

**Table 7.1: Top 25 down-regulated genes in the inner myometrium of adenomyotic uteri in the proliferative phase (cont.)**

Symbol	Gene ID	Fold changes	Chromosome	Definition	Synonyms	Ontology Component	Ontology process	Ontology function
<b>FABP5</b>	2171	-3	8	Fatty acid binding protein 5 (psoriasis-associated) (FABP5)	PA-FABP; PAFABP; E-FABP; EFABP	Cytoplasm	Transport; lipid metabolism; epidermis development	Fatty acid binding; protein binding
<b>WNT5A</b>	7474	-2	3	Wingless-type MMTV integration site family, member 5A (WNT5A)	hWNT5A	Extracellular region; extracellular space; soluble fraction	Morphogenesis; cell-cell signalling; signal transduction; frizzled-2 signaling pathway	Receptor binding; signal transducer activity
<b>SCUBE2</b>	57758	-2	11	Signal peptide, CUB domain, EGF-like 2 (SCUBE2)	Cegf1; CEGP1; FLJ16792; MGC133057; FLJ35234; Cegb1			Calcium ion binding
<b>H19</b>		-2	11	H19, imprinted maternally expressed transcript (H19) on chromosome 11.	MGC4485; D11S813E; ASM; ASM1; BWS; PRO2605			
<b>LOC439949</b>	439949	-2		PREDICTED: hypothetical gene supported by AY007155 (LOC439949)				
<b>C5orf23</b>	79614	-2	5	Chromosome 5 open reading frame 23 (C5orf23)	FLJ14054	Protein complex		
<b>SRPK3</b>	26576	-2	X	SFRS protein kinase 3 (SRPK3)	STK23; MGC102944; MSSK1		Protein amino acid phosphorylation	ATP binding; transferase activity; protein serine/threonine kinase activity; nucleotide binding

**Table 7.2: Top 25 up-regulated genes in the inner myometrium of adenomyotic uteri (compared to controls), in the proliferative phase, with associated gene ontology**

Symbol	Gene ID	Fold changes	Chromosome	Definition	Synonyms	Ontology Component	Ontology process	Ontology function
<b>IGSF10</b>	285313	19	3	Immunoglobulin superfamily, member 10 (IGSF10)	FLJ25972; CMF608		Protein amino acid phosphorylation	ATP binding; transferase activity; vascular endothelial growth factor receptor activity
<b>FLT1</b>	2321	8	13	Fms-related tyrosine kinase 1 (vascular endothelial growth factor/vascular permeability factor receptor) (FLT1)	VEGFR1; FLT	Extracellular space; membrane; integral to plasma membrane	Pregnancy; transmembrane receptor protein tyrosine kinase 234ignalling pathway; angiogenesis; positive regulation of cell proliferation; protein amino acid phosphorylation; cell differentiation	Nucleotide binding; receptor activity; transferase activity; ATP binding; vascular endothelial growth factor receptor activity
<b>STAC</b>	6769	6	3	SH3 and cysteine rich domain (STAC)	FLJ32331; STAC1	Soluble fraction	Intracellular 234ignalling cascade	Zinc ion binding; metal ion binding; diacylglycerol binding
<b>PCAF</b>	8850	5	3	p300/CBP-associated factor (PCAF)	GCN5L; GCN5L1; GCN5; P; P/CAF; CAF	Nucleus	Chromatin remodelling; transcription; negative regulation of cell proliferation; regulation of transcription, DNA-dependent; cell cycle; protein amino acid acetylation; cell cycle arrest	Transcription cofactor activity; transferase activity; histone deacetylase binding; N-acetyltransferase activity; histone acetyltransferase activity; protein binding
<b>PTH2R</b>	5746	5	2	Parathyroid hormone 2 receptor (PTH2R)		Integral to plasma membrane; membrane	G-protein coupled receptor protein 234ignalling pathway; signal transduction	Receptor activity; G-protein coupled receptor activity; parathyroid hormone receptor activity
<b>GABRB1</b>	2560	4	4	Gamma-aminobutyric acid (GABA) A receptor, beta 1 (GABRB1)		Integral to plasma membrane; postsynaptic membrane	Ion transport; signal transduction	Ion channel activity; GABA-A receptor activity; extracellular ligand-gated ion channel activity; chloride channel activity; neurotransmitter receptor activity
<b>STEAP4</b>	79689	4	7	STEAP family member 4 (STEAP4)	DKFZp666D049; STAMP2; TIARP; TNFAIP9; FLJ23153	Plasma membrane; integral to plasma membrane	Fat cell differentiation; electron transport	Oxidoreductase activity; iron ion binding; FAD binding

**Cont.**

**Table 7.2: Top 25 up-regulated genes in the inner myometrium of adenomyotic uteri in the proliferative phase (cont.)**

Symbol	Gene ID	Fold changes	Chromosome	Definition	Synonyms	Ontology Component	Ontology process	Ontology function
		4		cDNA FLJ44503 fis, clone UTERU3001158				
<b>ZFH4</b>	79776	4	8	Zinc finger homeobox 4 (ZFH4)	ZHF4; ZFH4; ZFH-4; FLJ20980; FLJ16514	Extracellular region; nucleus; intracellular	Regulation of transcription, DNA-dependent	Sequence-specific DNA binding; transcription factor activity; hormone activity; zinc ion binding; metal ion binding; nucleic acid binding
<b>ERCC6</b>	2074	3	10	Excision repair cross-complementing rodent repair deficiency, complementation group 6 (ERCC6)	CSB; COFS1; COFS; ARMD5; RAD26; CKN2	Nucleus	Transcription; transcription from RNA polymerase II promoter; regulation of transcription, DNA-dependent; DNA repair	RNA polymerase II transcription factor activity; hydrolase activity; nucleotide binding; DNA helicase activity; helicase activity; DNA binding; ATP binding; protein binding
<b>C18orf34</b>	374864	3	18	Chromosome 18 open reading frame 34 (C18orf34)	MGC163407; MGC111498; FLJ44050			
<b>C2</b>	717	3	6	Complement component 2 (C2)	CO2; DKFZp779M0311	Extracellular region; complement component C2 complex	Innate immune response; complement activation, classical pathway	Serine-type endopeptidase activity; peptidase activity; classical-complement-pathway C3/C5 convertase activity
<b>FMO3</b>	2328	3	1	Flavin containing monooxygenase 3 (FMO3), transcript variant 1	FMOII; dJ127D3.1; MGC34400	Integral to membrane; membrane; endoplasmic reticulum; intrinsic to endoplasmic reticulum membrane; microsome	Electron transport	NADP binding; dimethylaniline monooxygenase (N-oxide-forming) activity; monooxygenase activity; FAD binding
<b>SFRP2</b>	6423	3	4	Secreted frizzled-related protein 2 (SFRP2)	SDF-5; FRP-2; SARP1		Cell differentiation; Wnt receptor 235signalling pathway	
<b>KYNU</b>	8942	3	2	Kynureninase (L-kynurenine hydrolase) (KYNU), transcript variant 2		Cytoplasm	NAD biosynthesis; metabolism; tryptophan catabolism	Pyridoxal phosphate binding; hydrolase activity; kynureninase activity; peptidase activity; transaminase activity
<b>ZNF385A</b>	25946	3	12	Zinc finger protein 385A (ZNF385A)	DKFZP586G1122; RZF; HZF; ZFP385; ZNF385	Nucleus; intracellular	Regulation of transcription, DNA-dependent; transcription	Zinc ion binding; metal ion binding ; DNA binding

**Cont.**

**Table 7.2: Top 25 up-regulated genes in the inner myometrium of adenomyotic uteri, in the proliferative phase (cont.)**

Symbol	Gene ID	Fold changes	Chromosome	Definition	Synonyms	Ontology Component	Ontology process	Ontology function
<b>HOXC8</b>	3224	3	12	Homeobox C8 (HOXC8)	HOX3; HOX3A	Nucleus	Regulation of transcription, DNA-dependent; development	Sequence-specific DNA binding; transcription factor activity
<b>LILRB5</b>	10990	3	19	Leukocyte immunoglobulin-like receptor, subfamily B (with TM and ITIM domains), member 5 (LILRB5), transcript variant 2	LIR8; LIR-8; CD85C	Membrane; integral to membrane	Immune response; cell surface receptor linked signal transduction	Transmembrane receptor activity
		3		nad08f05.x1 NCI_CGAP_Pr28 cDNA clone IMAGE:3433088 3, mRNA sequence				
<b>SNX10</b>	29887	2	7	Sorting nexin 10 (SNX10)	MGC33054		Protein transport; intracellular signaling cascade	Phosphoinositide binding; protein binding
<b>PCOLCE2</b>	26577	2	3	Procollagen C-endopeptidase enhancer 2 (PCOLCE2)	PCPE2			Heparin binding
<b>BHLHB5</b>	27319	2	8	Basic helix-loop-helix domain containing, class B, 5 (BHLHB5)	CAGL85; Beta3; TNRC20	Nucleus	Regulation of transcription	Transcription regulator activity
		2		K-EST0187371 L5HLK1 cDNA clone L5HLK1-32-B12 5, mRNA sequence				
<b>HMOX1</b>	3162	2	22	Heme oxygenase (decycling) 1 (HMOX1)	HO-1; bK286B10	Membrane fraction; endoplasmic reticulum; microsome	Positive regulation of I-kappaB kinase/NF-kappaB cascade; heme oxidation	Oxidoreductase activity; metal ion binding; iron ion binding; signal transducer activity; heme oxygenase (decyclizing) activity
<b>PI16</b>	221476	2	6	Peptidase inhibitor 16 (PI16)	MSMBBP; MGC45378; DKFZp586B1817; PSPBP; CRISP9	Extracellular region		

**Table 7.3: Pathways analysis of genes differentially expressed between the inner myometrium of adenomyotic uteri (compared to controls), in the proliferative phase, fulfilling the criteria of  $p < 0.05$  and 2-fold change (all were over-represented)**

<b>PATHWAY</b>	<b>POSITIVE</b>	<b>MEASURED</b>	<b>TOTAL</b>	<b>Z SCORE</b>	<b>FUNCTIONAL HIERARCHY</b>	
<b>Antigen processing and presentation</b>	2	4	90	3.4	Cellular processes	Immune system
<b>Natural killer cell mediated cytotoxicity</b>	2	5	141	2.92	Cellular processes	Immune system
<b>Striated Muscle Contraction</b>	2	6	38	2.56	Physiological processes	
<b>Complement and coagulation cascades</b>	1	2	72	2.4	Cellular processes	Immune system
<b>Renin-angiotensin system</b>	1	2	24	2.4	Cellular processes	Endocrine system
<b>Type II diabetes mellitus</b>	1	2	52	2.4	Human diseases	Metabolic disorders
<b>Cardiac muscle contraction</b>	2	7	91	2.27	Cellular processes	Circulatory system
<b>GPCRs, Class A Rhodopsin-like</b>	2	8	268	2.03	Molecular function	

**Table 7.4: Top 25 down-regulated genes in the inner myometrium of adenomyotic uteri (compared to controls), in the secretory phase, with associated gene ontology**

Symbol	Gene ID	Fold changes	Chromosome	Definition	Synonyms	Ontology Component	Ontology process	Ontology function
<b>SLC3A1</b>	6519	-15	2	Solute carrier family 3 (cystine, dibasic and neutral amino acid transporters, activator of cystine, dibasic and neutral amino acid transport), member 1 (SLC3A1)	NBAT; CSNU1; ATR1; D2H; RBAT; FLJ34681	Membrane fraction; integral to plasma membrane; membrane	Transport; basic amino acid transport; L-cystine transport; carbohydrate metabolism; amino acid metabolism	L-cystine transporter activity; basic amino acid transporter activity; catalytic activity
<b>KRT86</b>	3892	-12	12	Keratin 86 (KRT86)	hHb6; KRTHB1; Hb1; FLJ25176; KRTHB6; MNX; HB6	Intermediate filament	Cytoskeleton organization and biogenesis	Structural molecule activity
<b>FOXQ1</b>	94234	-9	6	Forkhead box Q1 (FOXQ1)	HFH1	Nucleus	Regulation of transcription, DNA-dependent; transcription	Sequence-specific DNA binding; transcription factor activity
<b>TEKT1</b>	83659	-8	17	Tektin 1 (TEKT1)		Microtubule	Microtubule cytoskeleton organization and biogenesis	Structural molecule activity
<b>PROM1</b>	8842	-6	4	Prominin 1 (PROM1)	AC133; MSTP061; PROML1; CD133	Integral to plasma membrane; membrane	Visual perception	
<b>TFAP2C</b>	7022	-6	20	Transcription factor AP-2 gamma (activating enhancer binding protein 2 gamma) (TFAP2C)	AP2-GAMMA; TFAP2G; hAP-2g; ERF1	Nucleus	Transcription; cell-cell signaling; regulation of transcription from RNA polymerase II promoter	Protein dimerization activity; transcription factor activity
<b>PUNC</b>	9543	-5	15	Putative neuronal cell adhesion molecule (PUNC)	HsT18880	Membrane; integral to membrane		
<b>NPTX2</b>	4885	-4	7	Neuronal pentraxin II (NPTX2)	NARP; NP-II; NP2		Synaptic transmission	Sugar binding; calcium ion binding

**Cont.**

**Table 7.4: Top 25 down-regulated genes in the inner myometrium of adenomyotic uteri in the secretory phase (cont.)**

Symbol	Gene ID	Fold changes	Chromosome	Definition	Synonyms	Ontology Component	Ontology process	Ontology function
<b>OGDHL</b>	55753	-4	10	Oxoglutarate dehydrogenase-like (OGDHL)			Metabolism; glycolysis	Thiamin pyrophosphate binding; oxoglutarate dehydrogenase (succinyl-transferring) activity
<b>F3</b>	2152	-4	1	Coagulation factor III (thromboplastin, tissue factor) (F3)	TF; TFA; CD142	Plasma membrane; integral to membrane	Immune response; blood coagulation	Transmembrane receptor activity
<b>CD24</b>	934	-3	Y	CD24 molecule (CD24)	CD24A	Plasma membrane	Humoral immune response	GPI anchor binding
<b>MSTN</b>	2660	-3	2	Myostatin (MSTN)	GDF8	Extracellular space	Growth; muscle development; transforming growth factor beta receptor 239ignalling pathway	Cytokine activity; growth factor activity
<b>RBM24</b>	221662	-3	6	RNA binding motif protein 24 (RBM24)	FLJ37697; RNPC6; FLJ30829; dJ259A10.1; FLJ26355			RNA binding; nucleotide binding
<b>KIAA1199</b>	57214	-3	15	KIAA1199 (KIAA1199)	TMEM2L; CCSP1			
<b>LOC401089</b>	401089	-3	3	FLJ43329 protein (LOC401089)				
<b>WNT5A</b>	7474	-3	3	Wingless-type MMTV integration site family, member 5A (WNT5A)	hWNT5A	Extracellular region; extracellular space; soluble fraction	Morphogenesis; cell-cell 239ignalling; signal transduction; frizzled-2 signaling pathway	Receptor binding; signal transducer activity
		-3		MSTP131 (MST131) mRNA, complete cds				
		-3		cDNA FLJ20012 fis, clone ADKA03438				
<b>CYP3A5</b>	1577	-3	7	Cytochrome P450, family 3, subfamily A, polypeptide 5 (CYP3A5)	CP35; PCN3; P450PCN3	Membrane fraction; membrane; endoplasmic reticulum; microsome	Xenobiotic metabolism; steroid metabolism; electron transport	Heme binding; metal ion binding; unspecific monooxygenase activity; iron ion binding; oxygen binding; monooxygenase activity
<b>WNT2</b>	7472	-2	7	Wingless-type MMTV integration site family member 2 (WNT2)	IRP; INT1L1	Extracellular region	Development; frizzled-2 signaling pathway	Extracellular matrix structural constituent; signal transducer activity

**Cont.**

**Table 7.4: Top 25 down-regulated genes in the inner myometrium of adenomyotic uteri in the secretory phase (cont.)**

Symbol	Gene ID	Fold changes	Chromosome	Definition	Synonyms	Ontology Component	Ontology process	Ontology function
<b>LOC387934</b>	387934	-2		PREDICTED: similar to Fatty acid-binding protein, epidermal (E-FABP) (Psoriasis-associated fatty acid-binding protein homolog) (PA-FABP) (LOC387934)				
<b>SLC18A2</b>	6571	-2	10	Solute carrier family 18 (vesicular monoamine), member 2 (SLC18A2)	VAT2; MGC120477; SVAT; MGC26538; SVMT; VMAT2; MGC120478	Membrane; integral to plasma membrane; membrane fraction	Monoamine transport	Transporter activity; monoamine transporter activity
<b>PSD</b>	5662	-2	10	Pleckstrin and Sec7 domain containing (PSD)	KIAA2011; TYL	Intracellular	Signal transduction	ARF guanyl-nucleotide exchange factor activity; signal transducer activity
<b>NDP</b>	4693	-2	X	Norrie disease (pseudoglioma) (NDP)	EVR2; ND; FEVR	Extracellular space	Visual perception; cell-cell signaling; cell proliferation; vacuole organization and biogenesis; signal transduction	Growth factor activity
<b>SLC46A2</b>	57864	-2	9	Solute carrier family 46, member 2 (SLC46A2)	Ly110; TSCOT	Membrane; integral to membrane	Tetracycline transport; transport	Symporter activity; tetracycline:hydrogen antiporter activity

**Table 7.5: Top 16 up-regulated genes in the inner myometrium of adenomyotic uteri (compared to controls), in the secretory phase, with associated gene ontology**

Symbol	Gene ID	Fold changes	Chromosome	Definition	Synonyms	Ontology Component	Ontology process	Ontology function
<b>GLDN</b>	342035	10	15	Gliomedin (GLDN)	CRG-L2; UNC-112; CRGL2; CLOM; FLJ23917; COLM	Membrane; integral to membrane; cytoplasm	Cell differentiation; phosphate transport	
<b>PRPH</b>	5630	3	12	Peripherin (PRPH)	PRPH1; NEF4	Intermediate filament		Structural molecule activity
<b>MKX</b>	283078	3	10	Mohawk homeobox (MKX)	MGC39616; IFRX; IRXL1; C10orf48			
<b>PI16</b>	221476	3	6	Peptidase inhibitor 16 (PI16)	MSMBBP; MGC45378; DKFZp586B1817; PSPBP; CRISP9	Extracellular region		
<b>MYOT</b>	9499	3	5	Myotilin (MYOT)	LGMD1A; LGMD1; TTID	Actin cytoskeleton	Muscle contraction	Structural constituent of muscle; actin binding; protein binding
		3		nj92b10.x5 NCI_CGAP_Pr11 cDNA clone IMAGE:999931, mRNA sequence				
		2		cDNA FLJ37610 fis, clone BRCOC2011398				
<b>MAL</b>	4118	2	2	Mal, T-cell differentiation protein (MAL), transcript variant a		Lipid raft; insoluble fraction; membrane fraction; integral to plasma membrane; membrane; endoplasmic reticulum; apical plasma membrane; endosome	Apical protein localization; induction of apoptosis; lipid raft polarization; signal transduction; cell differentiation; central nervous system development; myelination	Apoptotic protease activator activity; structural constituent of myelin sheath; channel or pore class transporter activity; lipid binding
<b>LOC651268</b>	651268	2		PREDICTED: similar to protein phosphatase 1, regulatory (inhibitor) subunit 9A (LOC651268)				
<b>PDZRN4</b>	29951	2	12	PDZ domain containing RING finger 4 (PDZRN4)	SAMCAP3L; LNX4			Protein binding; metal ion binding; zinc ion binding
<b>FHL5</b>	9457	2	6	Four and a half LIM domains 5 (FHL5)	FLJ33049; dJ393D12.2; KIAA0776; ACT; RP3-393D12.2	Nucleus		Zinc ion binding; metal ion binding
<b>NTF3</b>	4908	2	12	Neurotrophin 3 (NTF3)	HDNF; NGF-2; NT3; NGF2; MGC129711		Anti-apoptosis; cell motility; cell-cell signaling; signal transduction	Growth factor activity

**Cont.**

**Table 7.5: Top 16 up-regulated genes in the inner myometrium of adenomyotic uteri in the secretory phase (cont.)**

Symbol	Gene ID	Fold changes	Chromosome	Definition	Synonyms	Ontology Component	Ontology process	Ontology function
<b>SNCG</b>	6623	2	10	Synuclein, gamma (breast cancer-specific protein 1) (SNCG)	BCSG1; SR	Cytoplasm		
<b>LOC196549</b>	196549	2	13	Similar to hypothetical protein FLJ20897 (LOC196549)				
<b>LPHN3</b>	23284	2	4	Latrophilin 3 (LPHN3)	LEC3; CIRL3	Integral to membrane; membrane	Neuropeptide signaling pathway; signal transduction	Latrotoxin receptor activity; receptor activity; G-protein coupled receptor activity; sugar binding
		2		cDNA FLJ37384 fis, clone BRAMY2026347				

**Table 7.6: Pathways analysis of genes differentially expressed between the inner myometrium of adenomyotic uteri (compared to controls), in the secretory phase, fulfilling the criteria of  $p < 0.05$  and 2-fold change.**

<b>PATHWAY</b>	<b>POSITIVE</b>	<b>MEASURED</b>	<b>TOTAL</b>	<b>Z SCORE</b>	<b>FUNCTIONAL HIERARCHY</b>	
<b><u>PATHWAYS WITH OVER-REPRESENTED GENES</u></b>						
Olfactory transduction	61	154	388	9.15	Cellular processes	Sensory system
Nuclear receptors in lipid metabolism and toxicity	9	19	43	3.91	Metabolic processes	
Graft-versus-host disease	4	6	45	3.5	Human diseases	Immune disorders
Bladder cancer	2	2	42	3.33	Human diseases	Cancers
gamma-Hexachlorocyclohexane degradation	2	2	85	3.33	Metabolism	Xenobiotics biodegradation and metabolism
Hypertrophy Model	2	2	21	3.33	Physiological processes	
IL-1 Signalling Pathway	2	2	39	3.33	Cellular processes	
Hematopoietic cell lineage	4	8	90	2.73	Cellular processes	Immune system
Focal Adhesion	1	1	190	2.35	Cellular processes	Cell communication
Notch Signaling Pathway	1	1	47	2.35	Environmental information processing	Signal transduction
Synthesis and degradation of ketone bodies	1	1	16	2.35	Metabolism	Lipid metabolism
Drug metabolism - cytochrome P450	4	10	161	2.18	Metabolism	Xenobiotics biodegradation and metabolism
Retinol metabolism	5	14	95	2.13	Metabolism	Metabolism of cofactors and vitamins
Metapathway biotransformation	13	52	188	1.99	Metabolic processes	

**Cont.**

**Table 7.6: Pathways analysis of genes differentially expressed between the inner myometrium of adenomyotic uteri (compared to controls), in the secretory phase, fulfilling the criteria of  $p < 0.05$  and 2-fold change (cont.)**

PATHWAY	POSITIVE	MEASURED	TOTAL	Z SCORE	FUNCTIONAL HIERARCHY	
<b><u>PATHWAYS WITH UNDER-REPRESENTED GENES</u></b>						
Pathways in cancer	1	34	344	-2.04	Human diseases	Cancers
Insulin signaling pathway	0	23	143	-2.06	Cellular processes	Endocrine system
Basal transcription factors	0	24	38	-2.11	Genetic information processing	Transcription
Alzheimer's disease	3	56	186	-2.13	Human diseases	Neurodegenerative diseases
N-Glycan biosynthesis	0	26	82	-2.2	Metabolism	Glycan biosynthesis and metabolism
Proteasome	0	35	52	-2.56	Genetic information processing	Folding sorting and degradation
Oxidative phosphorylation	0	36	68	-2.6	Metabolism	Energy metabolism
Proteasome Degradation	0	37	66	-2.64	Physiological processes	
Parkinson's disease	0	42	150	-2.82	Human diseases	Neurodegenerative diseases
Electron Transport Chain	0	44	116	-2.89	Metabolic processes	
Oxidative phosphorylation	2	67	237	-2.91	Metabolism	Energy metabolism
Huntington's disease	0	51	192	-3.12	Human diseases	Neurodegenerative diseases

**Table 7.7: Top 25 down-regulated genes in the outer myometrium of adenomyotic uteri (compared to controls), in the proliferative phase, with associated gene ontology**

Symbol	Gene ID	Fold changes	Chromosome	Definition	Synonyms	Ontology Component	Ontology process	Ontology function
<b>SERPINA5</b>	5104	-23	14	Serpin peptidase inhibitor, clade A (alpha-1 antiproteinase, antitrypsin), member 5 (SERPINA5)	PROCI; PAI3; PLANH3; PCI	Extracellular region; protein complex; membrane	Spermatogenesis; fusion of sperm to egg plasma membrane	Serine-type endopeptidase inhibitor activity; heparin binding
<b>GABRP</b>	2568	-18	5	Gamma-aminobutyric acid (GABA) A receptor, pi (GABRP)	MGC126386; MGC126387	Integral to membrane; postsynaptic membrane	Ion transport	Ion channel activity; GABA-A receptor activity; extracellular ligand-gated ion channel activity; chloride channel activity; neurotransmitter receptor activity
<b>LOC651957</b>	651957	-18		PREDICTED: hypothetical protein LOC651957 (LOC651957)				
<b>UGT2B7</b>	7364	-17		PREDICTED: UDP glucuronosyltransferase 2 family, polypeptide B7 (UGT2B7)				
<b>PRSS8</b>	5652	-17	16	Protease, serine, 8 (PRSS8)	PROSTASIN; CAP1	Plasma membrane; integral to membrane; extracellular region; extracellular space		Serine-type endopeptidase activity
<b>IGFN1</b>	91156	-17	1	Immunoglobulin-like and fibronectin type III domain containing 1 (IGFN1)	EEF1A2BP1; DKFZp434B1231			
<b>ASRGL1</b>	80150	-16	11	Asparaginase like 1 (ASRGL1)	ALP1; ALP; FLJ22316		Glycoprotein catabolism	Asparaginase activity
<b>SPDEF</b>	25803	-16	6	SAM pointed domain containing ets transcription factor (SPDEF)	bA375E1.3; PDEF; RP11-375E1__A.3	Nucleus	Regulation of transcription, DNA-dependent; development; transcription	Sequence-specific DNA binding; transcription factor activity; protein binding
		-12		7h36b03.x1 NCI_CGAP_Co16 cDNA clone IMAGE:3318029 3, mRNA sequence				
<b>CDH1</b>	999	-11	16	Cadherin 1, type 1, E-cadherin (epithelial) (CDH1)	CDHE; Arc-1; UVO; CD324; ECAD; LCAM	Membrane; integral to membrane	Homophilic cell adhesion; cell adhesion	Calcium ion binding; protein binding
<b>ABTB2</b>	25841	-11	11	Ankyrin repeat and BTB (POZ) domain containing 2 (ABTB2)	DKEFZP586C1619	Nucleus; nucleosome	Nucleosome assembly; chromosome organization and biogenesis (sensu Eukaryota); regulation of cell growth	DNA binding; protein binding

**Cont.**

**Table 7.7: Top 25 down-regulated genes in the outer myometrium of adenomyotic uteri (compared to controls), in the proliferative phase (cont.)**

Symbol	Gene ID	Fold changes	Chromosome	Definition	Synonyms	Ontology Component	Ontology process	Ontology function
<b>FOXL2</b>	668	-11	3	Forkhead box L2 (FOXL2)	BPES1; PINTO; BPES; POF3; PFRK	Nucleus	Ovarian follicle development; positive regulation of apoptosis; DNA fragmentation during apoptosis; positive regulation of transcription, DNA-dependent; transcription; cell differentiation	Sequence-specific DNA binding; transcription factor activity; protein binding
<b>LOC728811</b>	728811	-11	4	PREDICTED: similar to UDP glycosyltransferase 2 family, polypeptide B17 (LOC728811)				
<b>C1orf64</b>	149563	-10	1	Chromosome 1 open reading frame 64 (C1orf64)	RP11-5P18.4; MGC24047			
		-10		hx79b12.x1 NCI_CGAP_Kid11 cDNA clone IMAGE:3194015 3, mRNA sequence				
<b>EDN3</b>	1908	-10	20	Endothelin 3 (EDN3), transcript variant 3	MGC61498; MGC15067; ET3	Extracellular region; soluble fraction	Morphogenesis; regulation of vasoconstriction; pathogenesis; cell-cell 246ignalling; signal transduction	Receptor binding
<b>CDCA7</b>	83879	-8	2	Cell division cycle associated 7 (CDCA7), transcript variant 1	MGC34109; JPO1; FLJ14736; FLJ14722	Nucleus	Regulation of cell proliferation; regulation of transcription, DNA-dependent; transcription	
<b>KLK4</b>	9622	-8	19	Kallikrein-related peptidase 4 (KLK4)	PSTS; MGC116827; KLK-L1; ARM1; PRSS17; MGC116828; EMSP; EMSP1	Extracellular region		Serine-type endopeptidase activity [4252]
<b>SPINT2</b>	10653	-8	19	Serine peptidase inhibitor, Kunitz type, 2 (SPINT2)	Kop; PB; HAI-2; HAI2	Membrane; extracellular region; integral to membrane; soluble fraction	Cell motility	Serine-type endopeptidase inhibitor activity
<b>WNT4</b>	54361	-8	1	Wingless-type MMTV integration site family, member 4 (WNT4)	WNT-4	Extracellular region	Development; cell-cell 246ignalling; frizzled-2 signaling pathway	Extracellular matrix structural constituent; signal transducer activity

**Cont.**

**Table 7.7: Top 25 down-regulated genes in the outer myometrium of adenomyotic uteri (compared to controls), in the proliferative phase (cont.)**

Symbol	Gene ID	Fold changes	Chromosome	Definition	Synonyms	Ontology Component	Ontology process	Ontology function
<b>ISL1</b>	3670	-7	5	ISL1 transcription factor, LIM/homeodomain, (islet-1) (ISL1)	Isl-1	Nucleus	Regulation of transcription, DNA-dependent; development	Metal ion binding; zinc ion binding; transcription factor activity; sequence-specific DNA binding
<b>TERC</b>		-7	3	Telomerase RNA component (TERC) on chromosome 3.	TRC3; TR; hTR; SCARNA19			
<b>RORB</b>	6096	-7	9	RAR-related orphan receptor B (RORB)	NR1F2; RZRB; bA133M9.1; ROR-BETA	Nucleus	Regulation of transcription, DNA-dependent; transcription	Zinc ion binding; metal ion binding; sequence-specific DNA binding; transcription factor activity; steroid hormone receptor activity; protein binding
<b>LOC199897</b>	199897	-7	1	PREDICTED: hypothetical LOC199897 (LOC199897)				
<b>STRA6</b>	64220	-7	15	Stimulated by retinoic acid gene 6 homolog (mouse) (STRA6)	PP14296; MCOPS9; FLJ12541			

**Table 7.8: Top 25 up-regulated genes in the outer myometrium of adenomyotic uteri (compared to controls), in the proliferative phase, with associated gene ontology**

Symbol	Gene ID	Fold changes	Chromosome	Definition	Synonyms	Ontology Component	Ontology process	Ontology function
<b>LOC644964</b>	644964	145	19	PREDICTED: hypothetical protein LOC644964 (LOC644964)				
<b>PTGES</b>	9536	12	9	Prostaglandin E synthase (PTGES)	mPGES-1; MGST1L1; MGST1-L1; PIG12; TP53112; MGST-IV; PP102; MGC10317; PGES; PP1294	Membrane fraction; membrane; integral to membrane	Prostaglandin metabolism; antimicrobial humoral response (sensu Vertebrata); signal transduction	Prostaglandin-E synthase activity; isomerase activity
<b>C14orf19</b>		11	14	Chromosome 14 open reading frame 19 (C14orf19) on chromosome 14.				
<b>C18orf32</b>	497661	9	18	Chromosome 18 open reading frame 32 (C18orf32)	FLJ23458			
<b>ID4</b>	3400	8	6	Inhibitor of DNA binding 4, dominant negative helix-loop-helix protein (ID4)		Nucleus	Negative regulation of transcription; regulation of transcription from RNA polymerase II promoter	Transcription corepressor activity
<b>COL4A4</b>	1286	8	2	Collagen, type IV, alpha 4 (COL4A4)	CA44	Collagen type IV; collagen; cytoplasm	Phosphate transport; long-term strengthening of neuromuscular junction	Extracellular matrix structural constituent
<b>ZFHX4</b>	79776	8	8	Zinc finger homeobox 4 (ZFHX4)	ZHF4; ZFH4; ZFH-4; FLJ20980; FLJ16514	Extracellular region; nucleus; intracellular	Regulation of transcription, DNA-dependent	Sequence-specific DNA binding; transcription factor activity; hormone activity; zinc ion binding; metal ion binding; nucleic acid binding
<b>SNX10</b>	29887	7	7	Sorting nexin 10 (SNX10)	MGC33054		Protein transport; intracellular signaling cascade	Phosphoinositide binding; protein binding
<b>LOC649801</b>	649801	6		PREDICTED: similar to cell division cycle 10 isoform 1 (LOC649801)				
<b>LOC646706</b>	646706	6	19	PREDICTED: similar to vomeronasal 2, receptor, 14 isoform 1 (LOC646706)				
<b>PPIB</b>	5479	6	15	Peptidylprolyl isomerase B (cyclophilin B) (PPIB)	MGC14109; MGC2224; CYP-S1; SCYLP; CYPB	Endoplasmic reticulum; endoplasmic reticulum lumen	Protein folding	Peptide binding; peptidylprolyl cis-trans isomerase activity; unfolded protein binding; isomerase activity

**Cont.**

**Table 7.8: Top 25 up-regulated genes in the outer myometrium of adenomyotic uteri in the proliferative phase (cont.)**

Symbol	Gene ID	Fold changes	Chromosome	Definition	Synonyms	Ontology Component	Ontology process	Ontology function
<b>CCL19</b>	6363	6	9	Chemokine (C-C motif) ligand 19 (CCL19)	MIP3B; CKb11; MIP-3b; ELC; MGC34433; SCYA19	Extracellular region; extracellular space	Calcium ion homeostasis; inflammatory response; response to virus; signal transduction; chemotaxis	Chemokine activity
<b>AOC3</b>	8639	5	17	Amine oxidase, copper containing 3 (vascular adhesion protein 1) (AOC3)	SSAO; HPAO; VAP-1; VAP1	Plasma membrane; integral to membrane; cell surface	Amine metabolism; cell adhesion; inflammatory response; electron transport	Oxidoreductase activity; protein homodimerization activity; copper ion binding; amine oxidase activity; calcium ion binding; protein binding
<b>LOC402677</b>	402677	5		PREDICTED: similar to 40S ribosomal protein S3a (V-fos transformation effector protein), transcript variant 3 (LOC402677)				
<b>BMP8B</b>	656	5	1	Bone morphogenetic protein 8b (osteogenic protein 2) (BMP8B)	BMP8; MGC131757; OP2	Extracellular region; extracellular space	Ossification; cell differentiation; growth; cartilage development	Cytokine activity; growth factor activity
<b>HSD17B13</b>	345275	5	4	Hydroxysteroid (17-beta) dehydrogenase 13 (HSD17B13)	SCDR9; MGC138508; HMFN0376; NIIL497; MGC138510		Metabolism	Oxidoreductase activity
<b>TTRAP</b>	51567	5	6	TRAF and TNF receptor associated protein (TTRAP)	EAP2; AD022; MGC111021; MGC9099; dJ30M3.3; RP1-30M3.3	Nucleus	Cell surface receptor linked signal transduction	Transcription corepressor activity
<b>PPM2C</b>	54704	4	8	Protein phosphatase 2C, magnesium-dependent, catalytic subunit (PPM2C), nuclear gene encoding mitochondrial protein	PDPC; PDP1; FLJ32517; PDH; PDP; MGC119646	Protein serine/threonine phosphatase complex; mitochondrion	Protein amino acid dephosphorylation	Magnesium ion binding; calcium ion binding; catalytic activity; protein serine/threonine phosphatase activity
<b>TMEM167</b>	153339	4	5	Transmembrane protein 167 (TMEM167)	MGC23909; DKFZp68611152; FLJ30508	Membrane; integral to membrane		
		4		UI-E-EJ1-ajw-e-18-0-UI.r1 UI-E-EJ1 cDNA clone UI-E-EJ1-ajw-e-18-0-UI 5, mRNA sequence				

**Cont.**

**Table 7.8: Top 25 up-regulated genes in the outer myometrium of adenomyotic uteri in the proliferative phase (cont.)**

Symbol	Gene ID	Fold changes	Chromosome	Definition	Synonyms	Ontology Component	Ontology process	Ontology function
<b>ZBTB11</b>	27107	4	3	Zinc finger and BTB domain containing 11 (ZBTB11)	ZNF-U69274; FLJ13426; MGC133303	Nucleus; intracellular	Regulation of transcription, DNA-dependent; transcription	Zinc ion binding; metal ion binding; DNA binding; protein binding
<b>PI16</b>	221476	4	6	Peptidase inhibitor 16 (PI16)	MSMBBP; MGC45378; DKFZp586B1817; PSPBP; CRISP9	Extracellular region		
<b>DOHH</b>	83475	4	19	Deoxyhypusine hydroxylase/monooxygenase (DOHH)	HLRC1; MGC4293		Hypusine biosynthesis from peptidyl-lysine	Metal ion binding; binding; iron ion binding
<b>LPHN3</b>	23284	4	4	Latrophilin 3 (LPHN3)	LEC3; CIRL3	Integral to membrane; membrane	Neuropeptide signaling pathway; signal transduction	Latrotoxin receptor activity; receptor activity; G-protein coupled receptor activity; sugar binding

**Table 7.9: Pathways analysis of genes differentially expressed in the outer myometrium of adenomyotic uteri (compared to controls), in the proliferative phase, fulfilling the criteria of  $p < 0.05$  and 2-fold change**

PATHWAY	POSITIVE	MEASURED	TOTAL	Z SCORE	FUNCTIONAL HIERARCHY	
<b><u>PATHWAYS WITH OVER-REPRESENTED GENES</u></b>						
Olfactory transduction	67	194	388	8.57	Cellular processes	Sensory system
Renin-angiotensin system	3	3	24	4.14	Cellular processes	Endocrine system
Glycolysis / Gluconeogenesis	2	2	112	3.38	Metabolism	Carbohydrate metabolism
GPCRs, Class A Rhodopsin-like	14	45	268	3.12	Molecular function	
Biosynthesis of steroids	2	3	128	2.52	Metabolism	Lipid metabolism
Neuroactive ligand-receptor interaction	8	25	334	2.43	Environmental information processing	Signaling molecules and interaction
ACE Inhibitor Pathway	1	1	13	2.39	Drug development	Target based structure classification
Cholesterol Biosynthesis	1	1	30	2.39	Metabolic processes	
Glutathione metabolism	1	1	112	2.39	Metabolism	Metabolism of other amino acids
Glutathione metabolism	1	1	56	2.39	Metabolism	Metabolism of other amino acids
Glycolysis and Gluconeogenesis	1	1	60	2.39	Metabolism	Carbohydrate metabolism
<b><u>PATHWAYS WITH UNDER-REPRESENTED GENES</u></b>						
Alzheimer's disease	3	55	186	-2.03	Human diseases	Neurodegenerative diseases
Oxidative phosphorylation	1	36	68	-2.08	Metabolism	Energy metabolism
Calcium Regulation in the Cardiac Cell	0	28	153	-2.25	Physiological process	
mRNA processing	0	29	131	-2.29	Cellular processes	
Oxidative phosphorylation	3	68	237	-2.52	Metabolism	Energy metabolism
Proteasome	0	35	52	-2.52	Genetic information processing	Folding sorting and degradation
Proteasome Degradation	0	37	66	-2.6	Physiological processes	
Huntington's disease	1	51	192	-2.67	Human diseases	Neurodegenerative diseases

**Table 7.10: Top down-regulated genes in the outer myometrium of adenomyotic uteri (compared to controls), in the secretory phase, with associated gene ontology**

Symbol	Gene ID	Fold changes	Chromosome	Definition	Synonyms	Ontology Component	Ontology process	Ontology function
APCDD1L	164284	-5	20	Adenomatosis polyposis coli down-regulated 1-like (APCDD1L)	RP4-685L9.2; FLJ90166; MGC126807; MGC126809			
HSPB3	8988	-4	5	Heat shock 27kDa protein 3 (HSPB3)	HSPL27		Protein folding; response to unfolded protein	
MSLN	10232	-4	16	Mesothelin (MSLN), transcript variant 2	SMR; MPF; CAK1	Membrane	Cell adhesion	Peptide antigen binding; GPI anchor binding; protein binding
KCNK12	56660	-3	2	Potassium channel, subfamily K, member 12 (KCNK12)	THIK2; THIK-2	Membrane; integral to membrane	Ion transport; potassium ion transport	Potassium ion binding; potassium channel activity; voltage-gated ion channel activity
CILP	8483	-3	15	Cartilage intermediate layer protein, nucleotide pyrophosphohydrolase (CILP)	HsT18872	Extracellular region; extracellular matrix (sensu Metazoa)	Nucleobase, nucleoside, nucleotide and nucleic acid metabolism	Phosphoprotein phosphatase activity
HES6	55502	-3	2	Hairy and enhancer of split 6 (Drosophila) (HES6)	nucleus 5634] ; transcription factor complex 5667] [pmid 10851137] [evidence ISS]	Cell differentiation; regulation of transcription, DNA-dependent	Transcription cofactor activity; transcription factor activity	
PCDH17	27253	-3	13	Protocadherin 17 (PCDH17)	PCH68; PCDH68	Membrane; integral to membrane	Homophilic cell adhesion; cell adhesion	Calcium ion binding; protein binding
SLC22A16	85413	-3	6	Solute carrier family 22 (organic cation/carnitine transporter), member 16 (SLC22A16)	dJ261K5.1; OCT6; FLIPT2; OKB1; CT2	Plasma membrane; integral to membrane; membrane	Transport; sperm motility; organic cation transport; acid secretion; carnitine transport; fertilization (sensu Metazoa)	Transporter activity; carnitine transporter activity; ion transporter activity
WNT5A	7474	-2	3	Wingless-type MMTV integration site family, member 5A (WNT5A)	hWNT5A	Extracellular region; extracellular space; soluble fraction	Morphogenesis; cell-cell signaling; signal transduction; frizzled-2 signaling pathway	Receptor binding; signal transducer activity

Cont.

**Table 7.10: Top down-regulated genes in the outer myometrium of adenomyotic uteri in the secretory phase (cont.)**

Symbol	Gene ID	Fold changes	Chromosome	Definition	Synonyms	Ontology Component	Ontology process	Ontology function
<b>MC1R</b>	4157	-2	16	Melanocortin 1 receptor (alpha melanocyte stimulating hormone receptor) (MC1R)	SHEP1; MSH-R; MGC14337	Integral to plasma membrane; membrane	UV protection ; G-protein 253ignalling, coupled to cyclic nucleotide second messenger; development; signal transduction	Melanocyte stimulating hormone receptor activity; receptor activity; rhodopsin-like receptor activity
<b>CADPS2</b>	93664	-2	7	Ca2+-dependent activator protein for secretion 2 (CADPS2), transcript variant 1	KIAA1591; FLJ40851	Synapse; membrane	Protein transport; exocytosis	Lipid binding; calcium ion binding
<b>GPR37</b>	2861	-2	7	G protein-coupled receptor 37 (endothelin receptor type B-like) (GPR37)	hET(B)R-LP; EDNRBL; PAELR	Integral to plasma membrane; membrane	G-protein coupled receptor protein 253ignalling pathway; signal transduction	Receptor activity; G-protein coupled receptor activity, unknown ligand; rhodopsin-like receptor activity
<b>COL12A1</b>	1303	-2	6	Collagen, type XII, alpha 1 (COL12A1), transcript variant long	BA209D8.1; DJ234P15.1; COL12A1L	Collagen type XII; extracellular matrix (sensu Metazoa); cytoplasm	Collagen fibril organization; skeletal development; cell adhesion; phosphate transport	Extracellular matrix structural constituent conferring tensile strength; structural molecule activity; protein binding
<b>RASGRP3</b>	25780	-2	2	RAS guanyl releasing protein 3 (calcium and DAG-regulated) (RASGRP3)	GRP3; KIAA0846	Integral to plasma membrane; intracellular	Regulation of small GTPase mediated signal transduction; MAPKKK cascade	Rap GTPase activator activity; zinc ion binding; guanyl-nucleotide exchange factor; diacylglycerol binding; signal transducer activity; calcium ion binding; protein binding
<b>C6orf32</b>	9750	-2	6	Chromosome 6 open reading frame 32 (C6orf32), transcript variant 2	FAM65B; KIAA0386; DIFF48; DIFF40; PL48	Binding		
<b>PIGQ</b>	9091	-2	16	Phosphatidylinositol glycan anchor biosynthesis, class Q (PIGQ), transcript variant 2	GPI1; c407A10.1; hGPI1; MGC12693	Membrane; integral to membrane	GPI anchor biosynthesis; carbohydrate metabolism	Transferase activity, transferring glycosyl groups; phosphatidylinositol N-acetylglucosaminyltransferase activity

**Cont.**

**Table 7.10: Top down-regulated genes in the outer myometrium of adenomyotic uteri in the secretory phase (cont.)**

Symbol	Gene ID	Fold changes	Chromosome	Definition	Synonyms	Ontology Component	Ontology process	Ontology function
<b>PTCHD1</b>	139411	-2	X	Patched domain containing 1 (PTCHD1)	MGC149798; FLJ30296	Membrane	Hedgehog receptor activity	
<b>CALCRL</b>	10203	-2	2	Calcitonin receptor-like (CALCRL)	CGRPR; CRLR	Integral to plasma membrane; membrane	Signal transduction; G-protein signaling, coupled to cyclic nucleotide second messenger	Receptor activity; calcitonin receptor activity; G-protein coupled receptor activity
<b>LOC648470</b>	648470	-2		PREDICTED: similar to Caspase-4 precursor (CASP-4) (ICH-2 protease) (TX protease) (ICE(rel)-II) (LOC648470)				
<b>DENND2A</b>	27147	-2	7	DENN/MADD domain containing 2A (DENND2A)	KIAA1277; FAM31D			

**Table 7.11: Top up-regulated genes in the outer myometrium of adenomyotic uteri (compared to controls), in the secretory phase, with associated gene ontology**

Symbol	Gene ID	Fold changes	Chromosome	Definition	Synonyms	Ontology Component	Ontology process	Ontology function
LOC648343	648343	4		PREDICTED: similar to protein phosphatase 1 regulatory subunit 14B (LOC648343)				
LOC647436	647436	4		PREDICTED: similar to ribosomal protein L5, transcript variant 1 (LOC647436)				
PTMA	5757	4	2	prothymosin, alpha (PTMA), transcript variant 1	TMSA; MGC104802	Nucleus	Development; transcription	
LOC402644	402644	3		PREDICTED: similar to peptidylprolyl isomerase A isoform 1 (LOC402644)				
LOC641848	641848	3		PREDICTED: similar to ribosomal protein S3a (LOC641848)				
RAB33B	83452	3	4	RAB33B, member RAS oncogene family (RAB33B)	DKFZP434G099; MGC138182	Golgi apparatus	small GTPase mediated signal transduction 7264] ; protein transport 15031]	GTP binding 5525] ; nucleotide binding 166]
LOC647673	647673	3		PREDICTED: similar to Translationally-controlled tumor protein (TCTP) (p23) (Histamine-releasing factor) (HRF) (Fortilin) (LOC647673)				
PAPSS1	9061	3	4	3'-phosphoadenosine 5'-phosphosulfate synthase 1 (PAPSS1)	SK1; PAPSS; ATPSK1	Intracellular	Skeletal development; sulfate assimilation; nucleobase, nucleoside, nucleotide and nucleic acid metabolism	Sulfate adenylyltransferase (ATP) activity; adenylylsulfate kinase activity; nucleotide binding; ATP binding; nucleotidyltransferase activity
LOC441377	441377	2		PREDICTED: similar to 40S ribosomal protein S26 (LOC441377)				
LOC651202	651202	2		PREDICTED: similar to large subunit ribosomal protein L36a (LOC651202)				
LGALS3	3958	2	14	lectin, galactoside-binding, soluble, 3 (galectin 3) (LGALS3)	GAL3; MAC2; LGALS2; CBP35; GALBP	Extracellular region; cytoplasm; plasma membrane; nucleus		IgE binding; sugar binding
ANXA2P1		2	4	annexin A2 pseudogene 1 (ANXA2P1) on chromosome 4.	LPC2A; ANX2L1; ANX2P1			
LOC402221	402221	2		PREDICTED: similar to actin alpha 1 skeletal muscle protein (LOC402221)				
NUBPL	80224	2	14	nucleotide binding protein-like (NUBPL)	FLJ12660; C14orf127			ATP binding; nucleotide binding

**Table 7.12: Pathways analysis of genes differentially expressed in the outer myometrium of adenomyotic (compared to control uteri), in the secretory phase, fulfilling the criteria of  $p < 0.05$  and 2-fold change**

PATHWAY	POSITIVE	MEASURED	TOTAL	Z SCORE	FUNCTIONAL HIERARCHY	
<b>PATHWAYS WITH OVER-REPRESENTED GENES</b>						
Olfactory transduction	70	186	388	8.75	Cellular processes	Sensory system
GPCRs, Class A Rhodopsin-like	20	41	268	5.74	Molecular function	
Renin-angiotensin system	3	3	24	3.93	Cellular processes	Endocrine system
Peptide GPCRs	2	2	74	3.2	Molecular function	
ACE Inhibitor Pathway	1	1	13	2.26	Drug development	Target based structure classification
Glutathione metabolism	1	1	112	2.26	Metabolism	Metabolism of other amino acids
Monoterpenoid biosynthesis	1	1	41	2.26	Metabolism	Biosynthesis of secondary metabolites
Steroid Biosynthesis	1	1	22	2.26	Metabolism	Lipid metabolism
Neuroactive ligand-receptor interaction	8	25	334	2.15	Environmental information processing	Signaling molecules and interaction
GPCRs, Other	6	17	119	2.13	Molecular function	
<b>PATHWAYS WITH UNDER-REPRESENTED GENES</b>						
Alzheimer's disease	3	55	186	-2.24	Human diseases	Neurodegenerative diseases
TNF-alpha/NF-kB Signaling Pathway	0	25	188	-2.24	Cellular processes	
Axon guidance	0	27	130	-2.33	Cellular processes	Development
mRNA processing	0	29	131	-2.41	Cellular processes	
Parkinson's disease	1	42	150	-2.5	Human diseases	Neurodegenerative diseases
Electron Transport Chain	1	44	116	-2.58	Metabolic processes	
Proteasome	0	35	52	-2.66	Genetic information processing	Folding sorting and degradation
Proteasome Degradation	0	37	66	-2.74	Physiological processes	
Oxidative phosphorylation	2	67	237	-3.06	Metabolism	Energy metabolism
Huntington's disease	0	51	192	-3.24	Human diseases	Neurodegenerative diseases

## APPENDIX 3

### Publications arising from the thesis

1. Mehasseb MK, Brown LJ, Bell SC and Habiba MA. **Phenotypic characterization of the inner and outer myometrium in normal and adenomyotic uteri.** *Gynecol Obstet Inv (In Press)*. Accepted for publication 1 March 2010.
2. Mehasseb MK, Taylor AH, Pringle JH, Bell SC and Habiba MA. **Enhanced invasion of stromal cells from adenomyosis in a three-dimensional co-culture model is augmented by the presence of myocytes from affected uteri.** *Fertil Steril (In Press)*. Accepted for publication 08 April 2010.
3. Mehasseb MK, Bell SC and Habiba MA. **Neonatal administration of tamoxifen causes disruption of myometrial development but not adenomyosis in the C57/BL6J mouse.** *Reproduction* 2010; 139: 1067-1075.
4. Mehasseb MK, Bell SC, Pringle JH and Habiba MA. **Uterine adenomyosis is associated with ultrastructural features of altered contractility in the inner myometrium.** *Fertil Steril* 2010; 93: 2130–6.
5. Mehasseb MK, Bell SC and Habiba MA. **The effects of tamoxifen and estradiol on myometrial differentiation and organisation during early uterine development in the CD-1 mouse.** *Reproduction* 2009; 138: 341-350.
6. Mehasseb MK and Habiba MA. **Adenomyosis uteri: an update.** *The Obstetrician & Gynaecologist* 2009; 11: 41–47.

## APPENDIX 4

### Oral Presentations arising from the thesis

1. **Enhanced invasion of stromal cells from adenomyosis in a three-dimensional co-culture model is augmented by the presence of myocytes from affected uteri**, British International Congress of Obstetrics and Gynaecology, Belfast, July 2010 (*Winner of the best oral presentation in the Reproductive Sciences stream*).
2. **Histomorphometric analysis of gonadal steroid receptors distribution in uteri with and without adenomyosis through the menstrual cycle**, British International Congress of Obstetrics and Gynaecology, Belfast, July 2010 (*Winner of the best oral presentation in the Reproductive Sciences stream*).
3. **Endometrial stroma and myometrial interaction in uterine adenomyosis: a novel three-dimensional co-culture model**, Blair-Bell Research Society meeting, Manchester, December 2008.
4. **Pathogenesis of uterine adenomyosis**, Reproductive Sciences Section seminar, University of Leicester, Leicester, March 2008.
5. **Cyclical changes in the cellular density of the junctional zone myometrium in normal and adenomyotic uteri**, British International Congress of Obstetrics and Gynaecology, London, July 2007 (*Winner of the best oral presentation in the Reproductive Sciences stream*).
6. **Abnormal mesenchymal markers expression in adenomyosis uteri**, Blair-Bell Research Society meeting, Derby, June 2007.

7. **The role of endometrial-myometrial interface in the aetiopathology of uterine adenomyosis**, Reproductive Sciences Section seminar, University of Leicester, Leicester, October 2006.
8. **Disordered myometrial organisation during early uterine development in tamoxifen-induced adenomyosis**, Blair-Bell Research Society meeting, Leicester, October 2006.
9. **Phenotypic Characterization of the Myometrium in Normal and Adenomyotic uteri**, Blair-Bell Research Society meeting, Leicester, October 2006.

## APPENDIX 5

### Poster Presentations arising from the thesis

1. **Uterine adenomyosis is associated with ultrastructural features of altered contractility in the inner myometrium**, Society for Gynaecologic Investigation (SGI) meeting, Glasgow, UK, March 2009
2. **Endometrial stroma and myometrial interaction in uterine adenomyosis: a novel three-dimensional co-culture model**, Society for Gynaecologic Investigation (SGI) meeting, Glasgow, UK, March 2009.
3. **Strain-specific susceptibility to tamoxifen-induced adenomyosis in an animal model**, 10th World Congress of Endometriosis, Melbourne, Australia, March 2008. Also presented in the Society for Gynaecologic Investigation (SGI) meeting, Glasgow, UK, March 2009.
4. **Cellular density in myometrium and junctional zone in tamoxifen-induced and spontaneous adenomyosis**, 10th World Congress of Endometriosis, Melbourne, Australia, March 2008. Also presented in the Society for Gynaecologic Investigation (SGI) meeting, Glasgow, UK, March 2009.
5. **Study of proliferation and apoptosis indices in uterine adenomyosis**, 10th World Congress of Endometriosis, Melbourne, Australia, March 2008. Also presented in the Society for Gynaecologic Investigation meeting, Glasgow, UK, March 2009.

6. **The effects of estradiol and tamoxifen therapy on myometrial differentiation and organisation during early uterine development: an animal model**, British International Congress of Obstetrics and Gynaecology, London, July 2007.

## **APPENDIX 6**

### **Copy of Ethics Committee approval letters**

**DIRECTORATE OF RESEARCH AND DEVELOPMENT**

Director: Professor D Rowbotham  
Assistant Director: John Hampton  
Co-ordinator: G Davda  
Direct Dial: 0116 2584614  
Fax No: 0116 258 4226  
Email: Gemini.davda@uhl-tr.nhs.uk

Leicester General Hospital  
Gwendolen Road  
Leicester  
LE5 4PW

Tel: 0116 249 0490  
Fax: 0116 258 4666  
Minicom: 0116 258 8188

27 March 2006

Dr M Habiba  
University Hospitals of Leicester  
University Hospitals of Leicester  
c/o Research and Development Office  
Leicester General Hospital NHS Trust  
Leicester  
LE1 4PW

RECEIVED

- 4 APR 2006

Dear Dr Habiba

ID: 10020 Growth factors in uterine adenomyosis

LREC Ref: 06/Q2501/19 MREC Ref:

We have now been notified by the Ethics Committee that this project has been given a favourable opinion by the Ethics Committee (please see the attached letter from the Ethics Committee dated 15/02/06).

Since all other aspects of your UHL R+D notification are complete, I now have pleasure in confirming full approval of the project on behalf of University Hospitals of Leicester NHS Trust.

This approval means that you are fully authorised to proceed with the project, using all the resources which you have declared in your notification form.

The project is also now covered by Trust Indemnity, except for those aspects already covered by external indemnity (e.g. ABPI in the case of most drug studies).

We will be requesting annual and final reports on the progress of this project, both on behalf of the Trust and on behalf of the Ethical Committee.

Please note if you want to extend the study's end date you will have to submit an annual report available through the R&D website which will be forwarded and noted by the Trust and the relevant Ethics Committee. This allows you to continue working on the study under the previous arrangements covered by Trust Indemnity. Please note ethics approval is only granted until the proposed end date as reflected in A3 of the COREC form. You are no longer indemnified pass this date unless you have submitted the annual report form detailing this extension.

In the meantime, in order to keep our records up to date, could you please notify the Research Office if there are any significant changes to the start or end dates, protocol, funding or costs of the project.

I look forward to the opportunity of reading the published results of your study in due course.

Yours sincerely

  
John Hampton  
Assistant Director for Research and Development

**DIRECTORATE OF RESEARCH AND DEVELOPMENT**

Director: Professor D Rowbotham  
Assistant Director: John Hampton  
Co-ordinator: G Davda  
Direct Dial: 0116 2584614  
Fax No: 0116 258 4226  
EMail: Gemini.davda@uhl-tr.nhs.uk

Leicester General Hospital  
Gwendolen Road  
Leicester  
LE5 4PW  
Tel: 0116 249 0490  
Fax: 0116 258 4666  
Minicom: 0116 258 8188

09 March 2006

Dr M Habiba  
University Hospitals of Leicester  
University Hospitals of Leicester  
c/o Research and Development Office  
Leicester General Hospital NHS Trust  
Leicester  
LE1 4PW

Dear Dr Habiba

**ID: 10022 Uterine adenomyosis: The Clinical and Histopathological correlates.**

**LREC Ref: 06/Q2501/20 MREC Ref:**

We have now been notified by the Ethics Committee that this project has been given a favourable opinion by the Ethics Committee (please see the attached letter from the Ethics Committee).

Since all other aspects of your UHL R+D notification are complete, I now have pleasure in confirming full approval of the project on behalf of University Hospitals of Leicester NHS Trust.

This approval means that you are fully authorised to proceed with the project, using all the resources which you have declared in your notification form.

The project is also now covered by Trust Indemnity, except for those aspects already covered by external indemnity (e.g. ABPI in the case of most drug studies).

We will be requesting annual and final reports on the progress of this project, both on behalf of the Trust and on behalf of the Ethical Committee.

Please note if you want to extend the study's end date you will have to submit an annual report available through the R&D website which will be forwarded and noted by the Trust and the relevant Ethics Committee. This allows you to continue working on the study under the previous arrangements covered by Trust Indemnity. Please note ethics approval is only granted until the proposed end date as reflected in A3 of the COREC form. You are no longer indemnified past this date unless you have submitted the annual report form detailing this extension.

In the meantime, in order to keep our records up to date, could you please notify the Research Office if there are any significant changes to the start or end dates, protocol, funding or costs of the project.

I look forward to the opportunity of reading the published results of your study in due course.

Yours sincerely



John Hampton

**Assistant Director for Research and Development**  
Trust Headquarters, Gwendolen Road, Leicester, LE5 4QF  
Tel: 0116 258 8665 Fax: 0116 258 4666 Website: [www.uhl-tr.nhs.uk](http://www.uhl-tr.nhs.uk)  
Chairman Mr. Philip Hammersley CBE Chief Executive Dr Peter Reading

**DIRECTORATE OF RESEARCH AND DEVELOPMENT**

Director: Professor D Rowbotham  
Assistant Director: John Hampton  
Co-ordinator: G Davda  
Direct Dial: 0116 2584614  
Fax No: 0116 258 4226  
EMail: Gemini.davda@uhl-tr.nhs.uk

Leicester General Hospital  
Gwendolen Road  
Leicester  
LE5 4PW

Tel: 0116 249 0490  
Fax: 0116 258 4666  
Minicom: 0116 258 8188

09 March 2006

Dr M Habiba  
University of Leicester  
Reproductive Sciences Department  
Clinical Sciences Building  
Leicester University

Dear Dr Habiba

ID: 10021 **Immunohistopathologic features and characterization of uterine Adenomyosis**

LREC Ref: 06/Q2501/21 MREC Ref:

We have now been notified by the Ethics Committee that this project has been given a favourable opinion by the Ethics Committee (please see the attached letter from the Ethics Committee).

Since all other aspects of your UHL R+D notification are complete, I now have pleasure in confirming full approval of the project on behalf of University Hospitals of Leicester NHS Trust.

This approval means that you are fully authorised to proceed with the project, using all the resources which you have declared in your notification form.

The project is also now covered by Trust Indemnity, except for those aspects already covered by external indemnity (e.g. ABPI in the case of most drug studies).

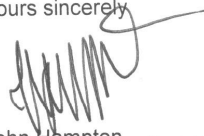
We will be requesting annual and final reports on the progress of this project, both on behalf of the Trust and on behalf of the Ethical Committee.

Please note if you want to extend the study's end date you will have to submit an annual report available through the R&D website which will be forwarded and noted by the Trust and the relevant Ethics Committee. This allows you to continue working on the study under the previous arrangements covered by Trust Indemnity. Please note ethics approval is only granted until the proposed end date as reflected in A3 of the COREC form. You are no longer indemnified pass this date unless you have submitted the annual report form detailing this extension.

In the meantime, in order to keep our records up to date, could you please notify the Research Office if there are any significant changes to the start or end dates, protocol, funding or costs of the project.

I look forward to the opportunity of reading the published results of your study in due course.

Yours sincerely



John Hampton

Trust Headquarters, Gwendolen House, Gwendolen Road, Leicester, LE5 4QF  
**Assistant Director for Research and Development** Website: [www.uhl-tr.nhs.uk](http://www.uhl-tr.nhs.uk)  
Chairman Mr. Philip Hammersley CBE Chief Executive Dr Peter Reading

## BIBLIOGRAPHY

- AHMED, A. I., MAHMOUD, A. E., FADIEL, A. A. & FREDERICK, N. 2007.  
Comparison of 2-, 3D and doppler ultrasound with histological findings in adenomyosis. *Fertil Steril*, 88, S82.
- AMSO, N. N., CROW, J. C. & SHAW, R. W. 1994. Comparative immunohistochemical study of oestrogen and progesterone receptors in the Fallopian tube and uterus at different stages of the menstrual cycle and the menopause. *Hum Reprod*, 9, 1027-1037.
- ARENDS, M. J. 1999. Apoptosis in the endometrium. *Histopathology*, 35, 174-178.
- ARNOLD, J. T., KAUFMAN, D. G., SEPPALA, M. & LESSEY, B. A. 2001.  
Endometrial stromal cells regulate epithelial cell growth in vitro: a new co-culture model. *Hum Reprod*, 16, 836-845.
- ASCHER, S. M., ARNOLD, L. L., PATT, R. H., SCHRUEFER, J. J., BAGLEY, A. S., SEMELKA, R. C., ZEMAN, R. K. & SIMON, J. A. 1994. Adenomyosis: prospective comparison of MR imaging and transvaginal sonography. *Radiology*, 190, 803-6.
- ATRI, M., REINHOLD, C., MEHIO, A. R., CHAPMAN, W. B. & BRET, P. M. 2000.  
Adenomyosis: US features with histologic correlation in an in-vitro study. *Radiology*, 215, 783-90.
- AZZIZ, R. 1989. Adenomyosis: current perspectives. *Obstet Gynecol Clin North Am*, 16, 221-35.

- BARANOVA, H., BOTHORISHVILLI, R., CANIS, M., ALBUISSON, E., PERRIOT, S., GLOWACZOWER, E., BRUHAT, M. A., BARANOV, V. & MALET, P. 1997. Glutathione S-transferase M1 gene polymorphism and susceptibility to endometriosis in a French population. *Mol Hum Reprod*, 3, 775-80.
- BARNICOT, N. A. 1967. A study of newt mitotic chromosomes by negative staining. *J Cell Biol*, 32, 585-603.
- BARRIER, B. F., MALINOWSKI, M. J., DICK, E. J., JR., HUBBARD, G. B. & BATES, G. W. 2004. Adenomyosis in the baboon is associated with primary infertility. *Fertil Steril*, 82 Suppl 3, 1091-4.
- BARTON, J. W., MCCARTHY, S. M., KOHORN, E. I., SCOUTT, L. M. & LANGE, R. C. 1993. Pelvic MR imaging findings in gestational trophoblastic disease, incomplete abortion, and ectopic pregnancy: are they specific? *Radiology*, 190, 163-168.
- BASKIN, G. B., SMITH, S. M. & MARX, P. A. 2002. Endometrial hyperplasia, polyps, and adenomyosis associated with unopposed estrogen in rhesus monkeys (*Macaca mulatta*). *Vet Pathol*, 39, 572-5.
- BATRA, S. 1990. Interaction of antiestrogens with binding sites for muscarinic cholinergic drugs and calcium channel blockers in cell membranes. *Cancer Chemother Pharmacol*, 26, 310-312.
- BAZOT, M., CORTEZ, A., DARAI, E., ROUGER, J., CHOPIER, J., ANTOINE, J. M. & UZAN, S. 2001. Ultrasonography compared with magnetic resonance imaging for the diagnosis of adenomyosis: correlation with histopathology. *Hum Reprod*, 16, 2427-33.

- BENSON, R. C. & SNEEDEN, V. D. 1958. Adenomyosis: a reappraisal of symptomatology. *Am J Obstet Gynecol*, 76, 1044-57; discussion 1057-61.
- BERGHOLT, T., ERIKSEN, L., BERENDT, N., JACOBSEN, M. & HERTZ, J. B. 2001. Prevalence and risk factors of adenomyosis at hysterectomy. *Hum Reprod*, 16, 2418-21.
- BIGSBY, R. M., AIXIN, L., LUO, K. & CUNHA, G. R. 1990. Strain differences in the ontogeny of estrogen receptors in murine uterine epithelium. *Endocrinology*, 126, 2592-2596.
- BIRD, C. C., MCELIN, T. W. & MANALO-ESTRELLA, P. 1972. The elusive adenomyosis of the uterus--revisited. *Am J Obstet Gynecol*, 112, 583-93.
- BLUM, M. 1981. Adenomyosis: study in a Jewish female population. *Int Surg*, 66, 341-3.
- BOYER, B., VALLES, A. M. & EDME, N. 2000. Induction and regulation of epithelial-mesenchymal transitions. *Biochem Pharmacol*, 60, 1091-1099.
- BREUILLER-FOUCHE, M., CHARPIGNY, G. & GERMAIN, G. 2007. Functional genomics of the pregnant uterus: from expectations to reality, a compilation of studies in the myometrium. *BMC Pregnancy Childbirth*, 7 Suppl 1, S4.
- BREUILLER-FOUCHE, M. & GERMAIN, G. 2006. Gene and protein expression in the myometrium in pregnancy and labor. *Reproduction*, 131, 837-50.
- BRODY, J. R. & CUNHA, G. R. 1989. Histologic, morphometric, and immunocytochemical analysis of myometrial development in rats and mice: II. Effects of DES on development. *Am J Anat*, 186, 21-42.

- BROMLEY, B., SHIPP, T. D. & BENACERRAF, B. 2000. Adenomyosis: sonographic findings and diagnostic accuracy. *J Ultrasound Med*, 19, 529-34; quiz 535-6.
- BROSENS, J. J., BARKER, F. G. & DE SOUZA, N. M. 1998. Myometrial zonal differentiation and uterine junctional zone hyperplasia in the non-pregnant uterus. *Hum Reprod Update*, 4, 496-502.
- BROSENS, J. J., DE SOUZA, N. M. & BARKER, F. G. 1995a. Uterine junctional zone: function and disease. *Lancet*, 346, 558-60.
- BROSENS, J. J., DE SOUZA, N. M., BARKER, F. G., PARASCHOS, T. & WINSTON, R. M. 1995b. Endovaginal ultrasonography in the diagnosis of adenomyosis uteri: identifying the predictive characteristics. *Br J Obstet Gynaecol*, 102, 471-4.
- BROWN, H. K., STOLL, B. S. & NICOSIA, S. V. 1991. Uterine junctional zone: correlation between histologic findings and MR imaging. *Radiology*, 179, 409-413.
- BULMER, J. N., JONES, R. K. & SEARLE, R. F. 1998. Intraepithelial leukocytes in endometriosis and adenomyosis: comparison of eutopic and ectopic endometrium with normal endometrium. *Hum Reprod*, 13, 2910-5.
- CAMARGO, F., GAYTAN, J., CALIGARA, C., SIMON, C. & PELLICER, A. 2001. Impact of ultrasound diagnosis of adenomyosis on recipients of sibling oocytes. *Fertil Steril*, 76, 150.

- CAMPBELL, S., YOUNG, A., STEWART, C. J. R., APLIN, J. D., CHURCH, H. J. & CAMERON, I. T. 1998. Laminin  $\beta 2$  distinguishes inner and outer layers of the human myometrium. *J Reprod Fertil Abstract Series*, 22, 12.
- CAPETANAKI, Y., NGAI, J. & LAZARIDES, E. 1984. Characterization and regulation in the expression of a gene encoding for the intermediate filament protein desmin. *Proc Natl Acad Sci*, 81, 6909-6912.
- CHIQUET-EHRISMANN, R., KALLA, P. & PEARSON, C. A. 1989. Participation of Tenascin and TGF-beta in reciprocal epithelial-mesenchymal interactions of MCF7 cells and fibroblasts. *Cancer Res*, 49, 4322-4325.
- CHRYSOSTOMOU, M., AKALESTOS, G., KALLISTROS, S., PAPADIMITRIOU, V., NAZAR, S. & CHRONIS, G. 1991. Incidence of adenomyosis uteri in a Greek population. *Acta Obstet Gynecol Scand*, 70, 441-4.
- COHEN, I., BEYTH, Y., SHAPIRA, J., TEPPER, R., FISHMAN, A., CORDOBA, M., BERNHEIM, J., YIGAEL, D. & ALTARAS, M. M. 1997. High frequency of adenomyosis in postmenopausal breast cancer patients treated with tamoxifen. *Gynecol Obstet Invest*, 44, 200-5.
- COHEN, I., BEYTH, Y., TEPPER, R., FIGER, A., SHAPIRA, J., CORDOBA, M., YIGAEL, D. & ALTARAS, M. M. 1995. Adenomyosis in postmenopausal breast cancer patients treated with tamoxifen: a new entity? *Gynecol Oncol*, 58, 86-91.
- COHEN, M. & BISCHOF, P. 2009. Coculture of decidua and trophoblast to study proliferation and invasion. *Methods Mol Biol*, 550, 63-72.

- COLE, W. C. & GARFIELD, R. E. 1989. Ultrastructure of the myometrium. *In*:  
WYNN, R. M. & JOLLIE, W. P. (eds.) *Biology of the uterus*. New York:  
Plenum.
- COTRAN, R. S., KUMAR, V. & ROBBINS, S. L. 1989. *Robbins pathological basis of  
disease*  
. Philadelphia: W.B. Saunders Company.
- CRAMER, D. W., HORNSTEIN, M. D., NG, W. G. & BARBIERI, R. L. 1996.  
Endometriosis associated with the N314D mutation of galactose-1-phosphate  
uridyl transferase (GALT). *Mol Hum Reprod*, 2, 149-52.
- CULLEN, T. S. 1908. Adenomyoma of the uterus. *JAMA*, L(2), 107-115.
- CUNHA, G. R. 1976. Stromal induction and specification of morphogenesis and  
cytodifferentiation of the epithelia of the mullerian ducts and urogenital sinus  
during development of the uterus and vagina in mice. *J Exp Zool*, 196, 361-370.
- CUNHA, G. R., BATTLE, E., YOUNG, P., BRODY, J., DONJACOUR, A.,  
HAYASHI, N. & KINBARA, H. 1992. Role of epithelial-mesenchymal  
interactions in the differentiation and spatial organization of visceral smooth  
muscle. *Epithelial Cell Biology*, 1, 76-83.
- CUNHA, G. R., YOUNG, P. & BRODY, J. R. 1989a. Role of uterine epithelium in the  
development of myometrial smooth muscle cells. *Biol Reprod*, 40, 861-871.
- CUNHA, G. R., YOUNG, P. & BRODY, J. R. 1989b. Role of uterine epithelium in the  
development of myometrial smooth muscle cells. *Biol Reprod*, 40, 821-871.

- CURTIS, K. M., HILLIS, S. D., MARCHBANKS, P. A. & PETERSON, H. B. 2002. Disruption of the endometrial-myometrial border during pregnancy as a risk factor for adenomyosis. *Am J Obstet Gynecol*, 187, 543-4.
- DAISLEY, H. 1987. Adenomyosis uteri. A prospective study in Trinidad & Tobago (January-May, 1986). *West Indian Med J*, 36, 166-73.
- DAVIES, H. G. & SPENCER, M. 1962. The variation in the structure of erythrocyte nuclei with fixation. *J Cell Biol*, 14, 445-458.
- DE VRIES, K., LYONS, E. A., BALLARD, G., LEVI, C. S. & LINDSAY, D. J. 1990. Contractions of the inner third of the myometrium. *Am J Obstet Gynecol*, 679-682.
- DEMAS, B. E., HRICAK, H. & JAFFE, R. B. 1986. Uterine MR imaging: effects of hormonal stimulation. *Radiology*, 159, 123-6.
- DEVLIEGER, R., D'HOOGHE, T. & TIMMERMAN, D. 2003. Uterine adenomyosis in the infertility clinic. *Hum Reprod Update*, 9, 139-47.
- DIMITROVA, I. K., RICHER, J. K., RUDOLPH, M. C., SPOELSTRA, N. S., RENO, E. M., MEDINA, T. M. & BRADFORD, A. P. 2009. Gene expression profiling of multiple leiomyomata uteri and matched normal tissue from a single patient. *Fertil Steril*, 91, 2650-63.
- DITO, W. R. & BATSAKIS, J. G. 1961. Norethynodrel-treated endometriosis: a morphological and histochemical study. *Obstet Gynecol*, 18, 1-12.
- DUEHOLM, M., LUNDORF, E., SORENSEN, J. S., LEDERTOUG, S., OLESEN, F. & LAURSEN, H. 2002. Reproducibility of evaluation of the uterus by

transvaginal sonography, hysterosonographic examination, hysteroscopy and magnetic resonance imaging. *Hum Reprod*, 17, 195-200.

EIDE, A. 1975. The effect of oestradiol on the DNA synthesis in neonatal mouse uterus and cervix. *Cell Tissue Res*, 156, 551-5.

EMGE, L. A. 1962. The elusive adenomyosis of the uterus. Its historical past and its present state of recognition. *Am J Obstet Gynecol*, 83, 1541-63.

ESPLIN, M. S., FAUSETT, M. B., PELTIER, M. R., HAMBLIN, S., SILVER, R. M., BRANCH, D. W., ADASHI, E. Y. & WHITING, D. 2005a. The use of cDNA microarray to identify differentially expressed labor-associated genes within the human myometrium during labor. *Am J Obstet Gynecol*, 193, 404-13.

ESPLIN, M. S., PELTIER, M. R., HAMBLIN, S., SMITH, S., FAUSETT, M. B., DILDY, G. A., BRANCH, D. W., SILVER, R. M. & ADASHI, E. Y. 2005b. Monocyte chemotactic protein-1 expression is increased in human gestational tissues during term and preterm labor. *Placenta*, 26, 661-71.

EYDEN, B. P., HALE, R. J., RICHMOND, I. & BUCKLEY, C. H. 1992. Cytoskeletal filaments in the smooth muscle cells of uterine leiomyomata and myometrium: an ultrastructural and immunohistochemical analysis. *Virchows Arch A Pathol Anat Histol*, 420, 51-58.

FANCHIN, R., RIGHINI, C., OLIVENNES, F., TAYLOR, S., DE ZIEGLER, D. & FRYDMAN, R. 1998. Uterine contractions at the time of embryo transfer alter pregnancy rates after in-vitro fertilization. *Hum Reprod*, 13, 1968-74.

- FEDELE, L., BIANCHI, S., DORTA, M., ARCAINI, L., ZANOTTI, F. & CARINELLI, S. 1992a. Transvaginal ultrasonography in the diagnosis of diffuse adenomyosis. *Fertil Steril*, 58, 94-7.
- FEDELE, L., BIANCHI, S., DORTA, M., ZANOTTI, F., BRIOSCHI, D. & CARINELLI, S. 1992b. Transvaginal ultrasonography in the differential diagnosis of adenomyoma versus leiomyoma. *Am J Obstet Gynecol*, 167, 603-6.
- FEDELE, L., BIANCHI, S., RAFFAELLI, R., PORTUESE, A. & DORTA, M. 1997. Treatment of adenomyosis-associated menorrhagia with a levonorgestrel-releasing intrauterine device. *Fertil Steril*, 68, 426-9.
- FERENCZY, A. 1979. Diagnostic electron microscopy in gynecologic pathology. *Pathol Annu*, 14, 353-381.
- FERENCZY, A. 1998. Pathophysiology of adenomyosis. *Hum Reprod Update*, 4, 312-22.
- FICICIOGLU, C., TEKIN, H. I., ARIOGLU, P. F. & OKAR, I. 1995. A murine model of adenomyosis: the effects of hyperprolactinemia induced by fluoxetine hydrochloride, a selective serotonin reuptake inhibitor, on adenomyosis induction in Wistar albino rats. *Acta Eur Fertil*, 26, 75-9.
- FRANKL, O. 1925. Adenomyosis uteri. *Am J Obstet Gynecol*, 10, 680-684.
- FRIEDERICI, H. H. R. & DECLOUX, R. J. 1968. The early response of immature rat myometrium to estrogenic stimulation. *J Ultrastruct Res*, 22, 402-412.

- FUJII, S., KONISHI, I. & MORI, T. 1989. Smooth muscle differentiation at endometrio-myometrial junction. An ultrastructural study. *Virchows Arch A Pathol Anat Histol*, 414, 105-112.
- FUJII, S., KONISHI, I. & MORI, T. 1990. Ultrastructure of smooth muscle tissue in the female reproductive tract: uterus and oviduct. *In*: MOTTA, P. M. (ed.) *Ultrastructure of smooth muscle*. Boston: Kluwer.
- FUJIMOTO, T. 1993. Calcium pump of the plasma membrane is localized in caveolae. *J Cell Biol*, 5, 1147-1157.
- FUNG, H. Y. M., WONG, Y. L., WONG, F. W. S. & ROGERS, M. S. 1994. Study of oestrogen and progesterone receptors in normal endometrium during the menstrual cycle by immunohistochemical analysis. *Gynecol Obstet Invest*, 38, 186-190.
- FUSI, L., CLOKE, B. & BROSENS, J. J. 2006. The uterine junctional zone. *Best Pract Res Clin Obstet Gynaecol*, 20, 479-91.
- GAETJE, R., KOTZIAN, S., HERRMANN, G., BAUMANN, R. & STARZINSKI-POWITZ, A. 1995. Invasiveness of endometriotic cells in vitro. *Lancet*, 346, 1463-4.
- GARCIA, E., BOUCHARD, P., DE BRUX, J., BERDAH, J., FRYDMAN, R., SCHAISON, G., MILGROM, E. & PERROT-APPLANAT, M. 1988. Use of immunocytochemistry of progesterone and oestrogen receptors for endometrial dating. *J Clin Endocrinol Metab*, 67, 80-87.

- GASTEIGER, E., HOOGLAND, C., GATTIKER, A., DUVAUD, S., WILKINS, M. R., APPEL, R. D. & BAIROCH, A. 2005. Protein identification and analysis tools on the ExPASy server. *In: WALKER, J. M. (ed.) The proteomics protocols handbook*. Humana Press.
- GOLDBLUM, J. R., CLEMENT, P. B. & HART, W. R. 1995. Adenomyosis with sparse glands. A potential mimic of low-grade endometrial stromal sarcoma. *Am J Clin Pathol*, 103, 218-23.
- GOMPEL, C. & SILVERBERG, S. G. 1994. Pathology in gynecology and obstetrics. Philadelphia: JB Lippencott Company.
- GOTO, Y., YOSHIKANE, H., HONDA, M., MORIOKA, S., YAMORI, Y. & MORIYAMA, K. 1993. Three-dimensional observation on sarcoplasmic reticulum and caveolae in myocardium of spontaneously hypertensive rats. *J Submicrosc Cytol Pathol*, 22, 535-542.
- GOUMENOU, A. G., ARVANITIS, D. A., MATALLIOTAKIS, I. M., KOUMANTAKIS, E. E. & SPANDIDOS, D. A. 2000. Loss of heterozygosity in adenomyosis on hMSH2, hMLH1, p16Ink4 and GALT loci. *Int J Mol Med*, 6, 667-71.
- GRAHAM, J. D. & CLARKE, C. L. 1997. Physiological action of progesterone in target tissues. *Endocrinol Rev*, 18, 502-509.
- GREAVES, P. & WHITE, I. N. 2006. Experimental adenomyosis. *Best Pract Res Clin Obstet Gynaecol*, 20, 503-10.

- GREEN, A. R., EDWARDS, R. E., GREAVES, P. & WHITE, I. N. 2003. Comparison of the effect of oestradiol, tamoxifen and raloxifene on nerve growth factor-alpha expression in specific neonatal mouse uterine cell types using laser capture microdissection. *J Mol Endocrinol*, 30, 1-11.
- GREEN, A. R., PARROTT, E., BUTTERWORTH, M., JONES, P. S., GREAVES, P. & WHITE, I. N. H. 2001. Comparisons of the effects of tamoxifen, toremifene and raloxifene on enzyme induction and gene expression in the ovariectomised rat uterus. *J Endocrinol*, 170, 555-564.
- GREEN, A. R., STYLES, J. A., PARROTT, E. L., GRAY, D., EDWARDS, R. E., SMITH, A. G., GANT, T. W., GREAVES, P., AL-AZZAWI, F. & WHITE, I. N. 2005. Neonatal tamoxifen treatment of mice leads to adenomyosis but not uterine cancer. *Exp Toxicol Pathol*, 56, 255-63.
- GUTTNER, J. 1980. Adenomyosis in mice. *Z Versuchstierkd*, 22, 249-51.
- HABAYEB, O. M. H., TAYLOR, A. H., BELL, S. C., TAYLOR, D. J. & KONJE, J. C. 2008. Expression of the endocannabinoid system in human first trimester placenta and its role in trophoblast proliferation. *Endocrinology*, 149, 5052-5060.
- HALL, J. B., YOUNG, R. H. & NELSON, J. H., JR. 1984. The prognostic significance of adenomyosis in endometrial carcinoma. *Gynecol Oncol*, 17, 32-40.
- HALL, L. L., BICKNELL, G. R., PRIMROSE, L., PRINGLE, J. H., SHAW, J. A. & FURNESS, P. N. 1998. Reproducibility in the quantification of mRNA levels by RT-PCR-ELISA and RT competitive-PCR-ELISA. *Biotechniques*, 24, 652-658.

- HARRIS, W. J., DANIELL, J. F. & BAXTER, J. W. 1985. Prior cesarean section. A risk factor for adenomyosis? *J Reprod Med*, 30, 173-5.
- HASHIMOTO, M., MOMORI, A., KOSAKA, M., MORI, Y., SHIMOYAMA, T. & AKASHI, K. 1960. Electron microscopic studies on the smooth muscle of the human uterus. *J Jpn Obstet Gynecol Soc*, 7, 115-121.
- HAUTH, E. A., JAEGER, H. J., LIBERA, H., LANGE, S. & FORSTING, M. 2007. MR imaging of the uterus and cervix in healthy women: determination of normal values. *Eur Radiol*, 17, 734-42.
- HAVELOCK, J. C., KELLER, P., MULEBA, N., MAYHEW, B. A., CASEY, B. M., RAINEY, W. E. & WORD, R. A. 2005. Human myometrial gene expression before and during parturition. *Biol Reprod*, 72, 707-19.
- HENDRICKSON, M. R. & KEMPSON, R. L. 1980. Non-neoplastic conditions of the myometrium and uterine serosa. *Surgical pathology of the uterine corpus*. W.B. Saunders, Philadelphia.
- HEVER, A., ROTH, R. B., HEVEZI, P. A., LEE, J., WILLHITE, D., WHITE, E. C., MARIN, E. M., HERRERA, R., ACOSTA, H. M., ACOSTA, A. J. & ZLOTNIK, A. 2006. Molecular characterization of human adenomyosis. *Mol Hum Reprod*, 12, 737-48.
- HIRAI, M., SHIBATA, K., SAGAI, H., SEKIYA, S. & GOLDBERG, B. B. 1995. Transvaginal pulsed and color Doppler sonography for the evaluation of adenomyosis. *J Ultrasound Med*, 14, 529-32.

- HOLDEREGGER, C. & KEEFER, D. 1986. The ontogeny of the mouse estrogen receptor: the pelvic region. *Am J Anat*, 177, 285-97.
- HORGAN, K., COOKE, E., HALLET, M. B. & MANSEL, R. E. 1986. Inhibition of protein kinase C mediated signal transduction by tamoxifen. *Biochem Pharmacol*, 35, 4463-4465.
- HU, J., GRAY, C. A. & SPENCER, T. E. 2004. Gene expression profiling of neonatal mouse uterine development. *Biol Reprod*, 70, 1870-6.
- HUSEBY, R. A. & THURLOW, S. 1982. Effects of prenatal exposure of mice to "low-dose" diethylstilbestrol and the development of adenomyosis associated with evidence of hyperprolactinemia. *Am J Obstet Gynecol*, 144, 939-49.
- IGUCHI, T. & SATO, T. 2000. Endocrine disruption and developmental abnormalities of female reproduction. *Am Zool*, 40, 402-411.
- IJLAND, M., EVERS, J. L., DUNSELMAN, G. A., VOLOVICS, L. & HOOGLAND, H. J. 1997. Relation between endometrial wavelike activity and fecundability in spontaneous cycles. *Fertil Steril*, 67, 492-6.
- IRISAWA, S. & IGUCHI, T. 1990. Critical period of induction by tamoxifen of genital organ abnormalities in female mice. *In Vivo*, 4, 175-9.
- IWAI, M., KANZAKI, H., FUJIMOTO, M., KOJIMA, K., HATAYAMA, H., INOUE, T., HIGUCHI, T., NAKAYAMA, H., MORI, T. & FUJITA, J. 1995. Regulation of sex steroid receptor gene expression by progesterone and testosterone in cultured human endometrial stromal cells. *J Clin Endocrinol Metab*, 80, 450-454.

- JEFFCOATE, T. N. & POTTER, A. L. 1934. Endometriosis as a manifestation of ovarian dysfunction. *J Obstet Gynaecol Br Commonw*, 41, 684-707.
- JEFFERSON, W. N., COUSE, J. F., BANKS, E. P., KORACH, K. S. & NEWBOLD, R. R. 2000. Expression of estrogen receptor beta is developmentally regulated in reproductive tissues of male and female mice. *Biol Reprod*, 62, 310-7.
- JIANG, X., HITCHCOCK, A., BRYAN, E. J., WATSON, R. H., ENGLEFIELD, P., THOMAS, E. J. & CAMPBELL, I. G. 1996. Microsatellite analysis of endometriosis reveals loss of heterozygosity at candidate ovarian tumor suppressor gene loci. *Cancer Res*, 56, 3534-9.
- JONES, J. L., ROYALL, J. E., CRITCHLEY, D. R. & WALKER, R. A. 1997. Modulation of myoepithelial-associated alpha6beta4 integrin in a breast cancer cell line alters invasive potential. *Exp Cell Res*, 235, 325-33.
- JONES, J. L., SHAW, J. A., PRINGLE, J. H. & WALKER, R. A. 2003. Primary breast myoepithelial cells exert an invasion-suppressor effect on breast cancer cells via paracrine down regulation of MMP expression in fibroblasts and tumour cells. *J Pathol*, 201, 562-572.
- JUANG, C. M., CHOU, P., YEN, M. S., TWU, N. F., HORNG, H. C. & HSU, W. L. 2007. Adenomyosis and risk of preterm delivery. *Bjog*, 114, 165-9.
- KALLURI, R. 2009. EMT: when epithelial cells decide to become mesenchymal-like cells. *J Clin Invest*, 119, 1417-1419.
- KALLURI, R. & NEILSON, E. G. 2003. Epithelial-mesenchymal transition and its implications for fibrosis. *J Clin Invest*, 112, 1776-1784.

- KANEHISA, M. & GOTO, S. 2000. KEGG: kyoto encyclopedia of genes and genomes. *Nucleic Acids Res*, 28, 27-30.
- KANEHISA, M., GOTO, S., FURUMICHI, M., TANABE, M. & HIRAKAWA, M. 2009. KEGG for representation and analysis of molecular networks involving diseases and drugs. *Nucleic Acids Res*.
- KANEHISA, M., GOTO, S., HATTORI, M., AOKI-KINOSHITA, K. F., ITOH, M., KAWASHIMA, S., KATAYAMA, T., ARAKI, M. & HIRAKAWA, M. 2006. From genomics to chemical genomics: new developments in KEGG. *Nucleic Acids Res*, 34, D354-7.
- KIDA, H. 1994. [Histological analysis of spontaneous adenomyosis-like changes in recombinant inbred mouse uterus (SMXA mouse)--a novel animal model for adenomyosis]. *Nippon Sanka Fujinka Gakkai Zasshi*, 46, 323-30.
- KILKKU, P., ERKKOLA, R. & GRONROOS, M. 1984. Non-specificity of symptoms related to adenomyosis. A prospective comparative survey. *Acta Obstet Gynecol Scand*, 63, 229-31.
- KING, A. 2000. Uterine leukocytes and decidualization. *Hum Reprod Update*, 6, 28-36.
- KING, R. J., TOWNSEND, P. T., WHITEHEAD, M. I., YOUNG, O. & TAYLOR, R. W. 1981. Biochemical analyses of separated epithelium and stroma from endometria of premenopausal and postmenopausal women receiving estrogen and progestins. *J Steroid Biochem*, 14, 979-987.
- KOCAK, I., YANIK, F. & USTUN, C. 1998. Transvaginal ultrasound in the diagnosis of diffuse adenomyosis. *Int J Gynaecol Obstet*, 62, 293-294.

- KONISHI, I., FUJII, S., OKAMURA, H. & MORI, T. 1984. Development of smooth muscle in the human fetal uterus: an ultrastructural study. *J Anat*, 139, 239-252.
- KORACH, K. S. 1994. Insights from the study of animals lacking functional estrogen receptor. *Science*, 266, 1524-1527.
- KOSHIYAMA, M., KONISHI, I., NANBU, K., NANBU, Y., MANDAI, M., KOMATSU, T., YAMAMOTO, S., MORI, T. & FUJII, S. 1995. Immunohistochemical localization of heat shock proteins hsp70 and hsp90 in the human endometrium: correlation with sex steroid receptors and ki-67 antigen expression. *J Clin Endocrinol Metab*, 80, 1106-1112.
- KOSTRZEWSKA, A., LAUDANSKI, T. & BATRA, S. 1997. Potent inhibition by tamoxifen of spontaneous and agonist-induced contractions of the human myometrium and intramyometrial arteries. *Am J Obstet Gynecol*, 176, 381-386.
- KRAUS, W. L. & KATZENELLENBOGEN, B. S. 1993. Regulation of progesterone receptor gene expression and growth in the rat uterus: modulation of estrogen actions by progesterone and sex steroid hormone antagonists. *Endocrinology*, 132, 2371-2379.
- KROEGER, E. A. & BRANDES, L. J. 1985. Evidence that tamoxifen is a histamine antagonist. *Biochem Biophys Res Commun*, 131, 750-755.
- KUNZ, G., BEIL, D., HUPPERT, P. & LEYENDECKER, G. 2000. Structural abnormalities of the uterine wall in women with endometriosis and infertility visualized by vaginal sonography and magnetic resonance imaging. *Hum Reprod*, 15, 76-82.

- KUNZ, G., BEIL, D., HUPPERT, P., NOE, M., KISSLER, S. & LEYENDECKER, G. 2005. Adenomyosis in endometriosis--prevalence and impact on fertility. Evidence from magnetic resonance imaging. *Hum Reprod*, 20, 2309-16.
- KUNZ, G., BELL, D., DEININGER, H., WILDT, L. & LEYENDECKER, G. 1996. The dynamics of rapid sperm transport through the female genital tract. Evidence from vaginal sonography of uterine peristalsis (VSUP) and hysterosalpingoscintigraphy (HSSG). *Hum Reprod*, 11, 627-632.
- KUNZ, G. & LEYENDECKER, G. 2002. Uterine peristaltic activity during the menstrual cycle: characterization, regulation, function and dysfunction. *Reprod Biomed Online*, 4 Suppl 3, 5-9.
- KURITA, T., COOKE, P. S. & CUNHA, G. R. 2001. Epithelial-stromal tissue interaction in paramesonephric (Mullerian) epithelial differentiation. *Dev Biol*, 240, 194-211.
- LAM, H. Y. 1984. Tamoxifen is a calmodulin antagonist in the activation of cAMP phosphodiesterase. *Biochem Biophys Res Commun*, 118, 27-32.
- LANE, B. P. 1965. Alterations in the cytologic detail of intestinal smooth muscle cells in various stages of contraction. *J Cell Biol*, 27, 199-213.
- LAZARIDES, E. 1980. Intermediate filaments as mechanical integrators of cellular space. *Nature (Lond.)*, 238, 249-256.
- LEE, J. K., GERSELL, D. J., BALFE, D. M., WORTHINGTON, J. L., PICUS, D. & GAPP, G. 1985. The uterus: in vitro MR-anatomic correlation of normal and abnormal specimens. *Radiology*, 157, 175-9.

- LEE, N. C., DICKER, R. C., RUBIN, G. L. & ORY, H. W. 1984. Confirmation of the preoperative diagnoses for hysterectomy. *Am J Obstet Gynecol*, 150, 283-7.
- LEE, S. L., BUSMANIS, I. & TAN, A. Year. 3D-angio of adenomyotic uteri. *In*: 2nd World congress on 3D Ultrasound in Obstetrics and Gynecology, October 1999 1999 Las Vegas.
- LEI, Z. M., RAO, C. V., LINCOLN, S. R. & ACKERMANN, D. M. 1993. Increased expression of human chorionic gonadotropin/human luteinizing hormone receptors in adenomyosis. *J Clin Endocrinol Metab*, 76, 763-8.
- LESSEY, B. A., KILLIAM, A. S. P., METZGER, D. A., HANEY, A. F., GREENE, G. L. & MCCARTY, K. S., JR. 1988. Immunohistochemical analysis of human uterine estrogen and progesterone receptors throughout the menstrual cycle. *J Clin Endocrinol Metab*, 67, 334-340.
- LEVGUR, M., ABADI, M. A. & TUCKER, A. 2000. Adenomyosis: symptoms, histology, and pregnancy terminations. *Obstet Gynecol*, 95, 688-91.
- LEWINSKI, H. 1931. Beitrag zur Frage der Adenomyosis. *Zentralbl Gynakol*, 55, 2163.
- LEYENDECKER, G., HERBERTZ, M., KUNZ, G. & MALL, G. 2002. Endometriosis results from the dislocation of basal endometrium. *Hum Reprod*, 17, 2725-36.
- LEYENDECKER, G., KUNZ, G., NOE, M., HERBERTZ, M. & MALL, G. 1998. Endometriosis: a dysfunction and disease of the archimetra. *Hum Reprod Update*, 4, 752-62.

- LEYENDECKER, G., KUNZ, G., WILDT, L., BEIL, D. & DEININGER, H. 1996. Uterine hyperperistalsis and dysperistalsis as dysfunctions of the mechanism of rapid sperm transport in patients with endometriosis and infertility. *Hum Reprod*, 11, 1542-51.
- LI, S. 1994. Relationship between cellular DNA synthesis, PCNA expression and sex steroid hormone receptor status in the developing mouse ovary, uterus and oviduct. *Histochemistry*, 102, 405-413.
- LIN, L. I.-K. 1989. A concordance correlation coefficient to evaluate reproducibility. *Biometrics*, 45, 255-268.
- LIN, L. I.-K. 2000. A note on the concordance correlation coefficient. *Biometrics*, 56, 324-325.
- LIN, Z., LU, M.-H., SCHULTHEISS, T., CHOI, J., HOLTZER, S., DILULLO, C., FISCHMAN, D. A. & HOLTZER, H. 1994. Sequential appearance of muscle-specific proteins in myoblasts as a function of time after cell division: evidence for a conserved myoblast differentiation program in skeletal muscle. *Cell Motil Cytoskeleton*, 29, 1-19.
- LIPSCHUTZ, A., IGLESIAS, R., PANASEVICH, V. I. & SALINAS, S. 1967. Pathological changes induced in the uterus of mice with the prolonged administration of progesterone and 19-nor-contraceptives. *Br J Cancer*, 21, 160-5.
- LIPTON, A. & MORRIS, I. D. 1986. Calcium antagonism by the antioestrogen tamoxifen. *Cancer Chemother Pharmacol*, 18, 17-20.

- LITOVKIN, K. V., IVANOVA, O. V., BAUER, A., HOHEISEL, J. D., BUBNOV, V. V. & ZAPOROZHAN, V. N. 2008. Microarray study of gene expression in uterine leiomyoma. *Exp Oncol*, 30, 106-11.
- LIU, P. & HWANG, J. T. 2007. Quick calculation for sample size while controlling false discovery rate with application to microarray analysis. *Bioinformatics*, 23, 739-746.
- LIVAK, K. J. & SCHMITTGEN, T. D. 2001. Analysis of relative gene expression data using real-time quantitative PCR and the 2(-Delta Delta C(T)) Method. *Methods*, 25, 402-408.
- LOUD, A. V., OLIVETTI, G. & ANVERSA, P. 1983. Morphometric measurement of cellular hypertrophy. *Lab Invest*, 49, 230-234.
- LOWY, J. & SMALL, J. V. 1970. The organization of myosin and actin in vertebrate smooth muscle. *Nature*, 227, 46-51.
- LUO, X., DING, L., XU, J. & CHEGINI, N. 2005a. Gene expression profiling of leiomyoma and myometrial smooth muscle cells in response to transforming growth factor-beta. *Endocrinology*, 146, 1097-1118.
- LUO, X., DING, L., XU, J., WILLIAMS, R. S. & CHEGINI, N. 2005b. Leiomyoma and myometrial gene expression profiles and their responses to gonadotropin-releasing hormone analog therapy. *Endocrinology*, 146, 1074-96.
- LYONS, E. A., TAYLOR, P. J., ZHENG, X. H., BALLARD, G., LEVI, C. S. & KRENTSER, J. V. 1991. Characterisation of subendometrial myometrial

- contractions throughout the menstrual cycle in normal fertile women. *Fertil Steril*, 55, 771-774.
- MAI, K. T., YAZDI, H. M., PERKINS, D. G. & PARKS, W. 1997. Pathogenetic role of the stromal cells in endometriosis and adenomyosis. *Histopathology*, 30, 430-42.
- MARCUS, C. C. 1961. Relationship of adenomyosis uteri to endometrial hyperplasia and endometrial carcinoma. *Am J Obstet Gynecol*, 82, 408-16.
- MARK, A. S., HRICAK, H., HEINRICHS, L. W., HENDRICKSON, M. R., WINKLER, M. L., BACHICA, J. A. & STICKLER, J. E. 1987. Adenomyosis and leiomyoma: differential diagnosis with MR imaging. *Radiology*, 163, 527-9.
- MARK, J. S. T. 1956. An electron microscopy study of uterine smooth muscle. *Anat Rec*, 125, 473-491.
- MARSH, E. E., LIN, Z., YIN, P., MILAD, M., CHAKRAVARTI, D. & BULUN, S. E. 2008. Differential expression of microRNA species in human uterine leiomyoma versus normal myometrium. *Fertil Steril*, 89, 1771-6.
- MARTIN, L., FINN, C. A. & TRINDER, G. 1973. Hypertrophy and hyperplasia in the mouse uterus after oestrogen treatment: an autoradiographic study. *J Endocrinol*, 56, 133-44.
- MCCANN, T. O. & MYERS, R. E. 1970. Endometriosis in rhesus monkeys. *Am J Obstet Gynecol*, 106, 516-23.
- MCCARTHY, S., SCOTT, G., MAJUMDAR, S. & AL., E. 1989a. Uterine junctional zone: MR study of water content and histologic examination of water content and relaxation properties. *Radiology*, 171, 241-243.

- MCCARTHY, S., SCOTT, G., MAJUMDAR, S., SHAPIRO, B., THOMPSON, S., LANGE, R. & GORE, J. 1989b. Uterine junctional zone: MR study of water content and relaxation properties. *Radiology*, 171, 241-3.
- MCCAUSLAND, A. M. 1992. Hysteroscopic myometrial biopsy: its use in diagnosing adenomyosis and its clinical application. *Am J Obstet Gynecol*, 166, 1619-26; discussion 1626-8.
- MCCORMACK, S. A. & GLASSER, S. R. 1980. Differential response of individual uterine cell types from immature rats treated with estradiol. *Endocrinology*, 106, 1634-1649.
- MERICKSAY, M., KITAJEWSKI, J. & SASSOON, D. 2004. Wnt5a is required for proper epithelial-mesenchymal interactions in the uterus. *Development*, 131, 2061-2072.
- MERTENS, H. J. M. M., HEINEMAN, M. J., THEUNISSEN, P. H. M. H., DE JONG, F. H. & EVERS, J. L. H. 2001. Androgen, estrogen and progesterone receptor expression in the human uterus during the menstrual cycle. *Eur J Obstet Gynecol Reprod Biol*, 98, 58-65.
- METAXA-MARIATOU, V., MCGAVIGAN, C. J., ROBERTSON, K., STEWART, C., CAMERON, I. T. & CAMPBELL, S. 2002. Elastin distribution in the myometrial and vascular smooth muscle of the human uterus. *Mol Hum Reprod*, 8, 559-565.
- MIKELS, A. J. & NUSSE, R. 2006. Purified Wnt5a protein activates or inhibits beta-catenin-TCF signaling depending on receptor context. *Plos Biology*, 4, e115.

- MILLER, C., PAVLOVA, A. & SASSOON, D. A. 1998. Differential expression patterns of Wnt genes in the murine female reproductive tract during development and the estrous cycle. *Mech Dev*, 76, 91-9.
- MILNER, D. J., WEITZER, G., TRAN, D., BRADLEY, A. & CAPETANAKI, Y. 1996. Disruption of muscle architecture and myocardial degeneration in mice lacking desmin. *J Cell Biol*, 134, 1255-1270.
- MOGGS, J. G., ASHBY, J., TINWELL, H., LIM, F. L., MOORE, D. J., KIMBER, I. & AL., E. 2004. The need to decide if all estrogens are intrinsically similar. *Environ Health Perspect*, 112, 1137-1142.
- MOLITOR, J. J. 1971. Adenomyosis: a clinical and pathological appraisal. *Am J Obstet Gynecol*, 110, 275-84.
- MOLL, R., LEVY, R., CZERNOBILSKY, B., HOHLWEG-MAJERT, P., DALLENBACH-HELLWEG, G. & FRANKE, W. W. 1983. Cytokeratins of normal epithelial and some neoplasms of the female genital tract. *Lab Invest*, 49, 599-610.
- MORI, T. & NAGASAWA, H. 1983. Mechanisms of development of prolactin-induced adenomyosis in mice. *Acta Anat (Basel)*, 116, 46-54.
- MORI, T., NAGASAWA, H. & NAKAJIMA, Y. 1982. Strain-difference in the induction of adenomyosis by intrauterine pituitary grafting in mice. *Lab Anim Sci*, 32, 40-1.
- MORI, T., NAGASAWA, H. & TAKAHASHI, S. 1981. The induction of adenomyosis in mice by intrauterine pituitary isografts. *Life Sci*, 29, 1277-82.

- MORI, T., NAKAHASHI, K., KYOKUWA, M., YAMASAKI, S. & NAGASAWA, H. 2002. A matrix metalloproteinase inhibitor, ONO-4817, retards the development of mammary tumor and the progression of uterine adenomyosis in mice. *Anticancer Res*, 22, 3985-8.
- MORI, T., SINGTRIPPOP, T. & KAWASHIMA, S. 1991. Animal model of uterine adenomyosis: is prolactin a potent inducer of adenomyosis in mice? *Am J Obstet Gynecol*, 165, 232-4.
- MYLONAS, I., JESCHKE, U., SHABANI, N., KUHN, C., BALLE, A., KRIEGEL, S., KUPKA, M. S. & FRIESE, K. 2004. Immunohistochemical analysis of estrogen receptor alpha, estrogen receptor beta and progesterone receptor in normal human endometrium. *Acta Histochem*, 106, 245-252.
- NATOLI, A. K., MEDLEY, T. L., AHIMASTOS, A. A., DREW, B. G., THEARLE, D. J., DILLEY, R. J. & KINGWELL, B. A. 2005. Sex steroids modulate human aortic smooth muscle cell matrix protein deposition and matrix metalloproteinase expression. *Hypertension*, 46, 1129-1134.
- NELSON, W. J. & NUSSE, R. 2004. Convergence of Wnt,  $\beta$ -Catenin, and Cadherin pathways. *Science*, 303, 1483-1487.
- NIETO, M. A. 2002. The snail superfamily of zinc-finger transcription factors. *Nat Rev Mol Cell Biol*, 3, 155-166.
- NIKKANEN, V. & PUNNONEN, R. 1980. Clinical significance of adenomyosis. *Ann Chir Gynaecol*, 69, 278-80.

- NOE, N., KUNZ, G., HERBERTZ, M., MALL, G. & LEYENDECKER, G. 1999. The cyclic pattern of the immunocytochemical expression of oestrogen and progesterone receptors in human myometrial and endometrial layers: characterization of the endometrial-subendometrial unit. *Hum Reprod*, 14, 190-197.
- NORTH, A. J., GALAZKIEWICZ, B., BYERS, T. J., GLENNEY, J. R. J. & SMALL, J. V. 1993. Complementary distributions of vinculin and dystrophin define two distinct sarcolemma domains in smooth muscle. *J Cell Biol*, 120, 1159-1167.
- NOYES, R. W. & HAMAN, J. O. 1953. Accuracy of endometrial dating; correlation of endometrial dating with basal body temperature and menses. *Fertil Steril*, 4, 504-17.
- O'BRIEN, M., MORRISON, J. J. & SMITH, T. J. 2008. Upregulation of PSCDBP, TLR2, TWIST1, FLJ35382, EDNRB, and RGS12 gene expression in human myometrium at labor. *Reprod Sci*, 15, 382-93.
- OEHLER, M. K., GRESCHIK, H., FISCHER, D. C., TONG, X., SCHUELE, R. & KIEBACK, D. G. 2004. Functional characterization of somatic point mutations of the human estrogen receptor alpha (hERalpha) in adenomyosis uteri. *Mol Hum Reprod*, 10, 853-60.
- OLIVER, C., MONTES, M. J., A., G. J. & AL., E. 1999. Human decidual stromal cells express  $\alpha$ -smooth muscle actin and show ultrastructural similarities with myofibroblasts. *Hum Reprod*, 14, 1599-1605.

- OSTRANDER, P. L., MILLS, K. T. & BERN, H. A. 1985a. Long-term responses of the mouse uterus to neonatal diethylstilbestrol treatment and to later sex hormone exposure. *J Natl Cancer Inst*, 74, 121-35.
- OSTRANDER, P. L., MILLS, K. T. & BERN, H. A. 1985b. Long-term responses of the mouse uterus to neonatal diethylstilbestrol treatment and to later sex hormone exposure. *J N C I*, 74, 121-135.
- OTA, H. & IGARASHI, S. 1993. Expression of major histocompatibility complex class II antigen in endometriotic tissue in patients with endometriosis and adenomyosis. *Fertil Steril*, 60, 834-8.
- OTA, H., IGARASHI, S., HATAZAWA, J. & TANAKA, T. 1998. Is adenomyosis an immune disease? *Hum Reprod Update*, 4, 360-7.
- OTA, H., IGARASHI, S., HATAZAWA, J. & TANAKA, T. 1999a. Endometriosis and free radicals. *Gynecol Obstet Invest*, 48 Suppl 1, 29-35.
- OTA, H., IGARASHI, S., HATAZAWA, J. & TANAKA, T. 1999b. Immunohistochemical assessment of superoxide dismutase expression in the endometrium in endometriosis and adenomyosis. *Fertil Steril*, 72, 129-34.
- OTA, H., IGARASHI, S., KATO, N. & TANAKA, T. 2000. Aberrant expression of glutathione peroxidase in eutopic and ectopic endometrium in endometriosis and adenomyosis. *Fertil Steril*, 74, 313-8.
- OTA, H., IGARASHI, S., SASAKI, M. & TANAKA, T. 2001a. Distribution of cyclooxygenase-2 in eutopic and ectopic endometrium in endometriosis and adenomyosis. *Hum Reprod*, 16, 561-6.

- OTA, H., IGARASHI, S. & TANAKA, T. 1996. Expression of gamma delta T cells and adhesion molecules in endometriotic tissue in patients with endometriosis and adenomyosis. *Am J Reprod Immunol*, 35, 477-82.
- OTA, H., IGARASHI, S. & TANAKA, T. 2001b. Xanthine oxidase in eutopic and ectopic endometrium in endometriosis and adenomyosis. *Fertil Steril*, 75, 785-90.
- OTA, H., MAKI, M., SHIDARA, Y., KODAMA, H., TAKAHASHI, H., HAYAKAWA, M., FUJIMORI, R., KUSHIMA, T. & OHTOMO, K. 1992. Effects of danazol at the immunologic level in patients with adenomyosis, with special reference to autoantibodies: a multi-center cooperative study. *Am J Obstet Gynecol*, 167, 481-6.
- OTA, H. & TANAKA, T. 1997. Integrin adhesion molecules in the endometrial glandular epithelium in patients with endometriosis or adenomyosis. *J Obstet Gynaecol Res*, 23, 485-91.
- OTA, H. & TANAKA, T. 2001. [Eutopic and ectopic endometrium in endometriosis]. *Nippon Rinsho*, 59 Suppl 1, 37-43.
- OTSUKI, Y., MISAKI, O., SUGIMOTO, O., ITO, Y., TSUJIMOTO, Y. & AKAO, Y. 1994. Cyclic bcl-2 gene expression in human uterine endometrium during menstrual cycle. *Lancet*, 344, 28-29.
- OWENS, G. K., RABINOVITCH, P. S. & SCHWARTZ, S. M. 1981. Smooth muscle cell hypertrophy versus hyperplasia in hypertension. *Proc Natl Acad Sci U S A*, 78, 7759-7763.

- OWOLABI, T. O. & STRICKLER, R. C. 1977. Adenomyosis: a neglected diagnosis. *Obstet Gynecol*, 50, 424-7.
- PAN, Q., LUO, X. & CHEGINI, N. 2008. Differential expression of microRNAs in myometrium and leiomyomas and regulation by ovarian steroids. *J Cell Mol Med*, 12, 227-40.
- PANDIS, N., KARAIKOS, C., BARDI, G., SFIKAS, K., TSERKEZOGLOU, A., FOTIOU, S. & HEIM, S. 1995. Chromosome analysis of uterine adenomyosis. Detection of the leiomyoma-associated del(7q) in three cases. *Cancer Genet Cytogenet*, 80, 118-20.
- PANGANAMAMULA, U. R., HARMANLI, O. H., ISIK-AKBAY, E. F., GROTEGUT, C. A., DANDOLU, V. & GAUGHAN, J. P. 2004. Is prior uterine surgery a risk factor for adenomyosis? *Obstet Gynecol*, 104, 1034-8.
- PARAZZINI, F., VERCELLINI, P., PANAZZA, S., CHATENOU, L., OLDANI, S. & CROSIGNANI, P. G. 1997. Risk factors for adenomyosis. *Hum Reprod*, 12, 1275-9.
- PARK, K.-Y., DALAKAS, M. C., SEMINO-MORA, C., LEE, H.-S., LITVAK, S., TAKEDA, K., FERRANS, V. J. & GOLDFARB, L. G. 2000. Sporadic cardiac and skeletal myopathy caused by a de novo desmin mutation. *Clin Genet*, 57, 423-429.
- PARROTT, E., BUTTERWORTH, M., GREEN, A., WHITE, I. N. & GREAVES, P. 2001. Adenomyosis--a result of disordered stromal differentiation. *Am J Pathol*, 159, 623-30.

- PENG, L., WEN, Y., HAN, Y., WEI, A., SHI, G., MIZUGUCHI, M., LEE, P.,  
HERNANDO, E., MITTAL, K. & WEI, J. J. 2009. Expression of insulin-like  
growth factors (IGFs) and IGF signaling: molecular complexity in uterine  
leiomyomas. *Fertil Steril*, 91, 2664-75.
- PHILLIPS, D. R. 1995. Endometrial ablation for postmenopausal uterine bleeding  
induced by hormone replacement therapy. *J Am Assoc Gynecol Laparosc*, 2,  
389-93.
- PICO, A., KELDER, T., VAN IERSEL, M., HANSPERS, K., CONKLIN, B. &  
EVELO, C. 2008. WikiPathways  
WikiPathways: pathway editing for the people. *PLoS biology*, 6, e184.
- PRENTICE, A., RANDALL, B. J., WEDDELL, A., MCGILL, A., HENRY, L.,  
HORNE, C. H. & THOMAS, E. J. 1992. Ovarian steroid receptor expression in  
endometriosis and in two potential parent epithelia: endometrium and peritoneal  
mesothelium. *Hum Reprod*, 7, 1318-25.
- PROPST, A. M., QUADE, B. J., GARGIULO, A. R., NOWAK, R. A. & STEWART,  
E. A. 2001. Adenomyosis demonstrates increased expression of the basic  
fibroblast growth factor receptor/ligand system compared with autologous  
endometrium. *Menopause*, 8, 368-71.
- QUINN, M. 2007. Uterine innervation in adenomyosis. *J Obstet Gynaecol*, 27, 287-91.
- RAJU, G. C., NARAYNSINGH, V., WOO, J. & JANKEY, N. 1988. Adenomyosis  
uteri: a study of 416 cases. *Aust N Z J Obstet Gynaecol*, 28, 72-3.

- RAO, B. N. & PERSAUD, V. 1982. Adenomyosis uteri. Report on a 15-year study (1966-1980) at the University Hospital of the West Indies. *West Indian Med J*, 31, 205-12.
- REINHOLD, C., ATRI, M., MEHIO, A., ZAKARIAN, R., ALDIS, A. E. & BRET, P. M. 1995. Diffuse uterine adenomyosis: morphologic criteria and diagnostic accuracy of endovaginal sonography. *Radiology*, 197, 609-14.
- REINHOLD, C., MCCARTHY, S., BRET, P. M., MEHIO, A., ATRI, M., ZAKARIAN, R., GLAUDE, Y., LIANG, L. & SEYMOUR, R. J. 1996. Diffuse adenomyosis: comparison of endovaginal US and MR imaging with histopathologic correlation. *Radiology*, 199, 151-8.
- REINHOLD, C., TAFAZOLI, F. & WANG, L. 1998. Imaging features of adenomyosis. *Hum Reprod Update*, 4, 337-49.
- RICHARDS, P. A., RICHARDS, P. D. G. & TILTMAN, A. J. 1998. The ultrastructure of fibromyomatous myometrium and its relationship to infertility. *Hum Reprod Update*, 4, 520-525.
- RIRIE, K. M., RASMUSSEN, R. P. & WITTEWER, C. T. 1997. Product differentiation by analysis of DNA melting curves during the polymerase chain reaction. *Anal Biochem*, 245, 154-160.
- ROBBOY, S. J., TAGUCHI, O. & CUNHA, G. R. 1982. Normal development of the human female reproductive tract and alterations resulting from experimental exposure to diethylstilbesterol. *Hum Pathol*, 13, 191-198.

- ROKITANSKY, K. 1860. Ueber uterusdruesen-neubildung. *Z Gesellschaft Aertze Wien*, 16, 577-581.
- ROMBERGER, D. J. 1997. Fibronectin. *Int J Biochem Cell Biol*, 29, 939-943.
- ROTH, T. M., KLETT, C. & COWAN, B. D. 2007. Expression profile of several genes in human myometrium and uterine leiomyoma. *Fertil Steril*, 87, 635-41.
- RUSSELL, P. & FRASER, I. S. 1998. The practical assessment of endometrial morphology and function. *In: CAMERON, I., FRASER, I. & SMITH, S. (eds.) Clinical disorders of the menstrual cycle and endometrium*. Oxford: Oxford University Press.
- SAHIN, A. A., SILVA, E. G., LANDON, G., ORDONEZ, N. G. & GERSHENSON, D. M. 1989. Endometrial tissue in myometrial vessels not associated with menstruation. *Int J Gynecol Pathol*, 8, 139-46.
- SAKAMOTO, S., MORI, T., SINGTRIPOP, T., KAWASHIMA, S., SUZUKI, S., KUDO, H., SAWAKI, K. & NAGASAWA, H. 1992. Increase of DNA synthesis in uterine adenomyosis in mice with ectopic pituitary isograft. *Acta Anat (Basel)*, 145, 162-6.
- SAMMOUR, A., PIRWANY, I., USUBUTUN, A., ARSENEAU, J. & TULANDI, T. 2002. Correlations between extent and spread of adenomyosis and clinical symptoms. *Gynecol Obstet Invest*, 54, 213-6.
- SANBORN, B. M., YUE, C., WANG, W. & DODGE, K. L. 1998. G protein signalling pathways in myometrium: affecting the balance between contraction and relaxation. *Review of Reproduction*, 3, 196-205.

- SAPINO, A., BOSCO, M., CASSONI, P., CASTELLANO, I., ARISIO, R., CSERNI, G., DEI TOS, A. P., FORTUNATI, N., CATALANO, M. G. & BUSSOLATI, G. 2006a. Estrogen receptor-beta is expressed in stromal cells of fibroadenoma and phyllodes tumors of the breast. *Modern Pathology*, 19, 599-606.
- SAPINO, A., BOSCO, M., CASSONI, P., CASTELLANO, I., ARISIO, R., CSERNI, G., DEI TOS, A. P., FORTUNATI, N., CATALANO, M. G. & BUSSOLATI, G. 2006b. Estrogen receptor- $\beta$  is expressed in stromal cells of fibroadenoma and phylloides tumors of the breast. . *Mod Pathol*, 19, 599-606.
- SASAKI, T., FASSLER, R. & HOHENESTER, E. 2004. Laminin: the crux of basement membranes assembly. *J Cell Biol*, 164, 959-963.
- SATO, T., OKAMURA, H., OHTA, Y., HAYASHI, S., TAKASUGI, N. & IGUCHI, T. 1992. Estrogen receptor expressin in genital tract of female mice treated neonatally with diethylstilbestrol. *In Vivo*, 6, 151-156.
- SCHARL, A., VIERBUCHEN, M., GRAUPNER, J., FISCHER, R. & BOLTE, A. 1988. Immunohistochemical study of distribution of estrogen receptors in corpus and cervix uteri. *Arch Gynecol Obstet*, 241, 221-233.
- SCOUTT, L., FLYNN, S. D., LUTHRINGER, D. J., MCCAULEY, T. R. & MCCARTHY, S. M. 1991. Junctional zone of the uterus: correlation of MR imaging and histologic examination of hysterectomy specimens. *Radiology*, 179, 403-407.
- SHAH, S. B., DAVIS, J., WEISLEDER, N., KOSTAVASSILI, I., MCCULLOCH, A. D., RALSTON, E., CAPETANAKI, Y. & LIEBER, R. L. 2004. Structural and

functional roles of desmin in mouse skeletal muscle during passive deformation. *Biophysical Journal*, 86, 2993-3008.

SHAIKH, H. & KHAN, K. S. 1990. Adenomyosis in Pakistani women: four year experience at the Aga Khan University Medical Centre, Karachi. *J Clin Pathol*, 43, 817-9.

SHIOZAWA, T., LI, S.-F., NAKAYAMA, K. & FUJII, S. 1996. Relationship between the expression of cyclins/cyclin-dependent kinases and sex-steroid receptors/Ki67 in normal human endometrial glands and stroma during the menstrual cycle. *Mol Hum Reprod*, 2, 745-752.

SNIJDERS, M. P., DE GOEJI, A. F., DEBETS-TE BAERTS, M. J., ROSCH, M. J., KOUDSTAAL, J. & BOSMAN, F. T. 1992. Immunocytochemical analysis of oestrogen receptors and progesterone receptors in the human uterus throughout the menstrual cycle and after the menopause. *J Reprod Fertil*, 94, 363-371.

STEPHANOU, A., ISENBERG, D. A., NAKAJIMA, K. & LATCHMAN, D. S. 1999. Signal transducer and activator of transcription-1 and heat shock factor-1 interact and activate the transcription of the Hsp-70 and Hsp-90b gene promoters. *J Biol Chem*, 274, 1723-1728.

STEVENSON, S., TAYLOR, A. H., MESKIRI, A., SHARPE, D. T. & THORNTON, M. J. 2008. Differing responses of human follicular and nonfollicular scalp cells in an in vitro wound healing assay: effects of estrogen on vascular endothelial growth factor secretion. *Wound Repair and Regeneration*, 16, 243-253.

STEWART, C. J. R., FARQUHARSON, M. A. & FOULIS, A. K. 1992. The distribution and possible function of gamma-interferon-immunoreactive cells in

- normal endometrium and myometrium. . *Virchows Arch A Pathol Anat Histol*, 420, 419-424.
- STUMPF, W. E., NARBAITZ, R. & SAR, M. 1980. Estrogen receptors in the fetal mouse. *J Steroid Biochem*, 12, 55-64.
- SUIRE, R. A., GOODMAN, D. G. & VALERIO, M. G. 1978. Female reproductive system. *In: BENIRSCHKE, K., GARNER, F. M. & JONES, T. C. (eds.) Pathology of laboratory animals*. New York: Springer-Verlag.
- TABIBZADEH, S. 1991. Induction of HLA-DR expression in endometrial epithelial cells by endometrial T-cells: potential regulatory role of endometrial T-cells in vivo. *J Clin Endocrinol Metab*, 73, 1352-1359.
- TABIBZADEH, S., SUN, X. Z., KONG, Q. F., KASNIC, G., MILLER, J. & SATYASWAROOP, P. G. 1993. Induction of a polarized micro-environment by human T cells and interferon-gamma in three-dimensional spheroids cultures of human endometrial epithelial cells. *Hum Reprod*, 8, 182-193.
- TAMAYA, T., MOTOYAMA, T., OHONO, Y., IDE, N., TSURUSAKI, T. & OKADA, H. 1979. Steroid receptor levels and histology of endometriosis and adenomyosis. *Fertil Steril*, 31, 396-400.
- TANWAR, P. S., LEE, H. J., ZHANG, L., ZUKERBERG, L. R., TAKETO, M. M., RUEDA, B. R. & TEIXEIRA, J. M. 2009. Constitutive activation of Beta-catenin in uterine stroma and smooth muscle leads to the development of mesenchymal tumors in mice. *Biol Reprod*, 81, 545-52.

- TAYLOR, A. H. & AL-AZZAWI, F. 2000. Immunolocalisation of oestrogen receptor beta in human tissues. *J Mol Endocrinol*, 24, 145-155.
- THIERY, J. P. 2002. Epithelial-mesenchymal transitions in tumour progression. *Nat Rev Cancer*, 2, 442-454.
- THOMAS, J. S., JR. & CLARK, J. F. 1989. Adenomyosis: a retrospective view. *J Natl Med Assoc*, 81, 969-72.
- THORNTON, M. J., TAYLOR, A. H., MULLIGAN, K. T., AL-AZZAWI, F., LYON, C. C., O'DRISCOLL, J. & MESSENGER, A. G. 2003. Oestrogen receptor beta is the predominant oestrogen receptor in human scalp skin. *Exp Dermatol*, 12, 181-190.
- TRAPIDO, E. J., BRINTON, L. A., SCHAIRER, C. & HOOVER, R. 1984. Estrogen replacement therapy and benign breast disease. *J Natl Cancer Inst*, 73, 1101-1105.
- TSAI, R. Y., KITTAPPA, R. & MCKAY, R. D. 2002. Plasticity, niches, and the use of stem cells. *Dev Cell*, 2, 707-712.
- TSENG, L. & ZHU, H. H. 1997. Regulation of progesterone receptor messenger ribonucleic acid by progesterin in human endometrial stromal cells. *Biol Reprod*, 57, 1360-1366.
- TULAC, S., NAYAK, N. R., KAO, L. C., VAN WAES, M., HUANG, J., LOBO, S., GERMEYER, A., LESSEY, B. A., TAYLOR, R. N., SUCHANEK, E. & GIUDICE, L. C. 2003. Identification, Characterization, and Regulation of the

Canonical Wnt Signaling Pathway in Human Endometrium. *J Clin Endocrinol Metab*, 88, 3860-3866.

TUXHORN, J. A., AYALA, G. E., SMITH, M. J., SMITH, V. C., DANG, T. D. & ROWLEY, D. R. 2002. Reactive stroma in human prostate cancer: induction of myofibroblast phenotype and extracellular matrix remodeling. *Clin Cancer Res*, 8, 2912-23.

UDUWELA, A. S., PERERA, M. A., AIQING, L. & FRASER, I. S. 2000. Endometrial-myometrial interface: relationship to adenomyosis and changes in pregnancy. *Obstet Gynecol Surv*, 55, 390-400.

UEKI, K., KUMAGAI, K., YAMASHITA, H., LI, Z. L., UEKI, M. & OTSUKI, Y. 2004. Expression of apoptosis-related proteins in adenomyotic uteri treated with danazol and GnRH agonists. *Int J Gynecol Pathol*, 23, 248-58.

VAN DER WALT, L. A., SANFILIPPO, J. S., SIEGEL, J. E. & WITTLIFF, J. L. 1986. Estrogen and progestin receptors in human uterus: reference ranges of clinical conditions. *Clin Physiol Biochem*, 4, 217-28.

VAN IERSEL, M., KELDER, T., PICO, A., HANSPERS, K., COORT, S., CONKLIN, B. & EVELO, C. 2008. Presenting and exploring biological pathways with PathVisio. *BMC Bioinformatics*, 9, 399.

VAVILIS, D., AGORASTOS, T., TZAFETAS, J., LOUFOPOULOS, A., VAKIANI, M., CONSTANTINIDIS, T., PATSIAOURA, K. & BONTIS, J. 1997. Adenomyosis at hysterectomy: prevalence and relationship to operative findings and reproductive and menstrual factors. *Clin Exp Obstet Gynecol*, 24, 36-8.

- VERCELLINI, P., PARAZZINI, F., OLDANI, S., PANAZZA, S., BRAMANTE, T. & CROSIGNANI, P. G. 1995. Adenomyosis at hysterectomy: a study on frequency distribution and patient characteristics. *Hum Reprod*, 10, 1160-2.
- VON RECKLINGHAUSEN, F. 1896. Die adenomyomata und cystadenomata der uterus und tubenwandug: ihre abkunft von resten des Wolff'schen koerpers. *August Hirschwald Verlag, Berlin*.
- WAHAB, M., THOMPSON, J., HAMID, B., DEEN, S. & AL-AZZAWI, F. 1999a. Endometrial histomorphometry of trimegestone-based sequential hormone replacement therapy: a weighted comparison with the endometrium of the natural cycle. *Hum Reprod*, 14, 2609-2618.
- WAHAB, M., THOMPSON, J. D. & AL-AZZAWI, F. 1999b. The distribution of endometrial leukocytes and their proliferation markers in trimegestone-treated postmenopausal women compared to the endometrium of the natural cycle: a dose-ranging study. *Hum Reprod*, 14, 1201-1206.
- WANG, H., MAHADEVAPPA, M., YAMAMOTO, K., WEN, Y., CHEN, B., WARRINGTON, J. A. & POLAN, M. L. 2003. Distinctive proliferative phase differences in gene expression in human myometrium and leiomyomata. *Fertil Steril*, 80, 266-76.
- WANG, P. H., SHYONG, W. Y., LIN, C. H., CHEN, Y. J., LI, Y. F., CHAO, H. T. & YUAN, C. C. 2002. Analysis of genetic aberrations in uterine adenomyosis using comparative genomic hybridization. *Anal Quant Cytol Histol*, 24, 1-6.
- WERTH, R. & GRUSDEW, W. 1898. Untersuchungen uber die entwicklung und morphologie der menschlichen uterusmuskulatur. *Arch Gynakol*, 55, 325-409.

- WETZSTEIN, R. 1965. Der Uterusmuskel: Morphologie. *Arch Gynecol*, 202, 1-13.
- WHITE, C. A., ROBB, L. & SALAMONSEN, L. A. 2004. Uterine extracellular matrix components are altered during defective decidualization in interleukin-11 receptor alpha deficient mice. *Reprod Biol Endocrinol*, 2, 76.
- WHITTED, R., ABADI, M. A., VOIGL, B. & MENDEZ, L. 2000. Does cesarean delivery increase the prevalence of adenomyosis? A retrospective review. *Obstet Gynecol*, 95, S83.
- WICZYK, H. P., JANUS, C. L., RICHARDS, C. J., GRAF, M. J., GENDAL, E. S., RABINOWITZ, J. G. & LAUFER, N. 1988. Comparison of magnetic resonance imaging and ultrasound in evaluating follicular and endometrial development throughout the normal cycle. *Fertil Steril*, 49, 969-72.
- WILDT, L., KISSLER, S., LICHT, P. & AL., E. 1998. Sperm transport in the human female genital tract and its modulation by oxytocin as assessed by hysterosalpingography, hysteronography, electronhysteroigraphy and Doppler sonography. *Hum Reprod Update*, 4, 655-666.
- WILKINS, M. R., GASTEIGER, E., APPEL, R. D. & HOCHSTRASSER, D. F. 1996. Protein identification with sequence tags. *Curr Biol*, 6, 1543-1544.
- WILKINS, M. R., GASTEIGER, E., TONELLA, L., KELI, O., TYLER, M., SANCHEZ, J. C., GOOLEY, A. A., WALSH, B. J., BAIROCH, A., APPEL, R. D., WILLIAMS, K. L. & HOCHSTRASSER, D. F. 1998. Protein Identification with N and C-terminal Sequence Tags in Proteome Projects. *J Mol Biol*, 278, 599-608.

- WOLF, D. M. & SPATARO, R. F. 1988. The current state of hysterosalpingography. *Radiographics*, 8, 1041-58.
- YAMAMOTO, T., NOGUCHI, T., TAMURA, T., KITAWAKI, J. & OKADA, H. 1993. Evidence for estrogen synthesis in adenomyotic tissues. *Am J Obstet Gynecol*, 169, 734-8.
- YAMASHITA, S., NEWBOLD, R. R., MCLACHLAN, J. A. & KORACH, K. S. 1989. Developmental pattern of estrogen receptor expression in female mouse genital tracts. *Endocrinology*, 125, 2888-2896.
- YEAMAN, G. R., COLLINS, J. E., CURRIE, J. K., GUYRE, P. M., WIRA, C. R. & FANGER, M. W. 1998. IFN-gamma is produced by polymorphonuclear neutrophils in human uterine endometrium and by cultured peripheral blood polymorphonuclear neutrophils. *J Immunol*, 160, 5145-5153.
- YEAMAN, G. R., GUYRE, P. M., FANGER, M. W., COLLINS, J. E., WHITE, H. D., RATHBUN, W., ORNDORFF, K. A., GONZALEZ, J., STERN, J. E. & WIRA, C. R. 1997. Unique CD8+ T cell-rich lymphoid aggregates in human endometrium. *J Leukocyte Biol*, 61, 427-435.
- ZAITSEVA, M., VOLLENHOVEN, B. J. & ROGERS, P. A. 2007. Retinoic acid pathway genes show significantly altered expression in uterine fibroids when compared with normal myometrium. *Mol Hum Reprod*, 13, 577-85.
- ZHU, Y. K., UMINO, T., LIU, X. D., WANG, H. J., ROMBERGER, D. J., SPURZEM, J. R. & RENNARD, S. J. 2001. Contraction of fibroblast-containing collagen gels: initial collagen concentration regulates the degree of contraction and cell survival. *In Vitro Cell Dev Biol*, 37, 10-16.

